Biomarker Discovery for Alzheimer's Disease Using NAPPA and *In Vivo* Crystallization in Baculovirus-Infected Insect Cells for Structural Biology

by

Yanyang Tang

A Dissertation Presented in Partial Fulfillment
of the Requirements for the Degree
Doctor of Philosophy

Approved March 2020 by the
Graduate Supervisory Committee:

Joshua LaBaer, Chair
Karen S. Anderson
Hao Yan

ARIZONA STATE UNIVERSITY

May 2020

ABSTRACT

Proteins are a large collection of biomolecules that orchestrate the vital cellular processes of life. The last decade has witnessed dramatic advances in the field of proteomics, which broadly include characterizing the composition, structure, functions, interactions, and modifications of numerous proteins in biological systems, and elucidating how the miscellaneous components collectively contribute to the phenotypes associated with various disorders. Such large-scale proteomics studies have steadily gained momentum with the evolution of diverse high-throughput technologies. This work illustrates the development of novel high-throughput proteomics platforms and their applications in translational and structural biology. In Chapter 1, nucleic acid programmable protein arrays displaying the human proteomes were applied to immunoprofiling of paired serum and cerebrospinal fluid samples from patients with Alzheimer's disease. This high-throughput immunoproteomic approach allows us to investigate the global antibody responses associated with Alzheimer's disease and potentially identify the diagnostic autoantibody biomarkers. In Chapter 2, a versatile proteomic pipeline based on the baculovirus-insect cell expression system was established to enable high-throughput gene cloning, protein production, *in vivo* crystallization and sample preparation for X-ray diffraction. In conjunction with the advanced crystallography methods, this end-to-end pipeline promises to substantially facilitate the protein structural determination. In Chapter 3, modified nucleic acid programmable protein arrays were developed and used for probing protein-protein interactions at the proteome level. From the perspective of biomarker discovery, structural proteomics, and protein interaction networks, this work demonstrated the power of high-throughput proteomics technologies in myriad applications for proteome-scale structural, functional, and biomedical research.

ACKNOWLEDGMENTS

This dissertation would not have been accomplished without the help from so many people during my journal of seeking for Ph.D. degree. I would like to express my fathomless appreciation and deepest gratitude to the following people who contributed to this work in different ways.

I would like to acknowledge my advisor, Dr. Joshua LaBaer, for providing the resourceful and collaborative research environment as well as the opportunity for me to work in his laboratory, the Center for Personalized Diagnostics in the Biodesign Institute at Arizona State University. His countless support and invaluable advice on my projects inspired me to overcome the challenges in the research development. I would also like to sincerely thank my committee mentors, Dr. Karen S. Anderson and Dr. Hao Yan, for their tremendous kindness and guidance to my research and life. Their insightful comments and precious encouragement have helped me to move this work forward.

During my study here, I was blessed to have met and become lifelong friends with many excellent scientists, Dr. Femina Rauf, Dr. Xiaofang Bian, Dr. Jingmin Shu, Dr. Weimin Gao, Dr. Lusheng Song, Dr. Jie Wang, Haoyu Wang, Anasuya Pal, Kristi Barker, and Justin Saul. I am very grateful for the constant care and help that I have been receiving from them. Special gratitude to Dr. Femina Rauf for her boundless encouragement, guidance, and help in every way of my research and life.

Many sincere thanks to my wonderful collaborators, Dr. Petra Fromme, Dr. Jose Martin Garcia, and Nirupa Nagaratnam for their valuable expertise in crystallography and their dedications in providing thoughtful feedback and suggestions that greatly improved this work. I also would like to thank Dr. Paul Coleman and Dr. Diego Mastroeni for their kind help with providing clinical samples

and training for the Alzheimer's disease project. They have been always there to generously share their thoughts and expertise when I needed advice.

I would like to thank my wonderful laboratory members, Dr. Ji Qiu, Dr. Jay Park, Dr. Vel Murugan, Dr. Mitch Magee, Mahasish Shome, Imtiazur Rahman, Seron Eaton, Vanessa Baack, Chenxi Xu, Huafang Lai, Kailash Karthikeyan, Melanie Sala, Danielle Brokaw, Jennifer Nolz, and Elaine Delvaux for all the unforgettable moments that we have spent together. It was really my honor and pleasure to work with them.

Lastly, I would like to sincerely express my deepest appreciation to my parents, Guangrong Chen and Shuqi Tang, and my husband, Jen-Yu Liao. I could not have anything done without the kind support, tremendous patience and unconditional love from my family.

TABLE OF CONTENTS

Page

CHAPTER Page

LIST OF TABLES

LIST OF FIGURES

Figure Page

LIST OF ABBREVIATIONS

Abbreviation	Full Name
2DE	Bidimensional gel electrophoresis
3D	Three-dimensional
AAbs	Autoantibodies
AAs	Amino acids
Aβ peptide	Amyloid-β peptide
AcMNPV	*Autographa californica* multicapsid nucleopolyhedrovirus
AD	Alzheimer's disease
ApoE	Apolipoprotein E
APP	Amyloid precursor protein
AT1R	Angiotensin 2 type 1 receptor
ATP5B	Acdenosine triphosphate synthase β subunit
AUC	Area under curve
BAC	Bacterial artificial chromosome
BBB	Blood brain barrier
BEVs	Baculovirus expression vectors
BV	Budded virion
CCP	Cyclic citrullinated peptides
CHAP	Chicago Health and Aging Project
chiA	Chitinase
CHO	Chinese hamster ovary
CNS	Central nerve system
CpGV	Granulovirus
C. pomonella	*Cydia pomonella*
CPV	Cypoviruses

CSF	Cerebrospinal fluid
Abbreviation	Full Name
DAB	3,3'-diaminobenzidine tetrahydrochloride
DI	Deionized
dsDNA	Double-stranded circular DNA
ECL	Electro-chemiluminescence
E. coli	*Escherichia coli*
EDTA	Ethylenediaminetetraacetic acid
FAD	Familial AD
FDA	American Food and Drug Administration
FDG	Fluorodeoxyglucose
GFAP	Glial fibrillary acidic protein
GFP	Green fluorescence protein
GOI	Gene of interest
GPCRs	G protein-coupled receptors
GST	Glutathione S-transferase
H. polymorpha	*Hansenula polymorpha*
HEK	Human embryonic kidney
HRP	Horseradish peroxidase
HT	High-throughput
IFN-β	Beta interferon
Ig	Immunoglobulin
IHC	Immunohistochemistry
IMR	Immuno-magnetic reduction
IP-MS	Immunoprecipitation coupled to mass spectrometry
IP-WB	Immunoprecipitation combined with Western blotting

IR	Infrared
IRBs	Institutional Review Boards
Abbreviation	Full Name
IVTT	*In vitro* transcription and translation
LB	Lysogeny broth
LC-ESI-MS	Liquid chromatography-electrospray ionization-tandem mass spectroscopy
LIC	Ligation independent cloning
LINAC	Linear accelerator
LOAD	Late-onset AD
MALDI-TOF	Matrix-assisted laser desorption/ionization-time of flight
MAP	Microtubule-associated protein
MCI	Mild cognitive impairment
MMSE	Mini-mental state examination
MNPV	Multicapsid nucleopolyhedrovirus
MOI	Multiplicity of infection
MS	Mass spectrometry
MT	Microtubule
MTG	Middle temporal gyrus
NAPPA	Nucleic Acid Programmable Protein Array
ND	Non-dementia
NDRC	Neurodegenerative Disease Research Center
NfL	Neurofilament light
NFTs	Neurofibrillary tangles
Ng	Neurogranin
Ni-NTA	Nickel-nitrilotriacetic acid

NPV	Nucleopolyhedrovirus
NSAIDs	Nonsteroidal anti-inflammatory drugs
OBs	Occlusion bodies
Abbreviation	Full Name
OD450	Optical density at 450 nm
ODV	Occlusion derived virion
ORFs	Open reading frames
PAGE	Polyacrylamide gel electrophoresis
PBS	Phosphate-buffered saline
PD	Parkinson's disease
PDB	Protein Data Bank
PET	Positron emission tomography
PHFs	Paired helical filaments
p.i.	Post infection
PMI	Post-mortem interval
PMSF	Phenylmethylsulfonyl fluoride
POIs	Proteins of interest
P. pastoris	*Pichia pastoris*
PPIs	Protein-protein interactions
proNGF	Pro nerve growth factor
pTau	Phosphorylated Tau
PTCD2	Pentatricopeptide repeat domain 2
PTMs	Post-translational modifications
PSEN1/2	Presenilin 1/2
R	Correlation coefficient
RABPT5	Rabaptin 5

RAGE	Receptor for advanced glycation end products
RAPID	Rapid Antigenic Protein In Situ Display
RNAP II	RNA polymerase II
ROC	Receive operating characteristic
Abbreviation	Full Name
RT	Room temperature
S. cerevisiae	*Saccharomyces cerevisiae*
SDS	Sodium dodecyl sulfate
SFX	Serial Femtosecond Crystallography
SHG	Second harmonic generation
SNPV	Single capsid nucleopolyhedrovirus
S/N	Signal to noise
SONICC	Second Order of Nonlinear Imaging of Chiral Crystals
sq	Secretory sequence
STMN4	Stathmin 4
T. brucei	*Trypanosoma brucei*
TEV	Tobacco etch virus
TMB	Tetramethylbenzidine
TREM2	Myeloid cells 2
tTau	Total Tau
UV	Ultraviolet
V-cath	Cathepsin
V. cholera	*Vibrio cholera*
WT	Wild-type
XFELs	X-ray free electron lasers
Y2H	Yeast two-hybrid

CHAPTER 1

1 IMMUNOPROFILING OF PAIRED SERUM AND CEREBROSPINAL FLUID IDENTIFIED STMN4 AS A NOVEL AUTOANTIGEN FOR ALZHEIMER'S DISEASE

1.1 Abstract

The participation of autoimmunity in pathogenesis of Alzheimer's disease (AD) is supported by compelling evidence and thus imposes impetus for the identification of novel autoantibodies (AAbs) to establish a diagnostic modality and to illuminate the disease mechanism at a molecular level. Although the research efforts on discovering AD-specific AAbs have been ongoing for years, no remarkable immunosignature-based diagnostic method has been developed mainly due to the inconsistent or non-specific performance of biomarkers. Furthermore, the potential correlation of global humoral immune responses in paired serum and cerebrospinal fluid (CSF) samples has not been discussed. The goal of this study was to identify novel neuronal antigenic targets specifically recognized by AAbs present in serum and CSF of AD patients for diagnostic purpose and to explore the possible association of antibody repertoire between serum and CSF. An immunoproteomic approach, namely nucleic acid programmable protein array (NAPPA), was applied to systemic AAb profiling of paired serum and CSF samples from 30 AD patients and 30 non-dementia (ND) controls. A stronger global immunoreactivity was observed in both serum and CSF of AD patients, which confirms the involvement of autoimmune components in AD. Antibody responses that were differentially represented in AD versus non-dementia (ND) controls were similar between serum and CSF. Specifically, antibodies present in CSF were also found in serum while no such correspondence was observed in reverse. This is in accordance with the autoimmune hypothesis for AD that circulating AAbs leak into the central nerve system (CNS) due to blood brain barrier (BBB) compromise in AD patients. Additionally, antibodies

showing strong immunoreactivity against serum of AD patients were also present in their CSF while no such correspondence was found in ND controls, suggesting a more severe penetration of circulating AAbs into the brain of AD patients due to the BBB deficiency. Antibody candidates discovered on NAPPA were subsequently verified and further validated by ELISA using an independent sample set comprising of additional 30 AD patients and 30 ND controls. This three-stage screening study led to identification of anti-STMN4 antibody as the top performer with a sensitivity of 28% and 15% in serum and CSF, respectively, at 90% specificity. The titer of anti-STMN4 antibody in paired serum and CSF of AD patients was significantly correlated (Spearman $r = 0.72$, $p < 0.0001$).

STMN4 is a microtubule-associated protein (MAP) highly expressed in the CNS. It functions as a microtubule destabilizer by inhibiting tubulin polymerization. Immunohistochemistry (IHC) staining of hippocampal tissue sections showed a significant increase in STMN4 protein level in CA1 neurons of AD patients relative to ND controls ($p < 0.0001$). On contrary, a significant reduction in STMN4 protein level was observed in the middle temporal gyrus (MTG) tissue lysates of AD patients analyzed by semi-quantitative Western blotting ($p = 0.0003$). Taken together, we proposed that the immunogenic STMN4 protein is overexpressed and released from diseased neurons, and induces continual production of anti-STMN4 antibody due to immune intolerance, which could exacerbate the disruption of neuronal structures and functions in AD. This study demonstrated the feasibility and value of using NAPPA to search for novel AAbs as a potential diagnostic tool that could differentiate AD from ND and contribute to the understanding of humoral immune responses in AD disease mechanism.

1.2 Introduction

1.2.1 Overview of Alzheimer's Disease (AD)

Alzheimer's Disease (AD) is a complex neurodegenerative disorder, representing the most common (60-70%) form of dementia that causes cognitive decline among the elderly population (Barker et al. 2002). It is characterized by a chain of neuropathological events, including abnormal formation and accumulation of senile plaques and neurofibrillary tangles, progressive neuronal loss and cortical atrophy, which over time severely impairs cognition and language abilities of affected individuals and results in death ultimately (Cacabelos et al. 2005; Goedert and Spillantini 2006; Holtzman, Morris, and Goate 2011; Querfurth and Laferla 2010). Current notion recognizes three stages of AD: 1) preclinical AD, 2) mild cognitive impairment (MCI), and 3) dementia due to AD (Petersen et al. 1999). Generally, patients with AD are subjected to an early onset followed by a long asymptomatic duration of 20 years or more prior to the disease manifestations.

AD is recognized as the 6th leading cause of death in the United States, exerting a substantial impact on public health (Heron 2018). According to 2010 U.S. Census and the Chicago Health and Aging Project (CHAP), an estimated 5.8 million Americans are living with AD in 2019, and 97% out of them are aged 65 or older (Association 2019; Hebert et al. 2013). There are 50 million people living with AD or other dementia worldwide in 2019, and this number is projected to reach 152 million by 2050 (Association 2019). The rapid growth in new and existing cases of AD is mainly due to the aging of baby boom generation and longer life expectancies. As a major cause of morbidity in the elderly, AD imposes a tremendous economic burden to the public healthcare system. The estimated worldwide cost of dementia is 1 trillion US$ in 2018 (Association 2019).

Relevant research efforts combining biochemistry, molecular and cellular biology, radiology, and transgenic modeling have partially uncovered a multifactorial pathology involving aging, genetic mutations (eg. APP, PSEN1/2), epigenetic modifications (DNA methylation, histone acetylation) (Huang and Mucke 2012), environmental factors (eg. education, nutrition), and other brain conditions (eg. cerebrovascular deterioration, traumatic brain injury), etc (Association 2019; Cacabelos et al. 2005; Huang and Mucke 2012). Despite these advances in our understanding of disease mechanism, the disease onset and/or progression of AD has not been fully explained yet. Unfortunately, to date almost no therapeutic interventions have proven effective to prevent, delay, or slow the AD onset and/or progression (Huang and Mucke 2012; Laske et al. 2015; Mehta et al. 2017). Since 1998, 100 drugs have been tested and most of them demonstrated no clinical benefits in individuals with AD (Association 2019). The possible explanations for this failure are that 1) clinical diagnostic accuracy for AD has been low, causing the inclusion of many trial subjects without significant AD neuropathology (Davis et al. 1992; Mehta et al. 2017), and 2) the trial drugs were administered too late in the disease course, when it is unlikely to reverse the permanent structural brain damage (Counts et al. 2017; Laske et al. 2015; Mehta et al. 2017). Therefore, therapeutics aimed at early pathological events have the greatest probability for effective modification if the disease is detected before the emergence of overt symptoms (Association 2019; Caselli et al. 2006; Holtzman et al. 2011). Unfortunately, no diagnostic modality yet has the needed accuracy, non-invasiveness, or cost-effectiveness for population screening of AD despite tremendous progress in radiological neuroimaging techniques (Caselli et al. 2006; Laske et al. 2015). Given the complex nature of AD pathophysiology, it is likely that the optimal diagnostic

method will require an integrated panel of different biochemical markers together with other clinical screening modalities (Counts et al. 2017; Jack et al. 2011).

1.2.2 Discovery of AD

In November 1901, Alois Alzheimer, a German psychiatrist and neuroanatomist, admitted a 51-year-old female patient, Auguste D., at Frankfurt Psychiatric Hospital because of her mental health issues including progressive memory loss, delusions, and hallucinations (Maurer, Volk, and Gerbaldo 1997). At that time, he specialized in clinical psychiatry and brain histopathology as a senior assistant at Municipal Institution for the Mentally Ill and Epileptics in Frankfurt, where he started the long-term extensive observation and detailed documentation of this unusual case study (Hippius and Neundörfer 2003). In 1903, Alzheimer moved to the University of Munich and was appointed as the head of the Anatomical Laboratory at the Royal Psychiatric Clinic. Soon after the patient's death in April 1906, her brain was sent to Munich for histological analysis. Alzheimer performed silver staining on the brain sample and observed peculiar histological changes, which were later known as neuritic plaques and neurofibrillary tangles (NFTs) (Alzheimer 1907). For the first time he described the neurofibrils: "In the center of an otherwise almost normal cell there stands out one or several fibrils due to their characteristic thickness and peculiar impregnability". He also reported on the typical plaques: "Numerous small miliary foci are found in the superior layers. They are determined by the storage of a peculiar material in the cortex".

In November 1906, Alzheimer presented the psychiatric illness and neurohistological abnormalities of this case at the 37th Meeting of South-West German Psychiatrists (37 Versammlung Südwestdeutscher Irrenärzte) in Tübingen, Germany. Although his remarkable lecture entitled "peculiar severe disease process of the cerebral cortex" (Über einen eigenartigen, schweren Erkrankungsprozeß der

Hirnrinde) failed to arouse an interest from the audience, it called great attention and support from one of the most prominent and influential psychiatrists in Germany, Emil Kraepelin, who was enthusiastic about the classification of psychiatric diseases (Alzheimer 1906, 1907). Later in the following years, Alzheimer and coworkers observed three additional cases comparable to Auguste D., and eventually published their clinical and histopathological findings of these cases (Alzheimer 1911; Perusini 1909). To recognize the significance of Alzheimer's work regarding this disease, Kraepelin first introduced the diagnostic term "Alzheimer's disease" in the 8th edition of his well-known text book *Psychiatrie* (Kraepelin 1910). However, in the following 50 years, relevant research remained silent due to rarely available cases for intensive studies (Hippius and Neundörfer 2003).

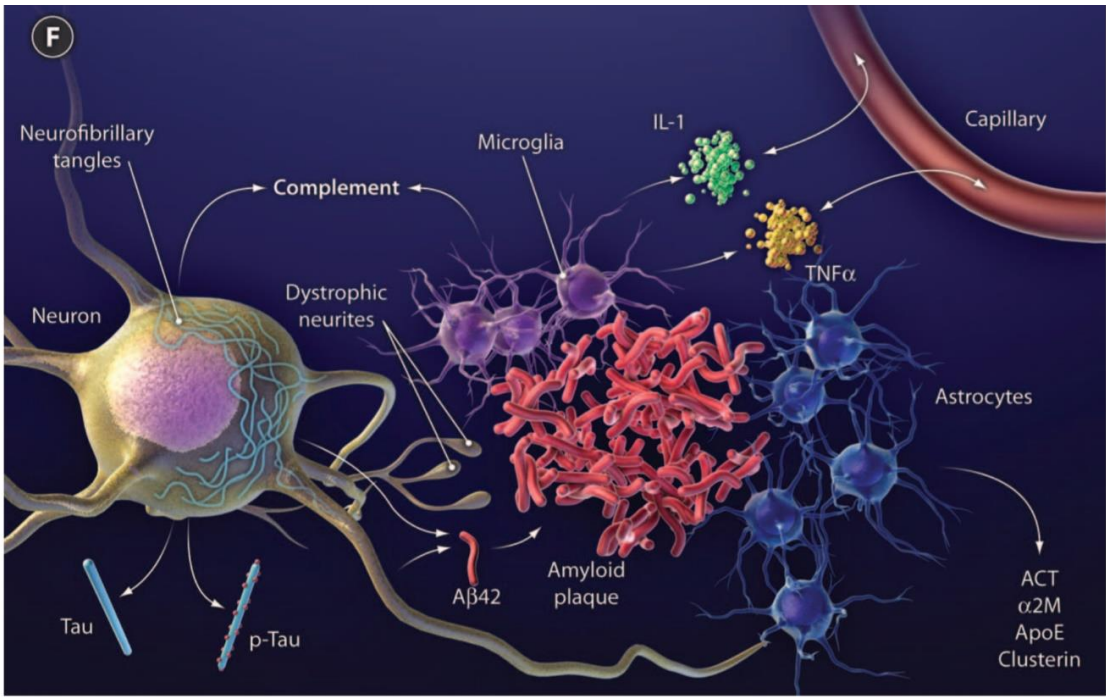

Figure 1-1. Diagram showing the two hallmark lesions of AD. Secreted Aβ42 aggregates to amyloid plaques in extracellular space. Hyperphosphorylated Tau assembles into NFTs and deposits in somatic and neuritic compartments. Figure adapted from Holtzman et al. 2011.

1.2.3 Hallmarks of AD

Although Alzheimer's discovery and description of the abnormal proteinaceous filaments greatly benefited the disease classification of AD, researchers at that time knew little about their molecular composition and role in the pathological process (Goedert and Spillantini 2006). Only until almost a century after the original case report, has a basic model of AD etiology centered around the two well-established pathological hallmarks, senile plaques and NFTs, become unveiled (Figure 1-1) (Goedert and Spillantini 2006; Holtzman et al. 2011; Querfurth and LaFerla 2010). The modern understanding of AD stemmed from the identification of molecular components and genetic alterations associated with the senile plaques and NFTs (Goedert and Spillantini 2006).

1.2.3.1 Plaque Pathology

The senile plaques are extracellular accumulations of filaments with a cross-β structure composed of amyloid-β (Aβ) peptides (Drolle et al. 2014; Querfurth and Laferla 2010). Aβ is a small secreted peptide consisting of 36-43 amino acids (AAs), which is derived from a much larger transmembrane protein, amyloid precursor protein (APP), through sequential enzymatic proteolysis (Holtzman et al. 2011; Querfurth and LaFerla 2010). It naturally exists in the CNS of both AD patients and healthy people with an unclear physiological function. The N and C terminus of Aβ is located in the extracellular and transmembrane domain of APP, respectively (Goedert and Spillantini 2006). The α-secretase cleaves in the middle of Aβ locus on APP, thus precluding its production. Alternatively, the cleavage of APP by β-secretase followed by γ-secretase give rise to the N and C terminus of Aβ, respectively (Figure 1-2) (Iwatsubo et al. 1994). The major species of Aβ are 40 or 42 AA in length, depending on the specific cleavage site of γ-secretase. While monomers of Aβ40 are naturally much more prevalent (Querfurth and Laferla 2010), Aβ42 is more of

significance in the pathological process of AD. As Aβ42 has two more hydrophobic AAs, it tends to form neurotoxic oligomers of 2-6 peptides, which are prone to aggregate into insoluble fibrils with β-sheet conformation (Goedert and Spillantini 2006; Querfurth and Laferla 2010). Such fibrillary structures further assemble into plaques, which are widely deposited in interneuronal space throughout the cerebral cortex over time, eventually leading to synaptic depression and neuronal cell death (Figures 1-1 and 1-2) (Goedert and Spillantini 2006; Palop and Mucke 2010; Querfurth and Laferla 2010).

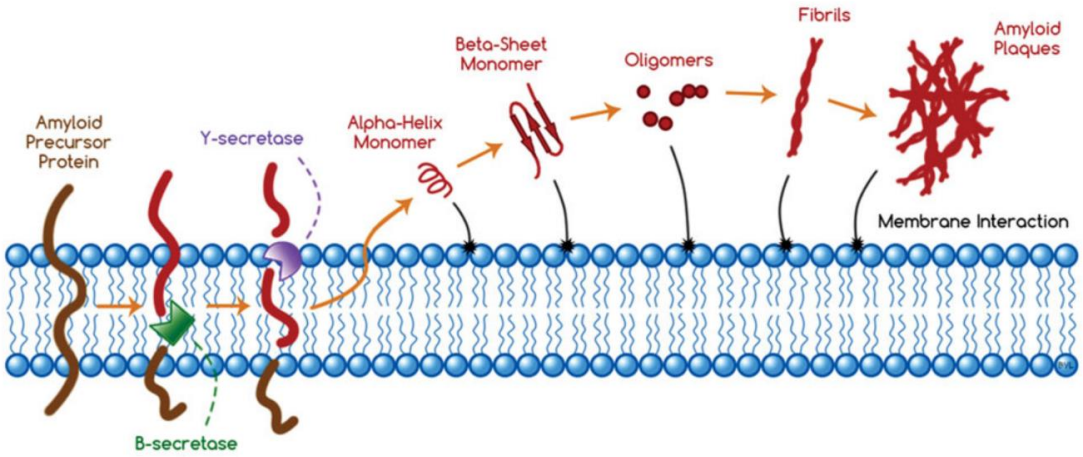

Figure 1-2. Scheme illustrating Aβ production, oligomerization and aggregation into amyloid plaques. Figure adapted from Drolle et al. 2014.

The impaired clearance of Aβ is often found present in AD patients (Bateman et al. 2006). Normally, a large fraction of Aβ generated by γ-secretase can be degraded in endosome by endothelin-cycling enzymes or other unidentified proteoses (J. Baranello et al. 2015). Alternatively, it might be transported into lysosome, where the secondary degradation occurs. Aβ that escapes from these proteolytic mechanisms may get drained into the cerebrospinal fluid (CSF) or peripheral blood circulation (Nicoll et al. 2004). Only Aβ off-targeted by these redundant pathways will aggregate and accumulate in cerebral parenchyma as senile plaques (J. Baranello et al. 2015).

Many studies have been dedicated in unmasking the complex plaque pathology over the past decades; it was suggested that different forms of Aβ can affect inflammatory responses, oxidative stress, DNA damage, ion channels, fluidity and permeability of lipid membranes. Although the exact toxicity mechanism induced by amyloid plaques is still under debate (Berthelot, Cullin, and Lecomte 2012), it is widely believed that the substantial plaque deposition, which is resulted from a disrupted balance between production, clearance, and oligomerization of Aβ, is an initiating factor underlying in AD onset (Querfurth and Laferla 2010).

1.2.3.2 Tangle Pathology

The molecular study of NFTs identified the aggregated hyperphosphorylated Tau (pTau) as the major component (Goedert et al. 1988; Grundke-Iqbal et al. 1986). Tau is an axonal protein ubiquitously present in pyramidal neurons and at low level in glial cells (Lopresti et al. 1995). It mediates microtubule (MT) polymerization as a MT stabilizer by directly binding to tubulin heterodimers (Kadavath et al. 2015; Kolarova et al. 2012; Weingarten et al. 1975). The primary structure falls into two functional domains, i.e. the N-terminal projection domain that docks to neuronal plasma membrane and the C-terminal MT-binding domain that attaches to axonal MT network (Figure 1-3) (Wang and Mandelkow 2016). Through this structural linkage between nerve cell bodies and neuritic processes, it regulates neural plasticity and MT stabilization (Wang and Mandelkow 2016). In nature, there are 6 CNS isoforms of Tau ranging from 352 to 411 AAs, which can be generated through alternative RNA splicing (Buée et al. 2000). Depending on the number (3 or 4) of MT-binding repeats, these isoforms can be categorized into two groups, which have approximately equal abundance in healthy people (Goedert and Spillantini 2006).

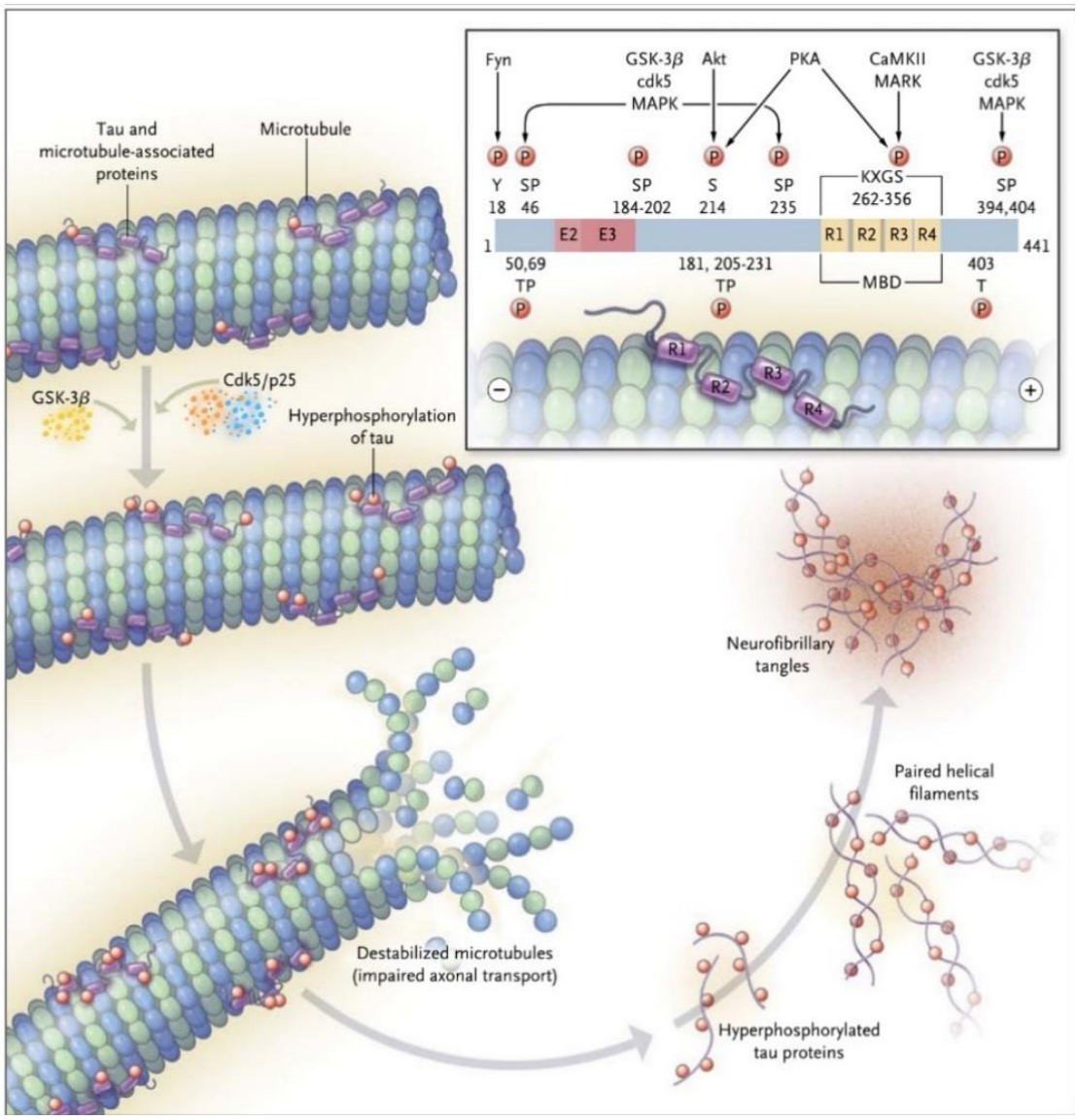

Figure 1-3. Scheme illustrating the domain structure of Tau and formation of NFTs. Figure adapted from Querfurth and Laferla 2010.

Tau can be phosphorylated/dephosphorylated at more than 30 serine or threonine sites by a wide range of kinases and phosphatases (Buée et al. 2000), whose dynamicity is essential for modulating Tau trafficking and binding affinity to MT (Biernat et al. 1993; Hirokawa et al. 1996). The site and degree of phosphorylation, which is mainly dependent on cellular compartments and development stage, in combination with the type of isoform, render diverse physical

and biochemical properties to Tau (Buée et al. 2000; Riederer and Binder 1994). Aberrantly phosphorylated Tau can lose its solubility as well as affinity to MT and assemble into paired helical filaments (PHFs) (Kidd 1963; Lee et al. 1991), which eventually form NFTs and accumulate in somatodendritic compartments as opposed to axons in normal condition (Figure 1-1 and 1-3) (Li and Götz 2017). In general, NFTs can be preferentially found in large pyramidal neurons from the hippocampus and the entorhinal cortex (Braak and Braak 1996). In addition to hyperphosphorylation, other factors may be also involved in the aggregation of NFTs, including ubiquitination (Mori, Kondo, and Ihara 1987), glycation (Ko et al. 1999), and oxidation of Tau (Ko et al. 1999).

Like Aβ oligomers, how NFTs directly exert neurotoxicity remains unclear (Goedert and Spillantini 2006). Nevertheless, it is assumed that a functional disconnection between damaged neurons or brain regions caused by these two prominent lesions is fundamental in the pathogenesis of AD (Araki, Sasaki, and Milbrandt 2004; Hoover et al. 2010). Although the tangle pathology occurs later than and is considered as a downstream pathological event of plaque pathology, the burden of NFTs is highly associated with the clinical progression and disease severity of AD (Götz et al. 2001; Lewis et al. 2001; Oddo et al. 2003), highlighting its significance as a potential target for AD diagnostics and therapeutics (Querfurth and Laferla 2010).

1.2.4 Familial AD (FAD)

Familial AD (FAD), representing only 1% of all cases, is inherited within families in an autosomal dominant manner (Holtzman et al. 2011). FAD patients have an early disease onset generally at 30-60 years old. Current research has identified several genetic risk factors that predominantly contribute to the development of FAD. Missense mutations adjacent to γ-secretase cleavage site in

APP gene result in elevated Aβ42 (Davis and Van Nostrand 1996; Grabowski et al. 2001; Van Nostrand et al. 2001). Also, a missense mutation near β-secretase cleavage site (Swedish mutation) or duplicated dosage of APP gene due to trisomy can lead to a higher level of total Aβ (Citron et al. 1992; Mullan et al. 1992; Rovelet-Lecrux et al. 2006). Another two highly homologous transmembrane proteins, presenilin 1/2 (PSEN1/2), are noted as the most common cause for FAD (Ring et al. 2007; Young-Pearse et al. 2010). PSEN1/2 serve as the catalytic subunits of γ-secretase complex (Edbauer et al. 2003; Takasugi et al. 2003), whose endoproteolytic enzymatic activity is dependent on 2 aspartates located in the transmembrane domain of PSEN1/2 (Wolfe et al. 1999). There are more than 160 mutations in PSEN genes identified, and some of them can increase Aβ42/Aβ40 ratio via reducing the γ-secretase activity (Citron et al. 1997; Strooper 2007; Strooper et al. 1998). In any case, these mutations in abovementioned genes contribute to the disease by promoting the production and accumulation of Aβ42. Besides, altered γ-secretase activity induced by PSEN mutations can also result in hyperphosphorylation of Tau (Doglio et al. 2006).

1.2.5 Late-onset AD (LOAD)

Unlike FAD, most AD cases are sporadic, and their dementia symptoms appear after 65 years old, which are thus referred to as late-onset AD (LOAD) (Holtzman et al. 2011). LOAD accounts for > 99% of all AD cases. To date, many risk factors have been identified to increase the chance of developing LOAD. Among them, apolipoprotein E (*ApoE*) is the only well-established genetic element (Strittmatter et al. 1993). There are 3 alleles of human *ApoE* gene, i.e. *ε2*, *ε3*, and *ε4*, which are distinguished by only one AA in sequence (Holtzman, Herz, and Bu 2012; Loy et al. 2014). The most and the least prevalent form are *ε3* and *ε2*, respectively (Rajan et al. 2017). Whereas *ε2* decreases the risk of LOAD, *ε4* is

associated with higher levels of Aβ deposits and and hemorrhage in the CNS (Corder et al. 1993; Greenberg et al. 1995; Schmechel et al. 1993; Strittmatter et al. 1993). One copy of ε4 can significantly increase the risk by 3 fold, and two copies by up to 12 fold (Michaelson 2014). Meta-analysis across a series of cohorts showed that 65% and 11% of Americans diagnosed with AD inherited one or two copies of ε4, respectively (Mayeux et al. 1998; Ward et al. 2012). ApoE is highly expressed in liver and CNS and known to regulate the lipoprotein metabolism and transport (Mahley 1988; Plump 1995). Compared to *ε4*, *ε2* displays a higher binding efficiency to Aβ, therefore accelerating its removal from the CNS via cellular uptake or vascular drainage into blood circulation (Kim, Basak, and Holtzman 2009). While it is certain that as an Aβ-binding protein, ApoE contributes to AD by directly affecting Aβ metabolism and possibly Tau phosphorylation as well (Holtzman et al. 2000; Reiman et al. 2009), the exact action mode is still not fully understood (Strittmatter et al. 1993). Other genetic risk factors of AD include *APOE2*, *CLU*, *CR1*, *PICALM*, *BIN1*, *SORL1*, *GAB2*, *ABCA7*, *MS4A4/MS4A6E*, *CD2AP*, *CD33*, *EPHA1*, and *HLA-DRB1/5* (Huang and Mucke 2012).

Age is another major risk factor. Over 97% of AD patients are 65 years old or older, and the incidence rises as the age increases (Hebert et al. 2003). The rapid growth of aging population in the upcoming decades will bring up the prevalence to 16 million in the United States by 2050 (Hebert et al. 2003). Normal aging alone causes synaptic loss (Lister and Barnes 2009; Masliah, Crews, and Hansen 2006), influencing the dentate gyrus in hippocampus. Traces of amyloid plaques and NFTs are also found in senior individuals without overt cognitive impairment (Braak and Braak 1991). Other than *ApoE* and aging, family history of AD, cardiovascular diseases, midlife obesity, education, etc. can all interact and collaboratively affect the development of AD. A variety of molecular mechanisms that could drive AD have

been proposed, such as inflammation, oxidative stress, calcium regulation, and cholesterol metabolism (Querfurth and LaFerla 2010). Such heterogeneity indicates the tangled mass of AD pathogenesis that cannot be clarified by a single linear chain.

1.2.6 Autoimmune Components

A large body of evidence supports that the immune system is intrinsically involved in AD neuropathogenesis (Colasanti et al. 2010; D'Andrea 2003, 2005; Sardi et al. 2011; Wyss-Coray and Rogers 2012). A dozen of naturally occurring anti-neuronal antibodies were consistently detected in serum and CSF of AD patients as reported in many studies (Colasanti et al. 2010; Counts et al. 2017; Wu and Li 2016). Immunolabeling of brains with AD also showed a significant increase in human immunoglobulin (Ig) positive neurons. These neurons also exhibited degenerative features which are not present in Ig negative neurons (D'Andrea 2003). Moreover, in a recent animal study, the triple transgenic AD (3xTg-AD) mice model demonstrated the systemic autoimmune manifestations with an elevated level of autoantibodies (AAbs) and an increased number of double-negative T splenocytes (Marchese et al. 2014). These mice also showed MCI prior to significant Aβ or Tau pathology. An epidemiological study reported an overlap of specific single-nucleotide polymorphisms in triggering receptor expressed on myeloid cells 2 (TREM2) and complement factors between AD and immune diseases, confirming that neurodegeneration and autoimmunity are genetically related (Yokoyama et al. 2016). Moreover, long-term use of nonsteroidal anti-inflammatory drugs (NSAIDs) is linked to reduced risk of developing AD (Lehrer and Rheinstein 2015; Lindsay et al. 2002; Stewart et al. 1997). Nevertheless, it remains mysterious that whether the autoimmune components play a neuroprotective or neurotoxic role in AD pathogenesis, as is with the cause-and-effect relationship between autoimmunity

and AD (Colasanti et al. 2010; Counts et al. 2017; Wu and Li 2016; Wyss-Coray and Rogers 2012).

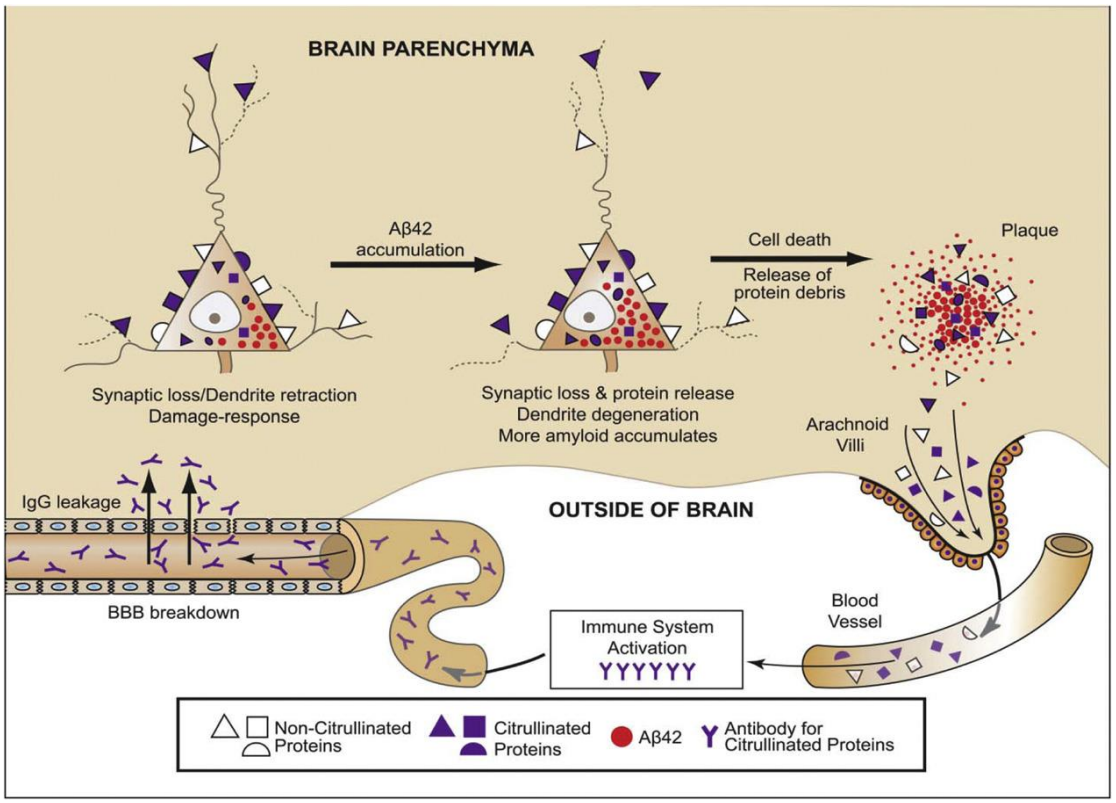

Figure 1-4. Hypothesized mechanism for the generation of autoantibodies (AAbs) detected in serum. Pre-existing pathological events, such as excessive accumulation of Aβ42 and pTau in AD brains, cause synaptic loss and neuronal cell death, releasing the autoantigens into the brain interstitium. Their degraded fragments may enter the general circulation and trigger AAb production Through the deficient blood brain barrier in AD patients, some AAbs may leak back to the brain parenchyma, where they bind to neurons and glia, thus potentially causing the autoimmunity-associated neurodegeneration. Figure adapted from Acharya et al. 2012.

As AD autoimmune hypothesis suggests, in the context of blood brain barrier (BBB) compromise, AAbs that would otherwise be restricted to blood circulation gain the entry into cerebral parenchyma and target specific neuronal proteins, resulting in apoptotic cell death (Figure 1-4) (Acharya et al. 2012; D'Andrea 2003, 2005; Sardi et al. 2011). Therefore, the immune system is regarded as a rich reservoir for AAbs indicative of AD. This concept highlights the importance of pursuing more novel

autoantigens to expand the current autoantigenome (D'Andrea 2005), which can greatly illuminate the disease mechanism and benefit the development of immunosignature-based diagnostics and therapeutics for AD.

Although AD-associated AAbs have been shown present in both CSF and serum, the latter is generally considered as a better biological fluid source in practice for a diagnostic method. CSF is physiologically generated through an ultrafiltration of arterial blood, where the circulating antibodies are maintained by the immune system. As a body fluid that envelopes and is in direct contact with the brain and spinal cord, CSF is often regarded as an indicator of many neuropathological states of brains (Counts et al. 2017; Fragoso-Loyo et al. 2008; Hu et al. 2015). However, CSF sampling through lumbar puncture is invasive and rarely performed as a routine practice (Zetterberg 2019). Furthermore, CSF volume in a normal adult is only 125-150 mL, leaving very limited amount of sample that can be collected for clinical analysis. In addition, the concentration of IgG in CSF is ~42 ± 21 mg/L, which is much less than that of serum (1118 ± 251 g/L) (Hu et al. 2015). Overall, these limitations largely compromise the invasiveness, applicability and convenience of using CSF-based AAbs for an efficient frontline community screening method. That being so, the discovery of blood-based AAbs would be of great significance to allow for the development of a less invasive and more convenient initial disease screening method for large-scale clinical implementation (Blennow 2017; Zetterberg 2019). In addition, the potential correlation of global humoral immune responses in paired serum and CSF samples, which has not been discussed, could also provide information on the compartmental distribution of autoimmune components in AD, enlightening its birth and role in relation to the pathogenesis.

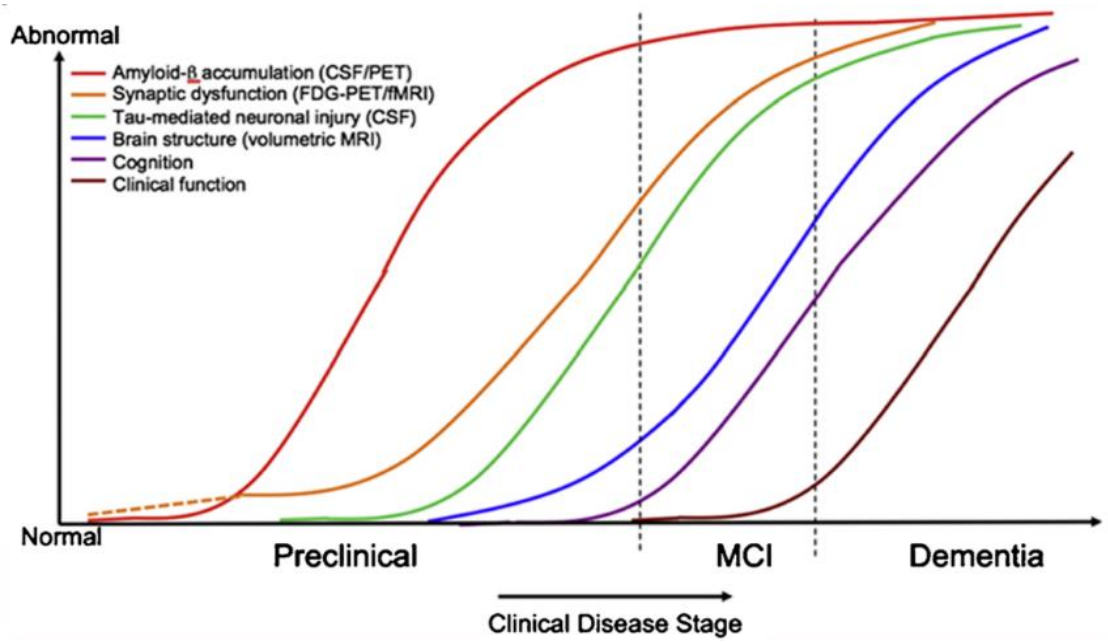

Figure 1-5. A hypothetical model of progression biomarkers for AD at preclinical, MCI, and dementia stages. Figure adapted from Counts 2017.

1.2.7 Diagnostics of AD

Because of the long pre-symptomatic phase of AD, therapeutic interventions aimed at the earliest pathological changes are counted on to delay or even prevent the cognitive decline. This concept proposes an impetus for developing a diagnostic tool for identifying individuals at the preclinical stage of AD (Figure 1-5). Besides, diagnostic modalities that can track disease progression have clinical utility for monitoring patients' response to disease-modifying therapies (Counts et al. 2017). Currently, the clinical diagnostic practice involves a medical examination, neuropsychological testing, neuroimaging, CSF and blood analysis (Figure 1-5) (Laske et al. 2015). Despite these gold standard procedures, currently, the definite diagnosis of AD relies on the neuropathological analysis of brain by autopsy from deceased suspected patients (Nussbaum and Ellis 2003; Wu and Li 2016). Furthermore, state-of-the-art diagnostic measures of AD are invasive (CSF analysis), expensive (neuroimaging), and time-consuming (neuropsychological assessment),

limiting their applicability for large-scale clinical implementation in primary care (Laske et al. 2015; Zetterberg 2019).

On the other hand, MCI is a heterogeneous syndrome as it can be caused by various forms of brain disorders such as AD, Parkinson's disease (PD), dementia with Lewy bodies, vascular dementia, frontotemporal dementia, traumatic brain injury, etc. In fact, only ~50% MCI cases progress to dementia with AD over years (Olsson et al. 2016). Such a heterogeneity in MCI amplifies the challenge for diagnostics of the early symptomatic stage of AD. Thus, the AD community is still in urgent need for an early diagnostic method that is reliable, relatively non-invasive, inexpensive, sensitive and specific (Jack et al. 2011; Laske et al. 2015).

1.2.7.1 CSF Biomarkers

Biomarkers are measurable identities within subjects that can indicate the presence or severity of a specific disease state. The core CSF biomarkers for AD include Aβ42, total Tau (tTau), and pTau (phosphorylated specifically at residue T181), which have been rigorously validated in numerous studies and demonstrated a high diagnostic performance for both MCI and dementia stages of AD (Figure 1-6) (Blennow 2017; Counts et al. 2017; Olsson et al. 2016; Zetterberg 2019). As the molecular components for senile plaques and NFTs, they were regarded as direct surrogates for the two lesions. Specifically, it is assumed that lower CSF Aβ42 levels correlate with accumulating plaque deposition, and higher CSF tTau and pTau levels correlate with progressive neuronal loss and tangle pathology, respectively (Counts et al. 2017; Olsson et al. 2016; Putnam et al. 2015; Zetterberg 2019). Using C-terminal antibodies against Aβ42, several studies consistently showed a ~50% decrease in Aβ42 in moderate AD compared with age-matched controls (Niels Andreasen et al. 1999; Andreasen and Blennow 2002; Mehta et al. 2000). Further analysis of CSF Aβ42 demonstrated a mean sensitivity of 86% and a mean specificity

of 89% (Blennow 2004), as well as an interchangeable performance with amyloid PET in evaluating the amyloid accumulation (Palmqvist et al. 2014). Alternatively, CSF Aβ42/Aβ40 ratio is 85-95% sensitive and specific in AD at both MCI and dementia stages.

	Number of comparisons included	Sensitivity		Specificity		LR+	LR−
		Mean (SD)	Min–max	Mean (SD)	Min–max		
AD VS. HEALTHY CONTROLS							
$A\beta_{42}$	11	83 (9)	63–97	80 (8)	67–92	4	0.2
T-tau	12	78 (9)	61–91	82 (14)	53–97	4	0.3
p-tau	12	78 (10)	61–89	77 (18)	37–92	3	0.3
Combination	25	87 (6)	70–98	84 (9)	53–97	5	0.2
AD VS. OTHER DEMENTIAS							
$A\beta_{42}$	5	85 (5)	82–95	61 (24)	22–80	2	0.2
T-tau	4	75 (14)	61–92	71 (22)	40–93	3	0.4
p-tau	4	80 (6)	77–88	78 (15)	56–88	4	0.3
Combination	19	86 (10)	67–100	78 (14)	36–97	4	0.2
MCI-C VS. MCI-S							
$A\beta_{42}$	9	79 (14)	55–91	63 (20)	36–96	2	0.3
T-tau	9	76 (12)	60–88	58 (17)	39–88	2	0.4
p-tau	7	78 (9)	64–85	56 (18)	30–90	2	0.4
Combination	19	84 (10)	57–98	63 (19)	36–95	2	0.3

AD, Alzheimer's disease; MCI, mild cognitive impairment (MCI-C: MCI-converters, MCI-S: MCI-stables); SD, standard deviation; LR+, positive likelihood ratio; LR−, negative likelihood ratio; sensitivity and specificity values are expressed in percentages.

Figure 1-6. Summary of diagnostic performance of core CSF biomarkers, including sensitivity, specificity, and likelihood ratios based on primary studies published. Figure adapted from Scott et al. 2017.

All isoforms of Tau irrespective of phosphorylation state were found to have an ~200-300% increase in AD (Blennow et al. 1995; Mori et al. 1995; Vigo-Pelfrey et al. 1995). Similarly, pTau phosphorylated at a series of sites associated with the formation of NFTs also increased by ~3 folds in AD patients (Hu et al. 2002; Kohnken et al. 2000; Vanmechelen et al. 2000). Analysis of CSF using ELISA showed

that tTau yielded a mean sensitivity of 81% and a mean specificity of 91%, whereas multiple forms of pTau also yielded a mean sensitivity of 81% and a mean specificity of 91% (Blennow 2004). Meta-analysis of results from 231 studies revealed that core CSF biomarkers are strongly associated with AD as well as with MCI due to AD (Olsson et al. 2016). Although both Aβ42 and tTau showed good ability of differentiating AD and ND controls, CSF pTau can further separate AD from other dementia that might exhibit similar symptoms or lesions with more than 80% specificity (Kang et al. 2013).

Apart from the core CSF biomarkers that directly relate to the plaque deposition and NFTs formation, other biomarkers have been identified capable of reflecting synaptic degeneration and loss, which is of significance as it correlates better with the cognitive deficits in AD (Counts et al. 2017). Neurofilament light (NfL) is a biomarker of axonal pathology as its increased level in AD reflects the release of such an axonal protein to CSF due to neuronal damage in AD (DeKosky and Scheff 1990; Terry et al. 1991). As opposed to the excellent specificity of CSF pTau, CSF NfL appears in a variety of neurodegenerative diseases, in which the higher NfL concentration in CSF has been widely observed (Khalil et al. 2018).

Neurogranin (Ng) is a calmodulin-binding protein that primarily expressed in dendritic spines of excitatory neurons in the cortex and hippocampus (Thorsell et al. 2010). Immunoprecipitation combined with Western blotting (IP-WB) performed to evaluate CSF Ng showed a marked increase in AD as compared with controls, implying the synaptic loss. This result was confirmed other studies using ELISA (Hellwig et al. 2015; Kvartsberg, Duits, et al. 2015; Kvartsberg, Portelius, et al. 2015). Longitudinal analysis also found that CSF Ng is strong correlated with CSF Tau but not Aβ42 levels (Portelius et al. 2015). Furthermore, this alteration is absent in other neurodegenerative diseases, augmenting its specificity as a biomarker for

AD (Wellington et al. 2016). In recent years, research efforts led to discovery of a series of novel CSF biomarkers, including neuronal calcium sensor VILIP-1 (Tarawneh et al. 2011), pro nerve growth factor (proNGF) (E. Counts et al. 2016), and proinflammatory chitinase YKL-40 (Craig-Schapiro et al. 2010). In addition to the potential clinical utility, the growing list of CSF biomarkers for AD also explicates the molecular changes involved in the pathogenesis, such as synaptic depression, cell survival, inflammation, etc.

1.2.7.2 Neuroimaging Biomarkers

In parallel with core CSF biomarkers, another reliable gold standard is molecular neuroimaging biomarkers (Laske et al. 2015). The development of radioactive tracers in conjunction with positron emission tomography (PET) largely benefit the clinical diagnostics of AD. Currently, there are three major groups of radioligands targeting plaques (amyloid PET), tangles (Tau PET), and neuronal dysfunction (fluorodeoxyglucose (FDG)-PET). Among them, amyloid PET yielded comparable diagnostic performance as the core CSF biomarkers (Palmqvist et al. 2015), while FDG-PET is correlated strongly with cognitive performance (Furst et al. 2012).

As the most widely used amyloid imaging agent, Pittsburgh compound B (PiB; [C-11]6-OH-BTA-1; [N-methyl-11C]2-(4’-methylaminophenyl)-6-hydroxybenzothiazole) can effectively differentiate AD from normal controls by PET (Klunk et al. 2004; Rowe et al. 2010). PiB has a high binding affinity to amyloid aggregates with β-sheet conformation so it assists in visualizing the location and density of plaque deposits in cortical regions (Levine 1995). It penetrates brain efficiently and clears fast, allowing for its application in primary care with PET (Mathis et al. 2003). Whereas PiB-PET has a strong concordance with CSF Aβ42 level, it doesn’t correlate with CSF Tau level (Fagan et al. 2006). Several longitudinal

studies reported that PiB positive subjects have a higher chance of converting to AD (Forsberg et al. 2008; Koivunen et al. 2011), augmenting its application in predicting MCI cases who will progress to dementia. However, it has been well established that ~20% AD patients are PiB negative while ~30% normal controls are PiB positive (Mintun et al. 2006; Mormino et al. 2012; Rowe et al. 2010). In any case, there is a likelihood for misdiagnosis (Mcdaniel, Lukovits, and Mcdaniel 1993).

To resolve the issue with the short radioactive half-life (~20 min) of PiB, a longer-lived PET tracer, fluorine-18 labeled [F-18] flutemetamol, has been developed to enhance the distribution in brain parenchyma (Landau et al. 2014). A multicenter phase II trial of [F-18] flutemetamol involving a mixed cohort of normal controls, MCI, and early AD subjects reported 93.1% sensitivity and 93.3% specificity (Vandenberghe et al. 2010). Analogs, like [F-18] florbetapir and [F-18] florbetaben, have been developed and demonstrated with high sensitivity and specificity (Barthel et al. 2011; Camus et al. 2012).

A range of Tau-selective PET radioactive tracers are emerging, including F-18]-labeled THK compounds (Harada et al. 2013); PBB compounds (Hashimoto et al. 2014); and [F-18]-labeled T807 and T808 compounds (Chien et al. 2013, 2014). However, off-target binding was noticed probably due to the heterogeneity of Tau isoform and phosphorylation in NFTs (Marquié et al. 2015). Therefore, more rigorous characterization and validation are required to claim its clinical utility (Villemagne 2016).

With respect to limitations with neuroimaging for AD, the sensitivity of PiB-PET has not been well characterized. Also, it remains to be defined what is the baseline for plaque and tangle burdens in normal controls and MCI cases, and how it should be tied to cognitive tests and CSF biomarkers (Counts et al. 2017).

1.2.7.3 Plasma Biomarkers

The plasma counterparts of core CSF biomarkers fail to exhibit comparable sensitivity and specificity in AD (Counts et al. 2017). Unlike CSF Aβ42, plasma Aβ42 level varies dramatically from study to study. Analysis of plasma Aβ42 level from more than 2,000 AD patients and 4,000 controls showed an increase, no change or a decrease in 27 different studies (Olsson et al. 2016). Meanwhile, no correlation was found in plasma and CSF Aβ42 titers (Hansson et al. 2010). This frustrating result may be attributed to the peripheral expression of APP, which interferes with the measurement of CNS-derived Aβ42 (Zetterberg 2019). A series of ultrasensitive assays, such as digital ELISA and immunoprecipitation coupled to mass spectrometry (IP-MS) (Ovod et al. 2017; Zetterberg et al. 2011), were used to assess Aβ in plasma to minimize the matrix interferences. These assays revealed a reduced plasma Aβ42/Aβ40 ratio in AD, which has a very high concordance with amyloid PET to predict the plaque deposition in a similar manner to CSF Aβ42/Aβ40 ratio, although with a weaker separation (Janelidze et al. 2016; Nakamura et al. 2018). However, meta-analysis revealed that plasma Aβ42 and Aβ40 concentrations are not associated with AD, thus they are not ideal analytes to use in clinical practice (Olsson et al. 2016).

In general, a major challenge of developing a screening tool with blood-based biomarkers resides in extremely low concentration of CNS-derived proteins in blood (Blennow 2017; Zetterberg 2019). Aβ is relatively abundant in CSF at a concentration of 10-20 ng/mL while its level is much lower in plasma (Golde et al. 1992; Haass et al. 1992; Seubert et al. 1992). A 100-fold difference was observed for Tau concentration in CSF (~2–300 pg/mL) versus plasma (~5 pg/mL) (Blennow et al. 1993; Zetterberg et al. 2013). Ultrasensitive detection methods, such as immuno-magnetic reduction (IMR) and single-molecule array (Simoa), are thus

required to measure the plasma level of proteins (Andreasson, Blennow, and Zetterberg 2016). An increase in plasma levels of tTau and pTau in AD patients has been consistently detected by both IMR and Simoa as well as by a recently developed electro-chemiluminescence (ECL) assay (Mielke et al. 2018; Tzen et al. 2014; Zetterberg et al. 2013). Similar to the situation of Aβ42, CSF and plasma Tau levels are poorly correlated (Mattsson et al. 2016), which is likely due to the peripheral expression in kidney and salivary glands and the varied stability in different biological fluids (Zetterberg 2019). Tau is stable in CSF for weeks but has a very short (~10 h) half-life in blood (Randall et al. 2013; Sato et al. 2018), which may undergo proteolytic degradation by various proteases in plasma (Yoshimura et al. 2008). This instability imposes a concern about the performance consistency of the blood-based biomarkers.

Many recent studies reported plasma NfL as a promising biomarker for blood test of AD (Lewczuk et al. 2018; Preische et al. 2019). A significant increase in plasma NfL was detected using Simoa in AD patients at both MCI and dementia stages (Mattsson et al. 2017), with a similar diagnostic accuracy to the core CSF biomarkers. At the cutoff value of 25.7 pg/mL, sensitivity, specificity, and accuracy of plasma NfL were 84%, 78%, and 82%, respectively (Lewczuk et al. 2018). Plasma and CSF NfL concentrations were strongly correlated in AD patients with a correlation coefficient of 0.75-0.97 (Gisslén et al. 2016; Zetterberg 2016). Just like CSF NfL, plasma NfL is not specific to AD and is present in most neurodegenerative diseases (Khalil et al. 2018). Nevertheless, it correlates well with cognitive disturbances and future brain atrophy, and thus could be used as a robust blood-based biomarker to reliably reflect the degree of neurodegeneration in AD and other dementia (Mattsson et al. 2017).

Several protein classifying panels have been reported as promising novel biomarkers using proteomic approaches. A multianalyte profiling of serum samples from over 500 AD patients and normal controls in two cohorts developed a biomarker panel consisted of 11 proteins that yielded a classification accuracy of 88% (O'Bryant et al. 2011). In another study, 120 signaling and inflammatory proteins in plasma were profiled by multivariate analysis (Ray et al. 2007), resulting in the identification of an 18-protein classifier that was able to distinguish AD dementia or MCI from controls with an accuracy of 89%. A recent study also reported a biomarker panel containing 18 proteins that identified AD patients with a sensitivity and specificity of 85% and 93%, respectively (Doecke et al. 2012). Some novel plasma biomarkers prove their effectiveness in detection of AD in early stages. Serum screening by capillary liquid chromatography-electrospray ionization-tandem mass spectroscopy (LC-ESI-MS) identified 59 potential biomarkers and 4 of them were validated to be able to separate controls from AD at very early stage with a 78% sensitivity at 80% specificity (Shah, Rohlfing, and Johnson 2016). Using SOMAscan platform, abundance of 1129 plasma proteins in AD patient and control blood samples were analyzed, and 5 proteins (S100A9, CD84, CD226, AIF1, and ESAM) were identified as an algorithm showing 90% sensitivity and 84% specificity in discovery study that discriminated AD from controls, and 97% sensitivity and 80% specificity in validation study that discriminated MCI from controls (Disease 2015). Finally, an unbiased mass spectrometric lipidomics approach was used to discover a plasma phospholipid panel of 10 lipids from peripheral blood that predicted the progression of cognitively normal elderly subjects to MCI or AD with > 90% accuracy (Mapstone et al. 2014). Despite these advancements in novel plasma biomarkers, none has been ready for clinical implementation concerning the variability and reproducibility due to a lack of

standardization in sample processing and analytical methods (Counts et al. 2017; Laske et al. 2015).

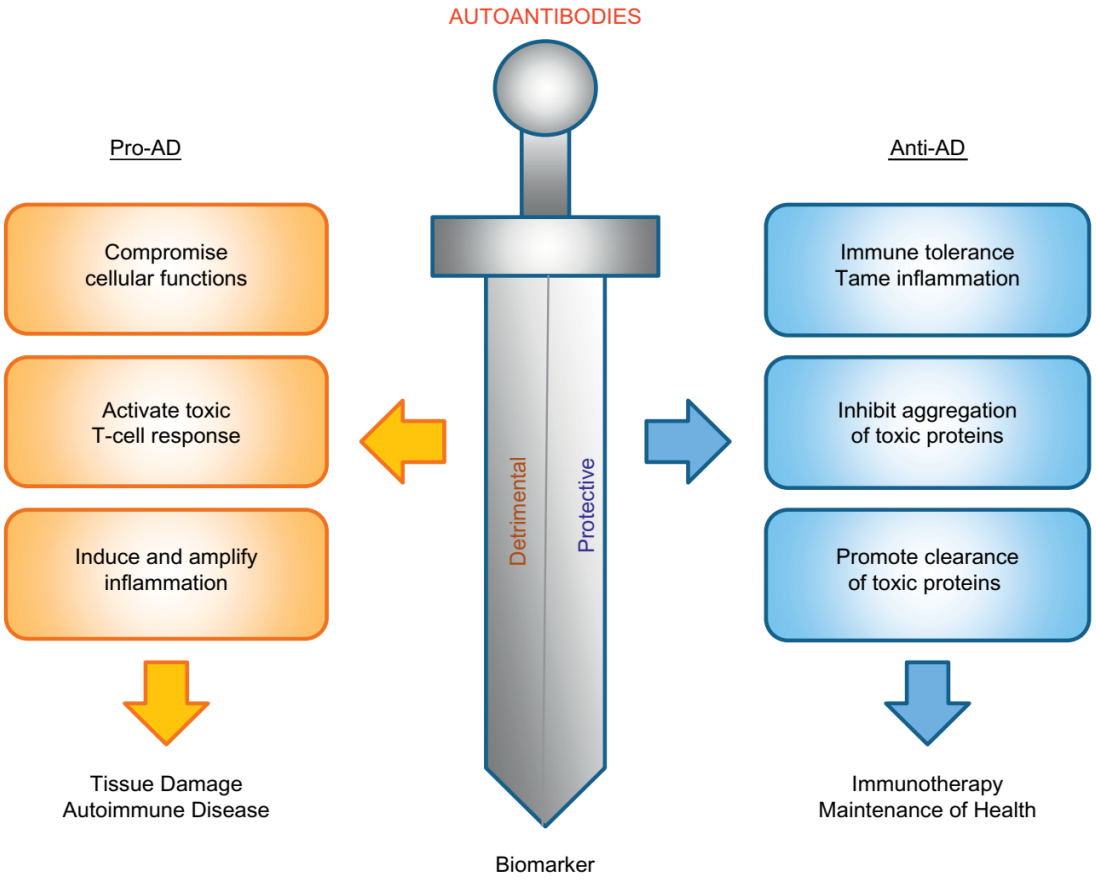

Figure 1-7. The binary role of AAbs in AD and the relevant molecular mechanism in which they are involved in. Figure adapted from Wu and Li 2016.

1.2.8 Identification of Autoantibodies (AAbs) for AD

The identification of AD-specific AAbs may not only benefit early accurate diagnosis but also shed light on AD pathogenesis. The identities of the antigens that have elicited AAbs may benefit the design of effective immunotherapies for AD. AAbs correlated with cognitive function or disease stages may also help stratify AD patients.

1.2.8.1 Known AD-Associated AAbs

Under physiological conditions, AAbs in IgM isotype with a moderate affinity are produced by B cells to recognize and clear the dead cellular components (Elkon and Silverman 2012). In case of breakdown of immune intolerance, AAbs in IgG isotype are produced to target self-proteins with a high affinity, which may eventually cause tissue injuries. Natural AAbs are abundant and ubiquitous in human sera and a subset of them is also present in CSF (Nagele et al. 2013). The AAb profiles in individuals is largely influenced by age, gender, disease conditions, etc. (Nagele et al. 2013). Given that AAbs directed against various neuronal proteins are reported detectable in AD patients by numerous studies, their potential as a diagnostic biomarker has been investigated by the AD research community (Jack et al. 2013). Some AAbs emerged as promising predictors of AD but the diversity in nature of these autoantigens renders ambiguity to their exact role in pathological process (Figure 1-7) (Colasanti et al. 2010; Wu and Li 2016).

While naturally occurring anti-Aβ antibody is present in both serum and CSF of AD patients as well as controls (Britschgi et al. 2009; Szabo, Relkin, and Weksler 2008), there are contradictory measurements of its level (Swamy-Mruthinti et al. 2004), which are presumably caused by discrepancy in unbound and bound forms of anti-Aβ antibody in the circulation. The titers of Aβ-IgG immune complexes measured by an improved ELISA assay were found to significantly increase in serum and CSF of AD patients whereas the levels of unbound anti-Aβ antibody measured by ELISA and dot blotting were significantly reduced in serum of AD patients compared with healthy controls (Gustaw et al. 2008; Maftei et al. 2013; Qu et al. 2014). Due to the variable measurements, neither the presence nor the levels of anti-Aβ antibody is correlated with the severity of AD (Klaver et al. 2011). It is reported that anti-Aβ antibody may be effective in removal of amyloid plaques through Ig-catalyzed

hydrolysis (Jack et al. 2010), therefore exerting a neuroprotective role. In contrast to Aβ, Tau is a very poor autoantigen as anti-Tau antibody is much less prevalent in neurodegenerative diseases (Terryberry, Thor, and Peter 1998). Using ELISA assay, anti-Tau antibody was found significantly elevated in patients with AD as well as multiple sclerosis (MS), which casts doubt on its value as a specific biomarker for AD (Bartos et al. 2012; Fialová et al. 2011).

AAbs against glial markers, including S100b, glial fibrillary acidic protein (GFAP), and microglia, measured by ELISA showed an elevated level in serum or CSF of AD patients (Dahlström et al. 1994; Gruden et al. 2007; Tanaka et al. 1989), suggesting a possible immune response to glial activation. These glial-derived proteins play a pivotal role in neuronal development and survival (Steiner and Schroeter 2011). Another study using ELISA measured the titers of AAb targeting cyclic citrullinated peptides (CCP), which accumulates in astrocytes, and found that it was positive in 71% AD patients and 2.4% controls (Satoh et al. 2010). It was shown that these glial-specific AAbs are associated with dysfunction of BBB and leakage of peripheral immune cells to CNS (Mecocci et al. 1995). However, it is questionable if the production of AAbs are resulted from age-related withering of BBB instead of being AD-specific pathological events (Mecocci et al. 1995).

Some microvasculature-related molecules were also identified as autoantigens in AD. Screening of serum samples against a human microvascular endothelial cell cDNA library revealed the presence of AAb against rabaptin 5 (RABPT5) (Delunardo et al. 2007), a cellular vesicle trafficking protein, in 65% AD patients but not in healthy controls. A 3-fold increase in the affinity purified human IgG from plasma reactive to the receptor for advanced glycation end products (RAGE) (Mruthinti et al. 2004), known to regulate Aβ transport across BBB, was noted in AD compared to age-matched controls (Deane et al. 2003). In a longitudinal study, ELISA was used

to measure the serum concentration of AAb against angiotensin 2 type 1 receptor (AT1R), a regulator of blood pressure and volume, and found that the AAb level is significantly increased in AD than in healthy controls (10.2 U/mL versus 8.1 U/mL, $p = 0.04$), and is associated with levels of tTau and pTau in CSF (Giil et al. 2015).

AAbs binding to cellular enzymes, such as adenosine triphosphate synthase β subunit (ATP5B) and aldolase which mediates glycolysis, were also differentially represented in AD patients versus controls. Immunoblotting of rat brain tissue lysates against human sera IgGs identified the positivity of anti-aldolase antibody in > 50% AD patients, 4% healthy controls, and 10% MS patients (Mor, Izak, and Cohen 2005). A later study identified ATP5B as a new autoantigen by the bidimensional gel electrophoresis (2DE) coupled with immunoproteomic approach using mouse brain proteins. Serum anti-ATP synthase antibody was present in 38% AD patients but not in aged-matched controls or patients with PD or atherosclerosis (Vacirca et al. 2012). Further analytical cytology studies, using SH-SY5Y neuroblastoma cell line, showed that anti-ATP synthase antibody could exert a pathogenic role by inhibiting of ATP synthesis and inducing cell apoptosis.

Although many AD-associated AAbs have been identified, their clinical utility as diagnostic biomarkers awaits further evaluation. Current issues with these known AAbs include 1) certain degree of overlap between different diagnostic groups (Mecocci et al. 1995), 2) a lack of sufficient or consistent diagnostic performance to meet clinical criteria (Schott et al. 1996), 3) little relationship between AAb titers and disease severity (Mitchell et al. 2010), and 4) small sample size used in studies (Rosenmann et al. 2006). Due to these drawbacks, their usefulness as a sensitive and specific indicator of AD has been limited for diagnostic purpose (Wu and Li 2016).

1.2.8.2 Methods for Identifying Novel AAbs

1.2.8.2.1 Target-Directed Assays

ELISA has been used as the most common technique to measure the abovementioned fluid biomarkers for AD. It is regarded as a gold standard assay since standardized materials and procedures have been established to resolve the variations in measurements between clinical laboratories (Mattsson et al. 2011), including an assay for measuring total Tau (Kuhlmann et al. 2017; Vanmechelen et al. 2000), pTau (N Andreasen et al. 1999), and Aβ42 (Olsson et al. 2016). Alternatively, immunoblotting technologies, such as dot blotting and Western blotting, are often used to probe the target proteins or antibodies in clinical samples. Nonetheless, prior knowledge of candidate biomarkers and AD pathogenesis is required to use these target-directed assays, limiting the efficiency of identifying potential biomarkers (Qu et al. 2014).

1.2.8.2.2 Immunoproteomic Approach

Given the heterogeneity of AD, it is plausible that a useful test for AD will demand a panel of proteins, rather than a single protein, contributing together towards a diagnostic tool (Counts et al. 2017; Jack et al. 2011). Proteomics technology is ideally suited to the discovery of novel disease-related AAbs for such a diagnostic set. Using immunoproteomic approach several studies have successfully identified a series of new AD-associated AAbs (Mor et al. 2005; Vacirca et al. 2012). Basically, mouse brain tissue homogenates were subjected to polyacrylamide gel electrophoresis (PAGE) for protein separation. Then sera or CSF from AD patients were screened against proteins in tissue homogenates by Western blotting. Coomassie blue-stained bands corresponding to the counterparts identified by Western blotting were recovered from the PAGE gels and analyzed with the matrix-assisted laser desorption/ionization-time of flight (MALDI-TOF) mass spectrometry

(MS) to determine the identity of immunoreactive proteins based on AA sequences of detected peptides. To confirm that human IgGs in serum and CSF bind to putative autoantigens, purified proteins were produced and challenged by sera or CSF from AD patients by immunoblotting or ELISA for quantitative analysis. Although this immunoprofiling approach has greatly expanded the searching scope to proteomic level, it engages labor-intensive sample preparation and protein purification. Also, the use of 2DE Western blotting against tissue lysates suffers from low resolution, interference from high abundant proteins, and incompatibility with membrane proteins.

The emergence of protein, peptide, and peptoid arrays has held the promise to provide a comprehensive representation of antibody repertoire in AD patients relative to ND controls. Reddy et al. screened a combinatorial library of approximately 15,000 unnatural synthetic molecules called peptoids (oligomers of N-substituted glycines) against sera from AD cases and controls for ligands that could capture AD-specific antibodies (Reddy et al. 2011). Three peptoids were identified that best distinguished the patients with AD from the controls with specificities ranging from 93.7% to 100% at a sensitivity of 93.7%. Using synthetic random peptide arrays of 10,000 20-mers, Restrepo et al. profiled serological AAbs and showed that dementia patients had distinguishable immunoprofiles compared to age-matched ND subjects (Restrepo et al. 2011; Restrepo, Stafford, and Johnston 2013). However, there was no confirmation of informative peptides using the discovery samples on an orthogonal platform, not to mention a validation. The use of synthetic peptoid or peptide arrays revealed the likelihood of immune differences between cases and controls, but it suffers from not only low coverage of search space but also the difficulty in interpreting the eliciting antigens. For example, immunosignatures

showed strong reactivity to many peptides even for commercial anti-Aβ antibody on synthetic peptide arrays (Restrepo et al. 2011).

One advantage of protein arrays is that each spot on the array displays a known and defined protein so that immune responses can be immediately tied back to known proteins and the underlying biology. Using conventional protein microarrays containing thousands of unique human antigens probed with sera from AD patients and healthy controls, Nagele et al. found a panel of 10 AAb biomarkers that can effectively classify AD cases and controls with a 96.0% sensitivity and 92.5% specificity (Nagele et al. 2011). Five biomarkers from this panel were also able to collaboratively differentiate AD from PD and breast cancer patients with a 90.0% sensitivity and 79.3% specificity. However, the validation based on dot blotting assay was low-throughput and semi-quantitative (Nagele et al. 2011). Also, autoantigens identified in the panel are proteins that have not been well characterized and their biological significance in AD remains vague (Wu and Li 2016). DeMarshall et al. performed immunoprofiling using human protein microarrays and identified a panel of 50 AAb biomarkers that could detect AD at MCI stage with 100% sensitivity and 100% specificity (DeMarshall et al. 2016). However, the validation of this work lacks stringency in that it relied on pure computational analysis rather than an independent immunoassay.

1.2.8.2.3 Nucleic Acid Programmable Protein Array (NAPPA)

The high-throughput proteomic-level AAb discovery platform built on the Nucleic Acid Programmable Protein Array (NAPPA) has very good potential to contribute towards the diagnosis and pathogenesis of AD. NAPPA entails programming cell-free protein expression extracts from HeLa cells with cDNAs to express the proteins *in situ* at the time of the assay without the need for labor-intensive and time-consuming protein purification (Grover et al. 2004). The cDNAs

encoding the full-length human proteins with an appended capture tag are printed at each feature of the array instead of printing protein (Figure 1-8). The DNA purification is more reliable and easier to control quality and is more time- and cost-effective than protein purification, which is inevitable in fabrication of conventional protein arrays. At the time of immunoprofiling against clinical samples, proteins are expressed from the cDNAs by a cell-free *in vitro* transcription and translation (IVTT) system and immobilized *in situ* by the anti-tag antibody co-printed on arrays (Figure 1-8). Producing proteins "just-in-time" for the assay abrogates concerns about protein stability during storage because the proteins are "fresh" for each assay.

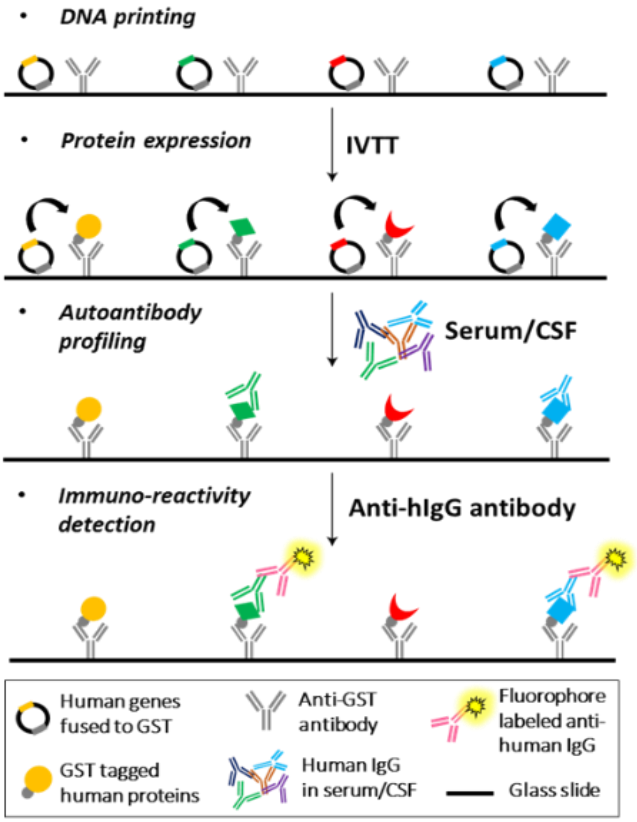

Figure 1-8. NAPPA diagram. Plasmids encoding GST tagged human proteins are co-printed with anti-GST antibody onto chemically modified glass slides. Proteins are expressed by cell-free IVTT system and subsequently immobilized in situ on arrays by anti-GST antibody. Serum or CSF samples are applied to challenge the displayed proteins. AAbs recognize and bind to antigens. Fluorophore-conjugated anti-human IgG is applied to detect any existent antigen-antibody responses.

One of the major advantages about NAPPA is that mammalian proteins are expressed in human milieu with an advanced protein translation machinery and chaperone proteins prepared from HeLa cells. This chemistry allows for the identification of conformational epitopes in that it increases the expression efficiency and protein integrity by encouraging natural folding. The success rate in displaying sequence-verified full-length proteins exceeds 95%, regardless of protein class or size. Furthermore, thousands of unique proteins are displayed on NAPPA at remarkably consistent levels. The yield of more than 93% of proteins are within two-fold of the average. As in all protein interactions, antibody-antigen binding is concentration dependent, making it difficult to interpret the array data when there are large variations in the amount of spotted proteins, as often occurs in conventional protein arrays due to the largely varied protein purification yields. This leaves a question that whether a spot with low immunoreactivity is a consequence of the little amount of antigen displayed on arrays or the low titer of AAb in clinical samples. Therefore, the consistent and reproducible display of proteins is crucial to array fabrication.

NAPPA circumvents many limitations of conventional protein arrays and has been extensively employed for AAb discovery in various cancers and autoimmune diseases (Bian et al. 2017; Grover et al. 2004; Wang et al. 2016, 2017). In addition to immunoprofiling, NAPPA also has successfully demonstrated a wide range of applications in identification of post-translationally modified autoantigens (Karthikeyan et al. 2016; Yu et al. 2014), humoral immune responses to infectious agents (Wagner R Montor et al. 2009), as well as protein-DNA and protein-protein interactions (Tang et al. 2017). All in all, this array-based "auto-antibodyomic"

technology that can provide an unbiased data-driven discovery of potential AAb biomarkers and show great promise as a diagnostic tool for AD.

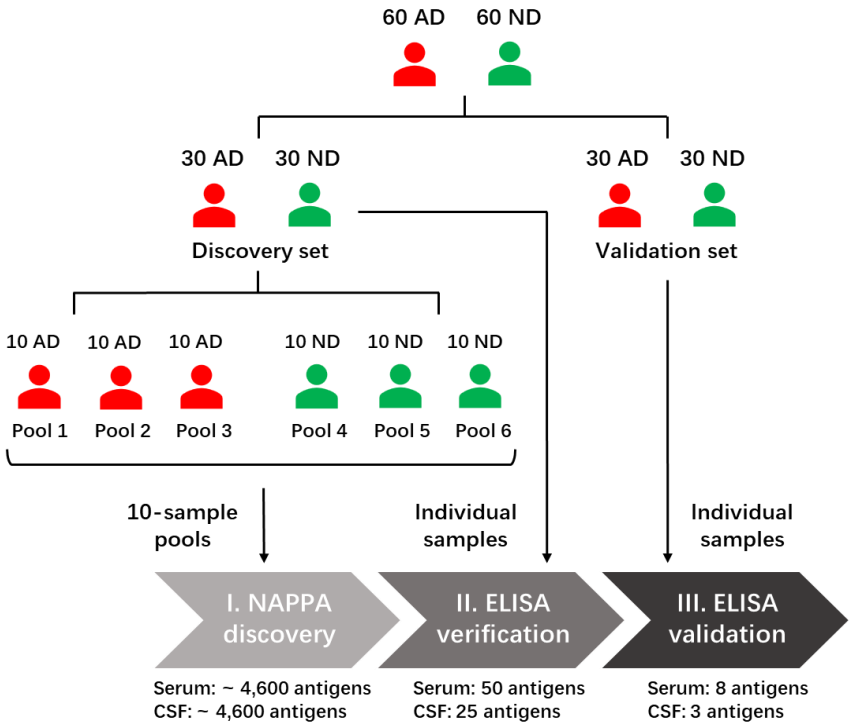

Figure 1-9. Study design. **I)** Discovery: 6 serum pools and 6 CSF pools from discovery sample set were screened against ~4,600 human proteins displayed on NAPPA arrays; **II)** Verification: 50 serum AAbs and 22 CSF AAbs were verified using individual samples from discovery sample set by RAPID-ELISA; **III)** Validation: 8 serum AAbs and 3 CSF AAbs were verified using individual samples from validation sample set by RAPID-ELISA.

1.3 Methods and Materials

1.3.1 Biological Samples

Paired serum and CSF samples from 60 AD patients and 60 ND controls were collected with written informed consent under the guidelines of the Institutional Review Boards (IRBs) at the Banner Health. The AD patients were neuropathologically diagnosed with a minimum of intermediate or high NIA-Reagan criteria. The ND controls had no dementia, Parkinsonism during life, or a major neuropathological diagnosis. Characteristics of study subjects were presented as

mean, range, and percentage in Table 1-1. All samples were collected within a short post-mortem delay interval of 3 hr on average. The blood was drawn postmortem by transthoracic puncture of the heart, and after clotting and centrifugation the serum aliquots were frozen at -80 °C. The CSF was drawn postmortem by puncture of the lateral ventricles while the brain was still in-situ, after removal of the skullcap, and the aliquots were frozen at -80 °C after centrifugation. The study samples were evenly split into two sets, i.e. the discovery and the validation set, with 30 AD and 30 ND in each (Figure 1-9). Every 10 random AD or ND samples from the discovery set were pooled and a total 12 sample pools (3 serum case pools, 3 serum control pools, 3 CSF case pools, and 3 CSF control pools) were prepared and used for NAPPA screening.

Brain tissue samples from the middle temporal gyrus (MTG) region of 23 AD patients and 41 ND controls were obtained from the ASU-Banner Neurodegenerative Disease Research Center (NDRC). All donors were from the same study set for serum/CSF samples. Tissues were frozen at autopsy and stored at -80 °C until use. Semi-quantitative Western blotting assays were performed to measure the protein expression level of STMN4 in MTG tissue lysates.

Table 1-1. Demographics of subjects.

Characteristics	Discovery set		Validation set	
	AD	**ND**	**AD**	**ND**
Number of subjects	30	30	30	30
Expired age (mean, range), y	80 (60-96)	85 (65-97)	81 (67-92)	85 (53-99)
Gender (male/%)	13 (43%)	18 (60%)	17 (57%)	20 (67%)
Brain weight (mean, range), g	1076 (875-1338)	1195 (934-1420)	1086 (750-1388)	1206 (975-1456)
Senile plaque density (0, A, B, C, NA)	0, 0, 1, 28, 1	10, 9, 11, 0, 0	0, 0, 2, 28, 0	12, 11, 7, 0, 0
NFT density (mean, range)	13.9 (10.5-15.0)	3.4 (1.0-6.5)	14.0 (8.8-15.0)	3.3 (0.8-6.5)
Braak stage (0, I, II, III, IV, V, VI)	0, 0, 0, 0, 0, 15, 15	0, 3, 11, 16, 0, 0, 0	0, 0, 0, 0, 0, 17, 13	0, 6, 5, 19, 0, 0, 0
MMSE (mean, range)	13 (0-28)	28 (25-30)	12 (0-26)	28 (23-30)
ApoE (2/2, 2/3, 2/4, 3/3, 3/4, 4/4, NA)	0, 0, 2, 8, 13, 5, 2,	2, 6, 0, 16, 5, 0, 1,	0, 1, 0, 10, 18, 1, 0	1, 6, 0, 17, 6, 0, 0

AD, Alzheimer's disease patients. ND, non-dementia controls. Senile plaque density: 0, none; A, sparse; B, moderate; C, frequent; NA, not available. NFT, neurofibrillary tangle. MMSE, Mini-Mental State Examination. ApoE, apolipoprotein E genotype.

Free-floating sections (40 μm) of paraformaldehyde-fixed hippocampal tissues from 4 AD patients and 4 ND controls were obtained from the ASU-Banner NDRC. All donors are from a separate study set and matched for age, gender, and post-mortem interval (PMI). Sections were stored in cryoprotectant at -20 °C until use. Immunohistochemistry (IHC) staining assays were performed to measure the protein expression level of STMN4 in individual CA1 neurons.

1.3.2 NAPPA Array Production and Quality Assessment

Open reading frames that encode human proteins used in this study were obtained from DNASU Plasmid Repository (http://dnasu.asu.edu/DNASU/) (Wiemann et al. 2016). NAPPA arrays were produced and controlled for the quality of DNA printing and protein displaying as previously described (Miersch and LaBaer 2011; Qiu and Labaer 2011; Sibani and LaBaer 2011). Briefly, plasmid DNAs that support *in vitro* expression of proteins with a C-terminal glutathione S-transferase (GST) fusion tag were spotted on modified glass slides (Figure 1-8). Upon screening, proteins were expressed using a HeLa cell lysate-based IVTT protein expression system. The GST-tagged proteins were then captured *in situ* by the anti-GST antibodies co-printed on arrays and displayed for subsequent AAb profiling. The correlation of protein expression between slides was compared to assess the reproducibility of array production.

1.3.3 Autoantibody Profiling on NAPPA

AAb profiling on NAPPA was performed as previously described (Figure 1-8) (Anderson et al. 2011; Bian et al. 2017; Miersch et al. 2013; Wang et al. 2016, 2017). Briefly, NAPPA arrays were blocked with the SuperBlock Buffer (Thermo Fisher Scientific, Waltham, MA) at room temperature (RT) for 1 hr with gentle shaking, and then rinsed with deionized (DI) water and dried by centrifugation. Arrays were sealed with the HybriWell hybridization sealing gaskets (Grace Bio-

Laboratories, Bend, OR), and 150 µL of IVTT (Thermo Fisher Scientific, Rockford, IL) was slowly injected over the arrays, followed by 3 hr incubation at 30 °C for protein expression and then 30 min incubation at 15 °C for protein *in situ* immobilization. Expressed arrays were washed with PBST (137 mM NaCl, 2.7 mM KCl, 10 mM Na2HPO4, 1.8 mM KH2PO4 pH 7.4, 0.2% (v/v) Tween-20) three times, then rinsed with DI water and dried. Arrays were loaded onto the HS 4800 Pro Hybridization Station (Tecan, Männedorf, Switzerland) and programmed with 1 hr blocking with 5% (w/v) milk-PBST at RT, 15 hr incubation with 150 µL of 1:30 diluted serum pool or 1:2 diluted CSF pool at 4 °C, followed by 1 hr incubation with 150 µL of 1:500 diluted Alexa Fluor 647 goat anti-human IgG (Jackson ImmunoResearch Laboratories, West Grove, PA) at RT. Finally, arrays were rinsed, dried, and then scanned with the Tecan PowerScanner (Tecan, Männedorf, Switzerland) under consistent settings.

1.3.4 Array Image Analysis

The scanned array images were examined using the ArrayPro Analyzer (Media Cybernetics Inc., Rockville, MD). Strong immuno-reactivity of AAbs from samples resulted in a saturated signal with diffusion around the local spot of antigens, the presence of which was defined as a ring (Figure 1-13). To capture real antibody responses that cannot be quantified by the image analysis software, all images were qualitatively examined to identify and confirm positive responses as previously described (Bian et al. 2017; Wang et al. 2016, 2017). Briefly, raw images were adjusted to extreme contrast and brightness, and each spot was graded at a scale of 0 to 5 based on the ring intensity and morphologic features. Any protein spots that exhibited a ring score of 1 or above was considered as a positive antibody response. Differences in ring counts and scores between AD and ND were used for selecting antibody candidates in both serum and CSF (Figure 1-10). Specifically, antibodies

were selected for verification when they met either of the following criteria: 1) to assure AAb prevalence across cases, their ring counts of AD minus ND is greater than or equal to 1, and 2) to assure AAb titer in samples, their ring score is greater than the arbitrary cutoffs set for each sample pool. Any uninformative antigens that showed no response or no appreciable difference in response were eliminated to facilitate the following stages.

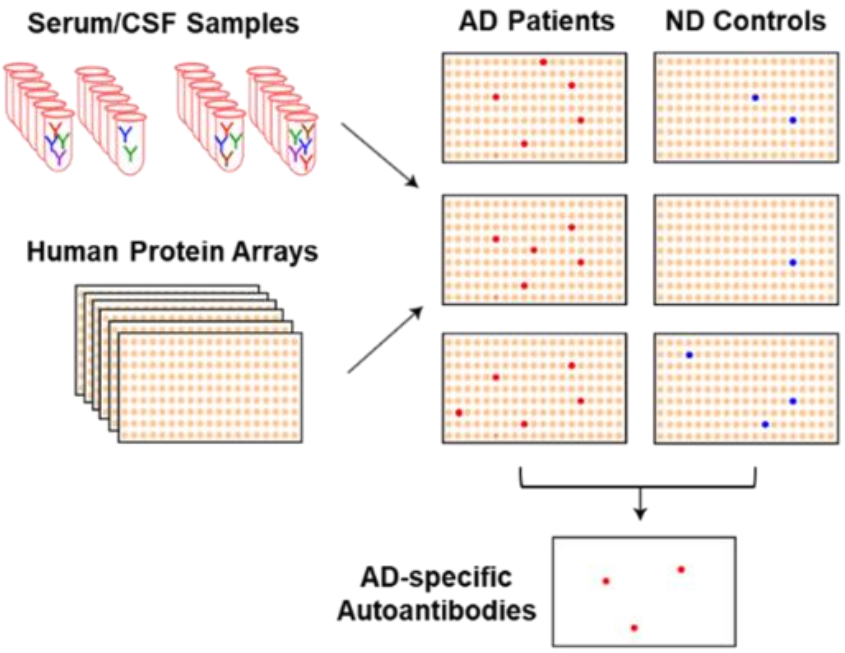

Figure 1-10. Workflow of screening for AD-specific AAbs. Paired serum or CSF samples from AD patients and ND controls were used to profile immunoreactivity of proteins displayed on NAPPA arrays. A comparison of "lighting-up" proteins between cases and controls led to the identification of AD-specific AAbs.

1.3.5 Rapid Antigenic Protein *In Situ* Display (RAPID)-ELISA

The Rapid Antigenic Protein In Situ Display (RAPID)-ELISA established in our lab is a robust, versatile and reliable immunoassay that has been widely used in AAb biomarker discovery studies (Bian et al. 2017; Karthikeyan et al. 2016; Wang et al. 2016, 2017). It works with the cell-free expression system, enabling the assessment of freshly produced proteins with no need for purification (Figure 1-11). The plate-

based detection allows us to assay a small number of protein targets against a large set of clinical samples. Here, the same plasmids printed on NAPPA arrays can be directly used for ELISA without further configuration. ELISA assays were performed to assess the immunoreactivity of selected autoantigen candidates as previously described (Bian et al. 2017; Wang et al. 2016, 2017). Briefly, 96-well High-Bind clear plates (Corning Life Sciences, Salt Lake City, UT) were coated with 50 µL of 10 µg/mL goat anti-GST antibody (GE Healthcare, Chicago, IL) in coating buffer (500 mM carbonate bicarbonate pH 9.6) overnight at 4 °C. All high-throughput liquid handlings were performed using the BioMek NxP Laboratory Automation Workstation (Beckman Coulter, Cincinnati, OH). On the next day, coated plates were washed five times with 100 µL of PBST and blocked with 100 µL of 5% milk-PBST for 1.5 hr at RT. Meanwhile, 200 ng/µL plasmid DNAs encoding GST-tagged autoantigens were incubated with IVTT for 1.5 hr at 30 °C for protein expression. Then 50 µL of 1:50 diluted protein was added to each well and incubated for 2 hr at RT on a shaker. Plates displaying autoantigens were washed and incubated with 50 µL of 1:300 diluted serum for 1 hr at RT on a shaker. Again, plates were washed and incubated with 50 µL of 1:10,000 diluted horseradish peroxidase (HRP)-conjugated goat anti-human IgG (Jackson ImmunoResearch Laboratories, West Grove, PA) for 1 hr at RT on a shaker. Finally, plates were washed and incubated with 50 µL of tetramethylbenzidine (TMB) substrate (Thermo Fisher Scientific, Waltham, MA) for 15 min at RT for colorimetric signal development, followed by 50 µL of 2 M sulfuric acid to quench reaction. Optical density at 450 nm (OD450) was measured immediately using the Envision Multilabel Reader (PerkinElmer, Waltham, MA).

Because the AAb concentration in CSF is much lower than that in serum, the chemiluminescent-based RAPID-ELISA assays were performed with 1:40 diluted CSF samples for higher detection sensitivity and larger dynamic range. Instead of using TMB substrate, SuperSignal ELISA Femto Substrate (Thermo Fisher Scientific, Waltham, MA) was applied to the secondary antibody and the chemiluminescent signal was immediately measured using the Envision Multilabel Reader.

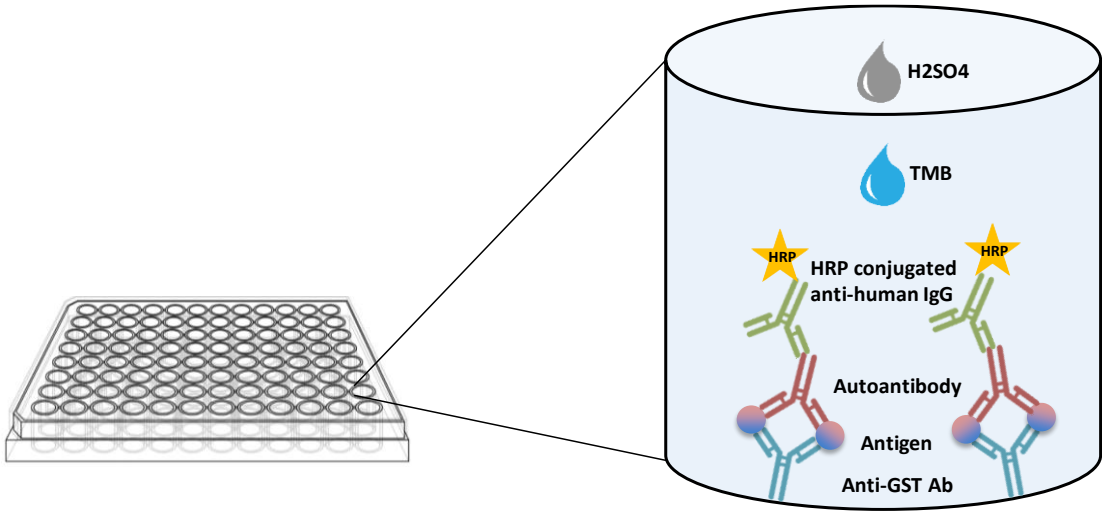

Figure 1-11. RAPID-ELISA diagram. Antigens fused to GST tag are in vitro expressed using cell-free IVTT system and captured to 96-well plate coated with anti-GST antibody. AAbs in sera or CSF recognize and bind to their antigen targets displayed in wells. HRP-conjugated anti-human IgG followed by TMB and H2SO4 are added to detect the immunoreactivity in each well.

1.3.6 Semi-quantitative Western Blotting

Two-color near-infrared fluorescence detection system was adopted for Western blotting to avoid the variations across blots as well as the errors introduced from stripping and reprobing. Briefly, 25 mg of frozen brain tissue from MTG region was homogenized on ice using an ultrasonic processor in 150 µL of protein solubilization buffer (20 mM Tris pH 7.5, 0.5% (v/v) octylphenoxy polyethoxyethanol (IGEPAL CA-630), 1 mM ethylenediaminetetraacetic acid (EDTA), 100 mM NaCl, 1

mM phenylmethylsulfonyl fluoride (PMSF), 1X Protease Inhibitor Cocktail I, II, and III (Sigma-Aldrich, St. Louis, MO)). The homogenate was incubated on ice for 20 min with vortexing every 5 min and then centrifuged at 14,000 x g for 15 min at 4 °C. Total protein concentration of supernatants was determined using the Pierce BCA Protein Assay Kit (Invitrogen, Carlsbad, CA) as described by the manufacturer. 10 µg of each protein lysate sample was resolved on 4-20% precast polyacrylamide gels (Bio-Rad Laboratories, Hercules, CA) under reducing conditions in running buffer (25 mM Tris, 192 mM glycine, 0.1% (w/v) sodium dodecyl sulfate (SDS)). Proteins in gels were semi-dry transferred onto the low background fluorescence Immobilon-FL PVDF Membranes (MilliporeSigma, Burlington, MA) in transfer buffer (25 mM Tris, 192 mM glycine, 20% (v/v) methanol) for 1 hr at 20 V. Membranes were air dried at RT for 1 hr, and then blocked in the Odyssey Blocking Buffer (LI-COR Biosciences, Lincoln, NE) for 1 hr at RT. Primary antibody incubation with 1:200 diluted STMN4 antibody (Proteintech Group, Rosemont, IL) and 1:20,000 diluted anti-β-Actin antibody (Cell Signaling Technology, Danvers, MA) was performed overnight at 4 °C in the Odyssey Blocking Buffer with 0.2 % Tween-20. After washing four times with TBST (50 mM Tris pH 7.5, 150 mM NaCl, 0.1% Tween-20), membranes were incubated with 1:10,000 680RD goat anti-rabbit IgG and 1:20,000 diluted IRDye 800CW goat anti-mouse IgG (LI-COR Biosciences, Lincoln, NE) in dark for 1 hr at RT in the Odyssey Blocking Buffer with 0.2 % Tween-20 and 0.01% SDS. For two-color detection, washed membranes were imaged with the Odyssey CLx Imager (LI-COR Biosciences, Lincoln, NE). Images were analyzed with the Empiria Studio 1.1 (LI-COR Biosciences, Lincoln, NE) for quantified and normalized signal intensity of protein bands.

1.3.7 Immunohistochemistry (IHC) staining

Free-floating brain sections were washed three times in 3 mL of PBS-TX (0.3% (v/v) Triton X-100) for 5 min at RT to remove any cryoprotectant residue. For antigen retrieval, sections were permeabilized with 1 mL of citrate buffer (10 mM Citric Acid pH 6.0, 0.05% Tween 20) at 95 °C for 10 min followed by two washes in PBS-TX. Sections were incubated in 3 mL of PBS-TX with 1% (v/v) H2O2 for 30 min at RT with gentle shaking to suppress endogenous peroxidase. After blocking in 2 mL of 3% (w/v) BSA-PBS-TX for 1 hr at RT, sections were incubated with 1 mL of 1:100 diluted STMN4 antibody (LSBio, Seattle, WA) overnight at 4 °C. Sections were then washed and incubated with 2 mL of 1:1,000 diluted biotinylated anti-rabbit IgG (Vector Laboratories, Burlingame, CA) for 2 hr at RT, followed by incubation with 2 mL of 1:1,000 diluted avidin-biotin complex solution (Vector Laboratories, Burlingame, CA) for 30 min at RT. Sections were exposed in 2 mL of reaction buffer (50 mM Tris pH 7.6, 0.01% (w/v) 3,3'-diaminobenzidine tetrahydrochloride (DAB), 0.04% H2O2, 4% (v/v) saturated nickel ammonium sulfate) for 10 min at RT. After washing three times in Tris buffer (50 mM Tris pH 7.6), sections were mounted and dehydrated for coverslip. Multiple adjacent images were taken from CA1 region per stained section at 40× magnification using an Olympus IX51 microscope (Olympus, Center Valley, PA). Images were analyzed in ImageJ for immunostaining intensity for individual neurons. Mean pixel value of each neuron was used to compare STMN4 protein level between cases and controls.

1.3.8 Statistical Analysis

Statistical analysis in this study was conducted using the GraphPad Prism 8.0.2 or R. $P < 0.05$ was considered statistically significant. Specifically, paired t test was performed to analyze the differences in antibody responses in different sample classes at different ring score cutoffs. Pearson’s correlation analysis was used to

investigate the correlation of antibody responses in serum versus CSF from NAPPA screening. Relative absorbance data from ELISA was calculated by subtracting the raw intensity of GST tag from that of tested GST-fused proteins. Mann-Whitney U test was performed to analyze the difference of STMN4 immunoreactivity in cases versus controls based on validation ELISA. Receive operating characteristic (ROC) analysis was used to analyze the diagnostic performance of serological anti-STMN4 antibody. Spearman's rank correlation analysis was used to test the correlation of STMN4 immunoreactivity between serum and CSF based on validation ELISA. Kruskal-Wallis test was used to analyze the association of anti-STMN4 antibody with subgroups of clinical parameters. Band intensity on Western blotting images was quantified and normalized to loading reference using Empiria Studio 1.1. Immunostaining intensity of CA1 neurons were quantified using ImageJ. Mann-Whitney U test was performed to analyze the difference of STMN4 protein abundance in cases versus controls. Venn diagrams were generated in Venny 2.1.0. Heatmap, scatter plots, bar plots, jitter plots, box plots, and ROC curve were generated in GraphPad Prism 8.0.2 or R. Gene set enrichment analysis was performed using Enrichr on proteins advanced to verification with customized reference and results were ranked according to p-value (Kuleshov et al. 2016).

1.4 Results

1.4.1 NAPPA Array Production and Quality Assessment

Consistent display of full-length proteins at high yield on arrays is the key to successful downstream applications. Prior to profiling antibodies in serum or CSF, *in situ* expressed and immobilized proteins on arrays were assessed by anti-GST antibody to confirm the robustness and consistency of inter-slide protein expression. Correlation coefficient (R) of fluorescent signal intensities from two randomly

selected slides stained with anti-GST antibody was 0.94 (Figure 1-12), assuring the reproducibility of array fabrication and protein display.

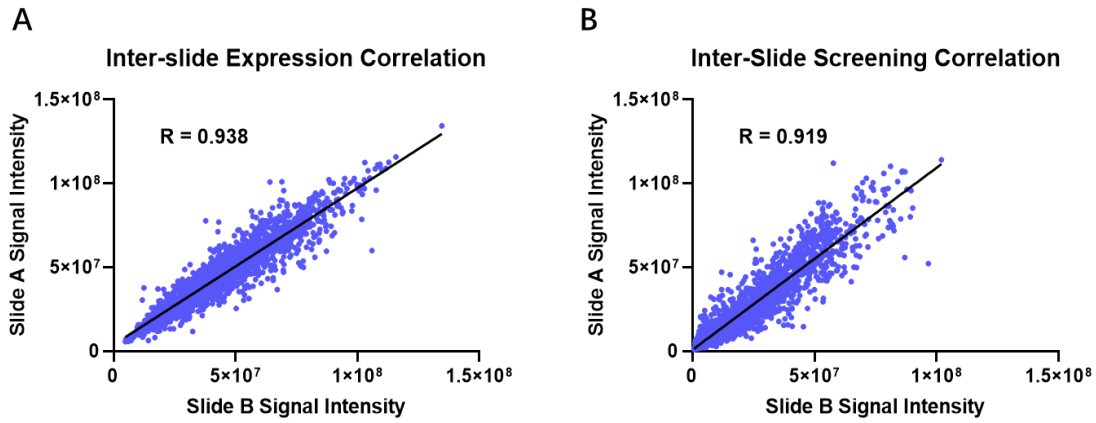

Figure 1-12. Quality assessment of protein expression and sample screening on NAPPA arrays. A) Scatter plot of signal intensities from two different NAPPA arrays stained with anti-GST antibody. Inter-slide correlation coefficient (R) for protein expression is 0.94. B) Scatter plot of signal intensities from two different NAPPA arrays challenged with the same serum sample. Inter-slide correlation coefficient (R) for sample screening is 0.92.

1.4.2 Autoantibody Profiling on NAPPA

To identify AD-associated AAbs, ~4,600 full-length human proteins displayed on NAPPA were challenged with clinical sample pools, including 3 case serum pools, 3 control serum pools, 3 case CSF pools, and 3 control CSF pools. Each 10-sample pool was prepared by mixing serum or CSF samples from 10 AD patients or 10 ND controls in the discovery set (Figure 1-9). We used pooled samples instead of individual samples so that we could survey AAb profiles in more samples in a cost-effective fashion. Overall antibody response in serum was much stronger than that in CSF for both cases and controls (Figure 1-13), which agrees with the fact that IgG concentration in serum is much higher than that in CSF (Hu et al. 2015).

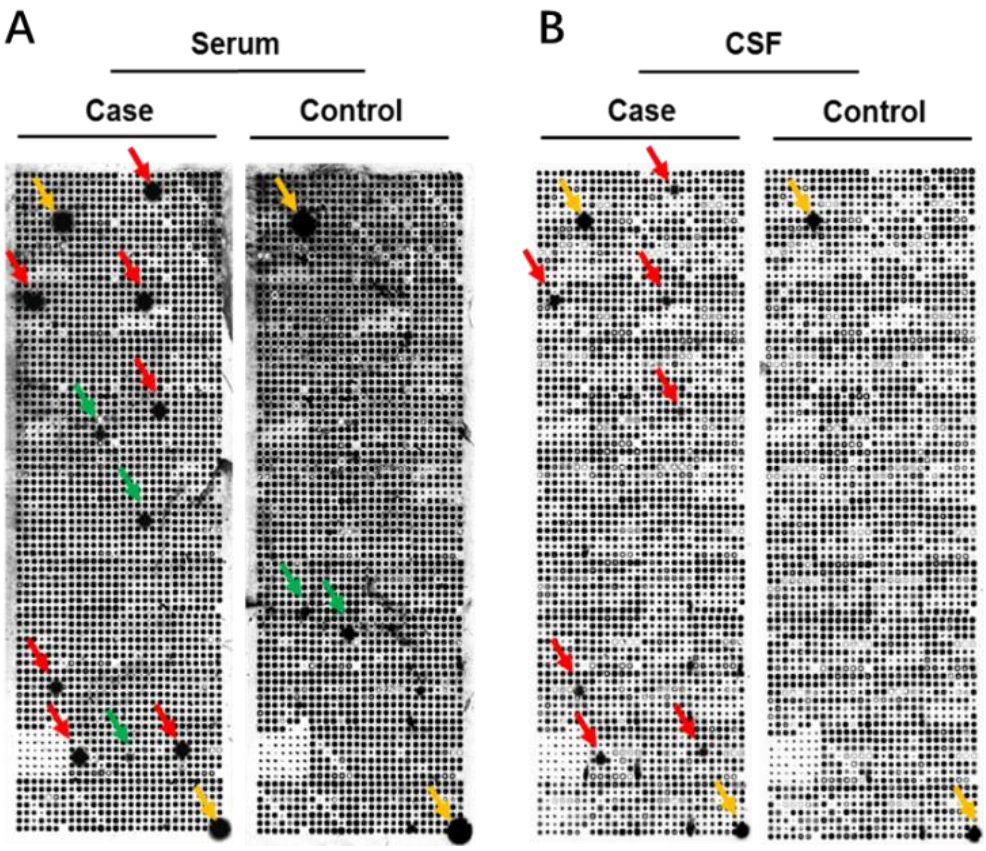

Figure 1-13. Array images of NAPPA slides challenged with paired **A)** serum or **B)** CSF of a case pool or a control pool. Strong antibody responses from samples resulted in a saturated signal with diffusion around the local spot of antigens, which was defined as a ring. Each spot was graded at a scale of 0 to 5 based on the ring intensity and morphologic features. Yellow arrows indicate array positive control protein EBNA. Red arrows indicate antibody responses shared by serum and CSF. Green arrows indicate antibody responses unique to serum.

Immunoreactivity analysis was performed for all array images, where any protein spot that exhibited a ring score of 1 or above was considered as a positive antibody response. For serum, there were a total of 249 antibodies showing positivity in at least one case or control pool, among which 157 were against at least one case pool and 126 against at least one control pool (Figure 1-14A). For CSF, there were a total of 50 antibodies showing positivity in at least one case or control pool, among which 31 were against at least one case pool and 25 against at least one control pool

(Figure 1-14A). Antigens that reacted to both cases and controls counted for 13.7% and 12.0% in all responses against serum and CSF, respectively (Figure 1-14A). In general, more antibody responses were observed in cases than controls for both serum and CSF, suggesting an overall stronger autoimmunity level in AD patients (Figures 1-14A and 1-13). When analyzing the immuno-reactivity with different ring score cutoffs (at a score of 1 through 4), the number of antibody responses against case pools was significantly higher than that of control pools for both serum ($p = 0.0123$) and CSF ($p = 0.0097$) (Figure 1-14B).

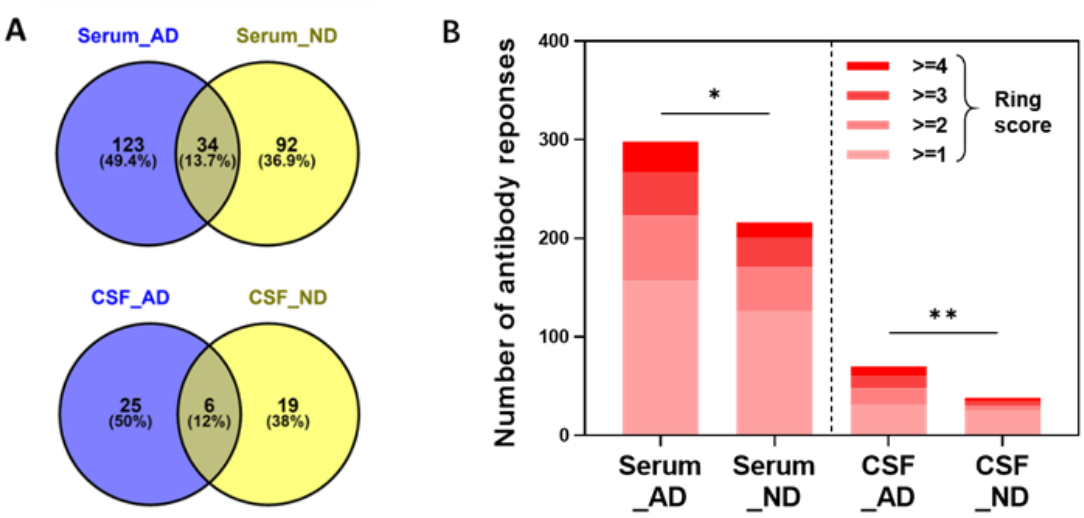

Figure 1-14. A) Venn diagrams of proteins showing immune positivity against the indicated sample classes on NAPPA arrays. There were 123 proteins responsive to serum cases, 92 proteins to serum controls, and 34 proteins to both. There were 25 proteins responsive to CSF cases, 19 proteins to CSF controls, and 6 proteins to both. **B)** Overview of antibody response intensity in indicated sample classes. Protein was counted as a positive antibody response if its ring score was equal to or greater than the indicated cutoffs. Frequency of antibody responses at different ring score cutoffs were represented in different red shades. $P < 0.05$ as *; $P < 0.01$ as **.

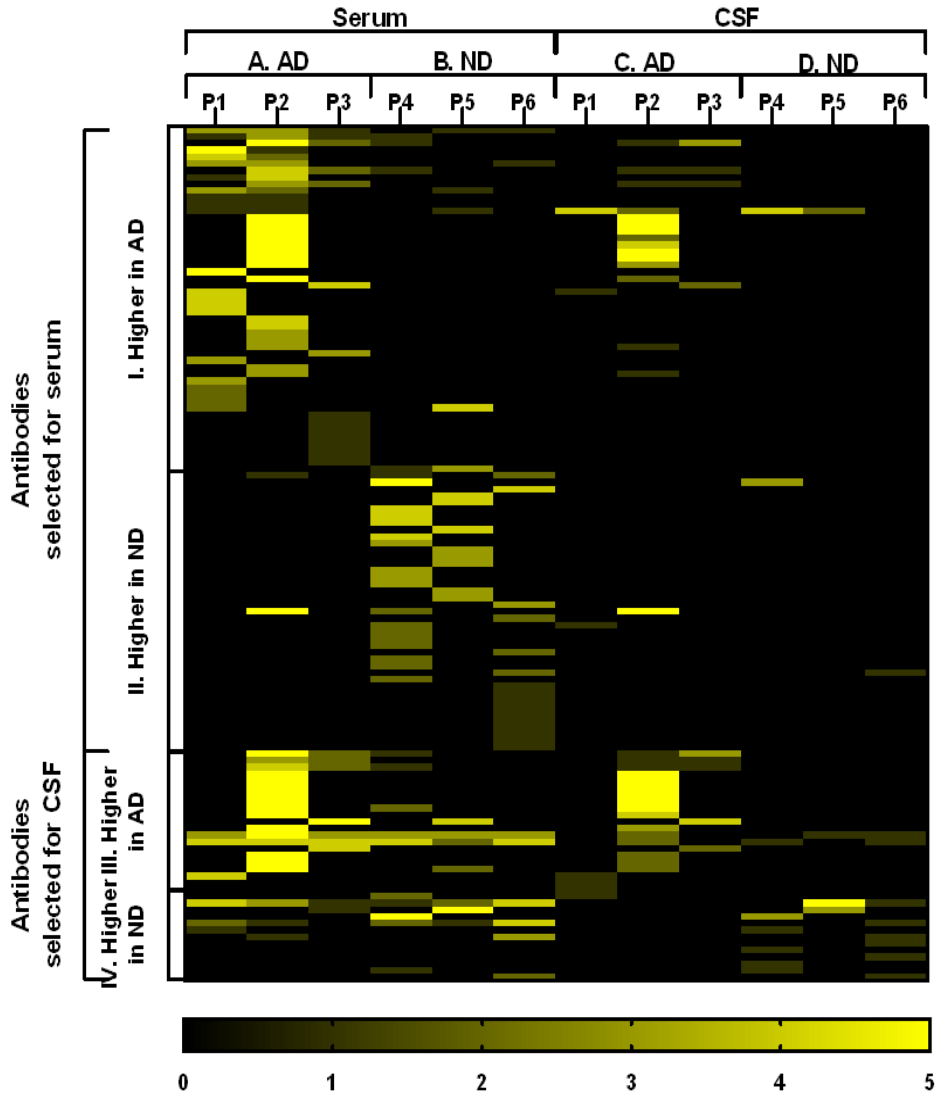

Figure 1-15. Heatmap of 126 proteins showing differential immunoreactivity to case pools (AD) versus control pools (ND) for serum and CSF. Proteins were clustered according to the indicated sample classes (Y axis) to which they were more reactive, including **I)** 50 proteins with higher reactivity to serum AD than ND; **II)** 42 proteins with higher reactivity to serum ND than AD; **III)** 22 proteins with higher reactivity to CSF AD than ND; **IV)** 12 proteins with higher reactivity to CSF ND than AD. Their immunoreactivity across all sample pools (X axis) were represented at a color scale for ring score of 1 to 5. Proteins with higher immunoreactivity to serum AD (AI) and CSF AD (CIII) were selected for ELISA verification. P: pool (n = 10).

A total of 126 antibodies, including 92 for serum and 34 for CSF, were

identified due to their differential immunoreactivity in cases versus controls. Specifically, 50 and 42 antibodies showed higher reactivity to serum cases (region A1 in Figure 1-15) and controls (region BII in Figure 1-15), respectively; 22 and 12 antibodies showed higher reactivity to CSF cases (region CIII in Figure 1-15) and controls (region DIV in Figure 1-15), respectively. A visual representation of their immunoreactivity across all sample pools was summarized in a heatmap (Figure 1-15). They were analyzed to understand the AD-specific autoimmune activities in two different types of extracellular biological fluids. Interestingly, it was noted that, similar reactivity patterns between serum and CSF were present in antibodies selected for CSF but not as much in those selected for serum. Specifically, for antibodies selected for CSF, strong correlations between serum and CSF were observed for both cases (Pearson $r = 0.79$, $P<0.0001$ for region AIII versus CIII in Figure 1-15) and controls (Pearson $r = 0.63$, $P<0.0001$ for region BIV versus DIV in Figure 1-15). In contrast, for antibodies selected for serum, no such strong correlations were seen for either cases (Pearson $r = 0.58$, $P<0.0001$ for region CI versus AI in Figure 1-15) or controls (Pearson $r = 0.29$, $P=0.001$ for region DII versus BII in Figure 1-15). This indicates to us that the presence of CSF AAbs (region CIII and DIV in Figure 1-15) is more indicative of serum AAbs (region AIII and BIV in Figure 1-15) than the reverse, implying that, irrespective of the health condition, AAbs in CSF are more likely to be originated from blood rather than be produced by leukocytes abnormally recruited to brain. Additionally, antibodies exhibiting strong reactivity in serum cases also showed strong reactivity in CSF cases (region CI versus AI in Figure 1-15); however, no such correspondence was noted in controls (region DII versus BII in Figure 1-15). The contrasting scenario between cases and controls may suggest a more severe leakage of AAbs from blood into brain through BBB damage in AD patients.

1.4.3 Verification of AD-Specific AAbs

The subsequent verification was focused on the antibodies showing higher reactivity to cases than controls to confirm their specificity in AD, which include 50 serum (region AI in Figure 1-15) and 22 CSF (region CIII in Figure 1-15) antibody candidates with 15 of them in common. Gene set enrichment analysis revealed that many of these candidates are significantly associated with neuronal cellular compartments as well as brain specific tissues (Figures 1-16A and 1-16B).

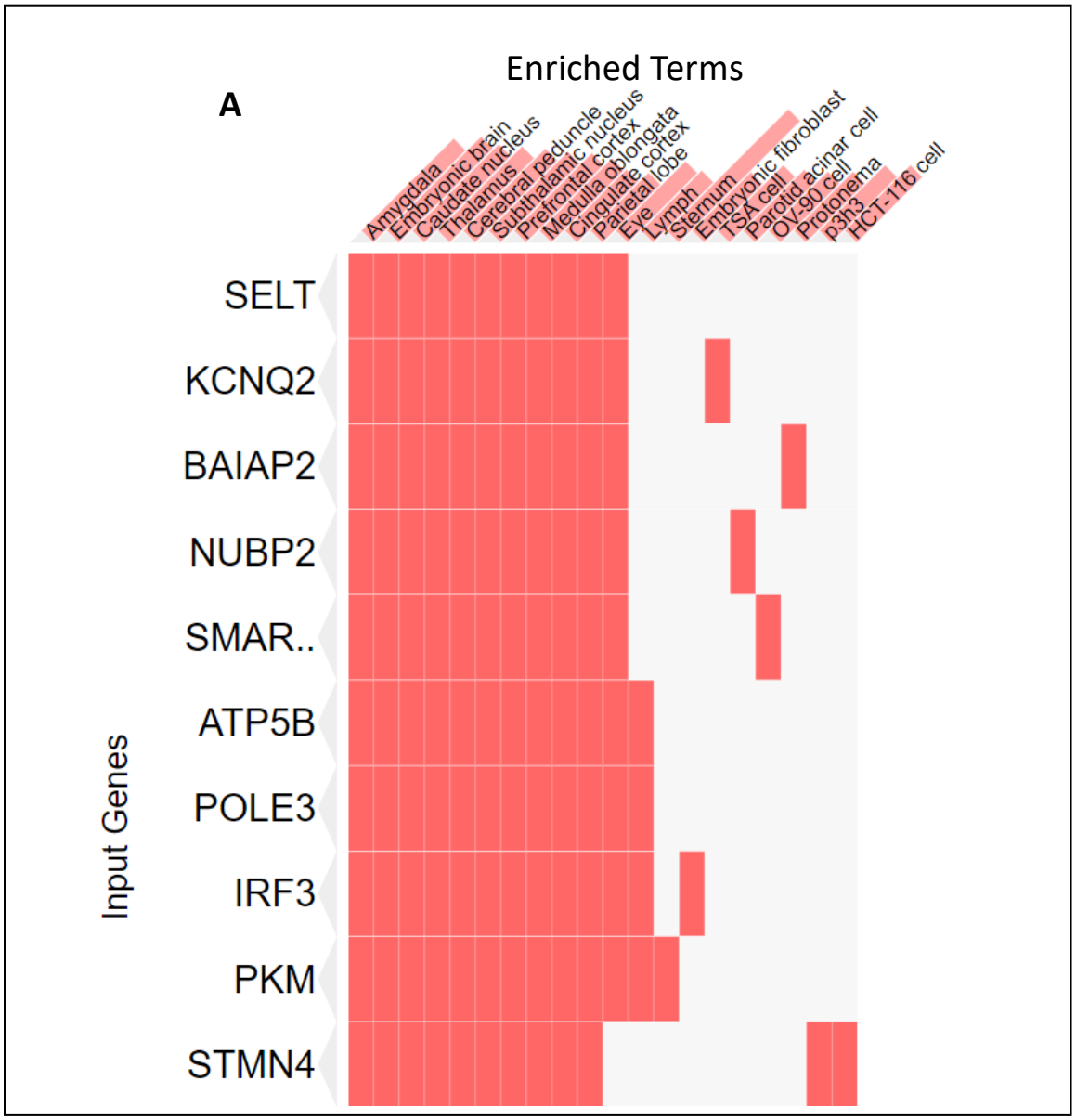

Figure 1-16. Gene ontology analysis of 72 antigens selected for verification identified significant associations with **A)** brain specific tissues and **B)** neuron cellular compartments.

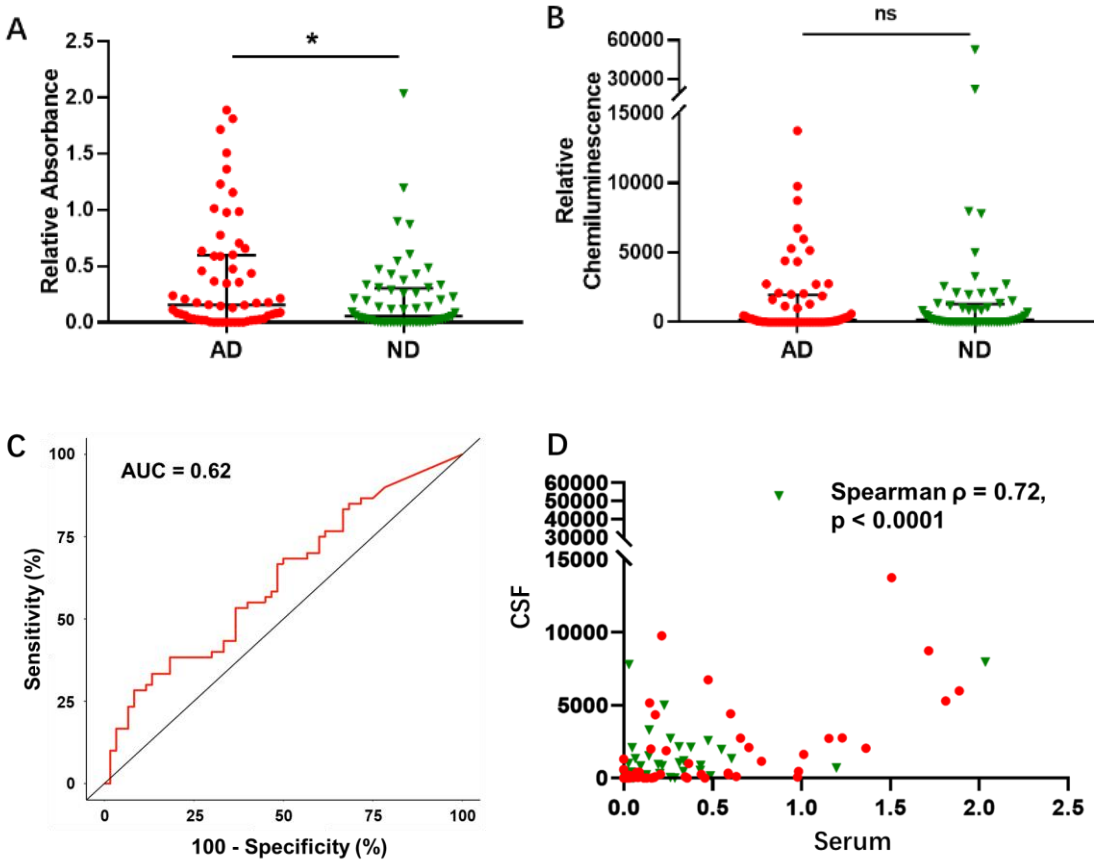

Figure 1-17. Jitter plots of STMN4 immunoreactivity against individual **A)** serum or **B)** CSF samples measured by ELISA in the entire sample set. The black lines indicate the median with interquartile range. $P < 0.05$ as *; $P \geq 0.05$ as not statistically significant (ns). **C)** ROC analysis of STMN4 immunoreactivity in serum showed an AUC of 0.62. **D)** Spearman's rank correlation analysis of anti-STMN4 antibody titers in serum versus CSF revealed a significant but moderate correlation (Spearman $\rho = 0.72$, $p < 0.0001$). Cases and controls were indicated by red circles and green triangles, respectively.

All selected antibody candidates were verified by ELISA using individual samples from the discovery set (Table 1-1) to unmask the antibody prevalence that was not demonstrated by NAPPA screening due to the use of pooled samples. They were ranked according to the sensitivity at the specificity of 90% that was calculated using the background subtracted ELISA signal intensity. To ensure that the potential AAb biomarkers possess a good distinguishing ability as well as readily detectable

concentration in clinical samples, two selection criteria need to be met at the same time to be selected for ELISA validation, i.e. 1) the sensitivity is equal to or greater than 15%; 2) the value of 90% specificity is above an arbitrary cutoff of 50th or 90th percentile of all ranked serum or CSF candidates, respectively. From there, 8 out of 50 serum candidates and 3 out of 22 CSF candidates were eventually advanced for validation (Table 1-2).

Table 1-2. Sensitivity of individual antibody at 90% specificity in different sample sets.

Sample type	**Antigen**	**Sensitivity (%) at 90% specificity**		
		Verification set	**Validation set**	**Overall set**
Serum	STMN4	20	33	28
	CPLX1	20	23	23
	SELT	17	17	17
	ZNF184	23	7	12
	PRKAG2	20	7	10
	IFI35	17	3	10
	CBFA2T3	23	3	8
	BAIAP2	20	0	5
CSF	STMN4	20	7	15
	PRKCZ	20	3	13
	CSN1S1	37	0	12

1.4.4 Validation of AD-Specific AAbs

In the validation stage, the 11 verified antibodies were assayed by ELISA using an independent sample set of 30 AD patients and 30 ND controls. A total of 4 antibody candidates (3 for serum, 1 for CSF) turned out with a sensitivity of equal to or greater than 15% in the entire sample set at 90% specificity (Table 1-2). Surprisingly, when ranking all antibody candidates according to the sensitivity in entire sample set, Stathmin 4 (STMN4) was noted as the top performer in both

serum and CSF with a sensitivity of 28% and 15%, respectively, at 90% specificity. A significant reactivity difference between cases and controls was observed for serum ($p = 0.027$) (Figure 1-17A) but not for CSF ($p = 0.97$) (Figure 1-17B) samples. ROC analysis of serological anti-STMN4 antibody showed an area under curve (AUC) of 0.62 (Figure 1-17C). Spearman's rank correlation analysis of anti-STMN4 antibody titers in serum versus CSF revealed a significant but moderate correlation (Spearman $\rho = 0.72$, $p < 0.0001$) (Figure 1-17D). In addition, the anti-STMN4 antibody titer in CSF was approximately 200-400 fold lower than that in serum when both samples were assayed with the same colorimetric-based ELISA (data not shown).

Table 1-3. P values of the hypothesis tests of association between STMN4 antibody level in serum and clinical characteristics. Significant values are shown in bold.

	Combined	**AD**	**ND**
Brain Weight	0.131	0.047	0.388
Gender	0.438	0.147	0.405
Expired age	0.025	0.435	0.067
Plaque density	0.086	0.195	0.792
Braak stage	0.153	0.354	0.622
MMSE	0.472	0.530	0.701
ApoE	0.273	0.311	0.431

Significant values are shown in bold.

1.4.5 Association of Anti-STMN4 Antibody with Clinical Characteristics

The association of anti-STMN4 antibody with clinical characteristics of samples were evaluated, including the age, gender, ApoE genotype, Braak stage, plaque density, brain weight, and mini-mental state examination (MMSE) (Table 1-3). No significant association was observed between anti-STMN4 antibody level in CSF and sub-grouped clinical characteristics (data not shown). Anti-STMN4 antibody level in

serum is significantly correlated to the brain weight of AD patients (p = 0.047) and the expired age of entire subjects (p = 0.025). Further subgroup analysis on brain weight revealed that the antibody level was significantly increased in AD patients with a brain size of less than 1000 g compared to those of greater than 1200 g (p = 0.037) (Figure 1-18A). Also, the antibody level was significantly lower in younger group (<= 74 y) than two older groups (p = 0.048 for 75-84 y; p = 0.025 for <= 85 y) (Figure 1-18B).

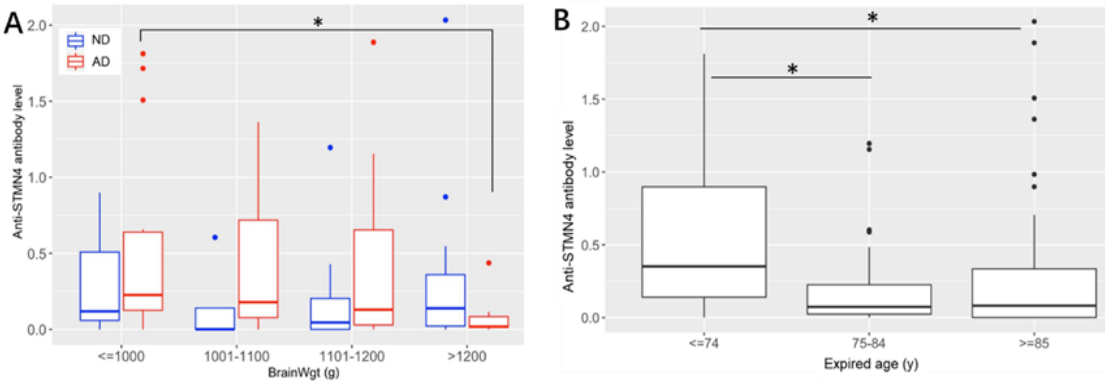

Figure 1-18. The association of anti-STMN4 antibody level in serum to **A)** brain weight of cases and controls separately and **B)** expired age of entire subjects. P < 0.05 as *.

1.4.6 Antigen Expression Level in Human Brain Tissues

According to human proteome databases and previous studies, STMN4 functions as a MT destabilizer and is specifically enriched in a wide range of CNS compartments, such as cerebellum, amygdala, hippocampus and spinal cord (Bateman 2019; Charbaut et al. 2001; Gaudet et al. 2017; Kim et al. 2014; Lin and Lee 2016; Proteome 2015). Therefore, we investigated if STMN4 protein level was affected by AD and how it was associated with its antibody. The protein abundance of STMN4 in MTG tissue lysates from 23 AD patients and 41 ND controls were measured by semi-quantitative Western blotting (Figure 1-19). A comparison of normalized band intensities indicated a significant reduction in STMN4 abundance in

MTG of cases than controls (p = 0.0003) (Figure 1-20A). However, no significant association between protein level and antibody titer in serum/CSF was found regardless of cases or controls (data not shown).

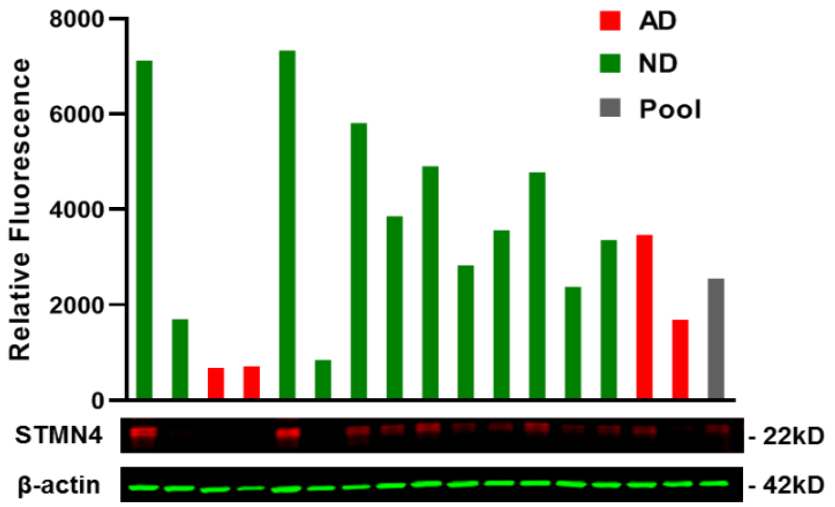

Figure 1-19. MTG tissue lysates were analyzed by Western blotting probed with antibodies against STMN4 and β-actin. Bar plot of quantified signal intensities for each band was shown. Cases (AD) and controls (ND) were coded in red and green, respectively. A pool sample (in grey) was included as a reference for normalization across different membranes.

As the hippocampus, specifically CA1, is the primary region to study synaptic malfunctions in AD, we further performed IHC of STMN4 using human hippocampal sections from 4 AD patients and 4 ND controls to investigate the protein expression level in individual CA1 neurons. Surprisingly, neuronal abundance of STMN4 in cases is significantly higher as opposed to controls (Figure 1-20B) (p < 0.0001). CA1 neurons displayed a stronger immunolabeling signal in cases compared to controls (Figure 1-20C and 1-20D). Besides, subcellular localization identified a ubiquitous but uneven distribution of STMN4 protein in somatodendrtic compartment of CA1 neurons (Figure 1-20C).

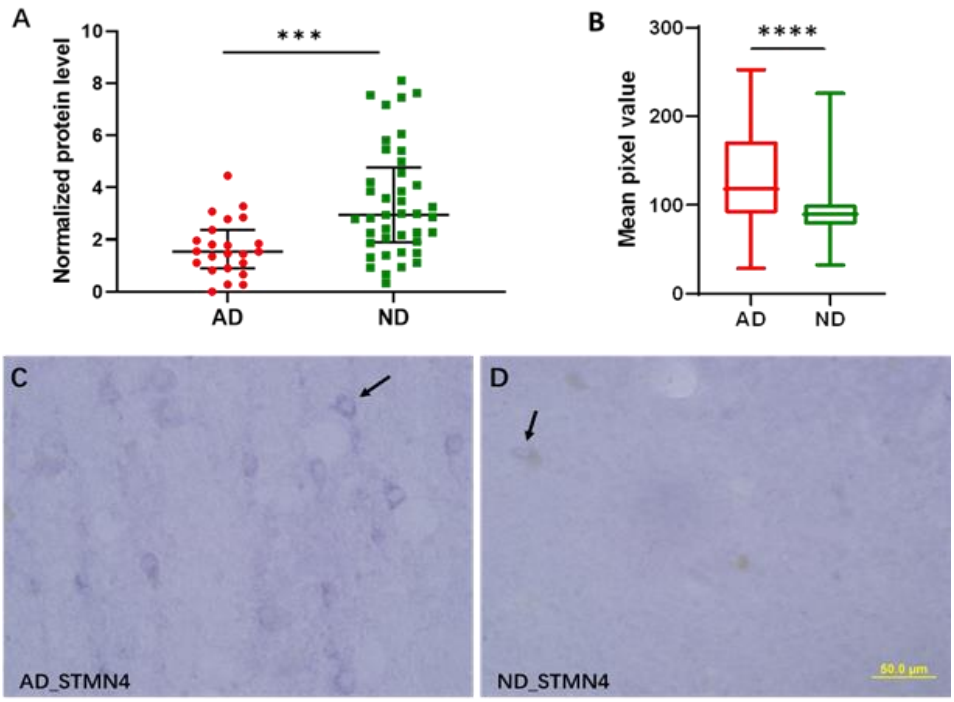

Figure 1-20. A) Jitter plot of STMN4 protein abundance in MTG tissue lysates of AD and ND measured by semi-quantitative Western blotting. The black lines indicate the median with interquartile range. **B)** Box and Whiskers plot of STMN4 protein abundance in individual CA1 hippocampal neurons of AD and ND measured by IHC staining. $P < 0.001$ as ***; $p < 0.0001$ as ****. Representative images of hippocampal sections from **C)** an AD patient (AD-0029) or D) an ND control (ND-0311) stained with anti-STMN4 antibody by IHC. STMN4 positive CA1 neurons were indicated by arrows.

1.5 Discussion

To the best of our knowledge, this is one of the first studies that investigated the systemic antibody repertoire of paired serum and CSF of AD in parallel and discussed the AD-associated correlation of AAbs in serum and CSF. We applied NAPPA to unbiased proteome-level profiling for AAbs that were differentially represented in AD and ND, and then evaluated the diagnostic performance of selected antibody candidates by ELISA using an independent sample set. Initial screening on NAPPA revealed a significantly higher overall immunoreactivity in cases than controls for both serum and CSF (Figure 1-14B and 1-13), which agrees with

the widely reported evidence that autoimmune components are intrinsically involved in AD (Colasanti et al. 2010; D'Andrea 2003, 2005; Sardi et al. 2011). On the other hand, many positive antibody responses on arrays challenged by CSF were also found in serum but with a stronger signal intensity (Figure 1-13), which can be explained by the fact that CSF is biologically formed through an ultrafiltration of arterial blood and thus contains much lower AAb titers (Brinker et al. 2014; Hu et al. 2015). Specifically, 24 out of 31 (77%) antibodies in CSF cases and 13 out of 25 (52%) antibodies in CSF controls were also observed in serum cases and controls, respectively (Figure 1-14A).

When analyzing antibodies that were differentially represented in cases versus controls, it was found that antibodies present in CSF also exhibited immune positivity in serum with a significantly strong correlation regardless of cases (Pearson $r = 0.79$, $P<0.0001$ for region AIII versus CIII in Figure 1-15) or controls (Pearson $r = 0.63$, $P<0.0001$ for BIV versus DIV in Figure 1-15), but no such correspondence was found in reverse (region CI versus AI for cases and region DII versus BII for controls in Figure 1-15). In general, the elevated prevalence of AAbs in the CNS compartments of AD patients has two-fold explanation: 1) leakage from circulating blood to peripheral CSF through BBB dysfunction (D'Andrea 2003, 2005; Lehrer and Rheinstein 2015), and 2) *in situ* production in CNS by leukocytes abnormally recruited through CSF flow (Correale and Villa 2007; Hatterer et al. 2008). The above findings of the antibody repertoire in CSF being a subset of that in serum favor the former hypothesis. Additionally, more antibody responses with strong reactivity were shared between serum and CSF in cases than controls (Figure 1-15), suggesting a more severe penetration of AAbs from blood into CSF due to the increased BBB permeability in AD patients. Altogether, the thoughts about the global

AAb similarity between serum and CSF in AD are consistent with previous reports on the CNS-targeted autoimmune responses in AD (D'Andrea 2005; Sardi et al. 2011).

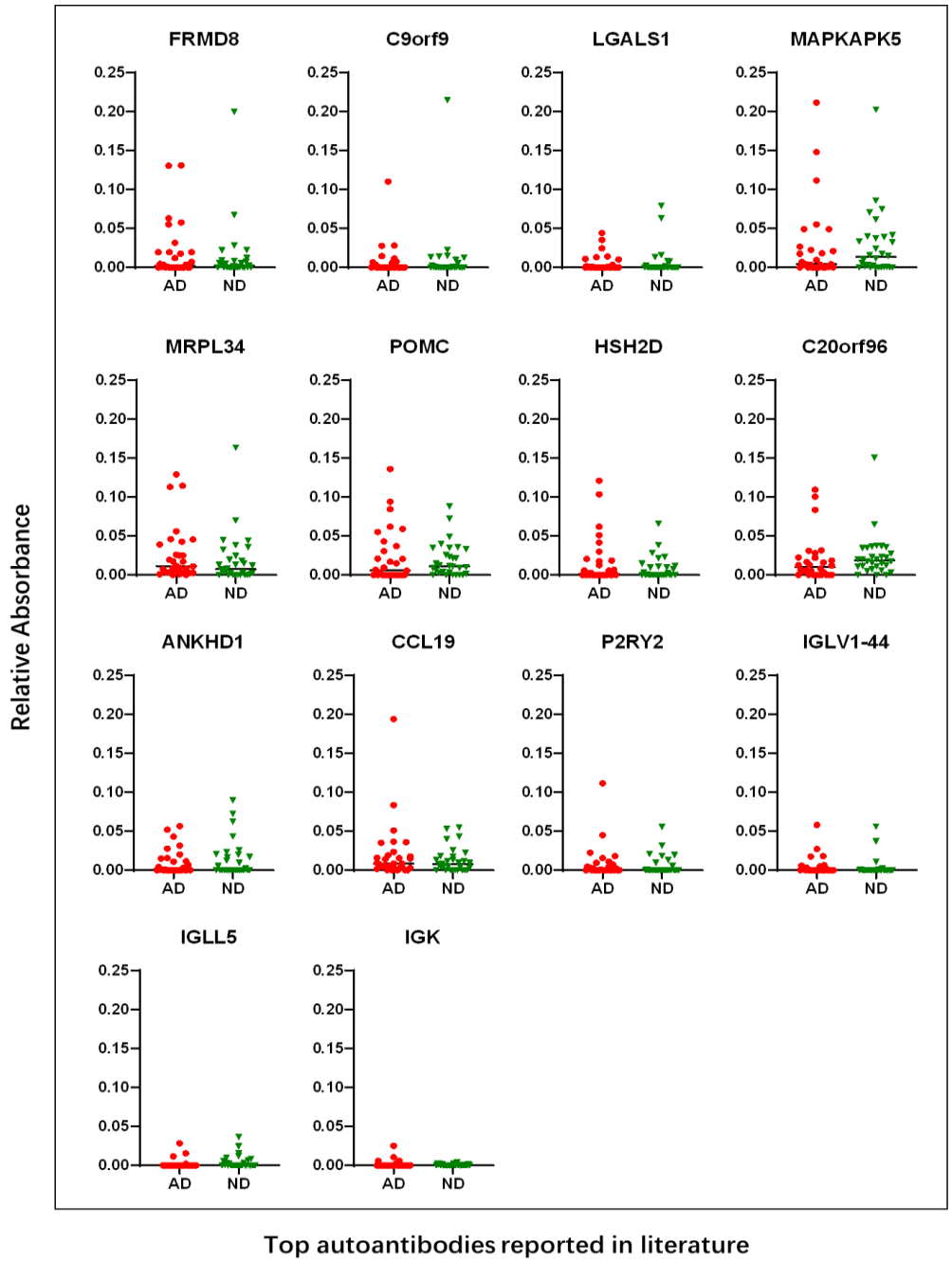

Figure 1-21. Jitter plots of top AAbs reported in literature. A total of 14 AAbs were selected from 2 different AD biomarker studies and tested by ELISA using serum samples from the discovery set. At a fixed specificity of 92.5%, the sensitivities of tested AAbs varied from 0-20%.

Gene ontology analysis of target antigens (50 for serum and 22 for CSF) showing higher reactivity to cases than controls revealed a significant association with brain specific tissues, including amygdala, embryonic brain, thalamus, prefrontal cortex, and cerebral peduncle (Figure 1-16A), as well as with neuron cellular compartments, including neuron projection, axon, and myelin sheath (1-16B). These results indicate that antibody profiling on NAPPA is capable of identifying neuronal antigens but not random targets. The presence of circulating AAbs targeted against diverse neuronal proteins is very intriguing, and they could play either a protective role (i.e. anti-Aβ antibody) by mediating the clearance of toxic autoantigens or a pathogenic role (i.e. anti-ATP synthase antibody) by directly participating in the pathogenic progress of disease progression (Du et al. 2003; Kellner et al. 2009; Vacirca et al. 2012).

Following verification, 8 serum and 3 CSF antibody candidates were validated by ELISA using an independent sample set to assure the stringency of biomarker assessment (Table 1-2). Among all, anti-STMN4 antibody had the best performance with 28% and 15% sensitivity in serum and CSF, respectively, at 90% specificity (Figures 1-17A and 1-17B). In this study, subjects with MCI, incidental Lewy bodies, and other tremor diseases were classified as ND controls, and no difference in anti-STMN4 antibody level was observed between MCI and non-MCI controls (data not shown). Therefore, anti-STMN4 antibody is expected to have the potential of distinguishing established AD from pre-AD stages or other dementia with similar neurological symptoms. This differentiation can be confirmed by further studies that involve longitudinal samples or patients diagnosed with other dementia. Also, the seroreactivity of anti-STMN4 antibody in cases was found to be significantly higher than that in controls (Figure 1-17A). The expired age does not contribute to this difference because cases and controls have similar mean of expired age (Table 1-1).

The compartmental analysis of anti-STMN4 antibody in CSF versus serum revealed that the antibody titers in paired serum and CSF samples of AD patients were significantly correlated (Spearman $\rho = 0.72$, $p < 0.0001$) (Figure 1-17D). On the other hand, the antibody titer in CSF was approximately 200-400 times lower than that in serum (data not shown). Similar findings were reported on the naturally occurring anti-Tau antibody in AD patients, implying that AAbs in CSF might not originate in brain but rather are produced in response to neuronal antigens leaking to the systemic circulation from CNS (Rosenmann et al. 2006). As a cross-validation, we also selected 14 top AD-associated AAbs with the extraordinary performance (> 96.0% sensitivity at > 92.5% specificity) that were reported in other studies, and tested them by ELISA using serum samples in the discovery set (DeMarshall et al. 2016; Nagele et al. 2011). Interestingly, these AAbs all showed relatively low titers and failed to repeat the sensitivity and specificity comparable to previous reports. At a fixed specificity of 92.5%, the sensitivities of tested AAbs varied from 0 to 20% (Figure 1-21). Such huge inconsistency dampens their clinical value and may result from variations in clinical samples and analytical methods, underlining the paramount importance of stringent validation in biomarker studies.

STMN4 is an intracellular MT-associated protein (MAP) that destabilizes MTs by inhibiting tubulin polymerization (Beilharz et al. 1998; Charbaut et al. 2001; Lin and Lee 2016). It belongs to the stathmin phosphoprotein family comprising of four MAP members (STMN1-4) highly expressed in CNS (Chauvin and Sobel 2015). Although they function similarly as a MT destabilizer, their differential spatio-temporal distribution in neurons suggest their partially distinct yet complementary roles in relation to regulating MT network and neuronal projection development (Charbaut et al. 2001; Gavet et al. 2002; Ozon, El Mestikawy, and Sobel 1999; Poulain and Sobel 2007). Previous reports have also linked the genetic redundancy

to a possible compensatory mechanism (Duncan et al. 2013). Indeed, STMN1 protein level was significantly lower in frontal and temporal cortices of AD patients (Cheon et al. 2001; Jin et al. 1996; Saitoh, Horsburgh, and Masliah 1993), and STMN1 knockout mice demonstrated an age-dependent axonopathy and significantly reduced nerve conduction velocity in motor neurons (Liedtke et al. 2002). Additionally, an upregulated expression of STMN4 is observed in these deficient mice (Yoshie et al. 2006). Taken together, it is likely that the synaptic damage in AD could induce STMN4 overexpression as a compensation for STMN1 loss to maintain microtubule network, which, on the other hand, could lead to the immune intolerance against STMN4 (Duda et al. 2017). This may explain the significant increase in STMN4 protein abundance in CA1 neurons as well as in anti-STMN4 antibody level in both serum and CSF of AD patients observed in this study (Figure 1-20B and 1-17A). On the other hand, STMN4 protein level was found to be significantly reduced in MTG tissue lysate of AD patients (Figure 1-20A). Despite the contradictory results from CA1 neurons and MTG lysates, these protein data are in accordance with STMN4 mRNA transcription data from independent studies. Particularly, in AD patients, STMN4 mRNA was shown significantly increased in NFT-bearing CA1 neurons but decreased in hippocampal homogenates compared to age-matched ND controls (Berchtold et al. 2008; Liang et al. 2008; Mastroeni et al. 2018). This discrepancy could be attributed to the cellular heterogeneity and "homogenate effect", which can mask the behavior of neurons by representing bulk populations of other glial cells. In addition, several earlier studies reported that the aberrant activity (either overdose or reduction) and localization of stathmins are related to a series of neurodegenerative events, including disordered neurogenesis, hyper-activation of signal transduction system, and NFT formation (Jin et al. 1996; Lin and Lee 2016; Saitoh et al. 1993). Neurogenesis, which takes place in the

dentate gyrus of hippocampus, is a pivotal event in neuron development during adulthood (Radad et al. 2017). Thus, it is likely that in AD aberrant STMN4 level affects the vulnerable hippocampus through disrupting the neurogenesis.

To fully understand the biological relevance of STMN4 in AD pathogenesis, neuronal cell lines can be incubated anti-STMN4 antibody and analyzed for their morphological and biochemical alterations. In vivo studies using mice immunized with anti-STMN4 antibody purified from AD patients might also provide insights to whether and how STMN4-specific immune response would affect the neuronal degeneration and cognitive decline. Given the multifactorial AD pathogenesis, it is plausible that the elevated STMN4 immunoreactivity merely represents one of the downstream alterations resulted from pre-existing underlying pathology, rather than an upstream triggering event. Indeed, further studies are required to enlighten the role of anti-STMN4 antibody in AD-associated molecular pathways (Gómez-Isla et al. 1996; Huang and Mucke 2012).

There are several limitations of this current study. 1) Postmortem samples were used for screening in this study considering physiological specimens obtained from living patients have significant uncertainty and unknown heterogeneity regarding both primary diagnosis and any other comorbid or secondary diagnoses. However, variations in PMI due to sample collection from deceased subjects could contribute to the poor outcomes of association analysis. 2) The usage of pooled samples for NAPPA screening may sacrifice the depth of immunoprofiling and lose individual information. 3) Due to a lack of subjects at early stages, it is difficult for us to gain a comprehensive understanding of how anti-STMN4 antibody level correlates with the cognitive function in subjects or develops over the disease course. 4) The current sample size is still too small for us to draw definite conclusions on its potential role for diagnosis as well as multivariate analysis of clinical characteristics.

Additional studies involving multiple-site cohorts, different disease stages, longitudinal samples, or cases with other neurodegenerative diseases are necessary to confirm the diagnostic utility of anti-STMN4 antibody for early detection of AD. 5) ~4,600 full-length human proteins, representing only one fourth of human proteome, were profiled in this study so it is likely that some potential autoantigens were missed. An expanded study incorporating ~18,000 human proteins available in DNASU Plasmid Repository (http://dnasu.asu.edu/DNASU/) may reveal more interesting AD-associated AAbs. 6) Native proteins used for screening lack some post-translational modifications (PTMs) that might be of importance in autoimmune responses occurring in AD. For example, Rosenmann et al. detected circulating AAbs against pathologically pTau protein in AD patients' sera (Rosenmann et al. 2006); Acharya et al. demonstrated that the pentatricopeptide repeat domain 2 (PTCD2) protein is present in a citrullinated form in AD brains as a target of a prominent circulating AAb (Acharya et al. 2012). Some degree of phosphorylation from the cell-free expression lysate has been observed, but most PTMs have not been thoroughly studied (Rauf et al. 2018). Accommodation of PTMs, such as glycosylation, oxidation, citrullination, and AMPylation, onto NAPPA is in progress to hopefully better address this concern in future (Karthikeyan et al. 2016; Yu et al. 2014).

1.6 Conclusion

In summary, we conducted an unbiased immunoprofiling of paired serum and CSF samples from AD patients and ND controls against ~4,600 full-length human proteins, followed by ELISA validation of selected AAb candidates. Stronger global antibody responses in both serum and CSF of AD patients suggest the participation of autoimmune components in AD. A comparative analysis of immunoreactivity in serum versus CSF indicates a possible more severe penetration of circulating AAbs into the CNS through impaired BBB in AD patients. This work identified anti-STMN4

antibody as a potential diagnostic biomarker for AD with 28% and 15% sensitivity in serum and CSF, respectively, at 90% specificity. Meanwhile, the STMN4 protein abundance was significantly increased in CA1 neurons, indicating a consequent immune intolerance against STMN4 in AD patients. However, further studies are needed to resolve the enigma whether altered anti-STMN4 antibody is a contributor, a consequence, or simply an epiphenomenon of AD. As more novel AD-specific AAbs discovered, an immunesignature-based biomarker panel is expected to be established as an accurate, reliable, non-invasive and inexpensive modality for early detection of AD (Colasanti et al. 2010; Wu and Li 2016). Such studies will also provide insights to the role of autoimmunity in AD disease mechanism and shed lights on the development of immunotherapies.

CHAPTER 2

2 CONSTRUCTION OF GATEWAY-COMPATIBLE BACULOVIRUS EXPRESSION VECTORS FOR HIGH-THROUGHPUT PROTEIN EXPRESSION AND *IN VIVO* MICROCRYSTAL SCREENING

2.1 Abstract

Proteins are the biomolecular machines that drive all important life activities in biology. Extensive research aimed to unmask the structure and function of proteins propose great needs for large quantities of purified and active proteins. Baculovirus-mediated insect cell expression system has been widely used for producing heterogeneous proteins. However, its applications in protein research has been largely restricted by the time-consuming cloning procedures and limited readily available resources of open reading frames (ORFs). The goal of this study is to establish an end-to-end pipeline built on the baculovirus-insect cell expression system that enables high-throughput (HT) gene cloning, protein production, cell screening for *in vivo* microcrystals and sample preparation for structural analysis. Particularly, we have generated a series of Gateway-compatible baculovirus expression vectors (BEVs) that allow HT integration of foreign genes into viral genome followed by generation of recombinant baculovirus in insect cells for target protein expression. The collection of BEVs also support the attachment of a variety of fusion tags to target proteins to meet the needs for different research applications. More importantly, this pipeline articulates with our readily available plasmid repository comprising of over 18,000 different human genes and tens of thousands of pathogen genes, which provides a ready source of materials for protein production. Using this pipeline, we have successfully demonstrated the mass parallel production of a protein collection with good reproducibility. Additionally, we explored the application of our pipeline in structural biology by combining it with the Second

Order of Nonlinear Imaging of Chiral Crystals (SONICC), a technology that visualizes thin and tiny protein crystals in living cells. We successfully identified *in vivo* microcrystals for 29 targets out of 56 overexpressed recombinant proteins. These SONICC positive hits can be advanced to the Serial Femtosecond Crystallography (SFX) for further protein structural characterization. This pipeline allows rapid screening of protein expression and *in vivo* crystallization, which promises to substantially facilitate the production of materials for myriad applications in structural, functional, and biomedical research.

2.2 Introduction

2.2.1 Overview

As the workhorses of almost all important life functions, proteins orchestrate the biological processes in living organisms through their interactions or manipulations of other biomolecules. There is great need for purified proteins in many aspects of protein characterization including structure determination, enzymatic activity analysis, protein-protein interaction and protein-small molecules interaction studies. The last decade has witnessed dramatic advances in the field of proteomics, which broadly includes understanding the composition, structure, and function of numerous proteins in biological systems, and how the various components collectively contribute to phenotypes. Yet, in post-genomic and proteomic era, the demand for stable and functional proteins for research and commercial uses still far outstrips the available supply. To produce a purified protein requires consideration of many factors, including host system, protein solubility, size, yield, purity, activity, etc., which makes it very challenging and time-consuming. Thus, a reliable and efficient high-throughput (HT) protein production pipeline is essential to empower translational research.

It is well known that transfection of cultured lepidopteran insect cells with the engineered baculovirus expression vector (BEV) encoding proteins of interest (POIs) generates the infectious bacoluvirus progeny, which can be used to infect insect cell cultures for high yield of proteins. As one of the most widespread protein expression systems, the baculovirus-insect cell system integrates the high production level in bacterial system and the eukaryotic protein processing cascades in mammalian system. Other advantages of this system include the improved protein solubility, high biosafety, and moderate maintenance cost, easy adaption to suspension culture for scaling and automation, making it an ideal choice for many protein research applications. Using insect cells to express proteins is not a new process. However, the procedures have been traditionally tedious, labor-intensive, and time-consuming regarding the insertion of foreign genes to viral genome and repeated rounds of plaque purification to isolate recombinant virus from the wild-type (WT) parental background, which largely compromises its development for mass parallel protein production.

To widen these bottlenecks, we have constructed a set of Gateway-compatible BEVs based on the pIEx/BacMagic system, which enable HT transfection followed by fast and convenient generation of recombinant baculovirus in insect cells for target protein expression. The BacMagic DNA, derived from *Autographa californica* multicapsid nucleopolyhedrovirus (AcMNPV) genome, has one essential gene ORF1629 partially deleted, therefore preventing the viral replication in insect cells. In pIEx BEVs that were constructed in this study, Gateway expression cassette is inserted at downstream of p10 promoter, which is flanked by viral genes, lef2/ORF603 and ORF1629, to facilitate the recombination. Once co-transfected into insect cells, the homologous recombination between pIEx BEVs and BacMagic DNA knocks in the expression cassette and restores ORF1629 flanking the insertion site.

Only recombinant baculovirus are replicative, thus yielding a homogeneous population of infectious recombinant progeny without the need for tedious and time-consuming plaque purification steps. In addition, Gateway technology was adapted to make pIEx BEVs suitable and efficient for HT cloning of genes encoding POIs. In brief, the target coding sequence in a Gateway donor vector can be conveniently transferred into the pIEx BEVs through one-step site-specific recombinational cloning. This also allows researchers to take advantages of over 14,000 full-length human genes as well as tens of thousands of pathogen genes already cloned in a Gateway donor vector, which are freely available from our existing DNASU plasmid repository (http://DNASU.org). Furthermore, these pIEx BEVs were modified with sequences encoding functional fusion tags at either amino- (n) or carboxy- (c) terminus of target coding sequence to support a variety of translational/structural research needs, including affinity tags for protein purification and detection, or fluorescent tags for imaging. Using our pIEx BEVs, we have established a mass protein production pipeline and successfully demonstrated the HT production of 40 recombinant proteins fused to various tags and purification of several targets from different species to verify the functionality of fusion tags, such as GST and His tags.

In summary, we have developed a versatile baculovirus-mediated expression pipeline by constructing a suite of Gateway-compatible pIEx expression vectors with various fusion tags, which enables HT protein expression and *in vivo* crystallization for functional and structural studies. In conjunction with the existing Gateway clone libraries and the advancement of XFEL technology, these vectors will enable proteomic-scale optimization of protocols for structure determination using *in vivo* microcrystals (Figure 2-1).

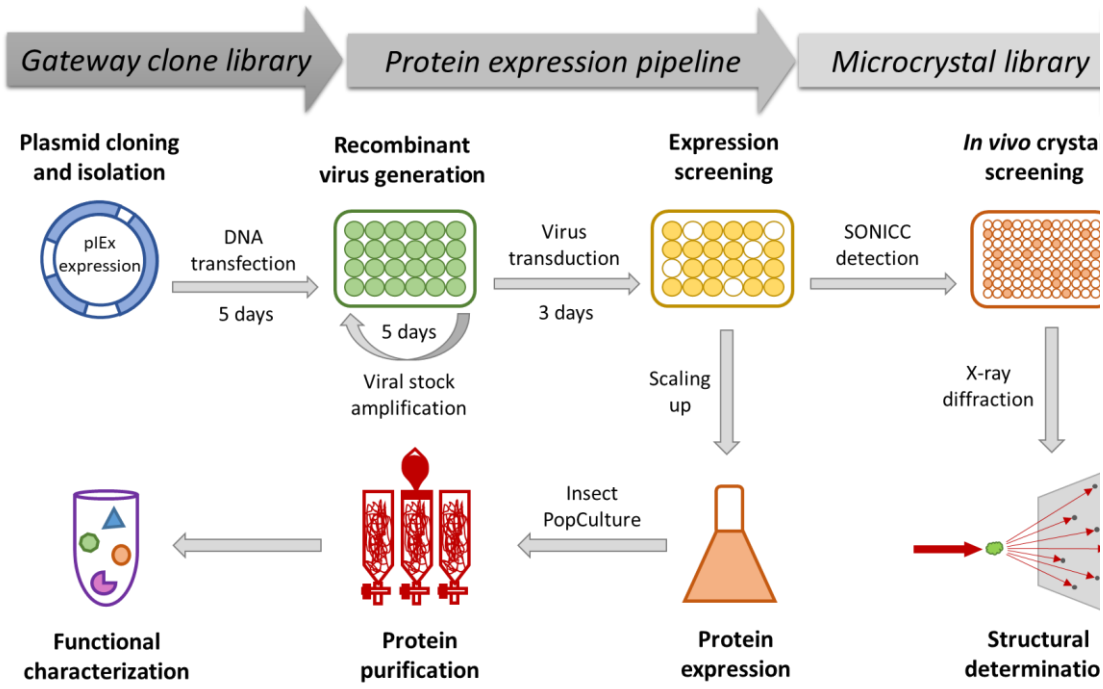

Figure 2-1. Workflow of the HT protein production and characterization pipeline. It enables: **1)** easy selection of ORFs encoding target proteins from any existing Gateway clone libraries; **2)** rapid and convenient HT construction of expression clones; **3)** mass parallel expression screening of recombinant proteins with various tags; **4)** affinity tag-based protein purification for functional characterization; and **5)** fast and sensitive screening for *in vivo* microcrystal targets.

2.2.2 Protein Expression Systems

Protein science involves characterizing any aspect of a protein, such as structure, function, modifications, trafficking and localization, etc. The very first essential step to this endeavor is to produce functional proteins of high quality. A variety of expression systems have been developed and widely used in research and industry, with the host organisms ranging from bacteria to mammalian cells. In 2009, out of 151 approved biopharmaceutical proteins, around 30% are produced in *Escherichia coli* (*E. coli*), 20% in yeast hosts, and 50% in higher eukaryotic cells, mainly mammalian cells (Ferrer-Miralles et al. 2009). Apart from manufacturing of

biopharmaceutical proteins, recombinant protein production has also been playing a critical role in structural biology. By 2013, *E. coli* has been used to produce more than 66,724 (88.6%) of all distinct protein chains in the Protein Data Bank (PDB), awarding it as the most prevalent microbial factory in structural biology (Fernández and Vega 2013). Insect cell expression system ranks as the second, accounting for 3,499 distinct protein chains (4.65%), while mammalian cells occupy the third position with 1,911 distinct protein chains (2.54%). Indeed, one single perfect expression system that works for all proteins does not exist. Each system has its own advantages and limitations regarding biosafety requirements, protein production scale, protein processing capabilities, maintenance cost, ease of manipulation and automation (Kost and Kemp 2016b), so it is important to select proper system based on specific research applications. Regardless of the diversity of expression systems, the general working principle is to introduce a DNA vector encoding the protein of interest into host cells and harness their own cellular machinery to produce desired proteins from the transfected DNA template.

2.2.2.1 Bacteria Expression System

Bacterial protein expression system is one of the most commonly used method in research as well as in industry (Figure 2-2). It has been demonstrated as a workhorse organism in numerous protein expression studies (Baneyx 1999). Several advantages of bacterial hosts include: 1) fast growth dynamics. The unparalleled short doubling time (~20 min) makes it possible for a starter culture to reach the stationary phase within only a few hours (Sezonov, Joseleau-Petit, and D'Ari 2007); 2) high cell density cultures. The density of a saturated *E. coli* liquid culture can reach up to 1×10^{13} viable cells/mL (Shiloach and Fass 2005), therefore guarantee the high recombinant protein yield of up to 50% biomass (Panda 1985); 3) low cost for maintenance and production. Culture media can be made from readily

available and inexpensive components; 4) easy and fast transformation of foreign DNA (Pope and Kent 1996). Competent bacterial cells with different properties have been well established to allow for convenient transformation of exogenous plasmid with high success rate (Froger and Hall 2007).

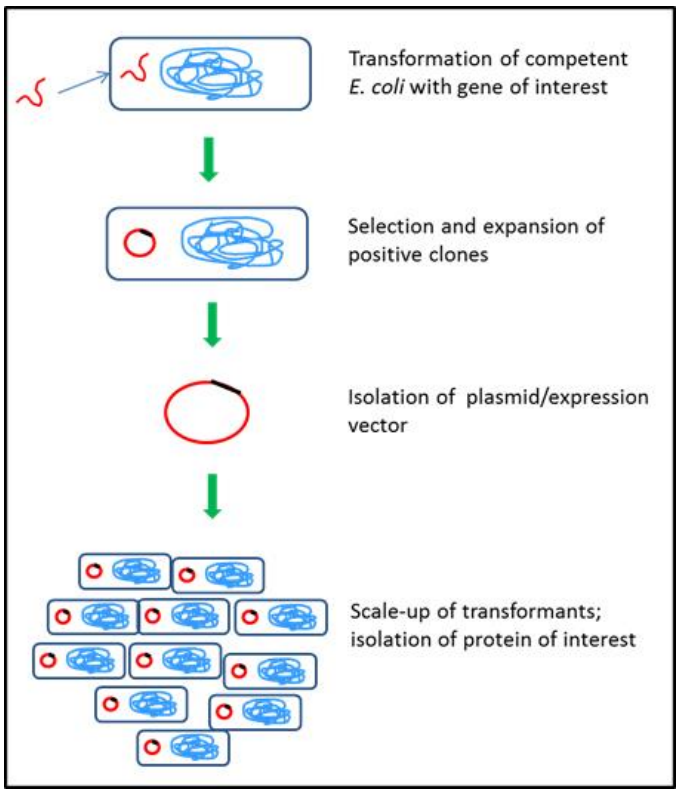

Figure 2-2. Bacteria protein expression system. Figure adapted from Millipore Sigma.

Substantial engineering has been devoted to bacteria to enable large-scale recombinant protein expression with relative ease. These efforts brought about a plasmid collection comprising of pET for medium copy number (15-60 copies per cell) (Bolivar et al. 1977), pUC for high copy number (500-700 copies per cell) (Minton 1984), pBAD for low copy number (10-12 copies per cell) (Guzman et al. 1995), as well as a series of engineered bacteria strains. As the most frequently used *E. coli* strain, BL21 was first described in 1986 after various modifications to the parental B

strains (Studier and Moffatt 1986). Its deficiencies in two proteases, Lon (Gottesman 1996) and OmpT (Grodberg and Dunn 1988), abolish the degradation of foreign proteins (Gottesman 1996; Grodberg and Dunn 1988). A genetic mutation in hsdSB derived from the parental strain (B834) effectively disrupts DNA methylation and degradation, thus preventing the plasmid loss (Baneyx 1999). These successful modifications are attributed to the wealthy knowledge about its physiology.

However, a very low success rate (2-20%) has been noted when expressing eukaryotic proteins in *E. coli* due to protein toxicity, insolubility, and aggregation (Service 2002). The lack of eukaryotic protein machinery in bacteria often leads to inactivity of multi-domain proteins because of unproper folding or incomplete post-translational modifications (PTMs) (Makrides 1996). Many proteins display poor solubility due to incorrect disulfide bonds (Derman et al. 1993) or insufficient chaperone molecules (Carrió and Villaverde 2002; Hoffmann and Rinas 2004). The aggravated hydrophobic interactions result in the formation of inclusion bodies composed of protein aggregates (Carrió and Villaverde 2002; Kane and Hartley 1988), which are very difficult to recover without harsh denaturant treatment and subsequent cumbersome protein-refolding procedures (Carrió and Villaverde 2002). Also, bacteria are not equipped with secretory mechanisms (Ni and Chen 2009), restraining it from the extensive usage for producing extracellular eukaryotic proteins. Protein size is another concern when using bacteria expression system, since proteins larger than 100 kD are generally difficult to be expressed by *E. coli* as they tend to become instable.

2.2.2.2 Yeast Expression System

Yeast cell factories have proven to be extremely useful for expressing and characterizing eukaryotic proteins (Mokdad-Gargouri et al. 2004; Strausberg and Strausberg 1995), and are ideally suited for large-scale production (Figure 2-3). It

combines the advantages of being unicellular organisms, such as fast growth and easy genetic manipulation, as well as eukaryotic features including secretory pathways leading to correct protein processing and many PTMs (Mokdad-Gargouri et al. 2004). Besides, it is easy to cultivate and less expensive than mammalian cells. Commonly used yeast strains include *Saccharomyces cerevisiae* (*S. cerevisiae*) (Reiser et al. 1990), *Pichia pastoris* (*P. pastoris*) (Macauley-Patrick et al. 2005), and *Hansenula polymorpha* (*H. polymorpha*) (Hitzeman et al. 1988). Among them, *S. cerevisiae* has long been used as a model eukaryotic microorganism in that its genetics (Romanos, Scorer, and Clare 1992), metabolism and biochemistry are well studied and documented.

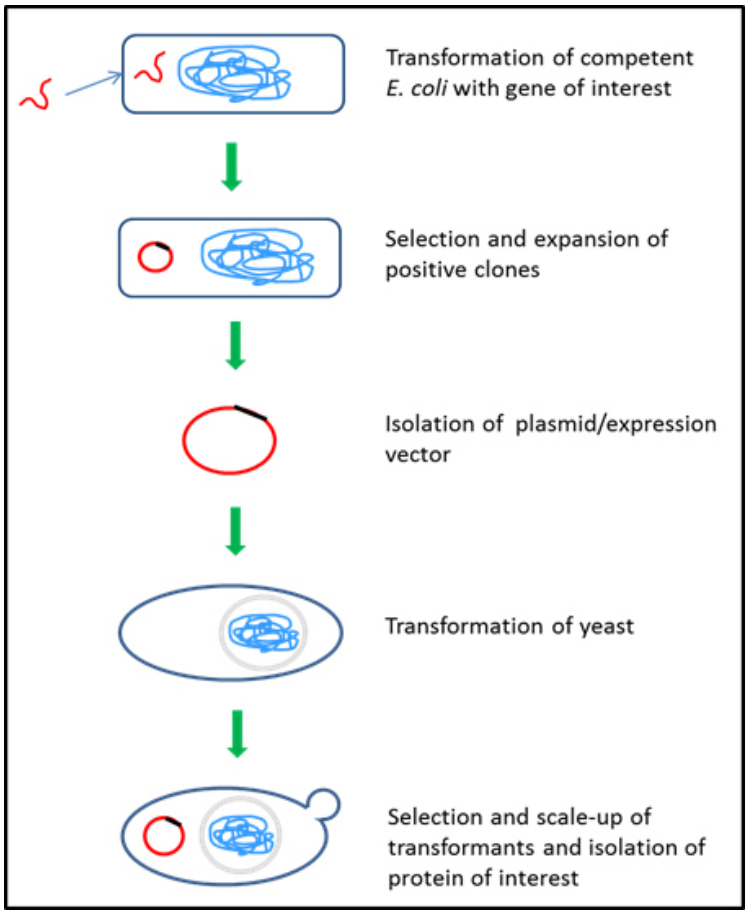

Figure 2-3. Yeast protein expression system. Figure adapted from Millipore Sigma.

Currently, the majority of yeast-derived products on the market are produced in *S. cerevisiae* (Hitzeman et al. 1981), which is recognized by the American Food and Drug Administration (FDA) as an organism generally regarded as safe (GRAS). The production of industrial enzymes by *S. cerevisiae* has far outweighed other microorganisms, with its share rivaling the total of microbial hosts (Ferrer-Miralles et al. 2009). Especially for the recombinant production of fungal enzymes, secretory expression in yeasts is often the best choice. Nevertheless, the strong fermentative metabolism of yeast can reduce the recombinant protein productivity. An undesirable hyper-glycosylation of protein products is often found in *S. cerevisiae* (Porro et al. 2000; Romanos et al. 1992), which can alter their original structural and functional properties.

2.2.2.3 Insect Expression System

Insect cells were chosen as the primary expression system for this study because of their relatively high protein production level and broad eukaryotic protein processing abilities (Jarvis 2009). As one of the most widely used higher eukaryotic expression systems, insect cells have a very wide range of PTMs, protein folding and trafficking pathways similar to mammalian cells (Contreras-Gómez et al. 2014; Jarvis 2009; McKenzie and Abbott 2018). These cellular and metabolic processes allow for production of recombinant proteins with proper conformation and function that cannot be achieved by prokaryotic systems. Whereas other expression systems rely on conventional physio-chemical gene delivery methods (Jha et al. 1992; Sridhar et al. 1994), genetically modified baculovirus is used to introduce the foreign DNA into insect cells for high expression of recombinant proteins (Figure 2-4) (Rooney, Butrovich, and Ware 2000). Generally, the yield can reach up to 25-50% of total cellular proteins or more than 100 mg of recombinant protein per liter of infected insect cell culture (Jarvis 2009; Possee 1993).

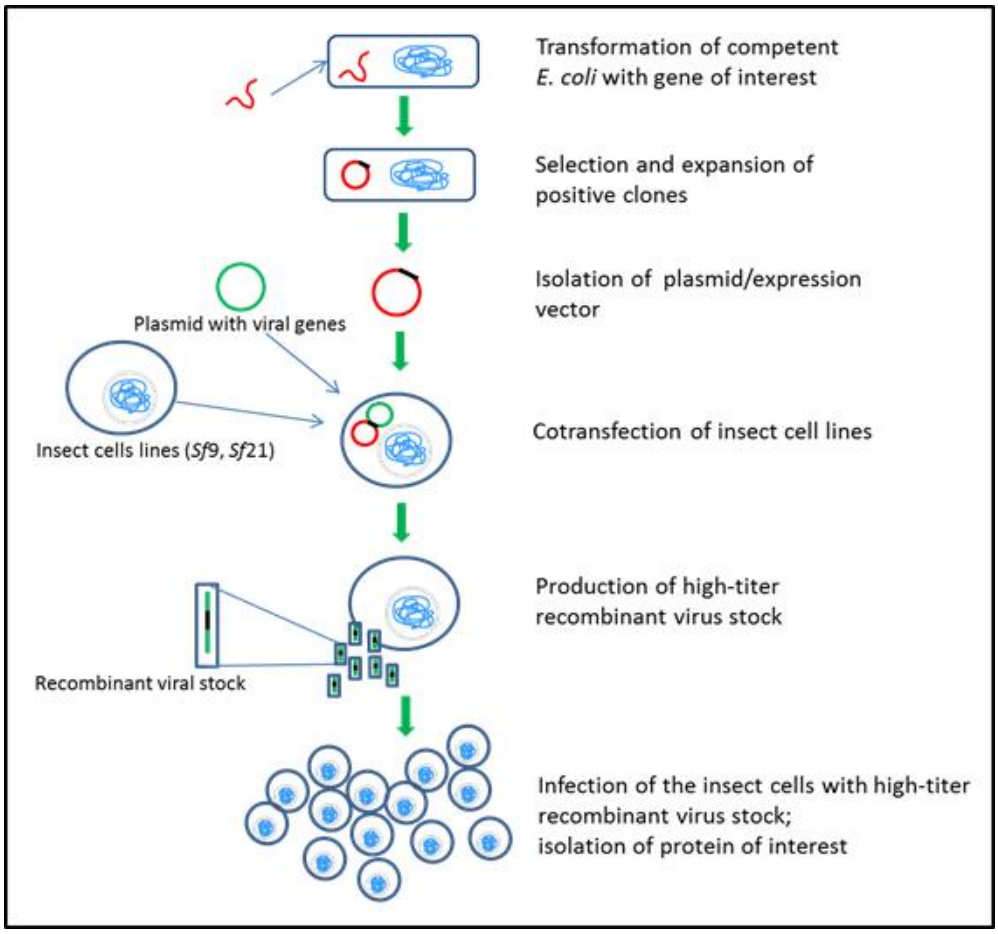

Figure 2-4. Insect cell expression system. Figure adapted from Millipore Sigma.

There are over 100 original cell lines described which are capable of being infected by baculovirus and yet have not been fully characterized. The insect cell lines mainly used in research and industrial settings are developed from the lepidopteran family. They are Sf9 and Sf21 cells (Max and Gale 1987; Vaughn et al. 1977), both derived from the *Spodoptera frugiperda* fall army worm pupal ovary, and High Five Tn-5B1-4 cells derived from the *Trichoplusia ni* cabbage looper embryo (Wickham and Nemerow 1993). These cell lines can be easily adapted to high cell density suspension cultures at 28 °C in absence of CO_2 for large-scale protein expression (van Oers 2011). These well-established culture conditions favor the ease

of handling and scaling up in contrast to mammalian cells (Vicente et al. 2011). These cells can also be maintained in serum free medium, which greatly saves the cost and facilitates secretory protein purification (McKenzie and Abbott 2018). In addition, this expression system has low risk biosafety profile as baculovirus strains display highly species-specific infection (Possee and King 2016). They are noninfectious to vertebrates and their promoters become inactive in mammalian cells. The lepidopteran insect cells established for research use are also known to be free of human pathogens (van Oers 2011).

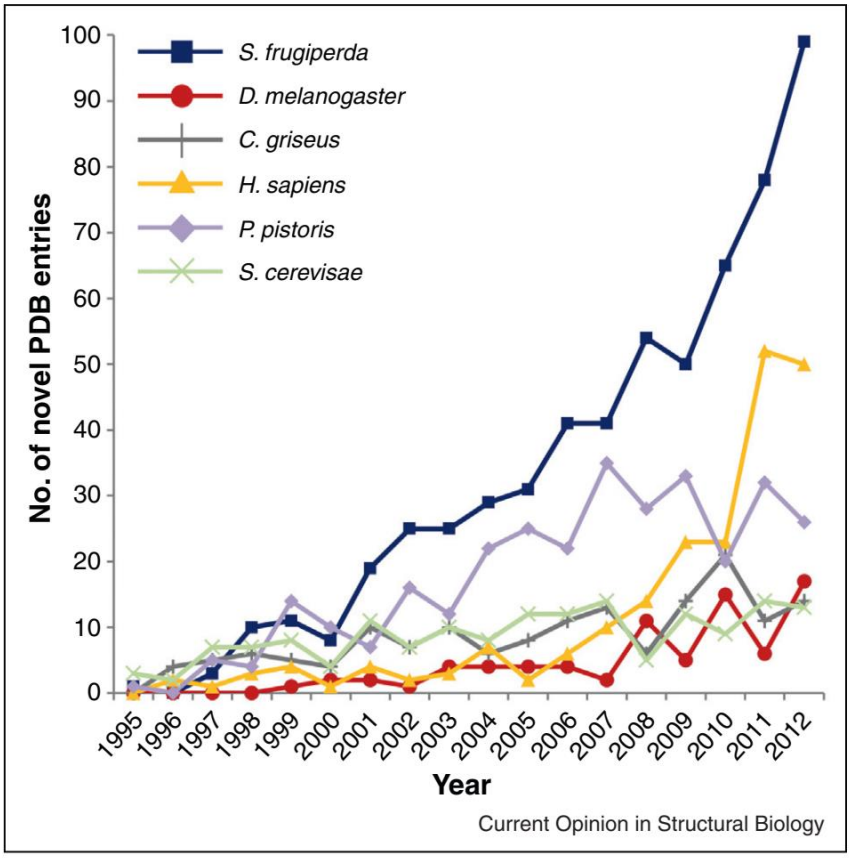

Figure 2-5. Impact and growth of different eukaryotic protein expression systems on structural biology. The graph shows the number of new, unique entries added to the Protein Data Bank (PDB) each year. *S. frugiperda* represents the baculovirus-mediated insect cell expression and *H. sapiens* represents HEK293 mammalian cell expression. Figure adapted from Assenberg et al. 2013.

The insect expression system has proven valuable for functional and structural studies of membrane proteins as well as for production of biopharmaceutical proteins (Kost, Condreay, and Jarvis 2005; Kost and Kemp 2016a). Among all eukaryotic expression systems, it is leading the way to producing proteins of high diffraction quality, tremendously contributing to the structural biology (Figure 2-5) (Assenberg et al. 2013). The structure of more than 70% known G protein-coupled receptors (GPCRs) were solved using insect expression system (Saarenpää, Jaakola, and Goldman 2015). Additionally, it has been successfully applied to commercial vaccine manufacturing (Mena and Kamen 2011; Metz and Pijlman 2011; Rychlowska et al. 2011). Examples include the human papilloma virus vaccine, Cervarix (Schiller et al. 2008), which is also the first FDA approved insect cell produced product, and the influenza virus vaccine, FluBlok (Krammer et al. 2010; Krammer and Grabherr 2010).

Traditionally, plaque purification for recombinant baculovirus has been cumbersome and time-consuming, therefore compromising the adaption of this system to automated HT protein production platforms. Also, the culture conditions are more challenging than prokaryotic systems. Despite the adequate capabilities of disulfide bond formation, PTMs and secretory mechanisms, insect cells are not completely interchangeable with mammalian cells unless they are modified with additional enzymes to create mammalian type structures. For example, one of the most notable difference is that N-linked glycosylation in insect cells is much simpler, restricted to small high mannose structures, and this might cause variations to the native form of protein products (McKenzie and Abbott 2018).

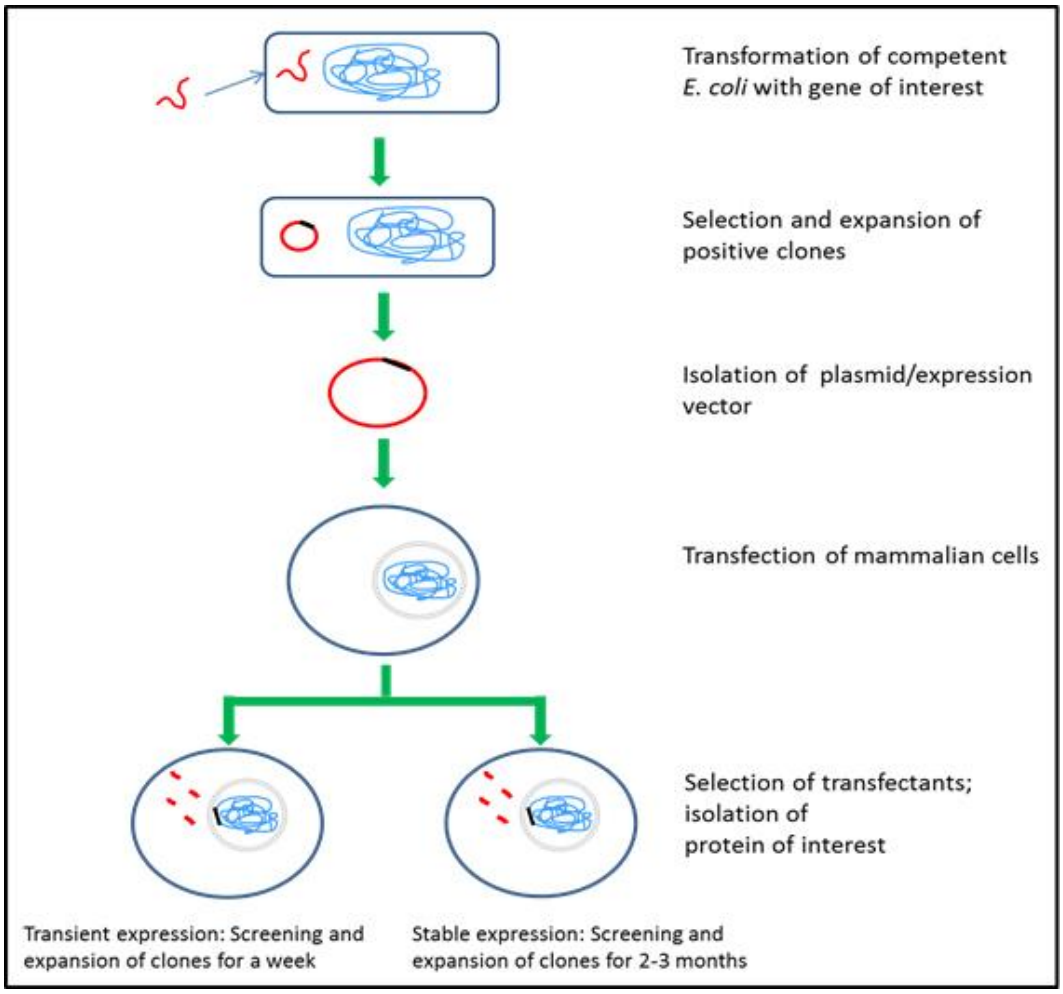

Figure 2-6. Mammalian cell expression system. Figure adapted from Millipore Sigma.

2.2.2.4 Mammalian Expression System

Mammalian expression system is the preferred method for the expression of complex mammalian proteins, such as antibodies (Kost and Kemp 2016b), secreted and membrane proteins, mainly because they offer native cellular environments for transcription and translation. This unique advantage, which cannot be matched by prokaryotic hosts, provides the physiologically relevant chaperones, secretory apparatus, redox milieu and PTMs that lead to properly folded and functionally active proteins very close to their native forms.

The two main expression host cell lines are Chinese hamster ovary (CHO) cells, which were originally isolated as spontaneously immortalized cells from primary CHO cultures, and human embryonic kidney (HEK) 293 cells (Puck, Cieciura, and Robinson 1958), which were originally established by transformation of HEK cells with sheared human adenovirus DNA (Graham et al. 1977). Both cell lines have a doubling time of ~24 hr and can grow to a high density of more than 5 million cells/mL (Hunter et al. 2019). A series of derivative cell lines have been constructed for enhanced transgene expression as well as suspension adapted cultures in serum free media (Liu et al. 2008; Rio, Clark, and Tjian 1985; Yates, Warren, and Sugden 1985). Mammalian expression system can be used to produce proteins transiently or through stable cell lines, where the DNA construct for expression is integrated into the host genome (Figure 2-6). While stable cell lines can be sustainably used over several generations, it takes a long time to isolate a stably transfected, high-yielding cell line with a selectable marker (Wurm 2004). Also, the integrated transgene in host genome might be affected by the chromatin positional effects, where the expression of transgene is negatively influenced or even silenced by the chromatin surrounding the integration site (Giraldo and Montoliu 2001). In contrast, transient gene expression can be conducted quickly and produces proteins in relatively high amounts. However, because the transgene tends to get lost during cell division, it suffers from a short-term effectiveness, with the protein yield peaking within 2 days after transfection followed by a rapid decline to the minimal level in approximately a week (Burkholder, Decker, and Ning-Sun Yang 1993; McKenzie and Abbott 2018; Yang et al. 1990). Major technical advances in the development of vector constructs and host cells have been made to mammalian expression system over the past decades to improve the efficiency and cut the cost (Barnes and Dickson 2006). Still, it is much more expensive to maintain and more difficult to scale up compared to

bacteria, yeast, and insect cell expression systems. Because mammalian cells are sensitive to environment fluctuations, such as pH (7.4), temperature (~37 °C), osmolality, CO_2 concentration (5-7%), they need more demanding culture conditions for the optimal protein expression, which requires specialized equipment and expertise.

2.2.2.5 Cell-Free Expression System

Unlike cell-based expression systems where protein expression takes place within various cell hosts, cell-free expression system favors *in vitro* synthesis of proteins by making use of whole cell extracts that contain all the macromolecules and components needed for transcription, translation and even PTMs (Katzen, Chang, and Kudlicki 2005). The essential components include RNA polymerase, regulatory protein factors, transcription factors, ribosomes and tRNA. Cell extracts are often prepared from *E. coli*, wheat germs (Katzen et al. 2005), rabbit reticulocytes, and HeLa cells. When supplemented with the DNA template, these cell extracts can produce proteins very quickly in a few hours without the hassle of cell culture and lysis.

Since cell-free expression system is independent of host cells, it allows for synthesis of cytotoxic and insoluble proteins (Klammt et al. 2007; Xu et al. 2005), novel proteins with modified amino acids (Bundy and Swartz 2010; Chattopadhaya, Tan, and Yao 2006), and proteins prone to be degraded by intracellular proteases. Coupled *in vitro* transcription and translation (IVTT) can be initiated using PCR products (Hanes and Plückthun 1997), avoiding the need for cloning of target genes into expression vectors as well as DNA transfection when using *in vivo* protein expression. Because of the easy manipulation and fast synthesis, cell-free expression system makes it simpler and more convenient to produce many different proteins simultaneously. Besides, this system is compatible with automation, which can

largely enhance the throughput of protein production and favor proteomic level studies (Vinarov et al. 2004; Yokoyama 2003).

A major limitation of cell-free expression system is the high cost, restricting its use to protein production of small quantities for analytical purposes and functional studies (Botte, Deniaud, and Schaffitzel 2016), rather than large-scale protein production. It is also documented that *in vitro* ribosomal machinery, mainly enzymes, become less active over time in cell extracts, which could dampen the expression inefficiency (Matsubayashi, Kuruma, and Ueda 2014). Also, the lack of essential chaperones and PTMs associated with prokaryotic extracts results in protein products without proper conformation or activity (Botte et al. 2016). On the other hand, eukaryotic extracts are often less productive due to the rate-limiting step of mRNA capping required for translation initiation (Swartz 2009), which represents a major barrier in activation of *in vitro* protein synthesis and results in low protein yields (Zemella et al. 2015).

2.2.3 Baculovirus Expression Vector System (BEVS)

2.2.3.1 Overview of Baculovirology

Baculovirus is a family of lytic, insect-pathogenic viruses that can replicate in the nucleus of infected insect cells (Contreras-Gómez et al. 2014; Ghosh et al. 2002; Van Oers and Vlak 1997). They have a large rod-shaped double-stranded circular DNA (dsDNA) genome of 80-180 kb (Funk, Braunagel, and Rohrmann 1997). Currently, there are 76 known species in this family (Harrison et al. 2018), which are categorized into 4 genera, i.e. alphabaculovirus, betabaculovirus, gammabaculovirus and deltabaculovirus. In nature, baculovirus can cause lethal disintegration to insect bodies, namely "wilting disease", by infecting and lysing the mid-gut cells of hosts and thus is often used as biological pesticides for pest control in agricultural industry (Mishra 1998; Moscardi et al. 2011). Baculovirus has a highly restricted host range.

Particularly, alphabaculovirus and betabaculovirus are only specific for the order Lepidoptera, gammabaculoviruses for Hymenoptera, while deltabaculoviruses for Diptera (Jehle et al. 2006).

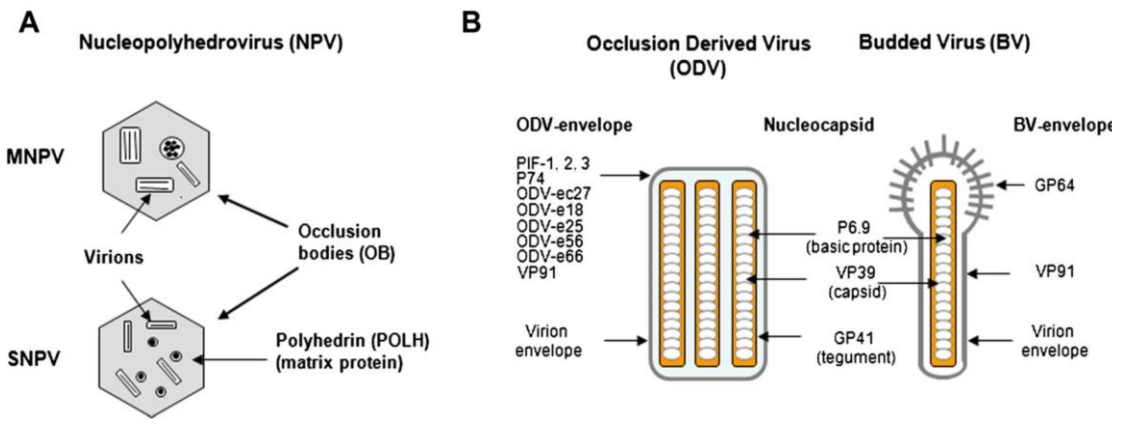

Figure 2-7. The biology of baculovirus. **A)** The ODVs of nucleopolyhedrovirus (NPV) containing either single (SNPV) or multiple (MNPV) nucleocapsids are occluded in polh protein matrix to form large OBs. **B)** Two forms of virions are genotypically same but phenotypically different. Depending on the virion types, either one (BV) or more (ODV) nucleocapsids are packaged into rod-shaped virion envelopes composed of different fusion proteins. Figure adapted from van Oers 2011.

2.2.3.1.1 Life Cycle of Baculovirus

Baculoviruses have a biphasic life cycle driven by the two structurally and functionally distinct forms of virions: occlusion derived virion (ODV) and budded virion (BV) (Figure 2-7B) (Possee et al. 2011). ODV is assembled entirely in the nucleus of infected cells and is occluded in a protein matrix composed of polyhedrin (polyh) or granulin to form occlusion bodies (OBs) of 0.15-5 μm in diameter. The initial primary infection occurs when the host feeds on plants contaminated with OBs (Figure 2-8) (Szewczyk et al. 2006). The protein matrix of OBs is dissolved by the alkaline environment in the host mid-gut, liberating embedded ODVs, which enter the susceptible epithelial cells through adsorptive endocytosis or fusion to cell membranes (Volkman and Goldsmith 1985). Through actin filaments mediated

transportation, viral nucleocapsid is directed to the host nucleus and uncoated for replication and transcription, producing new ODVs and BVs. BVs are budded out from cell membrane to spread the secondary systemic infection between cells and tissues within the infected insect larvae (Contreras-Gómez et al. 2014; Ghosh et al. 2002). As ODVs are accumulating in the cell nucleus, viral proteases lyse the host cells and degrade the chitinous exoskeleton of the insect, causing extensive cell lysis and eventually host death (Figure 2-8). When the larval body is disintegrated, millions of ODVs are dispersed into the environment for further horizontal transmission in a larval population (Contreras-Gómez et al. 2014).

Depending on the virus genus, distinct number of ODVs can be occluded in OBs of baculovirus (Contreras-Gómez et al. 2014; Jehle et al. 2006; Van Oers and Vlak 1997; Possee et al. 2011). Whereas granulovirus (genus betabaculovirus) produces granular OBs composed of granulin proteins that carry only one ODV, nucleopolyhedrovirus (NPV) (genera alphabaculovirus, gammabaculovirus and deltabaculovirus) produces large polyhedral shaped OBs composed of polh proteins that may harbor over 100 ODVs. Furthermore, depending on the virus species, one (single) or a variable number (multiple) of nucleocapsids may be packaged per ODV in single capsid nucleopolyhedrovirus (SNPV) or multicapsid nucleopolyhedrovirus (MNPV), respectively (Figure 2-7A) (Harrison et al. 2018). Another feature that distinguishes these genera is the glycoproteins displayed on BV envelope, which regulates BV budding from cells as well as attachment and fusion between viral and cellular membranes (Herniou and Jehle 2007). Specifically, group I alphabaculovirus expresses the glycoprotein gp64 as the BV envelope fusion protein, which forms into peplomer structures on the end of BV, to carry out the abovementioned processes (Figure 2-7B) (Monsma, Oomens, and Blissard 1996). On the other hand, it is the non-homologous F protein that performs these functions in group II

alphabaculovirus, betabaculovirus and deltabaculovirus (Ijkel et al. 2000). In contrast, gammabaculovirus infection is restricted to the host gut because they have no BV fusion proteins to spread systemic infection from cell to cell.

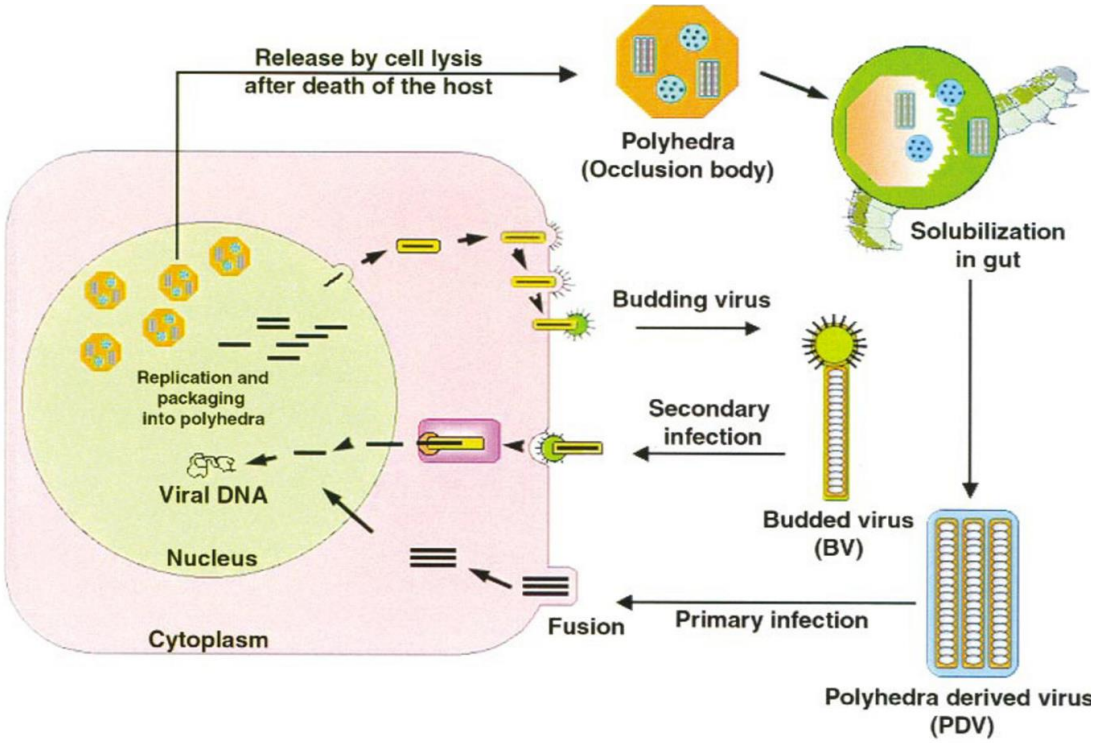

Figure 2-8. The natural life cycle of baculovirus. The primary infection occurs when ODVs are orally taken by insect larvae and released to infect mid-gut epithelial cells. Viral DNA is replicated and transcribed to produce new ODVs and BVs, and the latter infect other cells of the larvae host. The accumulation of OBs eventually leads to extensive lysis of cells and death of the host, liberating millions of new OBs to the environment for horizontal transmission. Figure adapted from Ghosh et al. 2002.

ODV and BV are genotypically the same but phenotypically very different (Figure 2-7B) (Possee et al. 2011). While generally only one nucleocapsid is packaged in the BV envelope, ODV can package more than one nucleocapsids. Except for a few common proteins for nucleocapsid formation, such as p6.9 and VP39, they assemble unique proteins of their own to the virion envelope. The lipid composition of the virion envelope is also different between the two virion forms in

that BV envelope consists of phosphatidylserine, while ODV envelope contains phosphatidylcholine and phosphatidylethanolamine (Braunagel and Summers 1994). NPVs survive outside their host in the form of OBs that consist of a proteinaceous matrix to shield embedded ODVs (Contreras-Gómez et al. 2014; Van Oers and Vlak 1997). Therefore, ODV is more resistant to heat and light inactivation. Although BV is more sensitive to environmental changes, it is noted as a perfect form of virion to be used for insect cell protein expression as it is more infectious than ODV by ~1,800 times (Volkman, Summers, and Hsieh 1976).

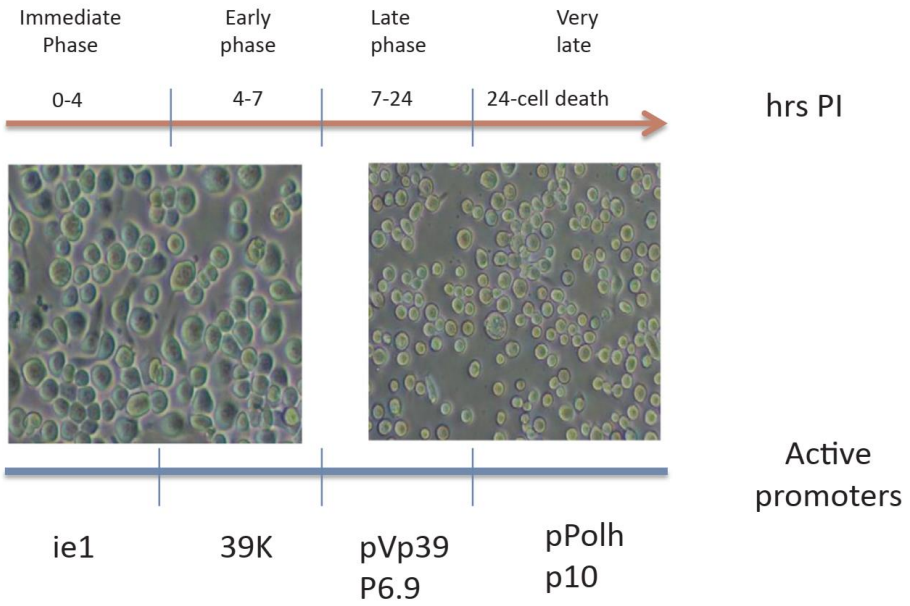

Figure 2-9. The four phases of the insect cell infection cycle. Phase-specific promoters become active at defined points to induce the expression of phase-specific genes. The schematic illustrates the typical cell morphological changes upon viral infection. Figure adapted from McKenzie and Abbott 2018.

2.2.3.1.2 Gene Expression Phases in Baculovirus

Baculovirus proteins are expressed in a temporally regulated, sequential fashion during the course of infection, which can be divided roughly into four successive phases: immediate-early, delayed-early, late, and very late phase

(Friesen 1997; Passarelli and Guarino 2007; Slack and Arif 2006). Early genes have host-like promoters, which can be recognized and transcribed by the host transcriptional machinery. This enables the initiation of viral gene expression at the very beginning of the infectious cycle in the absence of other baculovirus factors (Harrison and Jarvis 2016). Particularly, the **immediate-early genes** are transcribed by the host-encoded RNA polymerase II (RNAP II), which activate delayed-early and late genes. Subsequently, the **delayed-early genes** are also transcribed by host RNAP II, which encode proteins required for DNA replication and late gene expression, including DNA polymerase, helicase, a four-subunit viral RNA polymerase, and the late essential factors (Ahrens and Rohrmann 1995; Kool et al. 1995; Todd, Passarelli, and Miller 1995). The baculovirus is smart in that during this phase it also synthesizes proteins that prevent host defense system, such as apoptosis inhibitors, so that it can continuously make use of host materials and energy for its own reproduction (Clem 2007). In the late phase, the replication of viral genomic DNA is initiated followed by the expression of late genes (Passarelli and Guarino 2007), which is dependent on virus-encoded transcriptional machinery. As opposed to the host-like promoters in early genes, the late genes harbor virus-specific promoters that generally contain a typical TAAG motif to be recognized and transcribed by viral RNA polymerase, which is composed of four subunits: lef-4, lef-8, lef-9, and p47 (Passarelli 2007). The **late genes** encode nucleocapsid and viral envelope proteins, which are involved in virion assembly and virus budding. Similar to the late genes, the **very late genes** also have the virus-specific promoters containing the TAAG motif and an additional downstream ‘‘burst’’ sequence, which leads to hypertranscription of viral proteins involved in the production and assembly of OBs (Contreras-Gómez et al. 2014; Van Oers and Vlak 1997; Rychlowska et al. 2011). Particularly, in the very late phase, two viral proteins, polh (33 kD) and p10

(10 kD), are expressed in very large amounts under the control of two extremely strong promoters (Van Oers and Vlak 1997; Rohrmann 1986). Polh forms the crystalline protein matrix of OBs where ODVs are embedded, while p10 forms the fibrillar structure, which seems to be related to the release of OBs from the nucleus of infected cells towards the end of infection (Carpentier and King 2009).

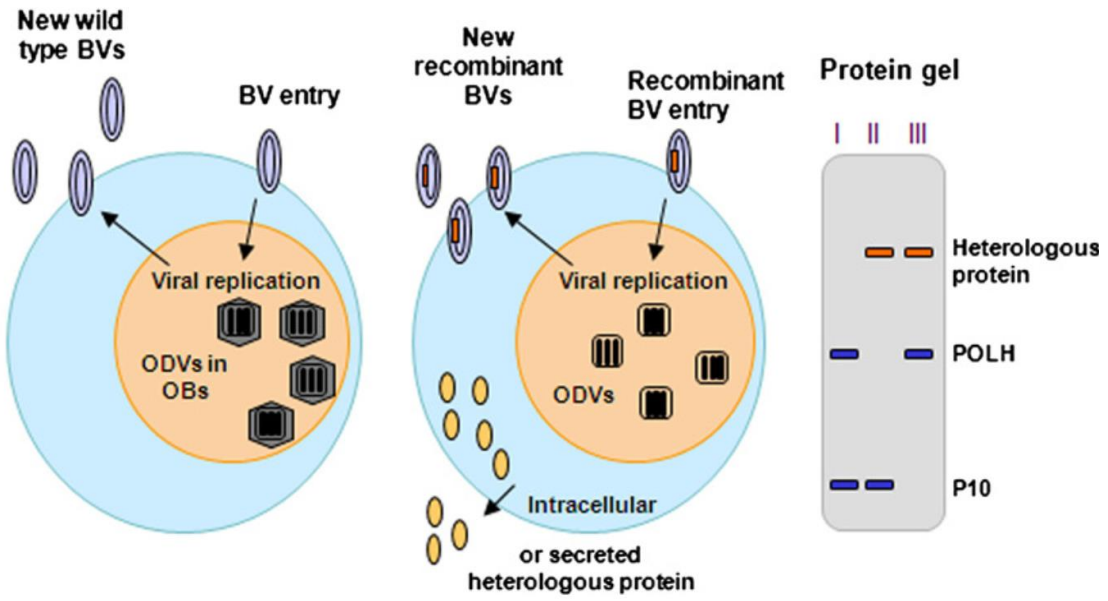

Figure 2-10. The working principle of BEVS. The left panel shows the infection of insect cells with WT BV, the middle panel with a recombinant BV where the polh promoter drives the expression of a foreign gene, resulting in the absence of OBs as well as the production of new recombinant BVs and heterologous target proteins. The right panel shows a schematic of a protein gel for insect cells infected with WT virus (I), polh (II), and p10 (III) promoter-based recombinant baculovirus. Figure adapted from van Oers 2011.

Baculovirus infection of cultured insect cells follows a similar temporal pattern comprising four defined stages (Figure 2-9) (McKenzie and Abbott 2018). During the immediate phase (0–4 hr pi), baculoviruses enter the insect cells and viral DNA is released from virion envelope into the nucleus. This is followed by the early phase (4–7 hr pi) when viral DNA replication occurs. During the late phase (7–24 hr pi), BVs are assembled and budded from infected cells, and secondary infection of

surrounding cells occurs. During the very late phase (24 hr until cell death) the stage specific promoters, like polh and p10 promoters, become active and ODVs are produced and embedded in OBs. Infected cells undergo apoptotic lysis, releasing the accumulated ODVs from the cell nucleus (Lynn and Harrison 2016).

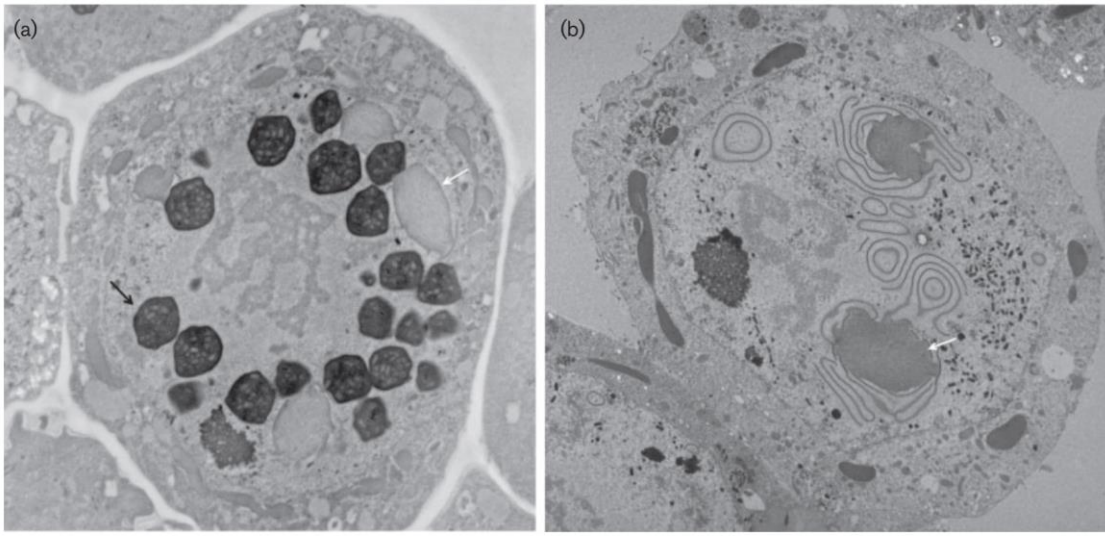

Figure 2-11. Electron micrographs of Sf21 insect cells infected with WT and recombinant AcMNPV. **A)** The black arrow points at a viral OB carrying ODV in the WT-infected cells. **B)** The cells infected with a polh promoter-based expression vector lack OBs and this characteristic is useful to select OB- recombinant viruses. Fibrillar structures composed of p10 protein are indicated by a white arrow. Figure adapted from van Oers, Pijlman, and Vlak 2015.

2.2.3.1.3 *Autographa Californica* Multicapsid Nucleopolyhedrovirus (AcMNPV)

The prototype of baculovirus, AcMNPV, is the first baculovirus strain that was completely sequenced in 1994 and consequently well characterized at the molecular level (Chambers et al. 2018). Its genomic DNA was found to be 134 kb in length with a maximum cloning capacity of at least 38 kb and encode 154 open reading frames (ORFs) (Ayres et al. 1994; Pidre et al. 2013). AcMNPV has a wide host range, being infectious and replicative in most cultured insect cell lines (Chambers et al. 2018; Luckow et al. 1993).

As the most commonly used baculovirus strain in insect expression system, it forms the basis of baculovirus expression vector system (BEVS). Several properties of AcMNPV that are beneficial to the development of BEVS include that: 1) the rod-shaped nature of the nucleocapsid and the large size of the genome allow for the insertion of multiple large segments of foreign DNA, supporting production of proteins or even complexes with large molecular weight (Van Oers, Pijlman, and Vlak 2015); 2) the extremely strong promoters of polh and p10 genes can be utilized for high expression of inserted foreign genes (Figure 2-10); 3) these promoters are not active until the very late phase of infection when BV production and budding is completed, such that polh and p10 are not essential factors for virus amplification in cell culture and can be replaced by foreign genes; 4) the absence of the polh protein can be used as a visible marker for the visual selection of the recombinant baculovirus that has no OB shield (Figure 2-11); 5) the peplomer structures formed by gp64 on the end of AcMNPV envelope effectively facilitate the viral attachment and fusion to cultured insect cells, assuring the high transduction efficiency; 6) AcMNPV transduction presents no toxic effects to insect cells even at high multiplicity of infection (MOI) so it does not disturb cell growth (Gao et al. 2002); 7) AcMNPV with transgene integrated to the genome are stable at 4 °C in dark for up to one year, providing good sustainability (Jorio, Tran, and Kamen 2006); and 8) AcMNPV is non-pathogenic to vertebrates, rendering the excellent inherent biosafety (Smith, Vlak, and Summers 1983).

2.2.3.2 Early Research on Baculovirus

A series of milestone discoveries along the way of baculovirus research revealed the biology of baculovirus and outlined the principle of BEVS (Van Oers et al. 2015). In 1971, the AcMNPV virus was first discovered and isolated from a single alfalfa looper (*Autographa californica*) specimen (Vail et al. 1971). It was later found

that the haemolymph of caterpillars infected by AcMNPV was highly infectious for cultured insect cells, which is crucial to the development of BEVS (Vaughn and Faulkner 1963). Further biological analysis of baculovirus life cycle led to understanding of two types of virions that are structurally and functionally different, i.e. BV and ODV (Volkman and Summers 1977). Subsequently, a study showed that transfection of cultured insect cells with purified DNA from AcMNPV could cause a successful infection, demonstrating the infectivity of baculovirus DNA (Burand, Summers, and Smith 1980).

In parallel with the biological studies, technological advances were also made. A plaque assay was developed to quantify infectious virus titers and isolate the recombinant from WT genotypes (Brown and Faulkner 1977). The genomic DNA of plaque-isolated AcMNPV strains were treated with restriction enzymes for sequence analysis (Lee and Miller 1978), and molecular cloning and mapping of individual genomic fragments eventually led to the representation of complete genomic DNA sequence of AcMNPV (Ayres et al. 1994; Lübbert et al. 1981). Analysis of time-dependent protein expression patterns in AcMNPV infected insect cells identified an extremely high expression of polh protein towards the end of infection, which accounted for > 25% of total cellular proteins (Smith, Vlak, et al. 1983), and its gene was mapped to AcMNPV genome. A follow-up study showed that polh protein is not essential to viral replication in infected insect cells, which is a significant finding and forms the basis of BEVS (Smith, Fraser, and Summers 1983).

The first BEVS for insect cells was described in 1983 by Smith et al. in the landmark publication on the production of recombinant human beta interferon (IFN-β) (Smith, Summers, and Fraser 1992). In this initial study, IFN-β gene was inserted at polh gene locus in AcMNPV genome, which was used as an expression vector for transfection. Biologically active interferon was produced and secreted from infected

Sf21 cells. Very soon thereafter, Pennock et al. reported the high expression of *E. coli* β-galactosidase in insect cells using an AcMNPV-derived expression vector (Pennock, Shoemaker, and Miller 1984). These pioneering studies hallmarked the birth of BEVS and brought the public attention to baculovirus-mediated insect cells as a potential powerful protein expression platform.

2.2.3.3 Development of BEVS

The general strategy of BEVS is to 1) construct a bacterial transfer plasmid carrying the gene of interest (GOI) flanked by sequences derived from polh gene and 2) co-transfect cultured insect cells with the transfer plasmid and the viral genomic DNA extracted from WT AcMNPV. Historically, the formation of recombinant virus relied on the spontaneous *in vivo* genetic recombination to integrate foreign genes into viral genome followed by selection based on altered viral phenotypes (King and Possee 1992). In the early years, the two major bottlenecks associated with the BEVS are the technically challenging and time-consuming processes of 1) cloning a GOI into a transfer plasmid for insertion into the viral genome (Hitchman, Possee, and King 2009) and 2) subsequently isolating recombinant viruses from non-recombinant parental viruses. Numerous attempts aimed at reducing time span, enhancing efficacy and user-friendliness of BEVS have been preceding in parallel to both viral genomic DNA and the transfer plasmid. For the latter, a variety of modifications have been designed and adopted to facilitate the identification of recombinant virus or the expression and purification of target proteins (Jarvis 2009). The introduction of a marker gene, such as LacZ that encodes *E. coli* β-galactosidase protein, to the transfer plasmid helps the differentiation of recombinant from non-recombinant virus through blue-white screening in a much easier way compared to OB- phenotype (D. R. O'Reilly, Miller, and Luckow 1992). Another type of modifications is aimed to make BEVS more versatile for different needs of protein

expression (Jarvis 2009), by adding the sequences encoding secretory signal peptides and amino- or carboxy-terminal purification tags. Also, the polh or p10 promoters have been replaced with alternative baculovirus promoters, such as ie1, as higher quality protein products can be obtained when expressing GOI under the control of immediate-early (ie) promoters (Jarvis, Weinkauf, and Guarino 1996).

The original procedure to generate recombinant viruses is by *in vivo* spontaneous homologous recombination between the viral genome and a transfer plasmid carrying the foreign gene placed under control of the polh or p10 promoter (Figure 2-12A) (Smith, Fraser, et al. 1983; Vlak et al. 1990). This foreign gene cassette is flanked by baculovirus genome fragments identical to the sequences up- and downstream of the desired insertion site, e.g. the polh or p10 locus, to facilitate recombination once co-transfected into insect cells. However, the spontaneous homologous recombination is a rare event with a typical frequency of 0.1-1% (Smith, Fraser, et al. 1983). The extremely low recombination efficiency associated with this method necessitates multiple virus isolation steps to avoid eventual outgrowth of the WT virus (Jarvis 2009; Van Oers et al. 2015). In general, repeated rounds of plaque assay using an agar overlay need to be performed (King and Possee 1992; J. J. O'Reilly et al. 1992), which is time-consuming and inefficient as it heavily relies on the visual inspection of plaques with OB- phenotype by trained research specialists under a dissecting microscope (Jarvis 2009). Later, a major improvement was made by linearizing the viral genome with a specific restriction enzyme *Bsu*36I that cleaves at polh locus (Kitts, Ayres, and Possee 1990). Recircularization of the viral genome, and the consequent generation of live and infectious baculovirus occurs upon recombination with a co-transfected transfer plasmid. This modification enhances the recovery of recombinant virus to ~30% as linearized viral genome cannot replicate and produce recombinant virus (Van Oers et

al. 2015). However, since *Bsu*36I restriction digestion is never 100% efficient, there is no guarantee for a homogenous population of recombinant progeny virus (Possee et al. 2008).

2.2.3.3.1 BacPAK6 System

Further engineering to the linearization approach gave birth to a more effective triple *Bsu*36I-digested viral genome, in which an engineered *E. coli* lacZ gene is incorporated for blue-white screening and a viral essential gene ORF1926 is disrupted by restriction enzyme digestion (Kitts and Possee 1993). ORF1629 is located downstream of the polh locus and encodes the phosphoprotein PP78/83, which is involved in nuclear actin filament formation during baculovirus infection and required for viral replication and infectivity (Ohkawa, Volkman, and Welch 2010). Upon recombination between the restricted viral genome and an appropriate transfer plasmid carrying the missing piece of ORF1629, GOI is incorporated into viral genome. Meanwhile, ORF1629 is restored and viral genome is recircularized, leading to production of infectious progeny virus (Figure 2-12B). This strategy, later commercialized as the BacPAK6 system (TaKaRa) along with the transfer plasmid pBacPAK6 (TaKaRa), dramatically increases the recombination frequency to over 90%, consequently eliminating the need for extensive plaque purification. This success stimulated the development, commercialization and popularization of BEVS for protein production in biomedical research community. Currently, there are several commercialized expression vector systems built on the AcMNPV genome, such as Bac-to-Bac, flashBAC (Possee et al. 2008), BacMagic, MultiBac, etc., that can generate the recombinant baculovirus by adopting various cloning strategies.

2.2.3.3.2 Bac-to-Bac System

In parallel with the homologous recombination, another new approach that relies on the genetic transposition has been developed to generate recombinant

virus. The construction of bacterial artificial chromosome (BAC) that is incorporated into a cloned copy of the entire AcMNPV genome, namely bacmid, permits the manipulation and maintenance of recombinant virus in *E. coli* DH10Bac strain (Figure 2-12C) (Luckow et al. 1993). The bacmid is engineered with a Tn7 transposition site and a mini-F replicon to allow low copy amplification of the viral genomic DNA in bacterial cells. Upon transformation of *E. coli* DH10Bac cells carrying the bacmid with a transfer plasmid containing a GOI, a polh or p10 promoter, and a reporter gene, such as green fluorescence protein (GFP), altogether flanked by the right and left ends of Tn7 (Tn7R and Tn7L), the GOI is transferred to bacmid by site-directed transposition with the help of Tn7 transposase, which is generally expressed by an independent helper plasmid in *E. coli* DH10Bac cells. The recombinant clones are then selected and amplified followed by extraction of recombinant bacmid to transfect cultured insect cells. Once inside the cells, the bacmid DNA is transcribed to initiate the expression cascade, and recombinant virus can be harvested from the culture supernatant and used to infect new cells to produce high titer seed stocks for recombinant protein production (Van Oers and Vlak 1997).

This *in vivo* transposition approach can produce recombinant virus with almost 100% efficiency without the need for plaque purification and has been commercialized as the Bac-to-Bac system (Invitrogen) (Jarvis 2009). Various transfer plasmid systems are also available to work with the Bac-to-Bac system, such as pFastBac1 and pFastBacDual (Invitrogen), which enables the expression of single or multiple proteins, respectively (Van Oers and Vlak 1997). Yet, a major disadvantage of this system is the loss of target protein expression after serial passage of recombinant virus in insect cells (Kohlbrenner et al. 2005), and this might be associated with the genetic instability due to the presence of bacterial replicon or transposition sequences retained in viral genome (Pijlman, van Schinjndel, and Vlak

2003). In addition, multiple time-consuming steps of selection, such as antibiotic selection, blue-white or reporter protein screening, followed by amplification of recombinant bacmid in bacteria are required prior to making recombinant virus, which slow down the process and result in a high cost when a large number of constructs need to be tested (Van Oers and Vlak 1997). These disadvantages compromise the popularity of Bac-to-Bac system in HT protein expression as well as its amenability to automation (Radner et al. 2012).

2.2.3.3.3 flashBAC System

A more recently developed system combines the concepts of *in vivo* homologous recombination and bacmid technology (Possee et al. 2008), allowing for the rapid one-step generation of recombinant virus and HT expression of heterogenous proteins in insect cells. In essence, a modified bacmid is built on a restricted AcMNPV genome that contains BAC at the polh locus and lacks a portion of downstream ORF1629 gene flanking the insertion site (Figure 2-12D) (Possee et al. 2008). These features permit the autonomous replication of bacmid in bacterial cells but not in insect cells, and the bacmid can thus be easily amplified and extracted from *E. coli*. Subsequently, the bacmid and transfer plasmid that carry GOI flanked by viral genes lef2/ORF603 and ORF1629 are co-transfected in insect cells, and upon homologous recombination ORF1629 gene essential for replication is restored, accompanied by the knock-out of BAC from the polh locus and the concomitant knock-in of GOI under the polh promoter. Since the non-recombinant virus is not able to replicate due to the defective ORF1926 gene, no further separation procedures are required, and recombinant virus can be easily recovered with an extremely high efficiency. This selection process is independent of a helper plasmid that provides Tn7 transposase as required for the conventional bacmid technology, thus remarkably reducing the time and complexity of producing recombinant virus

(Jarvis 2009). Also, the removal of BAC from recombinant viral DNA obviates the concern about the BAC associated genetic instability within insect cells (Jarvis 2009). This technology has been commercialized as flashBAC system (Oxford ET) and adapted to semi-automated protein production platforms using robotic arms (Hitchman, Possee, and King 2012). A series of transfer plasmids compatible with the flashBAC system are also commercially available as pOET (Oxford ET).

2.2.3.3.4 BacMagic System

The BacMagic system (Novagen) follows the same cloning principle as the flashBac system. The bacmid used in this system, i.e. BacMagic DNA, is an AcMNPV genome with a portion of ORF1629 deleted and a BAC in place of the polh coding region. In brief, the defective viral genome that fails to initiate viral propagation and infection in insect cells is rescued by homologous recombination with the transfer plasmid, thus achieving a positive selection of recombinant virus. Importantly, this allows 100% recombinant virus formation and often produces virus titers sufficient for test expression or scaled-up production directly from transfected cultures (Radner et al. 2012). The high virus titers generated using this method not only shorten the virus amplification process but also ensure the successful mass parallel protein expression using a universal volume-based virus-to-cell ratio without the need for performing titration assays on each individual virus stock. In this study, a virus-to-cell ratio of 1:200 (v/v) was used for all infections in place of the MOI ratio and able to produce proteins with high success rate. In addition, the latest bacmid in this system, BacMagic-3, has been further modified with deletions of several non-essential viral genes, such as chitinase (*chiA*), cathepsin (*v-cath*), *p10*, *p74*, and *p26*, which greatly improves the recombinant protein yield by reducing the protein degradation and increasing the recombinant biomass (Hitchman et al. 2010).

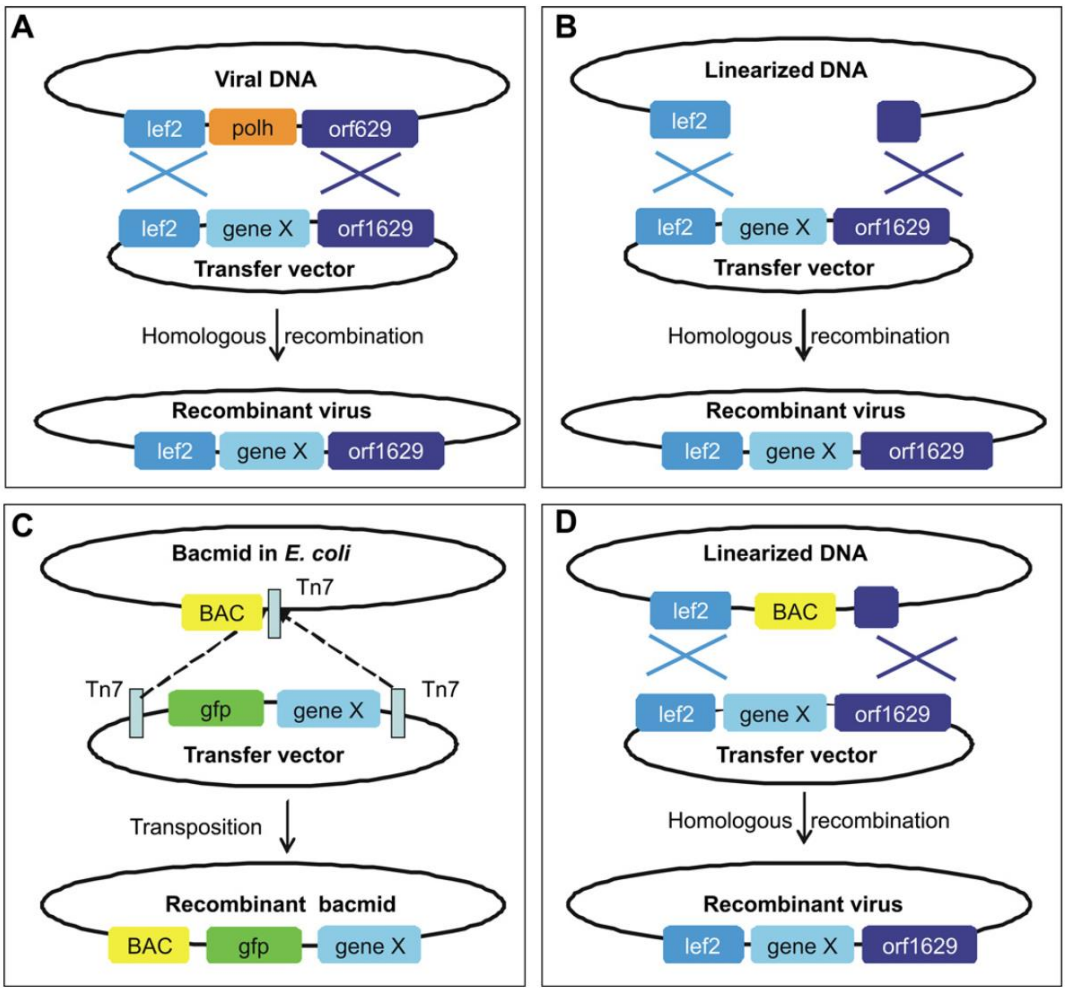

Figure 2-12. The schematic of BEVS using various strategies. **A)** Historically, recombinant baculovirus is generated through spontaneous homologous recombination. **B)** Subsequently, a linearized viral genome in which the disrupted essential gene orf1629 is restored upon recombination is used to increase the recombination efficiency. **C)** Bacmid technology is based on transposition of foreign gene X into a bacterial artificial chromosome (BAC) containing the baculovirus genome and which is amplified and manipulated in E. coli. **D)** Bacmid technology and the repair of an essential gene were combined to avoid bacterial sequences in the virus genome and further automated (flashback/BacMagic) for high-throughput recombinant virus generation. Figure adapted from van Oers 2011.

Various commercially available transfer plasmids, such as pIEx/Bac, pBAC, and pTriEx (Novagen), are designed to work with the BacMagic system for HT screening and robust protein expression. Unlike pBAC or pTriEx, which uses the polh

or p10 promoter, respectively, pIEx/Bac is featured with the incorporation of the hr5/ie1/p10/ie1 enhancer/promoter/terminator combination flanked by upstream lef2/ORF603 and downstream partial ORF1629. Transfer plasmids that only carry the p10 or polh promoter in the above-mentioned BEVS can only direct expression in the late/very late phase of baculovirus infection. In contrast, recombinant baculovirus created with the pIEx/Bac vector is capable of expressing target protein throughout the infection process, thus providing greater flexibility and optimization for insect cell expression (Radner et al. 2012). Specifically, the hr5 enhancer/ie1 promoter directs the plasmid-mediated and early baculovirus-mediated expression and the p10 promoter directs the late/very late baculovirus-mediated expression (Carpentier and King 2009; Jarvis et al. 1996; Pullen and Friesen 1995). It is recommended that when expressing a sensitive target protein or a protein requiring uniform post-translational modification, using earlier promoter-based transfer plasmids, like pIEx/Bac, may be optimal as this may result in improved glycosylation, solubility and overall yields (Jarvis et al. 1996; McKenzie and Abbott 2018).

2.2.4 Gateway Cloning

Given the above-mentioned advantages, the BacMagic-3 system along with the transfer plasmid pIEx/Bac were selected to build the protein production pipeline in this study. However, the insertion of target gene into the pIEx/Bac vector requires restriction and ligation cloning that is not compatible with HT screening of many expression constructs. Also, restriction enzymes might result in unwanted truncation of the insert and additional clean-up steps are required to process the restriction products. To reduce the time and resources needed to generate recombinant baculovirus at large scale, Radner et al. developed a ligation independent cloning (LIC) variant of pIEx/Bac vector that permits parallel LIC cloning and screening of expression constructs in insect cells (Radner et al. 2012). Alternatively, LIC-

compatible pIEx/Bac vector is also commercially available as pIEx/Bac LIC (Novagen). However, either multiple rounds of subcloning or substantial preparation of inserts from a genomic or cDNA template are required to obtain appropriately prepared PCR products prior to their insertion into the pIEx/Bac vector (Berrow et al. 2007).

Gateway recombination cloning technology circumvents these traditional restriction and ligation-based cloning limitations. More importantly, in conjunction with any existing Gateway clone libraries, it supports the easy and convenient one-step multiparallel transfer of any GOI in frame from their Gateway donor clones. Gateway cloning takes advantage of the well-characterized site-specific recombination system used by bacteriophage λ to integrate its DNA in the *E. coli* chromosome (Hartley, Temple, and Brasch 2000). The recombination reactions mediated by the λ integrase family are known to be conservative, resulting no net gain or loss of nucleotides (Landy 1989). With the help of proprietary recombinase, namely LR clonase, to recognize the "*att*" recombination sites, LR reaction is carried out such that DNA fragments flanked by *att*L1/2 and those flanked by *att*R1/2 are exchanged, as *att*L X *att*R → *att*B X *att*P. The fact that the *att*L1 can only recombine with *att*R1 but not *att*R2 enables the DNA fragments to maintain the original orientation during the *in vitro* recombination reaction (Hartley et al. 2000). Because the recombination sites, namely "*att*" sites, are much longer (25–242 bp) than restriction sites, they are extremely unlikely to occur by chance in DNA fragments. Therefore, the same recombinase can be used to robustly clone many different ORFs of variable size between plasmids in parallel reactions (Reece-Hoyes and Walhout 2018).

Two plasmids needed for LR reaction as the starting materials include a Gateway donor clone (*att*L1-ORF-*att*L2), which carries and donates the ORF to be

cloned, and a Gateway destination vector (*att*R1-*ccd*B-*att*R2), which receives the ORF for gene expression (Hartley et al. 2000). The LR clonase-mediated recombination reaction between the two plasmids accomplishes the transfer of ORF into the destination vector to replace the lethal *ccd*B gene. The resulting reaction mixture is transformed to *E. coli* followed by the ampicillin resistance (Amp^R) selection of transformants that only contain the expression clones ready for gene expression with various expression systems.

So far, multi-sited efforts by the research community over the last decades have led to the establishment of many large archives of Gateway donor clones that contain the vast majority of human ORFs cloned from human cDNA libraries or chemically synthesized. the ORFs from other species, such as mouse, rat, yeast, *Drosophila*, *Arabidopsis*, *Xenopus*, and many bacteria and viruses (e.g., Mammalian Gene Collection (http://mgc.nci.nih.gov/) (Lamesch et al. 2007), ORFeome Collaboration (http://www.orfeomecollaboration.org/) (Wiemann et al. 2016), DNASU (https://dnasu.org/DNASU/) (Seiler et al. 2014), Xenbase (https://www.xenbase.org/) (Karimi et al. 2017). The availability of these ORFeomes in Gateway donor clones allows the quick transfer of GOI into Gateway destination vectors to produce expression clones in a HT manner that facilitate the analysis of gene function and protein structure.

In the current study, we combined the BacMagic system and Gateway cloning technology by creating a suite of Gateway-compatible variants of the pIEx/Bac vector. In brief, the pIEx/Bac-based vector was modified by introducing the Gateway cassette (*att*R1-*ccd*B-*att*R2) to serve as a Gateway destination vector such that it can receive any GOI from a donor clone through one-step Gateway cloning to construct expression clones. With this suite of pIEx expression vectors, we were able

to build a protein expression pipeline that leverages our in-house DNASU Gateway donor clone repository.

2.2.5 *In Vivo* Protein Crystallization

One of the most crucial aspects of studying proteins is to understand their three-dimensional (3D) structures as the structural information can determine and elucidate the molecular function of a protein. Classical X-ray structure analysis relies heavily on the complicated and time-consuming screening of appropriate conditions for the growth of sufficiently large, well-diffracting crystals (Schönherr, Rudolph, and Redecke 2018). This has been one of the major bottlenecks in the process of obtaining the 3D structures of difficult-to-crystallize proteins particularly for membrane proteins and post-translationally modified proteins (Bill et al. 2011). Heterogeneously expressed proteins in baculovirus-insect cell system can spontaneously form crystals within living cells, although this was commonly perceived as a somewhat rare event and has only very recently been explored for structure determination (Doye and Poon 2006; Duszenko et al. 2015; Fan et al. 1996). The recent advances in X-ray crystallography, which were developed first at X-ray free electron lasers (XFELs) and later on at synchrotrons (Schönherr et al. 2018), allow data to be collected in a serial fashion from a stream of small nano or microcrystals for high-resolution structure determination (Koopmann et al. 2012; Redecke et al. 2013; Schönherr et al. 2018). This emerging concept of using serial crystallography with *in vivo* crystals opens new routes in structural biology of solving 3D protein structures (Koopmann et al. 2012; Redecke et al. 2013), and also highlights the significance of identifying novel *in vivo* crystal targets (Boudes et al. 2016; Duszenko et al. 2015; Gati et al. 2014). Thus, a high-throughput (HT) protein production pipeline built on baculovirus-insect cell system will be extremely beneficial

to the rapid screening for *in vivo* microcrystals that could be potentially advanced to serial crystallography for structure determination studies.

2.2.5.1 *In Vivo* Protein Crystals in Nature

In vivo protein crystallization is considered as a natural self-assembly process that occurs spontaneously and its mechanism is still poorly understood (Schönherr et al. 2018). It has been observed in nature in a few cases including seeds and cockroaches (Banerjee et al. 2018). It has also been observed as a consequence of heterologous protein expression in bacteria (Hofte and Whiteley 1989), insect cells (Anduleit et al. 2005; Fan et al. 1996) and mammalian cells (Gallat et al. 2014; Hasegawa et al. 2011). So far, all proteins that have been known to form *in vivo* crystals are cytosolic proteins.

2.2.5.1.1 Native *In Cellulo* Crystallization

The first reports on *in vivo* crystals date back to 1850, where protein crystals in human tissue and in the seeds of the Brazil nut were initially described (Charcot and Robin 1853; Hartig 1855). Most native *in cellulo* crystals were detected based on the regular morphology and dense packing, without much knowledge about the identity and function of the crystallized proteins. The natural crystallization have been found to occur in all kingdoms of life with no known preferences for particular cellular compartments (Schönherr et al. 2018). It is still not fully understood that whether the native *in cellulo* crystallization is restricted to a limited number of proteins because they are evolutionary optimized for natural crystallizability to provide a specific function, such as storage, nutrient source, and defense. The dense packing of crystalline lattice provides a space-efficient way for permanent or temporary storage of functional proteins. In plant seeds, the membrane-surrounded storage organelles consist of an amorphous matrix with embedded protein packed in a lattice is a frequent application of this strategy in nutrient storage (Jiang et al.

2000). Similarly, in oviparous animal species, such as mosquito (Snigirevskaya, Hays, and Raikhel 1997), frogs (Massover 1971), and bony fish (Lange, Grodziński, and Kilarski 1982), yolk proteins are crystallized in developing oocytes to provide a constant nutrient supply to the offspring.

Except for the use in the nutrient storage by plant and animals, crystallization is also adopted by viruses, fungi, or plants for protection of virions or stabilization of cell integrity. Filamentous fungi and plants use protein crystals to protect cells from harmful metabolic intermediates or to seal pores on the damaged cells, preventing cytoplasmic bleeding (Van Bel 2003; Plegaria and Kerfeld 2018; Yuan et al. 2003). Many viruses, including baculoviruses (NPV) and cypoviruses (CPV), form paracrystalline arrays in the infected host to encapsulate up to thousands of virions in the late stage of infection to survive in the harsh environment (Smith 1976). The embedded virus particles can be easily delivered to the host through oral-fecal routes as they remain stable and infectious in soil for years until digested by the insect larvae. Once the crystalline coat is dissolved in the alkaline environment in the insect midgut, the virus particles will be released to infect the insect cells (Payne and Mertens 1983). Due to the high crystallizability of polyhedrin protein produced by these viruses, it represents the most extensively studied viral crystalline so far. A comprehensive database containing the high-resolution structural information of polyhedrin from 3 NPV and 9 CPV enlightens the high evolutionary conservation in the polyhedra architecture regardless of the significant variability in the life cycles and polyhedrin sequences between NPV and CPV (Axford et al. 2014; Coulibaly et al. 2007, 2009; Ji et al. 2015).

2.2.5.1.2 Non-native *In Cellulo* Crystallization

In contrast to the native *in cellulo* crystals that provide advantageous functions for the organism, non-native abnormal crystallization of a usually soluble

protein is perceived as a disease-associated event. Although it is not clear if abnormal crystallization represents a causative trigger of the disease or simply a byproduct of harmfulness, so far there are only a few diseases that are known to be directly caused by abnormal protein crystallization (Doye and Poon 2006). More recently, the increasing evidence on intracellular crystals revealed that overexpression of recombinant proteins in host cells can also result in crystalline state, representing another route to non-native crystallization. The crystal growth as a consequence of heterogeneous protein expression has been reported in bacteria, yeast, plant, chicken and mammalian cells as well as in baculovirus-infected insect cells.

A total of four recombinant proteins are reported to form crystals in mammalian cells to date. In HEK293 cells transiently expressing human IgG, needle-shaped crystals of up to 50 μm in length formed in the ER lumen. Similar phenomenon has also been observed in CHO cells engineered for constitute overexpression of human IgG (Hasegawa et al. 2011). The crystal growth can take days until they exceed the cell size and eventually disrupt the plasma membrane. Another study later reported on the crystallization of Xpa, a genetically modified coral fluorescent protein, in transfected mammalian cells. Despite of the stability within cells, the crystals of Xpa are quickly dissolved after cell lysis (Tsutsui et al. 2015).

Crystalline states of five recombinant proteins have been reported in insect cell lines, including 1) an artificial variant of the heterodimeric phosphatase calcineurin, which forms up to three tetragonal, bipyramidal or cubic-shaped crystals in the cytosol of 20–40% of cell population (Fan et al. 1996); 2) firefly luciferase, which forms up to five needle-shaped crystals (Figure 2-13) in the peroxisomes of up to 50% of cell population (Schönherr et al. 2015); 3) inosine monophosphate

dehydrogenase from *Trypanosoma brucei* (*T. brucei*) (TbIMPDH), which forms several needle-shaped crystals in the peroxisomes of up to 90% of cell population (Koopmann et al. 2012); 4) glycosylated cathepsin B from T. brucei (TbCatB), which forms several needle-shaped crystals (Figure 2-13) in the ER of 70% of cell population (Koopmann et al. 2012; Redecke et al. 2013); and 5) the avian reovirus μNS protein linked to GFP (GFP-μNS), which forms single or multiple needle-shaped crystals per cell with a hexagonal cross section (Figure 2-13) in the cytosol of almost all cells (Brandariz-Nunez et al. 2010).

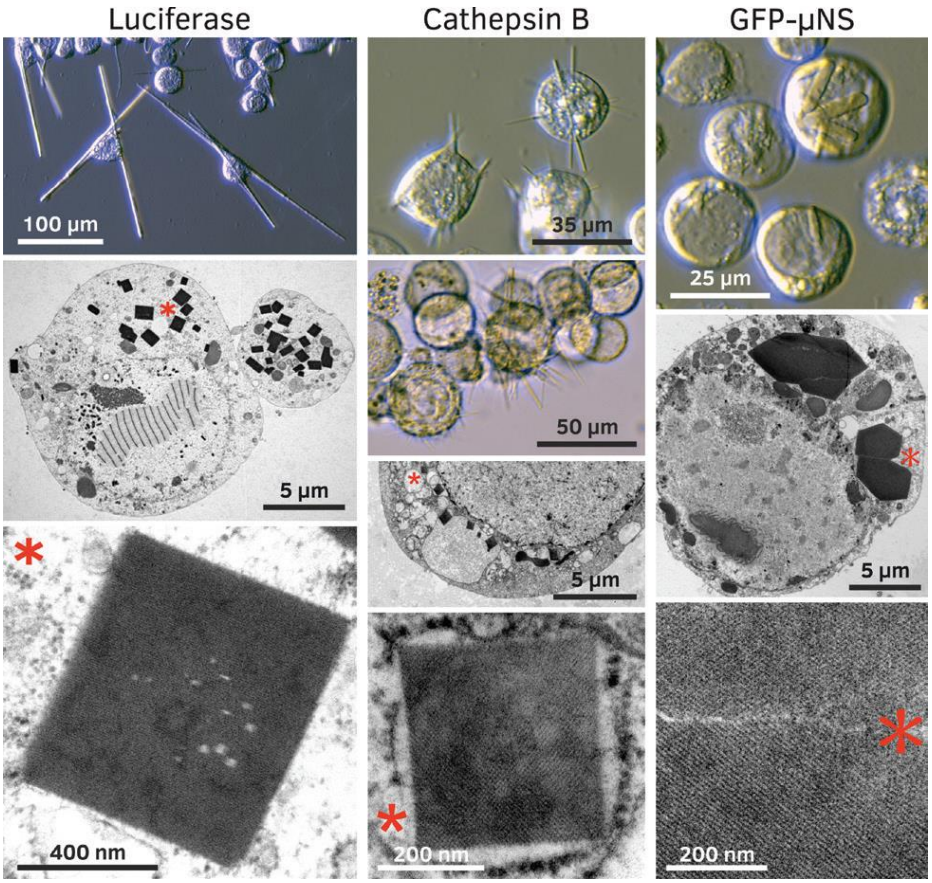

Figure 2-13. Non-native crystals of recombinant proteins overexpressed in insect cells. Left panel: Firefly luciferase crystals formed in HighFive cells. Middle panel: TbCatB crystals produced in HighFive cells. Right panel: Avian reovirus fusion protein GFP-μNS crystals produced in Sf9 cells. Asterisks denote crystals in magnified TEM images. Figure adapted from Schönherr et al. 2018.

These crystals differ in many features including crystal morphology, stability, dimensions, cellular localization, and dynamics (Schönherr et al. 2018). Although they seem to preferentially assemble into needle-like structures, the size of crystals varies from protein to protein. While GFP-μNS and calcineurin crystals generally do not exceed the regular cell dimension, TbCatB, TbIMPDH, and luciferase assemblies can grow to up to 200 μm in length, which can clearly extend out of the living cell without affecting cell viability. A unique feature about luciferase crystals is that it displays the growth period of dynamic degradation and re-assembly (Schönherr et al. 2015). There is no apparent preference for particular cellular compartments for crystallization in insect cells and the location depends on the native translocation signals carried in their protein sequences. Diffraction tests of TbIMPDH and GFP-μNS crystals have confirmed the crystalline state (Koopmann et al. 2012; Schönherr et al. 2015). Furthermore, X-ray diffraction of TbCatB crystals at XFEL source led to the determination of structure at a high resolution (Redecke et al. 2013). Luciferase crystals, however, tend to dissolve easily after cell lysis, preventing further studies on solving its structure (Schönherr et al. 2015).

2.2.5.2 *In Vivo* Protein Crystals in Structural Biology

In traditional *in vitro* crystallography, proteins need to be first expressed at a very high yield (~10 mg/mL) and then the highly purified fractions (> 95% purity) are used for screening for appropriate crystal growth conditions to obtain sufficiently large and homogeneous single crystals of diffraction quality. Regardless of numerous strategies developed to facilitate the *in vitro* crystal growth (Chayen and Saridakis 2008), there is no guarantee for crystal formation, particularly for membrane proteins and post-translationally modified proteins (Bill et al. 2011). On the contrary, the application of *in vivo* crystals in crystallography eliminates the need for the extremely labor-intensive and time-consuming procedures associated with

purification and crystallization. Besides, being processed in the native cellular environment, proteins can be properly folded and modified with adequate conformational and structural homogeneity, which is necessary for the formation of well-layered crystal lattice (Schönherr et al. 2018). Thus, *in cellulo* crystallization could offer exciting new possibilities for solving proteins structures that would be otherwise unobtainable applying conventional approaches. However, in contrast to countless efforts devoted to *in vitro* crystallization over the past decades, the potential of *in vivo* crystals in structural biology has not yet been fully valued and exploited, mainly because the relatively small microcrystals formed in vivo are sensitive to radiation damage caused by the conventional synchrotron X-ray radiation sources (Gallat et al. 2014).

Nevertheless, this challenge has been recently overcome by the emerging serial femtosecond X-ray crystallography (SFX) technique, which uses extremely bright and ultrashort X-ray pulses from XFEL sources to irradiate nano or microcrystals and record their diffraction before destruction occurs (Chapman et al. 2011), therefore boosting the applicability of in vivo crystallization in structural biology (Gallat et al. 2014; Koopmann et al. 2012). XFEL takes advantage of the linear accelerator (LINAC) and a magnetic field-based undulator, through which the electrons are first expedited to the speed of light and then forced to travel in wiggling motion to gain extremely powerful energy. With this set-up, XFEL can generate X-ray pulses a billion times brighter than those previously available at synchrotrons, with the pulse length ranging from 0.2 to 200 fs, a timescale on which the motion of atoms can be seen and tracked. Meanwhile, the advent of SFX provides improved serial data collection strategies. Instead of using one large crystal, thousands of nano or microcrystals are continuously delivered one by one so that when an X-ray pulse hits the sample, the diffraction pattern is captured before

each particle is destroyed. By supplying a stream of crystal particles, thousands of diffraction patterns at random orientation can be obtained followed by combination and analysis to solve the protein structure.

In 2007, the first structure of a natively crystallizing protein, cypoviral polyhedra, was reported by Coulibaly and coworkers using the synchrotron diffraction approach (Coulibaly et al. 2007). This approach was subsequently applied to the structural characterization of baculoviral polyhedra protein using *in vivo*-grown microcrystals purified from insect cells, resulting in the determination of the 2.2 Å resolution (Coulibaly et al. 2009). Despite of this success, the quick deterioration of diffraction quality largely restricts the data resolution. The application of SFX to micron-sized crystals at an XFEL source solves the limitations associated with crystal dimensions and radiation damage (Spence 2017). This concept was proved in 2013 by Redecke and co-workers that intracellular crystals formed by a recombinant, not naturally crystallizing protein can also be used to extract high-resolution structural information (Redecke et al. 2013). They revealed

the 2.1 Å resolution structure of TbCatB protein, representing the first successful synergy of *in vivo* crystallization and SFX technology. TbCatB is a protozoan parasite that can cause sleeping sickness and degrade the red blood cells of host. This breakthrough experiment demonstrated that structural information can be obtained by the "diffraction-before-destruction" approach of SFX from thousands of microcrystals that are delivered to the XFEL beam in a liquid jet in their mother liquor (Gallat et al. 2014). This approach was subsequently applied to determine the structure of polyhedrin from CPV type 17 at 1.75 Å (Ginn et al. 2015) and the structure of granulin from *Cydia pomonella* (*C. pomonella)* granulovirus (CpGV) at 2 Å and 2.56 Å by two groups (Gati et al. 2017; Oberthuer et al. 2017).

With the development of data processing strategies and sample injection techniques, fewer diffraction patterns can be used to solve the protein structure, which dramatically reduces the sample consumption and experimental time from several hours to less than 10 min to obtain a complete dataset. In 2017, Oberthuer et al. developed a double-flow focusing nozzle which improved the jet stability for more reliable and efficient delivery of fresh crystals across the beam of XFEL (Oberthuer et al. 2017). In the same year, Roedig et al. reported that a novel sample delivery approach based on the micropatterned silicone chips and a high-speed goniometer has greatly improved the crystal particle hit-rate from 10% to approximately 70%, compared to the currently used liquid micro-jet (Roedig et al. 2017).

2.3 Methods and Materials

2.3.1 Construction of pIEx Expression Vectors

The Gateway-compatible pIEx expression vector series were modified from the pIEx-cyto vector (obtained as a gift from Drs. James Love and Scott Garforth at Albert Einstein College of Medicine; available in DNASU) as illustrated in Figure 2-14.

Briefly, the cloning efforts were structured in two steps, with the pIEx-nGST expression vector shown as an example here. To generate pIEx-nGST expression vector, the pIEx-cyto vector was first digested with *Nco*I and *Bsu*36I, followed by gel purification to remove the original insert. In parallel, the GST tag coding sequence was amplified from pANT7-cGST vector (available in DNASU). The purified PCR product of GST tag was inserted to the linearized pIEx-cyto vector via In-Fusion reaction, to generate the pIEx-nGST empty vector. The In-Fusion product was transformed to *E. coli* DH5α competent cells (NEB) for colony selection. Following the plasmid isolation and sequence verification, the pIEx-nGST empty vector was digested with *Sgf*I and *Bsu*36I, followed by gel purification to remove the original insert. In parallel, the Gateway death cassette was amplified from a modified pANT7-cGST-DC vector (available in DNASU). The purified PCR product of the death cassette was inserted into the linearized pIEx-nGST empty vector via In-Fusion reaction, to generate pIEx-nGST expression vector. The final In-Fusion product was transformed to *E. coli* ccdB survival-competent cells (Invitrogen) for colony selection.

The resulting pIEx expression vectors were sequence verified for the presence of both the death cassette and fusion tags, which enable the insertion of target gene through Gateway LR reaction as well as the production of N- or C-terminally tagged fusion proteins through homologous recombination with BacMagic-3 DNA. Maps and sequences of these Gateway-compatible pIEx expression vectors are available in DNASU (https://dnasu.org/DNASU/Home.do). The plasmid DNA of all expression vectors was prepared using the NucleoBond Plasmid Maxiprep Kit (Macherey-Nagel).

2.3.2 Protein Selection

A test collection of 40 full-length proteins were selected to assess the expression capability of our pipeline (Supplementary Table S1). These proteins were chosen if their full-length ORFs were available in a Gateway donor clone in DNASU.

The selected proteins 1) range in size from ~8 to 130 kDa, 2) localize in different subcellular compartments, and 3) function in diverse biological processes. The donor clones for selected ORFs in the test collection were acquired from DNASU to construct the pIEx expression clones for protein expression with various tags in insect cells. These ORFs were annotated as either "closed" or "fusion" to indicate if a stop codon is present (closed) or is absent (fusion) in an ORF insert. Fusion format clones are used for producing a C-terminally tagged version of an ORF.

2.3.3 Gateway Subcloning of pIEx Expression Clones

The Gateway LR cloning was performed to construct multiple pIEx expression clones in parallel. The LR cloning reaction was set up by mixing 300 ng of Gateway donor clone, 300 ng of pIEx expression vector, 1 µL of Gateway LR Clonase II Enzyme Mix (Invitrogen), and then incubated for 1 h at 25 °C (Figure 2-15A). The cloning reaction mix was transformed into 20 µL of *E. coli* DH5α competent cells and incubated in 150 µL of S.O.C medium (Thermo Scientific) for 1 h at 37 °C, 250 rpm in an orbital shaker. The entire cell suspension was plated on lysogeny broth (LB) agar with 100 µg/mL of ampicillin followed by an overnight incubation at 37 °C. Positive colonies selected from the agar plates were inoculated to LB medium with 100 µg/mL of ampicillin. The plasmid DNA of the resulting pIEx expression clones was isolated from the bacteria culture using the NucleoSpin Plasmid Miniprep Kit (Macherey-Nagel). All LR cloning products were sequence verified prior to transfection of insect cells.

2.3.4 Insect Cell Culture

Spodoptera frugiperda Sf9 cells (Invitrogen) were maintained in Sf-900 III Serum Free Medium (Gibco) and incubated at 27 °C, 140 rpm without CO_2 exchange in a non-humidified orbital shaker. Suspension culture was passaged when reaching a density of 2E6 viable cells/mL and was seeded at 0.5E6 viable cells/mL. Cell

counting was performed on the suspension culture using Trypan Blue (Invitrogen) to determine the cell density and viability at every passage.

2.3.5 Recombinant Baculovirus Generation and Amplification in 24-Well Plate Format

The pIEx/BacMagic-3 co-transfection was performed for multiple expression clones to generate recombinant baculovirus in parallel. For each transfection, a reaction was assembled by mixing 1 mL of Sf-900 III Serum Free Medium, 5 µL of Insect GeneJuice Transfection Reagent (Sigma-Aldrich), 100 ng of BacMagic-3 DNA (Novagen), and 500 ng of pIEx expression clone (Figure 2-15B). The transfection reaction was gently agitated and incubated at room temperature (RT) for 30 min to allow complexes to form. The entire reaction was then slowly added to 1 mL of Sf9 cells at 1E6/mL in a 24-well deepwell plate (Thomson Instrument Company) for recombinant virus production. Plates were sealed with an adhesive silicone film (Analytical Sales & Services) to allow air exchange, and crucially, to avert evaporation. Cultures were incubated for 120 h at 27 °C, 140 rpm. Subsequently, the culture was centrifuged at 1,000 x g for 5 min to remove cell debris and the supernatant containing recombinant budded viruses was harvested. The resulting first generation (P1) of virus was then amplified through a second round of Sf9 cell infection to generate P2 virus. Briefly, 4 mL of Sf9 cells at 2E6/mL were infected with 20 µL of P1 virus stock in a 24-well deepwell plate, sealed with silicone film, and incubated for 120 h at 27 °C, 140 rpm. The generated P2 virus was verified via the expression screening for the working stock prior to protein expression.

2.3.6 Protein Expression in 24-Well Plate Format

In a 24-well deepwell plate, 4 mL of Sf9 cells at 1E6/mL were infected with 20 µL of P2 virus stock which had been confirmed for protein expression, and incubated for 72 h at 27 °C, 140 rpm. Alternatively, suspension culture was scaled up in a

sterile Optimum Growth Flask (Thomson Instrument Company) by adding P2 virus stock proportionally with the same virus-to-cell ratio. After centrifugation of infected culture, the insect cell pellet was collected for SDS-PAGE analysis on 4-20% precast polyacrylamide gels (Bio-Rad). Gels were stained with Coomassie SimplyBlue SafeStain (Invitrogen) to visualize the protein bands. A target was considered as "expressed" if a novel band at expected size was present only in infected cells but not in uninfected cells.

2.3.7 Protein Purification

One tablet of Protease Inhibitor Cocktail (Roche), 500 µL of Insect Popculture (Millipore), and 1.6 µL of Benzonase (Millipore) were added to 10 mL of Sf9 cell culture expressing the target protein and incubated for 15 min at RT. The resulting lysate was subjected to purification using different types of affinity beads, depending on the fusion tag.

For His-tagged proteins, 400 µL of 50% Ni-NTA agarose (QIAGEN) was washed and equilibrated with 1 mL of equilibration buffer (50 mM Tris, 300 mM NaCl, 1 mM DTT, 5% (v/v) glycerol, 1% (v/v) Triton X-100, pH 7.5), and incubated with 10 mL of total lysate for 1 h at 4 °C with agitation. Agarose beads were then washed twice subsequentially with 10 mL of wash buffer 1 and 2 (20 mM and 50 mM imidazole in equilibration buffer) to remove unbound particles, and then were incubated with 500 µL of elution buffer (250 mM imidazole in equilibration buffer) for 5 min at RT with agitation to elute the His-tagged protein targets.

For GST-tagged proteins, 100 µL of 25% Glutathione Magnetic Agarose Beads (Thermo Scientific) were washed twice with 500 µL of wash buffer (125 mM Tris, 150 mM NaCl, 1 mM DTT, 1 mM EDTA, pH 7.4). Lysate was centrifuged at 2,000 x g for 5 min at 4 °C and the resulting supernatant was incubated with agarose beads for 1 h at RT with agitation. Agarose beads were washed twice with 500 µL of wash buffer to

remove unbound particles, and then were incubated with 250 µL of elution buffer (50 mM reduced glutathione in wash buffer) for 10 min at RT with agitation to elute the GST-tagged protein targets.

2.3.8 SONICC Screening for Microcrystals within Living Sf9 Cells

Sf9 cells infected with recombinant virus were tested for *in cellulo* crystallization using a SONICC instrument. Briefly, at 24, 48, 72, 96, and 120 h p.i., 1 mL of each suspension culture was harvested and centrifuged at 500 x g for 5 min at 4 °C. The supernatant containing the culture medium was discarded, and the insect cell pellet was gently re-suspended in 50 µL of PBS (phosphate-buffered saline) buffer. Next, 2 µL of high-density cell suspension was loaded into a 96-well 2-drop MRC Crystallization Plate (Swissci) and immediately imaged with SONICC imager (Formulatrix) using visible light and the SHG technology to visualize and identify the *in vivo*-grown protein crystals. In a typical SONICC image, crystals appear white against a stark black background that helps to identify crystals even in murky environments like those from the extremely complex and crowded cellular environments. Image tuning was utilized to adjust the brightness and contrast of the SONICC images to remove any noise visible from the drops of each target. In our experiment, the signal intensity of the images was auto tuned per drop by default settings in Rock Maker (Formulatrix) and compared against the control drop containing the non-infected Sf9 cells to determine the positive hits.

2.4 Results

2.4.1 pIEx Expression Vector Construction

A suite of pIEx-based expression vectors for baculovirus-insect cell system have been generated to enable the rapid cloning of target genes into expression clones using Gateway technology. To construct a Gateway-compatible pIEx expression vector, the Gateway death cassette containing the ccdB lethal gene

flanked by bacteriophage l site-specific recombination sites (*att*R1 and *att*R2) was introduced downstream of the very late p10 promoter in the pIEx-cyto backbone (Figure 2-14). When mediated by LR clonase, target genes in frame from a Gateway donor clone replace the death cassette in pIEx expression vectors, resulting in pIEx expression clones (Figure 2-15A). Upon co-transfecting Sf9 cells with a pIEx expression clone and BacMagic-3 viral DNA, homologous recombination at viral-specific sequences (Lef2/ORF603 and ORF1629) occurs, which consequently inserts the expression cassette (i.e. the target gene and fusion tag) and restores the essential gene ORF1629 flanking the insertion site to eventually form recombinant viral DNA (Figure 2-15B).

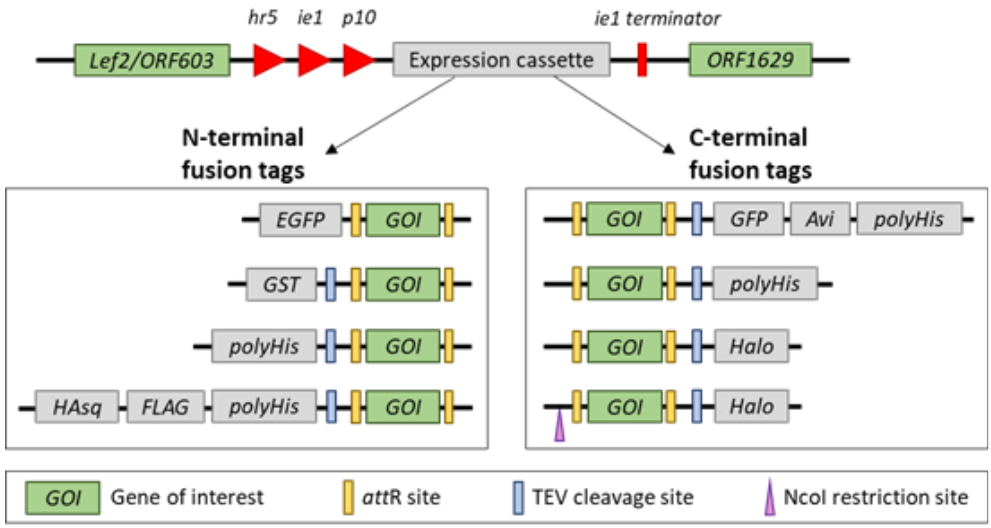

Figure 2-14. Schematic drawing of pIEx expression vectors. The pIEx expression vectors were derived from the pIEX-cyto vector containing baculovirus homologous region *Lef2/ORF603* and *ORF1629*, the enhancer *hr5* and early immediate promoter *ie1*. Through In-Fusion cloning, the Gateway death cassette flanked by *att*R recombination sites was introduced downstream of the baculovirus very late promoter *p10* and upstream of the *ie1* terminator. Sequences encoding fusion tags were inserted in the appropriate reading frame as indicated either upstream or downstream of the death cassette, which is later replaced by the GOI upon Gateway LR reaction with the donor clone. An *Nco*I restriction site that contains ATG start codon initiates translation before the *att*R1 site.

In addition, a series of fusion tags were introduced to the pIEx vector collection to support the expression of fusion proteins with nEGFP, cGFP-Avi-His, cHalo, nHis, cHis, nGST, or nHA secretory sequence (sq)-FLAG-His tags (Figure 2-14 and Table 1). Thus, this pIEx vector collection provides a variety of options to tag target proteins depending on the desired downstream applications. Particularly, there are two variants of pIEx expression vector with cHalo tag: one initiates translation at the start codon before the *att*R1 site (named "pIEx-NcoI-cHalo") and the other supports the translation initiation using the natural start codon located within the ORF insert following the *att*R1 site (named "pIEx-cHalo") (Figure 2-14). Additionally, a tobacco etch virus (TEV) protease cleavage site was also introduced before or after the C-terminal or N-terminal tag so that, if desired, the fusion tags can be readily removed from the recombinant proteins with TEV protease (Figure 2-14).

Table 2-1. Gateway-compatible pIEx expression vector collection.

Vector	Gateway cloning	Fluorescent imaging	Purification	TEV cleavage	Translation start site
pIEx-nEGFP	✓	✓			Fusion Tag
pIEx-cHalo	✓	✓[1]	✓	✓	Inserted ORF
pIEx-nGST	✓		✓	✓	Fusion Tag
pIEx-nHis	✓		✓	✓	Fusion Tag
pIEx-nHAsq-FLAG-His (pIEx-nHFH)	✓	✓[2]	✓	✓	Fusion Tag
pIEx-cGFP-Avi-His (pIEx-cGAH)	✓	✓	✓	✓	Inserted ORF
pIEx-cHis	✓		✓	✓	Inserted ORF
pIEx-NcoI-cHalo (pIEx-N-cHalo)	✓	✓[1]	✓	✓	Gateway junction

[1] Via HaloTag fluorescent ligand (Promega) staining; [2] Via immunofluorescence staining.

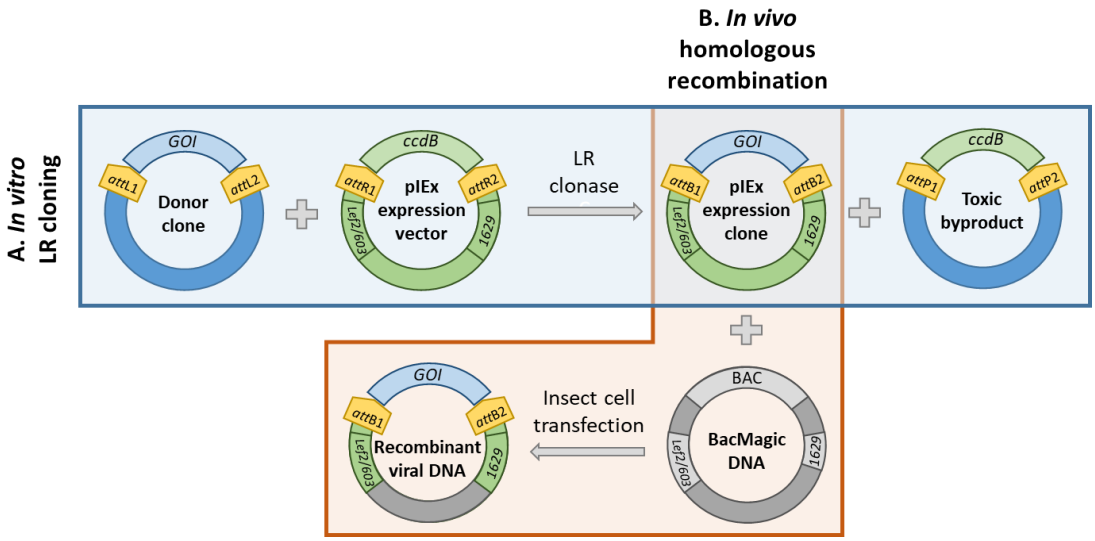

Figure 2-15. Working principle of the Gateway-compatible pIEx/BacMagic-3 expression system. **A)** A GOI in a donor clone is transferred to replace the death cassette containing the *ccdB* lethal gene in pIEx expression vector via Gateway recombination between *att*L and *att*R sites, producing a pIEx expression clone. **B)** Sf9 cells are co-transfected with a pIEx expression clone and BacMagic-3 DNA, where the expression cassette flanked by *Lef2/ORF603* and *ORF1629* is integrated into recombinant viral DNA through homologous recombination, thus replacing the bacteria artificial chromosome (BAC) and repairing the defective gene *ORF1629*.

2.4.2 High-throughput Protein Expression Analysis

To demonstrate the mass parallel expression of recombinant proteins, a test collection of ORFs encoding 40 individual full-length proteins in Gateway donor clone were transferred into the pIEx expression vectors. These target proteins were selected from a diverse range of molecular weight (8-130 kDa) and host organisms, including human, fungus, bacteria, and virus (Figure 2-16). Additionally, these proteins are located in different subcellular compartments of their original organisms as well as involved in various biological processes. Successful parallel protein expression from each pIEx expression vector was demonstrated by SDS-PAGE (Figure 2-17). For proof-of-principle, selected proteins were tested in certain vectors.

Notably, five target proteins, including ALD2, MLF2, ARHGEF18, tufA, and RBM45, were successfully expressed in all pIEx expression vectors (Figure 2-18). These 5 target proteins, including 3 from human, 1 from *S. cerevisiae*, and 1 from *Vibrio cholera* (*V. cholera*), range in size from ~25 to 130 kDa. These results indicate that the protein production pipeline built on the suite of Gateway-compatible pIEx expression vectors can achieve rapid mass parallel cloning and expression of recombinant proteins with various fusion tags.

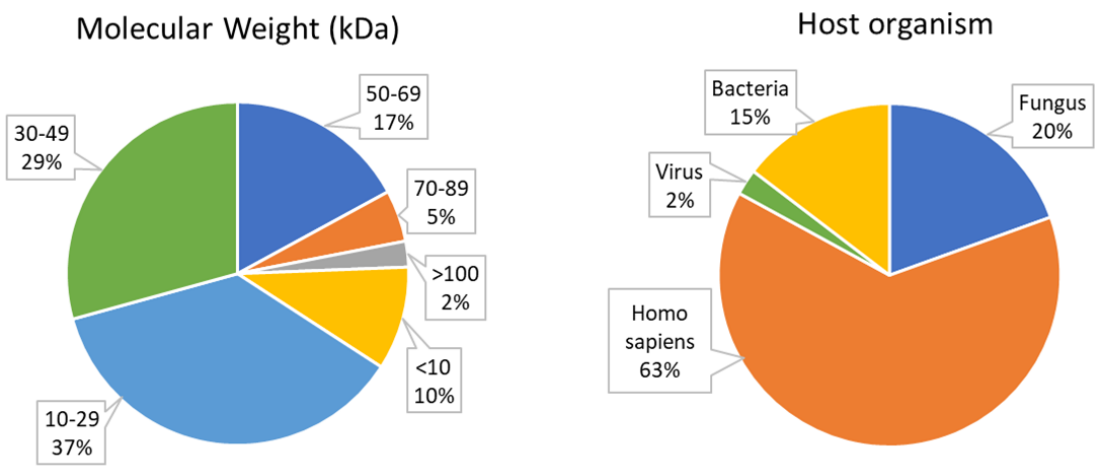

Figure 2-16. Host organisms and molecular weight range of the test collection. Proteins selected for the test collection are derived from a variety of species, including human, fungus, bacteria, and virus, with molecular weights ranging from ~8 to 130 kDa as indicated.

To assess the reproducibility of protein production using our pipeline, expression assays were performed repeatedly for pIEx expression clones encoding nEGFP-WWTR1, nEGFP-MLF2, nEGFP-RGS13, and nEGFP-STAT4. SDS-PAGE analysis of Sf9 cells infected with recombinant viruses from different batches showed similar expression levels (Figure 2-19), suggesting that the pipeline is capable of producing recombinant proteins stably and reproducibly.

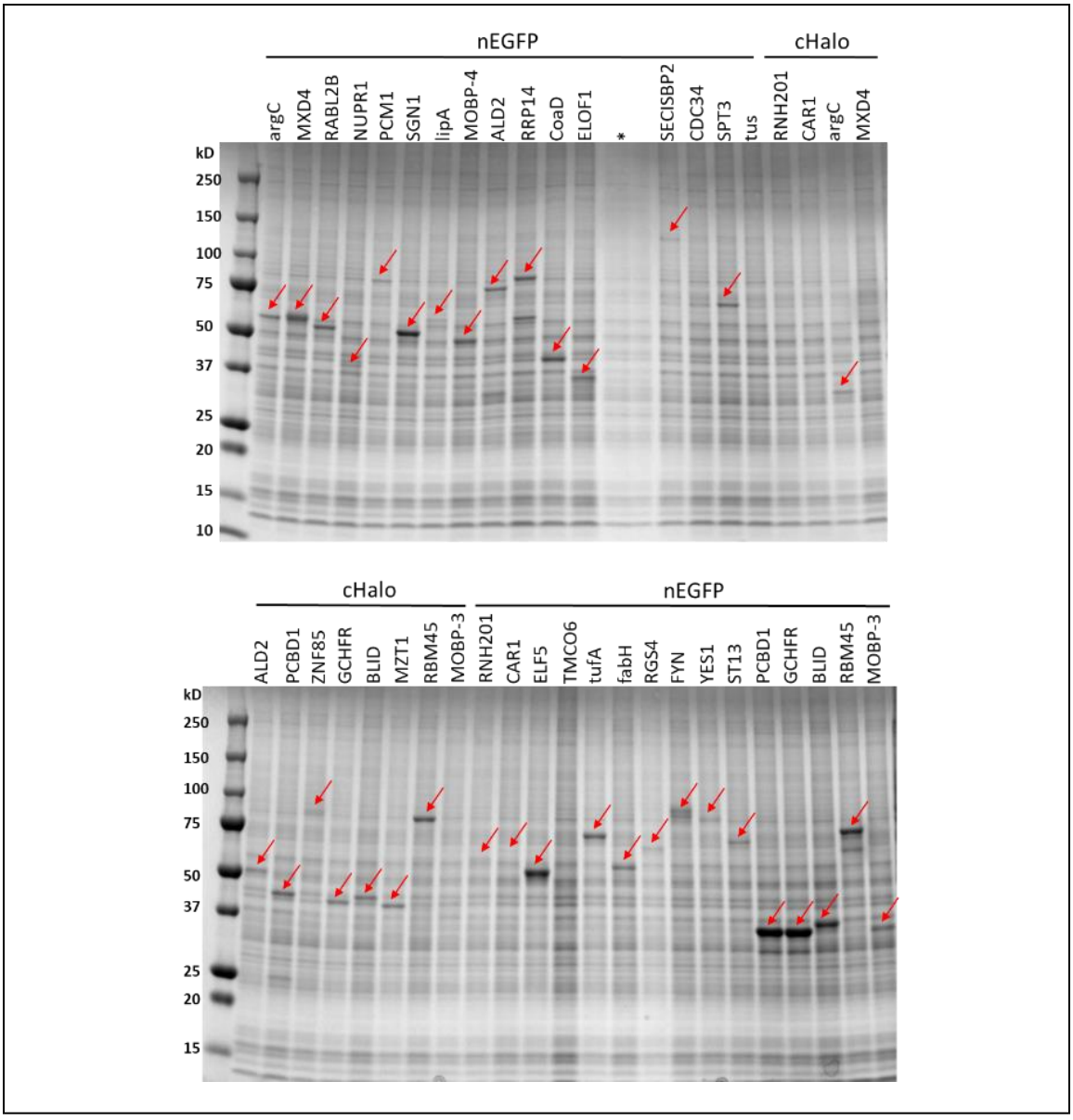
nEGFP
cHalo
argC
MXD4
RABL2B
NUPR1
PCM1
SGN1
lipA
MOBP-4
ALD2
RRP14
CoaD
ELOF1
*
SECISBP2
CDC34
SPT3
tus
RNH201
CAR1
argC
MXD4
kD
250
150
100
75
50
37
25
20
15
10
cHalo
nEGFP
ALD2
PCBD1
ZNF85
GCHFR
BLID
MZT1
RBM45
MOBP-3
RNH201
CAR1
ELF5
TMCO6
tufA
fabH
RGS4
FYN
YES1
ST13
PCBD1
GCHFR
BLID
RBM45
MOBP-3
kD
250
150
100
75
50
37
25
20
15

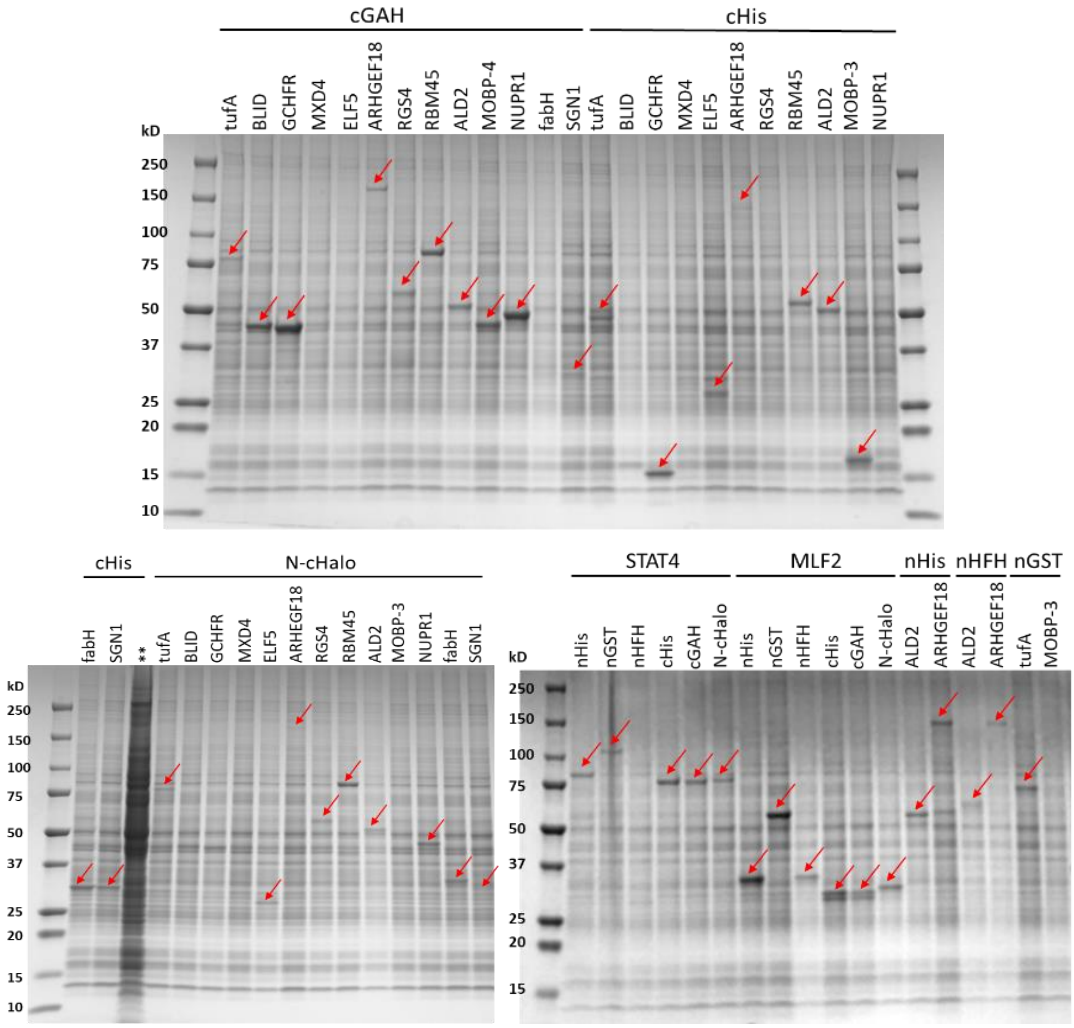

Figure 2-17. Successful mass parallel expression of recombinant proteins fused to various fusion tags. Target proteins in the test collection were expressed using the indicated pIEx expression vectors and analyzed by Coomassie-stained SDS-PAGE. A target was considered as "expressed" if a novel band (red arrow) was present at the expected molecular weight but absent in the non-infected Sf9 cells. Closed format clones were attached with no fusion tags when expressed using pIEx vectors carrying C-terminal tags. * indicates an inter-lane sample diffusion due to the broken gel well; ** indicates a sample overloading.

2.4.3 High-throughput Protein Expression Protocol Development

The imperative of HT production is to express as many proteins as possible using the uniform protocol. Many parameters were tested to optimize the overall

protein expression capability of our pipeline, including evaluating plasmid DNA concentration, cell density, virus amplification, multiplicity of infection (MOI), and infection duration. For the generation of recombinant baculovirus, conditions for DNA templates recommended by manufacturer was found to be the most efficient for most POIs. In common baculovirus-mediated protein production protocols, a recombinant virus stock generally needs to be amplified for at least three consecutive rounds before being used to infect insect cells for expression. In the current protocol, thanks to pIEx/BacMagic system, this process was largely shortened as one round of amplification is usually necessary to reach the required viral titer for expression screening.

Traditionally, the optimal MOI needs to be determined by titrating each individual virus stock followed by testing a variety of titer ratios to achieve the highest protein yield. To avoid the time-consuming and tedious procedures of virus titration, we adopted a universal volume-based ratio in this pipeline aimed for HT protein production. Several recombinant virus stocks that showed relatively weak expression were selected to be studied to assure that the determined MOI would work for most POIs. After measuring the virus titer, a range of MOI as 2, 5, 20, and 50 were performed for cell infection. The subsequent Western blot analysis revealed that for tested targets the yield increased from low to high MOI, with MOI 5, 20, and 50 showing similar protein expression. To tolerate titer variations among individual virus stocks, the middle MOI 20 was used for infecting cells, which was further converted, based on virus titer of tested targets, to a volume-based virus-to-cell ratio of 1:200 on average to enable HT viral transduction with relative ease.

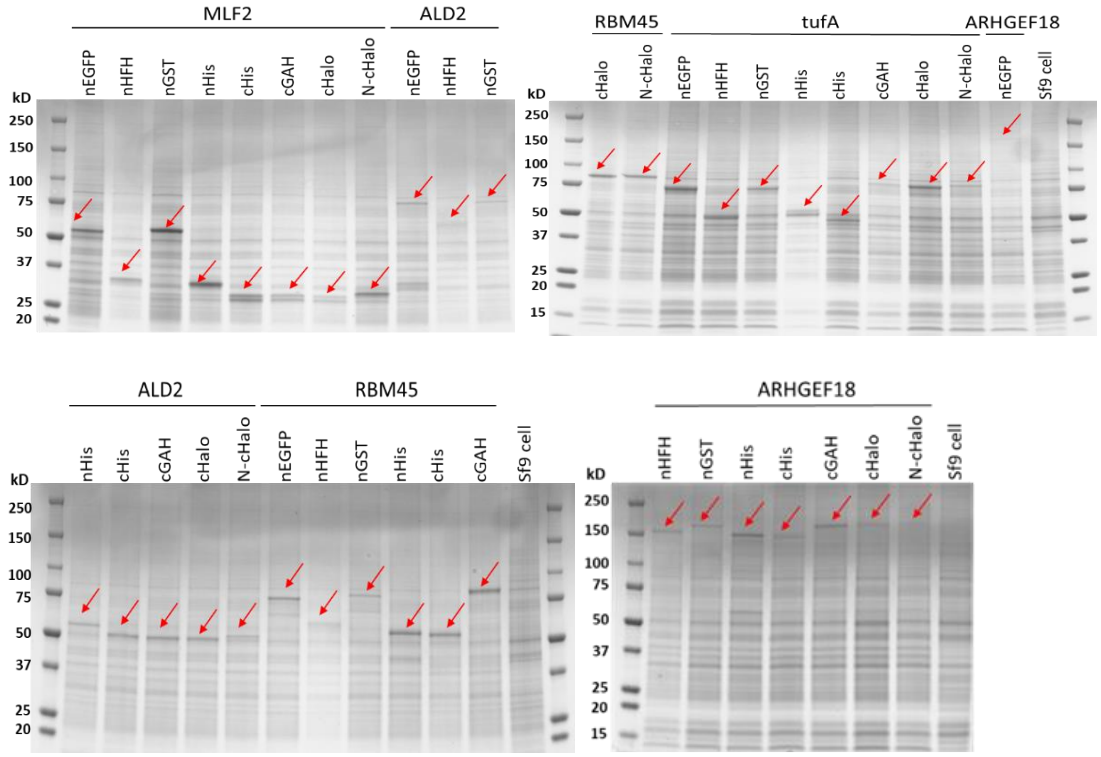

Figure 2-18. Successful parallel expression of target proteins. As expected, the two closed format clones, MLF2 and ALD2, were attached with no fusion tags when expressed using pIEx vectors carrying C-terminal tags.

To maximize protein yield, different harvest times were also assessed. It was found that protein expression initiated around 24 hr post infection (p.i.) and continuously increased in a time-dependent manner up to 72 hr pi, with an almost equal or slightly higher level compared to 96 hr pi. This subtle protein level decrease might result from mild proteolysis or degradation that generally coincided with longer incubation times. Taken together, 72 hr p.i. was determined as the optimal harvest time for stable and economical protein expression. Using optimized conditions described in Methods and Materials section, the majority of constructs were expressed successfully in the pipeline.

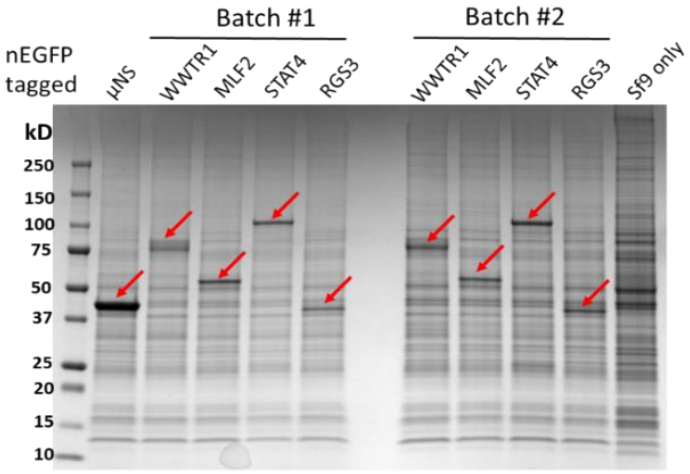

Figure 2-19. Reproducibility of protein expression. The pIEx expression clones for the indicated targets were introduced into the pipeline repeatedly. Harvested cultures were analyzed by Coomassie-stained SDS-PAGE to assess the inter-batch variations in protein expression. In both batches, all proteins were overexpressed (red arrows) compared to uninfected Sf9 cells. The nEGFP-μNS was included as a positive control for expression.

2.4.4 Protein Purification with His- or GST-tag

To demonstrate that pIEx destination vectors support protein purification, cultures expressing His or GST tagged proteins were subjected to affinity binding to nickel-nitrilotriacetic acid (Ni-NTA) agarose or magnetic glutathione resin, respectively. The resin was washed to remove unbound proteins, and POIs were released by imidazole or reduced glutathione for His or GST tagged proteins, respectively. To optimize protein purification, numerous parameters were tested, including the methods of cell lysis, resin-to-sample ratio, the amount of protease inhibitors, binding time, number of washes, equilibration/wash/elution buffers, and type of detergent. Notably, for many tested POIs, the majority of protein was found in pellet after cell lysis as the insoluble fraction rather than in the supernatant when the cells were lysed with sonication or French press. This abnormality of protein aggregation was observed for nGST, nHis, and cHis tagged proteins ranging from

~40 to 160 kD. To tackle this issue, lysis buffers with different salt concentrations (100-500 mM) were used to lyse cells in hope of reducing protein aggregation. An increased concentration of detergent, osmolyte and reducing reagent, such as 1% Triton X-100, 5% glycerol and 1 mM DTT, was supplemented to the lysis buffer to help solubilize the aggregates. Cultures harvested at different time points were also tested to see if lower endogenous protein concentration would alleviate the formation of protein aggregates caused by misfolding.

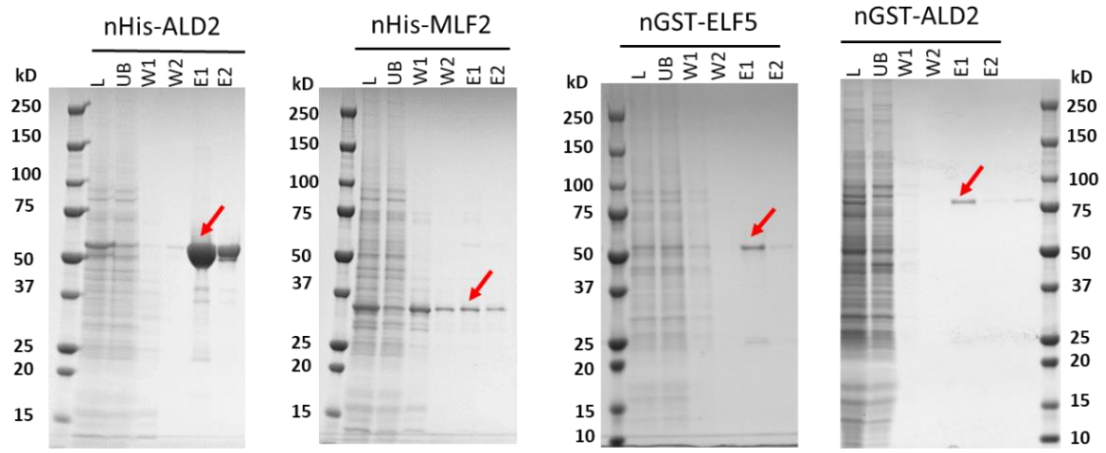

Figure 2-20. Protein purification. Recombinant proteins fused to nHis or nGST tags were successfully purified (red arrows) and analyzed by Coomassie-stained SDS-PAGE. L, lysate; UB, unbound; W, wash; E, elution.

Using the optimal conditions described in the Methods and Materials section, several proteins were isolated from the Sf9 cell cultures expressing His-tagged or GST-tagged proteins and analyzed by SDS-PAGE (Figure 2-20). Specifically, His-tagged MLF2 and ALD2 recombinant proteins were successfully purified from expression constructs, pIEx-nHis-MLF2 and pIEx-nHis-ALD2, respectively, using nickel-nitrilotriacetic acid (Ni-NTA) agarose. Similarly, GST-tagged ALD2 and ELF5 recombinant proteins were successfully purified from expression constructs, pIEx-nGST-ALD2 and pIEx-nGST-ELF5, respectively, using magnetic glutathione resin.

2.4.5 *In Vivo* Crystallization

To explore the feasibility of employing our tools in a HT structural biology pipeline using *in vivo* crystals, SONICC screening was performed to test for *in vivo* crystallization of recombinant proteins expressed using our pipeline. The SONICC method detects the presence of crystals as small as 100 nm of chiral molecules by second harmonic generation (SHG) (Wampler et al. 2008). When two infrared (IR) photons at 1024 nm hit a chiral crystal with <10 fs time difference, frequency doubling occurs by SHG whereby the crystal emits a green photon. Protein crystals in living insect cells are thereby detected by the green photons emitted. For amorphous precipitates or proteins in solution, the second harmonic signals cancel out. The SONICC measurements can be carried out in 96-well plates and thereby can be performed in a HT fashion.

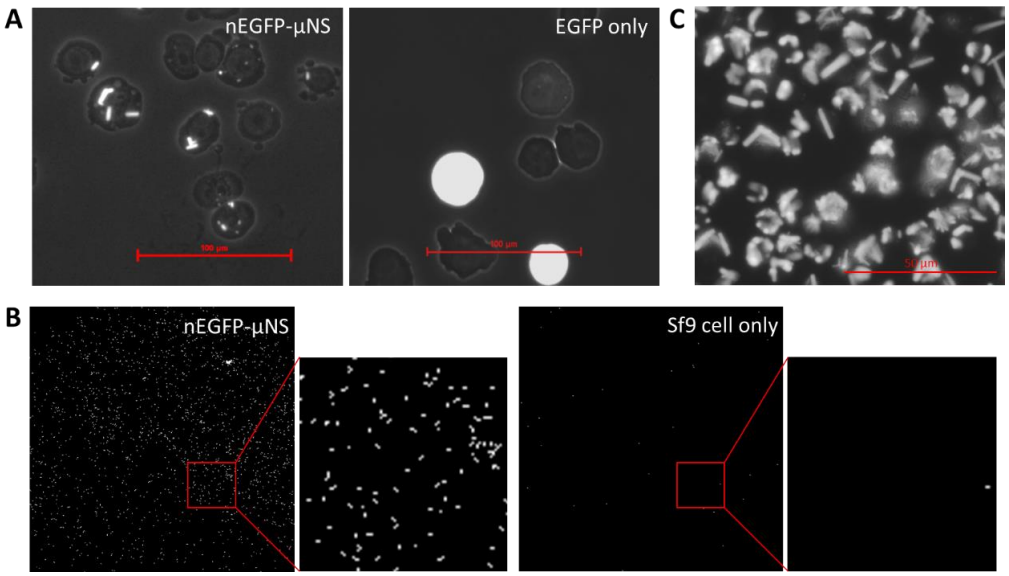

Figure 2-21. Characterization of *in vivo* crystallization in Sf9 cells expressing nEGFP-μNS. **A)** UV fluorescence images revealed one or more rod-shaped crystals in Sf9 cells expressing nEGFP-μNS but not in cells expressing EGFP tag alone. **B)** SONICC detected the positive signal for Sf9 cells infected with nEGFP-μNS while no signal for non-infected control. A zoomed-in view was shown for the red boxed area. **C)** UV fluorescence image showed intact nEGFP-μNS crystal particles in suspension after the culture was stored at 4 °C for 2 weeks.

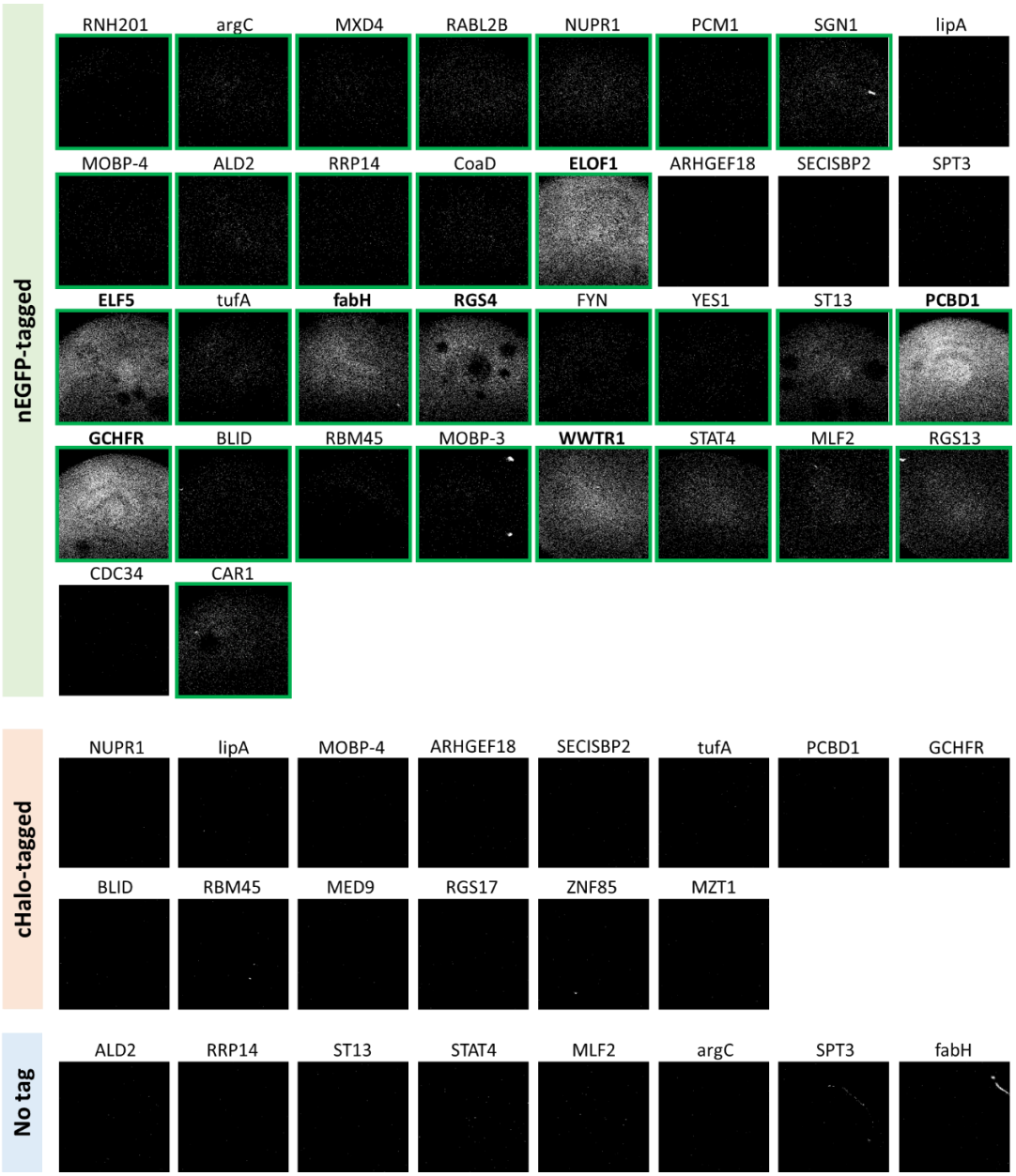

Figure 2-22. High-throughput screening for *in vivo* crystals. SONICC images of Sf9 cells expressing the indicated target proteins at 48 h p.i. Among nEGFP-tagged proteins, 29 targets were identified as positive hits as shown in green boxes, and 7 of them showed very strong SONICC signals with their names shown in bold. No signal was observed for proteins with cHalo tag or those without a tag.

As nEGFP-μNS has been reported to form *in vivo* crystals in living insect cells (Schönherr et al. 2015), we included this target in our study as a positive control. In

agreement with Schönherr et al., we observed a strong intrinsic tendency of crystallization for nEGFP-μNS expressed in Sf9 cells (Figure 2-21). Around 72 h p.i., the accumulation of rod-shaped structures, which were developed from the tiny spots representing the initial crystal nuclei, became visible within Sf9 cells under ultraviolet (UV) fluorescence microscopy (Figure 2-21A). In contrast, no fluorescent particles nor crystals were detected in cells expressing only the EGFP tag. In addition, positive SONICC signal was detected in cells expressing nEGFP-μNS but not in non-infected cells (Figure 2-21B). Further investigation on the formation of nEGFP-μNS microcrystals and their diffraction characterization can be found in the recent report by Nagaratnam and co-workers (Nagaratnam et al.).

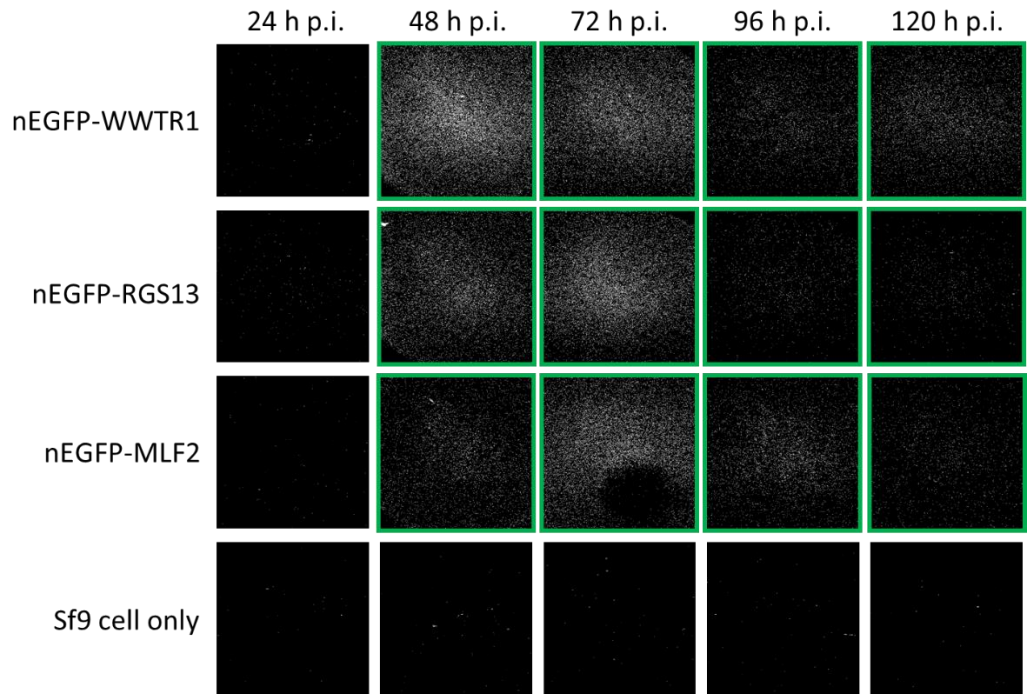

Figure 2-23. Time course of *in vivo* crystal formation. SONICC images of Sf9 cells expressing the indicated recombinant proteins or non-infected cells at 24, 48, 72, 96, and 120 h p.i. Targets that showed positive SONICC signals were shown in green boxes.

To test whether the pipeline could identify any novel protein crystal targets, we expanded the SONICC detection to a large set of recombinant proteins for HT

screening of *in vivo* microcrystals. A test collection of 34 proteins with nEGFP tag, 14 with cHalo tag, and 8 without a tag were produced and Sf9 cells expressing these recombinant proteins were imaged and analyzed by SONICC at 48 h p.i. (Figure 2-22). Excitingly, positive SONICC signals, which indicates the presence of crystals grown in the living insect cells, were observed for 29 proteins, representing ~52% of all tested protein targets. Among them, 7 targets showed extremely strong signals, indicating the presence of abundant crystalline particles that can be potentially be used for further X-ray diffraction studies.

Furthermore, we monitored time-dependent changes in protein crystallization by assessing target-expressing Sf9 cells harvested at different time points post infection. Three target proteins, MLF2, WWTR1, and RGS13, were expressed with the nEGFP tag, and were inspected by SONICC for the *in cellulo* crystallization signals over time. None of the tested target proteins exhibited positive SONICC signals before or at 24 h p.i. (Figure 2-23). A strong signal was first observed for nEGFP-WWTR1 at 48 h p.i., which slowly dropped over time until no crystals could be detected anymore after 120 h p.i. The first moderate signal was observed for nEGFP-RGS13 at 48 h p.i., followed by an increase to the maximal signal intensity after 72 h p.i., then a subsequent rapid decline. By comparison, nEGFP-MLF2 showed a mild signal at 48 h p.i., which subsequently increased to the maximal signal intensity after 72 h p.i., followed by a slight decrease in the signal intensity. These results may represent the protein-dependent variations in the growth dynamics of *in vivo* microcrystals. We hypothesize that crystals require a critical protein concentration in the cell for crystal formation, which is reached for most proteins after 48 h p.i. Crystal growth continues and maximizes after 72 h p.i. The decline of the crystals follows the decrease in cell viability. In addition, nEGFP-MLF2 and nEGFP-WWTR1 proteins displayed a punctate fluorescence pattern in particular region of cells

whereas nEGFP-RGS13 features an unevenly diffuse fluorescence in cells (Figure 2-24). Such differentiated fluorescence patterns might be associated with the difference in protein localization.

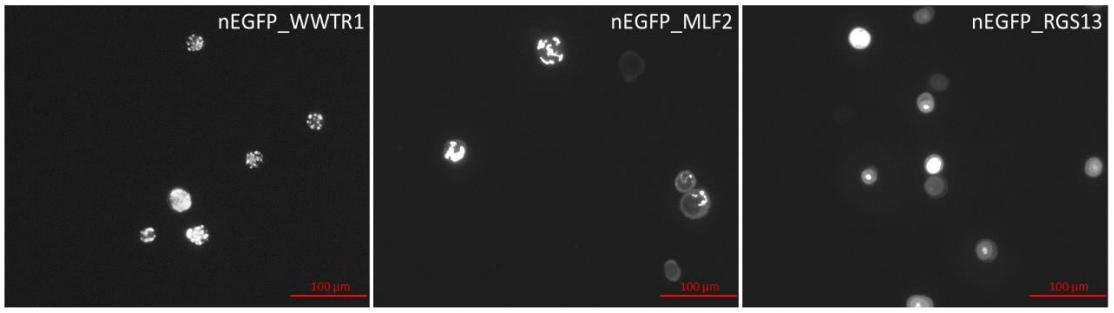

Figure 2-24. UV fluorescence images of the indicated SONICC positive targets. The Sf9 cells expressing the indicated SONICC positive hits showed different fluorescence patterns. Punctate fluorescence was observed for nEGFP-WWTR1 and nEGFP-MLF2 while uneven, diffuse fluorescence was observed for nEGFP-RGS13.

2.5 Discussion

In this study, we have established a BEVS-based protein production pipeline to enable mass parallel recombinant protein expression and rapid screening for *in vivo* microcrystals. We took advantage of the pIEx/BacMagic-3 expression vector system and Gateway cloning technology, and constructed a suite of pIEx-based expression vectors that support: 1) convenient HT construction of expression clones by single-step Gateway recombinational cloning; and 2) mass parallel expression of target proteins with different fusion tags of choice at either the N- or C-terminus to meet various protein research needs. We first demonstrated the successful application of our new vectors for overexpression of proteins in Sf9 cells (Figures 2-17 and 2-18) and their subsequent protein purification (Figure 2-20). We further demonstrated that the new system can be used for *in vivo* crystallization screening prior to scaled-up production of microcrystals for structural and functional studies

using a set of target proteins that vary in their host organism, molecular weight, and subcellular localization (Figures 2-16 and 2-22).

Insect cells were chosen as the primary expression system for this pipeline because of their relatively high protein production level and broad eukaryotic protein processing abilities (Jarvis 2009). In vivo protein crystallization has been observed in nature in a few cases including seeds and cockroaches (Banerjee et al. 2018). It has also been observed as a consequence of heterologous protein expression in bacteria (Hofte and Whiteley 1989), insect cells (Anduleit et al. 2005; Fan et al. 1996) and mammalian cells (Gallat et al. 2014; Hasegawa et al. 2011). However, in contrast to countless efforts devoted to *in vitro* crystallization over the past decades, the potential of *in vivo* crystals in structural biology has not yet been fully valued and exploited, mainly because the relatively small microcrystals formed *in vivo* are sensitive to radiation damage caused by conventional synchrotron X-ray radiation sources (Gallat et al. 2014). However, this challenge has been recently overcome by the emerging serial femtosecond X-ray crystallography (SFX) technique, which uses extremely bright and ultrashort X-ray pulses from XFEL sources to irradiate nano or microcrystals and record their diffraction before destruction occurs, therefore boosting the applicability of *in vivo* crystallization in structural biology (Gallat et al. 2014; Koopmann et al. 2012). The first study reporting the successful synergy of *in vivo* crystallization and SFX technology was published in 2013 by Redecke and co-workers (Redecke et al. 2013), in which they revealed the 2.1 Å resolution structure of TbCatB protein. This breakthrough experiment demonstrated that structural information can be obtained by the "diffraction-before-destruction" approach of SFX from thousands of microcrystals that are delivered to the XFEL beam in a liquid jet in their mother liquor (Gallat et al. 2014).The feasibility of solving protein structures using *in vivo*-grown microcrystals entails a HT pipeline to optimize protein

expression, *in vivo* crystal formation and structure determination protocols. We included nEGFP-μNS in our study as a positive control for *in vivo* crystallization and achieved high expression and good crystal formation (Figure 2-21). Similar results were observed in repeated experiments, suggesting such crystallization in living insect cells is highly reproducible. During the course of infection, the number of crystals continuously increased until most cells contained one or multiple crystals bundled together. The size of nEGFP-μNS crystals generally did not exceed the living insect cell dimensions (~15-20 μm) (Figure 2-21A). Interestingly, no obvious degradation of nEGFP-μNS crystals was observed after crystal-containing cells were stored at 4 °C for up to 2 weeks, although some crystal particles were seen floating freely in the medium or attached to cell remnants (Figure 2-21C). This indicates the good intrinsic stability of nEGFP-μNS crystals in agreement with the previous work by Schönherr and co-workers (Schönherr et al. 2015). We further used these nEGFP-μNS crystals successfully in SFX diffraction experiments being able to build the first electron density maps of the nEGFP-μNS protein (Nagaratnam et al. n.d.), which demonstrates the feasibility of using *in vivo*-grown crystals produced from our pipeline for structural studies.

The rapid HT *in cellulo* screening built on the current pipeline largely accelerates the identification of protein candidates that can form microcrystals prior to proceeding with in-depth structural characterization by SFX. Here, apart from μNS, we detected *in vivo*-grown crystals for 29 out of the 56 recombinant proteins tested (Figure 2-22), suggesting that when proteins are overexpressed in insect cells, the formation of microcrystals might be a more frequent event than previously known (Doye and Poon 2006; Schönherr et al. 2018). Interestingly, all positive hits identified in this study were nEGFP-tagged proteins, while no SONICC signals were observed for any target proteins expressed without tags or with the cHalo tag (Figure

2-22). Thereby, EGFP seems to be an efficient tag in promoting the crystallization of fusion proteins and enhancing microcrystal detection (Schönherr et al. 2015). Further X-ray diffraction of isolated crystals by SFX can be performed in the future to confirm the results and potentially determine the protein structures at high resolution; however, experimental "beamtime" at XFELs is quite limited as only 5 XFELs exist so far worldwide, and only one experiment can be performed at a given time. Microfocus beamlines at Synchrotrons with high flux and µm focus have also been recently used for successful structure determination of larger *in vivo*-grown crystals using serial microsecond X-ray crystallography (SMX). With even more SMX synchrotron beamlines under development and new developments in compact XFEL technology at Arizona State University (Graves et al. 2018) and in Germany at DESY (Kärtner et al. 2016), *in vivo*-grown crystals may soon become a commonly used route for protein crystallography.

Time-dependent monitoring of SONICC signals of three nEGFP-tagged proteins revealed that microcrystal formation of different target proteins followed various temporal patterns in terms of signal intensity and duration, which further emphasizes the importance of a HT pipeline to optimize the conditions for growth of structure-grade *in vivo* microcrystals. The nEGFP-WWTR1 protein showed a strong signal early at 48 h p.i., which slightly declined over time and lasted for up to 120 h p.i. The nEGFP-MLF2 and nEGFP-RGS13 proteins developed a mild-to-moderate signal around 48 h p.i., which subsequently reached a peak at 72 h p.i. and then decreased at different rate (Figure 2-23). As the intracellular crystallization process is highly dynamic (Schönherr et al. 2015), such protein-dependent variations in crystallization dynamics may indicate that crystal growth and degradation kinetics may vary for different protein targets depending on their expression level and subcellular localization (Schönherr et al. 2015). In addition, different fluorescence

patterns were observed within Sf9 cells expressing these target proteins (Supplementary Figure 2-24), although it is not yet clear how such difference relates to the *in vivo* crystallization process. In the future, further proteomic-scale investigation on a larger set of target proteins could provide even more insights to how the time-dependent crystal formation and/or fluorescence morphology correlate with promising X-ray diffraction results.

The incorporation of Gateway cloning technology into pIEx/BacMagic-3 system not only makes the pipeline amenable for HT construction of expression clones but also leverages the readily available ORF libraries for functional proteomics (Festa et al. 2013; Katzen 2007; Walhout et al. 2000). For example, our DNASU plasmid repository comprises ORFs encoding the proteomes for human, yeast, Drosophila, Arabidopsis, Xenopus, and hundreds of different bacteria and viruses. This provides plentiful starting materials to satisfy researchers' needs to study their proteins of interest.

Other than studying protein structure, there are many other applications where the protein production pipeline can be used as discussed in the following. 1) Enzymatic activity study. We have demonstrated that proteins produced from our pipeline can be successfully purified and remain functionally capable of catalyzing their substrates in biochemical reactions (unpublished data). This will enable researchers to explore how enzymatic proteins control crucial reactions in many key biochemical functions. 2) Protein interaction identification. A very crucial aspect of protein studies is to understand the crosstalk among millions of proteins to carry out various life functions. Previously, we developed Nucleic Acid Programmable Protein Array (NAPPA), which is capable of displaying and probing thousands of protein interactions at one time (Tang et al. 2017; Yu et al. 2015). In conjunction with our protein production system, we can further zoom in on specific interactions by

producing these proteins to assess interaction strength and dynamics. 3) Drug target screening. Protein malfunctions cause many human diseases, and one common therapeutic approach is designing drugs that hinder the abnormal behavior of key proteins in disease-relevant pathways. Current facilities in our lab allow HT screening for potential novel drug targets followed by producing them for further investigation on drug accuracy and efficiency (Rauf et al. 2018). Plasmids with multiple promoters, allowing for the simultaneous expression of two or more protein subunits, have also been developed for this classical recombination system (Belyaev and Roy 1993; Weyer and Possee 1991). Moreover, this protein expression pipeline in insect cells is highly amenable to automation (Possee et al. 2008). The infrastructure we have established at CPD for HT DNA preparation and protein production provides all major instrumentation needed to produce proteins from the insect cells in a HT fashion.

2.6 Conclusion

In summary, we have developed a HT protein production and microcrystal screening pipeline built on baculovirus-mediated insect expression system, which will feed target proteins for functional and structural studies. In this study, we constructed a set of Gateway-compatible pIEx destination vectors with various fusion tags and demonstrated successful mass parallel production of recombinant proteins and functional characterization of purified proteins using our pipeline. In conjunction with our existing DNASU plasmid repository and SONICC facility, this protein production pipeline supports translational research by enabling researchers to 1) select ORFs encoding POIs from DNASU; 2) HT express POIs using our protein production pipeline; 3) purify target proteins using affinity fusion tags; 4) screen for *in vivo* microcrystals with SONICC; and 5) perform detailed functional or structural characterization on target proteins (Figure 2-1). We believe this multi-facility pipeline will significantly benefit the protein research and ultimately lead to an in-depth

understanding of structure and functionality of proteins that are highly significant in human diseases or major biological pathways.

CHAPTER 3

3 DISCOVERING PROTEIN-PROTEIN INTERACTIONS USING NUCLEIC ACID PROGRAMMABLE PROTEIN ARRAYS

This chapter has been published:

Yanyang Tang, Ji Qiu, Matthias Machner, and Joshua LaBaer. Discovering protein-protein interactions using nucleic acid programmable protein arrays. Current Protocol Cell Biology. 2017 Mar 3;74:15.21.1-15.21.14. doi: 10.1002/cpcb.14.

3.1 Abstract

Proteins are the biomolecular machines that drive all important life functions. Proteins orchestrate the cellular processes of life through their interaction with and/or manipulation of other biomolecules. Identifying the interactors of proteins is essential to deciphering their biological functions. This unit provides a protocol for elucidating protein-protein interactions (PPIs) at the proteome scale on Nucleic Acid Programmable Protein Array (NAPPA) in a high-throughput multiplexed fashion without the need of purifying target or query protein. We have developed a protocol enabling the study of PPIs at the proteome level using *in vitro* synthesized proteins. Assay preparation requires molecular cloning of the query gene into a vector that supports *in vitro* transcription/translation (IVTT) and appends a HaloTag to the query protein of interest. In parallel, protein microarrays are prepared by printing plasmids encoding GST-tagged target proteins onto a carrier matrix/glass slide coated with antibody directed against GST. At the time of experiment, the query protein and the target proteins are produced separately using IVTT. The query protein is then applied to NAPPA arrays that display thousands of freshly produced target proteins captured by the antibody. Interactions between the query and immobilized target proteins are detected through addition of a fluorophore-labeled HaloTag ligand. Our protocol allows the elucidation of PPIs in a high-throughput fashion using proteins produced *in*

vitro, obviating the scientific challenges, high cost, laborious work, as well as concerns about protein stability present in protocols using conventional protein arrays. Chaperone proteins present in the human cell lysate further assists in protein folding during IVTT. Furthermore, the specific covalent bond between the HaloTag and its added ligand allows the detection of interactions without the need for anti-tag antibody or chemical labeling of the query protein. The "programmability" of our NAPPA protocol supports the study of query proteins with different tag configurations and/or refined studies of protein domains or regions important for the observed interactions with target proteins.

3.2 Introduction

Discovering Protein-Protein Interactions Using Protein Arrays Protein-protein interactions (PPIs) are fundamental to understanding biological systems. Proteomic techniques such as protein arrays allow profiling of PPIs at the proteome level (Jones et al. 2006; Kaushansky et al. 2008; Ramachandran et al. 2004, 2008; Ramani et al. 2012). Most conventional methods for studying PPIs on protein arrays require purified proteins, both query and target (Ramani et al. 2012), and the detection of interactions on arrays is usually achieved by either chemically labeling the query protein (with a fluorophore or with biotin), or using anti-tag or query protein-specific antibodies (Jones et al. 2006; Kaushansky et al. 2008). Despite demonstrated feasibility of these methods, protein arrays have not gained ground mainly due to methodical challenges (Ramachandran et al. 2004, 2008). For instance, the purification of full-length human or eukaryotic proteins is technically challenging and requires extensive optimization. Some proteins are extremely difficult to produce in surrogate hosts such as bacteria, yeast or insect cells. Also, the storage and/or chemical labeling can denature or mask epitopes or domains that are important for protein interactions. In addition, protein-specific antibodies may not be available or

lack specificity, leading to false positives or low signal-to-noise ratios (Yu et al. 2015).

To address some of these deficiencies, we have developed a protocol to study PPIs using *in vitro* synthesized query and target proteins. Our protocol begins with cloning of the query-encoding gene into the pJFT7_nHALO_DC expression vector which upon incubation with a HeLa cell lysate-based protein production system, enables the transcription and subsequent translation of a HaloTagged-query protein (Ramachandran et al. 2008). Our protocol was developed to work with NAPPA, which is an innovative protein platform that displays thousands of human target proteins without the need for protein purification (Miersch and LaBaer 2011; Qiu and Labaer 2011; Ramachandran et al. 2004, 2008). The human target genes are cloned into the pANT7_cGST expression vector which encodes for a carboxy-terminal GST-tag. Once the plasmids have been spotted on the array, the GST-tagged target proteins are freshly produced through IVTT using cell-free lysate, captured on the array by co-spotted anti-GST antibody, and displayed for the query to bind. Detailed protocols for the manufacturing of NAPPA arrays have been published before (Miersch and LaBaer 2011; Qiu and Labaer 2011; Sibani and LaBaer 2011).

The detection of interactions between HaloTagged query proteins and putative target proteins on the NAPPA arrays is achieved by addition of a fluorophore-conjugated HaloTag ligand. The HaloTag, used as a solubility enhancing fusion tag, is a modified haloalkane dehalogenase engineered to form a covalent bond with haloalkanes, including the fluorescent ligand (Saul et al. 2014). This ligand-based approach overcomes many of the detection challenges discussed above. Furthermore, the flexibility of using plasmid DNA and the on-demand protein production capability of NAPPA enables easy manipulation of the query proteins, including alterations in the tag configuration and fine mapping of interaction

sequence or domains by analyzing protein variants. Although our protocol uses NAPPA as an example, the concept is generally applicable to other protein platforms.

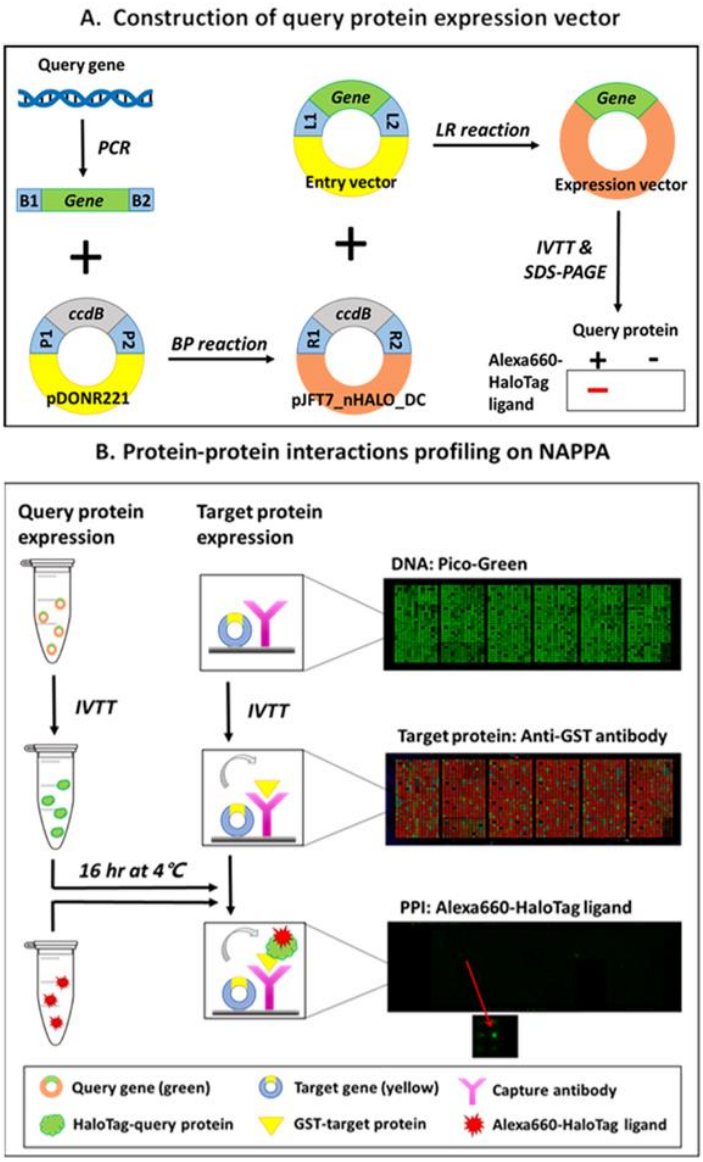

Figure 3-1. Flow scheme of protein interaction assay using NAPPA. **A)** Construction of query vector. Homologous recombination-based cloning of the query gene of interest into the expression vector. Size, amount, and stability of query proteins can be assessed by SDS-PAGE. **B)** PPI profiling on NAPPA. DNA printing and immobilization are validated with Pico Green staining (green); production and display of GST-tagged target proteins are examined with anti-GST antibody (red) after IVTT; binding of HaloTagged query protein to its interactors on NAPPA is detected using Alexa Fluor 660–conjugated HaloTag ligand.

As is true for most protein array technologies, the NAPPA protocol presented here does not eliminate all possible drawbacks. For example, the display of properly folded membrane proteins in the absence of a lipid bilayer is challenging (Katzen, Peterson, and Kudlicki 2009). Also, cDNA for all query and target proteins is needed in order to generate IVTT-compatible vectors. Moreover, cellular proteins within the cell-free expression system may result in false negatives by interfering with protein interactions. And lastly, proteins produced *in vitro* using the cell-free expression system might either lack critical post-translational modifications (PTMs) or display atypical ones (Ramachandran et al. 2008). Despite these potential downsides, the fact that NAPPA is a highly flexible platform makes it possible to counteract some of these issues, for example by adding missing enzymes and substrates required for PTMs or by including detergent and other critical reagents. In the past, we have been actively improving our protocol to specifically address these challenges (Yu and Labaer 2015).

This protocol describes the detailed procedures for proteome-level PPI profiling using freshly produced proteins without the need for protein purification. Basically, NAPPA arrays displaying thousands of human candidate target proteins are probed with a query protein fused to a HaloTag that allows the query to be visually detected by binding to fluorescently labeled ligand probes. This protocol consists of 5 components: (1) Query gene cloning: insertion of the gene encoding the query protein into the pJFT7_nHALO_DC expression vector (Figure 3-1A); (2) Query protein synthesis: IVTT of the expression vector to produce HaloTagged query protein (Figure 3-1B); (3) Target protein synthesis: expression of target gene DNA spotted on NAPPA using IVTT (Figure 3-1B); (4) PPI profiling: incubation of HaloTagged query protein with immobilized target proteins on the array and detection of interactions using an Alexa Fluor 660-conjugated HaloTag ligand (Figure

3-1B); (5) Imaging and data analysis: Extraction of fluorescence intensity information from each spot on the array and identification of candidate target proteins using appropriate quality criteria.

3.3 Methods and Materials

3.3.1 Construct Query Gene Expression Vectors

1) Obtain pDONR221_query_gene expression vector or construct by cloning the gene encoding the query protein into the Gateway entry vector pDONR221 (Park, Throop, and LaBaer 2015). Besides pDONR221, other common entry vectors supporting recombinational cloning, such as pDONR201 and pDONR223, can also be used. More than ~32,600 genes in pDONR221 vector are available from DNASU (https://dnasu.org/DNASU/) (Seiler et al. 2014). Check availability before cloning.
2) Obtain the destination expression vector pJFT7_nHALO_DC from DNASU (Saul et al. 2014). pJFT7_nHALO_DC adds an N-terminal HaloTag to recombinant proteins. It has an in-frame stop codon and can work with a query gene with or without a stop codon in pDONR221 entry vector. If using a different expression vector without an in-frame stop codon, the gene cloned into the pDONR221 entry vector must have its own stop codon. If using an expression vector with a C-terminal tag, the gene in the pDONR221 entry vector must not have a stop codon. There are ~6,000 human genes in pJFT7_nHALO_DC vector in DNASU. Check availability before cloning.
3) Prepare 10 µL of Gateway LR reaction mix as follows in a chilled tube: 6 µL of ice-cold DEPC nuclease-free water (Ambion, cat. no. 9906), 1 µL of 150 ng/µL pDONR221_query_gene, 1 µL of 150 ng/µL pJFT7_nHALO_DC, and 2 µL of 2 µg/µL Gateway LR Clonase Enzyme mix (Thermo Fisher Scientific, cat. no. 11791019). Incubate the reaction mix for 1 hr at 25 °C. Mix fresh just before use

by pipetting up and down several times. Do not vortex the reaction mix and be gentle when operating. Keep all reagents on ice.

4) Put the tube containing Gateway LR reaction mix on ice for at least 5 min.
5) Transfer 5 µL of Gateway LR reaction mix to a chilled tube, add 40 µL of *E. coli* DH5-alpha competent cells (Thermo Fisher Scientific, cat. no. 18258012) and keep on ice for 30 min.
6) Heat shock the competent cells in a 42 °C water bath for 45 s, and then keep on ice for at least 2 min.
7) Add 200 µL of S.O.C medium (Thermo Fisher Scientific, cat. no. 15544034) and incubate with agitation at ~700 rpm for 30 min at 37 °C.
8) Pre-warm the LB agar plate supplemented with 100 µg/mL ampicillin (Sigma-Aldrich, cat. no. A9518-25G) at 37 °C.
9) Spread the mixture on the LB agar plate using a sterile applicator and grow overnight at 37 °C.
10) Pick single colonies with pipette tips, inoculate in 5 mL of LB medium supplemented with 5 µL of 100 mg/mL ampicillin, and culture overnight at 250 rpm at 37 °C in a ground shaker.
11) Dispense 300 µL of culture into 700 µL of 80% glycerol and store at −80 °C as a glycerol stock for future use.
12) Miniprep the query gene using the QIAprep Spin Miniprep kit (Qiagen, cat. no. 27106) and quantify DNA concentration with the NanoDrop Spectrophotometer (Thermo Fisher Scientific, cat. no. ND-8000-GL). While both DNA miniprep and maxiprep are able to produce DNA of good quality as well as adequate concentration for sequencing or cloning purpose, the former is more time-efficient and can be done for a relatively large amount of DNA samples each time.

Therefore, DNA miniprep is a better option for sequencing confirmation of query gene.

13) Confirm the sequence of the miniprepped query gene using forward and reverse primers for identity confirmation. Sequencing primers for pJFT7_nHALO_query_gene are shown as follows: forward: AAGCCTGCCTAACTGCAA; reverse: TTTTTGTTTAAACTACCACTTT.

14) Maxiprep the query gene using the Nucleobond xtra Maxi kit (Macherey-Nagel, cat. no. 740 414.50), and quantify DNA concentration with the NanoDrop Spectrophotometer and store at −20 °C. Compared to DNA miniprep, maxiprep produces DNA of higher concentration, which can be used for PPI assay on NAPPA and other downstream validation studies to ensure consistency in terms of DNA quality and concentration.

15) Express the gene and check protein level using Alexa Fluor 660-HaloTag ligand (Promega, cat. no. G8471) (Saul et al. 2014). Besides confirmation by sequencing, it is recommended to confirm the correct size as well as to assess the production of the query protein from the expression vector before performing the PPI assay.

    a) Prepare 4 µL of IVTT mix as follows using the 1-step Human Coupled IVT Kit (Thermo Fisher Scientific, cat. no. 88881): 2.5 µL of HeLa lysate, 0.5 µL of Accessory proteins, and 1 µL of Reaction mix. Gently mix the IVTT mix with 1 µL of 200 ng/µL pJFT7_nHALO_query_gene and incubate at 30 °C for 2 hr in the EchoTherm programmable incubator. The volume showed here is just for one query gene sample and can be scaled up accordingly. The reaction can be prepared in PCR tube for a very small volume. Mix fresh just before use by pipetting up and down several times. Incubation at 30 °C is key to the efficient protein expression.

b) Add 2.5 µL of 4 µM Alexa Fluor 660-HaloTag ligand to the expression mixture and incubate for 20 min at room temperature. Cover the tube with black shields to keep the light out. Alexa Fluor 660 is light sensitive.

c) Add 2.5 µL of 4X Laemmli sample buffer (Bio-Rad, cat. no. 1610747) and boil the mixture for 5 min at 95 °C.

d) Run 10 µL of the resulting sample on SDS-PAGE until satisfactory separation. Include appropriate molecular weight markers. Cover the gel apparatus with black shields to keep the light out.

e) Rinse the gel with Milli-Q water 5 times. Minimize light exposure during washes.

f) Image the gel with the Typhoon FLA 9500 Scanner (GE Healthcare, cat. no. 28-9969-43) using 630/670 nm ex/em and 450 V PMT voltage.

g) Compare the band mobility against the expected molecular weight of query protein plus HaloTag. Ideally, a single band of the correct molecular weight is observed on the gel image. The molecular weight of HaloTag is ~34 kDa.

3.3.2 Express Target Genes on NAPPA

16) Obtain or prepare NAPPA arrays. NAPPA with more than 10,000 sequence-verified, full-length human open reading frames in pANT7_cGST vector can be obtained from NAPPA Protein Array Core (http://nappaproteinarray.org/) in standard or customized format. If homemade arrays are desired, refer to (Miersch and LaBaer 2011; Qiu and Labaer 2011; Ramachandran et al. 2008; Sibani and LaBaer 2011) for NAPPA manufacture procedures. Follow the following steps to clone target genes of interest into the expression vector pANT7_cGST if not available in DNASU. When working with a new set of NAPPA arrays, it is recommended to assess the target protein display with anti-GST (26H1) antibody (Cell Signaling Technologies, cat. no. 2624S) (Ramachandran et al. 2004, 2008).

In addition to using individual arrays for each HaloTagged query protein (pJFT7_nHALO_query_gene), an additional array should also be included for the HaloTag only (pJFT7_nHALO_empty) as a negative control.

17) Transfer arrays to a CELLSTAR FourWell plate (VWR, cat. no. 30617-596), add ~3 mL of SuperBlock (Pierce, cat. no. 37535) and incubate for 1 hr at room temperature on a rocker for 60 tilts per min.

18) Place arrays in a slotted slide rack, briefly rinse with Milli-Q water, and remove excess liquid with centrifugation at 1,000*g* for 2 min at 4 °C. Continue to the next step immediately after centrifugation.

19) Carefully align the HybriWell gasket (Grace Bio-Labs, cat. no. 440904) to the slide surface at the top, slowly apply to the slide and seal by rubbing the adhesive areas with a wooden stick. Avoid touching the HybriWell gasket to the printed spots on arrays. Make sure the printing area is in the center of the chamber. Do not press down too hard, otherwise it will be difficult for the IVTT mix to flow through the HybriWell chamber.

20) Prepare 160 µL of IVTT mix per slide as follows: 80 µL of HeLa lysate, 16 µL of Accessory proteins, 32 µL of Reaction mix, and 32 µL of DEPC nuclease-free water. Slowly inject from the entry port on the HybriWell gasket into the chamber. Both ports of the HybriWell gasket must be open for the IVTT mix to flow properly. Make sure the IVTT mix spreads over the entire array to get similar yields of all proteins. Remove air bubbles generated during injection out of the ports by gently tapping or massaging the HybriWell gasket. The presence of air bubbles may affect the production efficiency and display of proteins on NAPPA arrays. Mix fresh just before use by pipetting up and down several times. Any remaining IVTT mix can be stored at −80 °C for <1 month. However, the solution

should be used within three freeze/thaw cycles to avoid a substantial loss in activity.

21) Seal both ports with the round stickers using tweezers. Inadequate sealing will lead to significant artifacts on the arrays.

22) Place arrays on a Corning Square BioAssay Dish and incubate for 1.5 hr at 30 °C, followed by 30 min at 15 °C in the EchoTherm programmable incubator. Incubation at 30 °C is key for efficient protein production.

23) Remove the HybriWell gasket and wash arrays for 5 min with ~5 mL of PBST 3 times in a CELLSTAR FourWell plate on a rocker.

24) Place arrays in a slotted slide rack, thoroughly rinse with Milli-Q water 15 times.

3.3.3 Produce Query Protein *In Vitro*

25) Mix 20 µL of 500 ng/µL pJFT7_nHALO_query_gene or pJFT7_nHALO_empty with 180 µL of IVTT mix (see Step 15 (a)) per slide and incubate for 2 hr at 30 °C in the EchoTherm programmable incubator. The control vector pJFT7_nHALO_empty supports *in vitro* production of HaloTag without the query protein. It will be used as a negative control to detect protein interactions mediated by the tag (see Step 29). Store the freshly synthesized query proteins on ice before use (at Step 29).

3.3.4 Profile Protein-Protein Interactions on NAPPA

26) Transfer arrays (from Step 24) into a CELLSTAR FourWell plate, add ~3 mL of PPI blocking buffer and incubate for 2 hr at 4 °C on a rocker for 60 tilts per min.

27) Place arrays in a slotted slide rack, briefly rinse with Milli-Q water, and remove excess liquid with centrifugation at 1,000*g* for 2 min at 4 °C. Continue to the next step immediately after centrifugation.

28) Carefully align the HybriWell gasket to the slide surface at the top, slowly apply to the slide and seal by rubbing the adhesive areas with a wooden stick.

29) Slowly inject 180 µL of query protein or HaloTag IVTT mixture (from Step 25) from the entry port on the HybriWell gasket into the chamber. Incubate one array with HaloTagged query protein and one with HaloTag only as a control. In our experience, the HaloTag interacts only weakly with human proteins. However, it is highly recommended to probe one array with HaloTag as a negative control when working with a new set of target-protein arrays in order to assess background signals for data analysis purpose (see Step 50 (b)). Make sure the query fluid spreads over the entire array. Remove air bubbles generated during injection out of the ports by gently tapping or massaging the HybriWell gasket. The presence of air bubbles may affect the protein-protein interactions.
30) Seal both ports with the round stickers using tweezers. Inadequate sealing will lead to significant artifacts on the arrays.
31) Place arrays on a Corning Square BioAssay Dish (Fisher Scientific, cat. no. 06-443-22) and incubate for 16 hr at 4 °C.
32) Remove the HybriWell gasket and gently wash arrays for 5 min with ~1 mL of PPI washing buffer 3 times in a CELLSTAR FourWell plate on a rocker to remove unbound molecules.
33) Place arrays in a slotted slide rack, briefly rinse with Milli-Q water, and remove excess liquid with centrifugation at 1,000*g* for 2 min at 4 °C. Continue to the next step immediately after centrifugation.
34) Carefully align the HybriWell gasket to the slide surface at the top, slowly apply to the slide and seal by rubbing the adhesive areas with a wooden stick.
35) Prepare 12.5 µM Alex Fluor 660-HaloTag ligand in PPI washing buffer, and slowly inject 180 µL from the entry port on the HybriWell gasket into the chamber. Make sure the HaloTag ligand solution spreads over the entire array. Remove air bubbles generated during injection out of the ports by gently tapping or

massaging the HybriWell gasket. The presence of air bubbles may affect the binding of HaloTag ligand to HaloTag and therefore protein interactions.

36) Seal both ports with the round stickers using tweezers. Inadequate sealing will lead to significant artifacts on the arrays.

37) Place arrays on the StainTray slide staining system and incubate in the dark for 2 hr at 4 °C. Cover the StainTray slide staining system with black shields to keep light out.

38) Remove the HybriWell gasket and gently wash arrays in the dark for 5 min with ~1 mL of PPI washing buffer 3 times in a CELLSTAR FourWell plate on a rocker. Cover the CELLSTAR FourWell plate with black shields to keep light out. Minimize light exposure during washes.

39) Place arrays in a slotted slide rack, briefly rinse with Milli-Q water, and remove excess liquid with centrifugation at 1,000*g* for 2 min at 4 °C.

40) Scan the slides using the Tecan PowerScanner (Tecan) with appropriate settings (Resolution 10 um; Channel 2: 676/37; without autogain). With 'autogain', an automatic gain will be assigned for each individual slide, and the scanning parameters may change from slide to slide. Herein the 'autogain' is not recommended.

41) Save the array images in 16-bit TIFF format.

3.3.5 Select Target Candidates

42) Open array images in the Array-Pro Analyzer (Media Cybernetics) microarray software and examine the spot shape, dust and nonspecific binding to remove any possible false positive signals. Most commercial microarray analyzing software can be used for this work, such as ScanArray Express (PerkinElmer) and GenePix (Molecular Devices).

43) Quantify the average florescence signal intensity from microarray spots in an array image and produce a data file (.csv) using the Array-Pro Analyzer.
44) Open the data file (.csv) using the program Microsoft Excel 2013.
45) Estimate the background from nonspecific binding of probes by the first quartile of the printing-buffer-only spots as a negative control.
46) Adjust the raw signal intensity of each spot by subtracting the nonspecific binding background.
47) Normalize signal by dividing the background-adjusted signal intensity of each spot by the median background-adjusted value of all proteins on array. The aim of data normalization is to decrease the background variation between individual arrays.
48) Calculate Z-score using the normalized value for each spot on all arrays.
49) Select target candidates based on the following criteria: a) Z-score greater than or equal to 3; b) Z-score ratio of query to the negative control (HaloTag) higher than 1.5; c) The targets have to meet the previous criteria in two independent experiments; d) In addition, we also selected some potential candidates based on visual inspection of the luminous radiation ("ring/halo") around the spots. Previous work showed that these rings are best identified using the Array-Pro Analyzer by adjusting the contrast of microarray image, especially when the Z-score is low (Wagner R. Montor et al. 2009; Yu et al. 2015).

3.4 Commentary

3.4.1 Background Information

Proteins are the workhorses that undertake a variety of essential biological processes, including gene replication and expression, cell growth and proliferation, intercellular communications, and so on. While a single protein may function properly, the majority of these activities are executed and coordinated through a

network of interactions, or interactome. Therefore, studying proteins in the context of their interacting partners is of great importance to fully understand a protein's function and its role within the context of living systems.

Early attempts at experimental proteome-scale interactome network mapping started in the mid-1990s. In the past decade, significant steps have been taken towards the generation of comprehensive protein-protein interaction (PPI) network maps, including the first human interactome (Calderwood et al. 2007; Jäger et al. 2012; Krogan et al. 2006; Rozenblatt-Rosen et al. 2012; Shapira et al. 2009; Tafforeau, Rabourdin-Combe, and Lotteau 2012; Uetz et al. 2000), However, high quality protein-protein interactome datasets that emerged from these approaches were often low in coverage, and more than 80-90% of the interactions within the human proteome remain to be mapped (Tyagi et al. 2012; Venkatesan et al. 2009). Yeast two-hybrid (Y2H) and immunoprecipitation/mass spectrometry (IP/MS) are two platforms that have been routinely applied for the high-throughput study of protein interaction networks. Despite their demonstrated feasibility, both Y2H and IP/MS technologies also have a number of disadvantages. Y2H is often troubled with false negatives due to the limitation of the repertoire of proteins that can be produced, properly folded, and transported into the nucleus, and the limited coverage of the search space of all possible pairwise interactions (Calderwood et al. 2007; Rozenblatt-Rosen et al. 2012; Shapira et al. 2009; Tafforeau et al. 2012; Uetz et al. 2000). While IP/MS is invaluable to determine the constituents of protein complexes, it is not always the best method to detect direct interactions. IP/MS also suffers from the interference by abundant proteins and the failure to detect low abundance interactors or those that are not produced in a particular cell type (Jäger et al. 2012; Krogan et al. 2006).

Protein arrays offer a third high-throughput platform to interrogate the interactions between the query protein and thousands of target proteins on a microscopic glass slide (Jones et al. 2006; Kaushansky et al. 2008; Ramachandran et al. 2004, 2008; Ramani et al. 2012). This technology has several advantages over Y2H and IP/MS. First, it will only detect binary interactions between a query protein and the displayed target proteins, whereas the detection of misleading bridging interactions is unlikely to happen. Second, because proteins are individually organized on the array, interaction results are interpreted immediately. Third, the experimental set-up to study query proteins of interest against thousands of target proteins is extremely fast and easy. Finally, it is worth noting that the same plasmids used to produce both query proteins and target proteins on NAPPA can be immediately deployed for more detailed interaction studies once a new interaction has been detected on the array.

3.4.2 Critical Parameters

Our generic protocol works well for many query proteins we have tested and should serve as the starting point for assay optimization. Critical parameters affecting PPIs include the buffer components, query protein concentrations, and incubation time and temperature. Optimization of these parameters requires a balanced approach and depends on specific experimental goals. High salt/detergent concentrations and excessive washing will reduce background, but also diminish weak signals. High incubation temperature and long incubation time may result in high background, but it also gives high signals that may be needed to detect weak interactions. Short incubation time at a low temperature may result in high signal to noise (S/N) ratio if only strong interactions are of interest. Similarly, high query protein concentration will lead to strong signals and, probably, high background. On the other hand, low concentration may only reveal strong interactions. To obtain a

strong S/N ratio, a balance needs to be reached by optimizing the parameters discussed above. Apart from these general considerations of PPIs, individual query proteins may have unique requirements for buffer, temperature and tag configuration to preserve protein conformation for native interactions.

Some protocol steps where vulnerable reagents are involved should be performed with special care. For example, the HeLa cell lysate-based IVTT system will lose its activity due to repeated freeze-thaw cycles and needs to be aliquoted. Furthermore, cell-free protein production requires stringent control of temperature for maximal efficiency.

3.4.3 Troubleshooting

Troubleshooting advice can be found in Table 3-1.

Table 3-1. Troubleshooting table.

Step	Problem	Possible reason	Solution
43	No/low signals	Array slides were loaded upside down in the hybridization chamber, resulting in no target hybridization of probes (Steps 19, 28 and 34).	Repeat the experiment and ensure that the hybridization chamber is covered on the slide surface with microarray spots.
		Low levels of the query protein (Step 25).	Check the human cell-free expression system for protein production *in vitro*, as it may lose its activity during shipment and storage.
			Check protein amounts using fluorophore-conjugated HaloTag ligand.
		Low production level of target proteins on NAPPA (Step 22).	Check the human cell-free expression system for protein production *in vitro*, as it may lose its activity during shipment and storage.
			Check the protein amount on NAPPA using monoclonal mouse GST-specific antibody.
		Array slides are loaded upside down in the Tecan PowerScanner (Step 40).	Load the slide again in the Tecan PowerScanner with the microarray spots facing up.
		A wrong laser is chosen for array scanning (Step 40).	Choose the laser with appropriate excitation and emission wavelengths.
45	High background	The concentration of query protein may be too high (Steps 25 and 29)	Decrease the concentration of query proteins.
			Increase the washing cycles using PPI washing buffer.
		The query protein is sticky.	Optimizing assay parameters such as a lower incubation temperature and a more stringent washing buffer.

3.4.4 Anticipated Results

PPI profiling on NAPPA should ideally result in the detection of one or more interacting candidates. In other words, interactions between the query and select target proteins should lead to bright microarray spots on the array. The relative fluorescence intensities of spots correlate with the binding strength between interaction partners. A higher intensity, at times with the luminous radiation ("ring/halo") around the spot, is observed primarily for a stronger interaction. A ring is observed when the query protein binds to target proteins that "bleed" into the neighboring areas around spots during protein production and immobilization. This signal information is subject to data quantification and analysis, eventually leading to identification of interacting partners for the query protein of interest.

Figure 3-2 shows the representative results of PPI profiling of a HaloTagged version of the Legionella pneumonia effector LidA as a query protein against ~2,000 human target proteins on NAPPA array. Interactions between Rab1B and Rab27B with LidA are visually distinctive and have the highest Z-scores among all targets on arrays (Figure 3-2).

3.4.5 Time Considerations

The time required for the entire procedure depends on the experimental design, such as the number of query proteins to be studied and the number of NAPPA arrays to be probed. For construction of pJFT7_nHAO_query_gene expression vector, Gateway LR reaction and transformation require 2.5 hr, followed by plating on agar and overnight incubation. The *in vitro* generation of target proteins on NAPPA, including blocking and IVTT mix incubation, takes ~4 hr. The PPI profiling on NAPPA, including blocking, query protein binding, and Alexa Fluor 660-HaloTag ligand detection, takes ~21 hr, much of which is time for incubation. Scanning NAPPA

arrays requires ~7 min per slide with one setting cycle. Data quantification and candidate selection requires 12 hr.

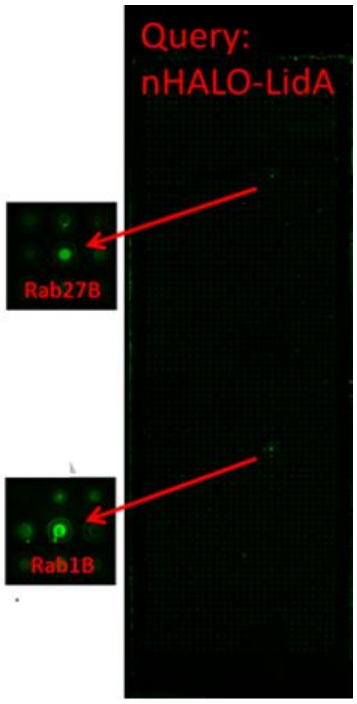

Figure 3-2. A representative image from PPI assay using NAPPA arrays. The slide was probed with HaloTag-LidA to identify the host interacting targets for L. pneumophila effectors. Interactors of interest are enlarged and marked with an arrow.

REFERENCES

Acharya, Nimish K., Eric P. Nagele, Min Han, Nicholas J. Coretti, Cassandra DeMarshall, Mary C. Kosciuk, Paul A. Boulos, and Robert G. Nagele. 2012. "Neuronal PAD4 Expression and Protein Citrullination: Possible Role in Production of Autoantibodies Associated with Neurodegenerative Disease." *Journal of Autoimmunity* 38(4):369–80.

Ahrens, Christian H. and George F. Rohrmann. 1995. "Replication of Orgyia Pseudotsugata Baculovirus DNA: Lef-2 and Ie-1 Are Essential and Ie-2, P34, and Op-Iap Are Stimulatory Genes." *Virology* 212(2):650–62.

Alzheimer, Von A. 1906. "Über Einen Eigenartigen Schweren Erkrankungsprozess Der Hirninde." *Neurologisches Centralblatt* 25:1134.

Alzheimer, Von A. 1907. "Über Eine Eigenartige Erkrankung Der Hirnrinde." *Zentralbl. Nervenh. Psych.* 18:177–79.

Alzheimer, Von A. 1911. "Über Eigenartige Krankheitsfälle Des Späteren Alters." *Z Ges Neurol Psychiatr* 4:356–85.

Anderson, Karen S., Sahar Sibani, Garrick Wallstrom, Ji Qiu, Eliseo A. Mendoza, Jacob Raphael, Eugenie Hainsworth, Wagner R. Montor, Jessica Wong, Jin G. Park, Naa Lokko, Tanya Logvinenko, Niroshan Ramachandran, Andrew K. Godwin, Jeffrey Marks, Paul Engstrom, and Joshua LaBaer. 2011. "Protein Microarray Signature of Autoantibody Biomarkers for the Early Detection of Breast Cancer." *Journal of Proteome Research* 10(1):85–96.

Andreasen, N. and K. Blennow. 2002. "β-Amyloid (Aβ) Protein in Cerebrospinal Fluid as a Biomarker for Alzheimer's Disease." *Peptides* 23:1205–1214.

Andreasen, N, L. Minthon, A. Clarberg, P. Davidsson, J. Gottfries, E. Vanmechelen, H. Vanderstichele, B. Winblad, and K. Blennow. 1999. "Sensitivity, Specificity, and Stability of CSF-Tau in AD in a Community-Based Patient Sample." *Neurology* 53(7):1488–94.

Andreasen, Niels, Camilla Hesse, Davidsson Pia, Lennart Minthon, Anders Wallin, Bengt Winblad, Hugo Vanderstichele, Eugeen Vanmechelen, and Kaj Blennow. 1999. "Cerebrospinal Fluid β-Amyloid (1-42) in Alzheimer Disease: Differences between Early-and Late-Onset Alzheimer Disease and Stability during the Course Of." *Arch Neurol* 56(6):673–80.

Andreasson, Ulf, Kaj Blennow, and Henrik Zetterberg. 2016. "Update on Ultrasensitive Technologies to Facilitate Research on Blood Biomarkers for Central Nervous System Disorders." *Alzheimer's and Dementia: Diagnosis, Assessment and Disease Monitoring* 3:98–102.

Anduleit, Karin, Geoff Sutton, Jonathan M. Diprose, Peter P. C. Mertens, Jonathan M. Grimes, and David I. Stuart. 2005. "Crystal Lattice as Biological Phenotype for Insect Viruses." *Protein Science* 14(10):2741–43.

Araki, Toshiyuki, Yo Sasaki, and Jeffrey Milbrandt. 2004. "Increased Nuclear NAD Biosynthesis and SIRT1 Activation Prevent Axonal Degeneration." *Science* 305(5686):1010–13.

Assenberg, Rene, Paul T. Wan, Sabine Geisse, and Lorenz M. Mayr. 2013. "Advances in Recombinant Protein Expression for Use in Pharmaceutical Research." *Current Opinion in Structural Biology* 23(3):393–402.

Association, Alzheimer. 2019. *2019 Alzheimer's Disease Facts and Figures*. Vol. 15.

Axford, Danny, Xiaoyun Ji, David I. Stuart, and Geoff Sutton. 2014. "In Cellulo Structure Determination of a Novel Cypovirus Polyhedrin." *Acta Crystallographica Section D: Biological Crystallography* 70(5):1435–41.

Ayres, Martin D., Stephen C. Howard, Miguel Lopez-Ferber, Miguel Lopez-Ferber, and Robert D. Possee. 1994. "The Complete DNA Sequence of Autographa Californica Nuclear Polyhedrosis Virus." *Virology* 202(2):586–605.

Banerjee, Sanchari, Pierre Montaville, Leonard M. G Chavas, and S. Ramaswamy. 2018. *The New Era of Microcrystallography*. Vol. 98.

Baneyx, François. 1999. "Recombinant Protein Expression in Escherichia Coli." *Current Opinion in Biotechnology* 10(5):411–21.

Barker, Warren W., Cheryl A. Luis, Alice Kashuba, Mercy Luis, Dylan G. Harwood, David Loewenstein, Carol Waters, Pat Jimison, Eugene Shepherd, Steven Sevush, Neil Graff-Radford, Douglas Newland, Murray Todd, Bayard Miller, Michael Gold, Kenneth Heilman, Leilani Doty, Ira Goodman, Bruce Robinson, Gary Pearl, Dennis Dickson, and Ranjan Duara. 2002. "Relative Frequencies of Alzheimer Disease, Lewy Body, Vascular and Frontotemporal Dementia, and Hippocampal Sclerosis in the State of Florida Brain Bank." *Alzheimer Disease and Associated Disorders*.

Barnes, Louise M. and Alan J. Dickson. 2006. "Mammalian Cell Factories for Efficient and Stable Protein Expression." *Current Opinion in Biotechnology* 17(4):381–86.

Barthel, Henryk, Hermann-Josef Gertz, Stefan Dresel, Oliver Peters, Peter Bartenstein, Buerger Katharina, Florian Hiemeyer, Sabine M. Wittemer-Rump, John Seibyl, Cornelia Reininger, and Osama Sabri. 2011. "Cerebral Amyloid-β PET with Fl Orbetaben (^{18}F) in Patients.Pdf." 424–35.

Bartos, Ales, Lenka Fialová, Jana Sřvarcová, and Daniela Ripova. 2012. "Patients with Alzheimer Disease Have Elevated Intrathecal Synthesis of Antibodies against Tau Protein and Heavy Neurofilament." *Journal of Neuroimmunology* 252(1–2):100–105.

Bateman, Alex. 2019. "UniProt: A Worldwide Hub of Protein Knowledge." *Nucleic Acids Research* 47(D1):D506–15.

Bateman, Randall J., Ling Y. Munsell, John C. Morris, Robert Swarm, Kevin E. Yarasheski, and David M. Holtzman. 2006. "Human Amyloid-β Synthesis and Clearance Rates as Measured in Cerebrospinal Fluid in Vivo." *Nature Medicine*

12(7):856–61.

Beilharz, Erica J., Eugene Zhukovsky, Anthony A. Lanahan, Paul F. Worley, Karoly Nikolich, and Laurie J. Goodman. 1998. "Neuronal Activity Induction of the Stathrnin-like Gene RB3 in the Rat Hippocampus: Possible Role in Neuronal Plasticity." *Journal of Neuroscience* 18(23):9780–89.

Van Bel, A. J. E. 2003. "The Phloem, a Miracle of Ingenuity." *Plant, Cell and Environment* 26(1):125–49.

Belyaev, A. S. and P. Roy. 1993. "Development of Baculovirus Triple and Quadruple Expression Vectors: Co-Expression of Three or Four Bluetongue Virus Proteins and the Synthesis of Bluetongue Virus-like Particles in Insect Cells." *Nucleic Acids Research* 21(5):1219–23.

Berchtold, Nicole C., David H. Cribbs, Paul D. Coleman, Joseph Rogers, Elizabeth Head, Ronald Kim, Tom Beach, Carol Miller, Juan Troncoso, John Q. Trojanowski, H. Ronald Zielke, and Carl W. Cotman. 2008. *Gene Expression Changes in the Course of Normal Brain Aging Are Sexually Dimorphic*.

Berrow, Nick S., David Alderton, Sarah Sainsbury, Joanne Nettleship, Rene Assenberg, Nahid Rahman, David I. Stuart, and Raymond J. Owens. 2007. "A Versatile Ligation-Independent Cloning Method Suitable for High-Throughput Expression Screening Applications." *Nucleic Acids Research* 35(6).

Berthelot, Karine, Christophe Cullin, and Sophie Lecomte. 2012. "Mini-Review What Does Make an Amyloid Toxic: Morphology, Structure or Interaction with Membrane?"

Bian, Xiaofang, Clive Wasserfall, Garrick Wallstrom, Jie Wang, Haoyu Wang, Kristi Barker, Desmond Schatz, Mark Atkinson, Ji Qiu, and Joshua LaBaer. 2017. "Tracking the Antibody Immunome in Type 1 Diabetes Using Protein Arrays." *Journal of Proteome Research* 16(1):195–203.

Biernat, J., N. Gustke, G. Drewes, E. Mandelkow, and E. Mandelkow. 1993. "Phosphorylation of Ser262 Strongly Reduces Binding of Tau to Microtubules: Distinction between PHF-like Immunoreactivity and Microtubule Binding." *Neuron* 11(1):153–63.

Bill, Roslyn M., Peter J. F. Henderson, So Iwata, Edmund R. S. Kunji, Hartmut Michel, Richard Neutze, Simon Newstead, Bert Poolman, Christopher G. Tate, and Horst Vogel. 2011. "Overcoming Barriers to Membrane Protein Structure Determination." *Nature Biotechnology* 29(4):335–40.

Blennow, K., A. Wallin, H. Ågren, C. Spenger, J. Siegfried, and E. Vanmechelen. 1995. "Tau Protein in Cerebrospinal Fluid - A Biochemical Marker for Axonal Degeneration in Alzheimer Disease?" *Molecular and Chemical Neuropathology* 26(3):231–45.

Blennow, Kaj. 2004. "Cerebrospinal Fluid Protein Biomarkers for Alzheimer's Disease." *NeuroRx* 1(2):213–25.

Blennow, Kaj. 2017. "A Review of Fluid Biomarkers for Alzheimer's Disease: Moving from CSF to Blood." *Neurology and Therapy* 6:15–24.

Blennow, Kaj, Pam Fredman, Anders Wallin, Carl-Gerhard Gottfries, Ingmar Skoog, Carsten Wikkelsö, and Lars Svennerholm. 1993. "Protein Analysis in Cerebrospinal Fluid." *European Neurology* 33(2):134–42.

Bolivar, F., R. L. Rodriguez, P. J. Greene, M. C. Betlach, H. L. Heynker, H. W. Boyer, J. H. Crosa, and S. Falkow. 1977. "Construction and Characterization of New Cloning Vehicles. II. A Multipurpose Cloning System." *Biotechnology (Reading, Mass.)* 2(2):95–113.

Botte, Mathieu, Aurélien Deniaud, and Christiane Schaffitzel. 2016. "Cell-Free Synthesis of Macromolecular Complexes." Pp. 79–95 in *Advances in Experimental Medicine and Biology*. Vol. 896. Springer New York LLC.

Boudes, Marion, Damià Garriga, Andrew Fryga, Tom Caradoc-Davies, and Fasséli Coulibaly. 2016. "A Pipeline for Structure Determination of in Vivo-Grown Crystals Using in Cellulo Diffraction." *Acta Crystallographica Section D: Structural Biology* 72(4):576–85.

Braak, H. and E. Braak. 1991. "Neuropathological Stageing of Alzheimer-Related Changes." *Acta Neuropathologica* 82(4):239–59.

Braak, Heiko and E. Braak. 1996. "Evolution of the Neuropathology of Alzheimer's Disease." *Acta Neurologica Scandinavica* 94(SUPPL.165):3–12.

Brandariz-Nunez, A., R. Menaya-Vargas, J. Benavente, and J. Martinez-Costas. 2010. "Avian Reovirus NS Protein Forms Homo-Oligomeric Inclusions in a Microtubule-Independent Fashion, Which Involves Specific Regions of Its C-Terminal Domain." *Journal of Virology* 84(9):4289–4301.

Braunagel, Sharon C. and Max D. Summers. 1994. "Autographa Californica Nuclear Polyhedrosis Virus, PDV, and ECV Viral Envelopes and Nucleocapsids: Structural Proteins, Antigens, Lipid and Fatty Acid Profiles." *Virology* 202(1):315–28.

Brinker, Thomas, Edward Stopa, John Morrison, and Petra Klinge. 2014. "A New Look at Cerebrospinal Fluid Circulation." *Fluids and Barriers of the CNS* 11(1).

Britschgi, M., C. E. Olin, H. T. Johns, Y. Takeda-Uchimura, M. C. Lemieux, K. Rufibach, J. Rajadas, H. Zhang, B. Tomooka, W. H. Robinson, C. M. Clark, A. M. Fagan, D. R. Galasko, D. M. Holtzman, M. Jutel, J. A. Kaye, C. A. Lemere, J. Leszek, G. Li, E. R. Peskind, J. F. Quinn, J. A. Yesavage, J. A. Ghiso, and T. Wyss-Coray. 2009. "Neuroprotective Natural Antibodies to Assemblies of Amyloidogenic Peptides Decrease with Normal Aging and Advancing Alzheimer's Disease." *Proc. Nati. Acad. Sci. USA* 106:12145–50.

Brown, M. and P. Faulkner. 1977. "A Plaque Assay for Nuclear Polyhedrosis Viruses Using a Solid Overlay." *Journal of General Virology* 36(2):361–64.

Buée, Luc, Thierry Bussière, Valérie Buée-Scherrer, André Delacourte, and Patrick R.

Hof. 2000. "Tau Protein Isoforms, Phosphorylation and Role in Neurodegenerative Disorders." *Brain Research Reviews* 33(1):95–130.

Bundy, Bradley C. and James R. Swartz. 2010. "Site-Specific Incorporation of p-Propargyloxyphenylalanine in a Cell-Free Environment for Direct Protein-Protein Click Conjugation." *Bioconjugate Chemistry* 21(2):255–63.

Burand, John P., Max D. Summers, and Gale E. Smith. 1980. "Transfection with Baculovirus DNA." *Virology* 101(1):286–90.

Burkholder, Joseph K., Jerilyn Decker, and Ning-Sun Yang. 1993. "Rapid Transgene Expression in Lymphocyte and Macrophage Primary Cultures after Particle Bombardment-Mediated Gene Transfer." *Journal of Immunological Methods* 165(2):149–56.

Cacabelos, Ramon, Lucia Fernandez-Novoa, Valter Lombardi, Yasuhiko Kubota, and Masatoshi Takeda. 2005. "Molecular Genetics of Alzheimer's Disease and Aging." *Methods and Findings in Experimental and Clinical Pharmacology* 27 Suppl A:1–573.

Calderwood, Michael A., Kavitha Venkatesan, Li Xing, Michael R. Chase, Alexei Vazquez, Amy M. Holthaus, Alexandra E. Ewence, Ning Li, Tomoko Hirozane-Kishikawa, David E. Hill, Marc Vidal, Elliott Kieff, and Eric Johannsen. 2007. "Epstein-Barr Virus and Virus Human Protein Interaction Maps." *Proceedings of the National Academy of Sciences of the United States of America* 104(18):7606–11.

Camus, V., P. Payoux, L. Barré, B. Desgranges, T. Voisin, C. Tauber, R. La Joie, M. Tafani, C. Hommet, G. Chételat, K. Mondon, V. De La Sayette, J. P. Cottier, E. Beaufils, M. J. Ribeiro, V. Gissot, E. Vierron, J. Vercouillie, B. Vellas, F. Eustache, and D. Guilloteau. 2012. "Using PET with 18F-AV-45 (Florbetapir) to Quantify Brain Amyloid Load in a Clinical Environment." *European Journal of Nuclear Medicine and Molecular Imaging* 39(4):621–31.

Carpentier, David C. J. and Linda A. King. 2009. "The Long Road to Understanding the Baculovirus P10 Protein." *Virologica Sinica* 24(4):227–42.

Carrió, M. M. and A. Villaverde. 2002. "Construction and Deconstruction of Bacterial Inclusion Bodies." *Journal of Biotechnology* 96(1):3–12.

Caselli, Richard J., Thomas G. Beach, Roy Yaari, and Eric M. Reiman. 2006. "Alzheimer's Disease a Century Later." *Journal of Clinical Psychiatry* 67(11):1784–1800.

Chambers, Adam C., Mine Aksular, Leo P. Graves, Sarah L. Irons, Robert D. Possee, and Linda A. King. 2018. "Overview of the Baculovirus Expression System." *Current Protocols in Protein Science* 91(1):5.4.1-5.4.6.

Chapman, Henry N., Petra Fromme, Anton Barty, Thomas A. White, Richard A. Kirian, Andrew Aquila, Mark S. Hunter, Joachim Schulz, Daniel P. Deponte, Uwe Weierstall, R. Bruce Doak, Filipe R. N. C. Maia, Andrew V. Martin, Ilme Schlichting, Lukas Lomb, Nicola Coppola, Robert L. Shoeman, Sascha W. Epp, Robert Hartmann, Daniel Rolles, Artem Rudenko, Lutz Foucar, Nils Kimmel, Georg Weidenspointner,

Peter Holl, Mengning Liang, Miriam Barthelmess, Carl Caleman, Sébastien Boutet, Michael J. Bogan, Jacek Krzywinski, Christoph Bostedt, Săa Bajt, Lars Gumprecht, Benedikt Rudek, Benjamin Erk, Carlo Schmidt, André Hömke, Christian Reich, Daniel Pietschner, Lothar Ströder, Günter Hauser, Hubert Gorke, Joachim Ullrich, Sven Herrmann, Gerhard Schaller, Florian Schopper, Heike Soltau, Kai Uwe Kühnel, Marc Messerschmidt, John D. Bozek, Stefan P. Hau-Riege, Matthias Frank, Christina Y. Hampton, Raymond G. Sierra, Dmitri Starodub, Garth J. Williams, Janos Hajdu, Nicusor Timneanu, M. Marvin Seibert, Jakob Andreasson, Andrea Rocker, Olof Jönsson, Martin Svenda, Stephan Stern, Karol Nass, Robert Andritschke, Claus Dieter Schröter, Faton Krasniqi, Mario Bott, Kevin E. Schmidt, Xiaoyu Wang, Ingo Grotjohann, James M. Holton, Thomas R. M. Barends, Richard Neutze, Stefano Marchesini, Raimund Fromme, Sebastian Schorb, Daniela Rupp, Marcus Adolph, Tais Gorkhover, Inger Andersson, Helmut Hirsemann, Guillaume Potdevin, Heinz Graafsma, Björn Nilsson, and John C. H. Spence. 2011. "Femtosecond X-Ray Protein Nanocrystallography." *Nature* 470(7332):73–78.

Charbaut, Elodie, Patrick A. Curmi, Sylvie Ozon, Sylvie Lachkar, Virginie Redeker, and André Sobel. 2001. "Stathmin Family Proteins Display Specific Molecular and Tubulin Binding Properties." *Journal of Biological Chemistry* 276(19):16146–54.

Charcot, J. M. and C. Robin. 1853. "Observation of Leukocytosis." *CR Mem. Soc. Biol.* 5:450–54.

Chattopadhaya, Souvik, Lay Pheng Tan, and Shao Q. Yao. 2006. "Strategies for Site-Specific Protein Biotinylation Using in Vitro, in Vivo and Cell-Free Systems: Toward Functional Protein Arrays." *Nature Protocols* 1(5):2386–98.

Chauvin, Stéphanie and André Sobel. 2015. "Neuronal Stathmins: A Family of Phosphoproteins Cooperating for Neuronal Development, Plasticity and Regeneration." *Progress in Neurobiology* 126:1–18.

Chayen, Naomi E. and Emmanuel Saridakis. 2008. "Protein Crystallization: From Purified Protein to Diffraction-Quality Crystal." *Nature Methods* 5(2):147–53.

Cheon, M. S., M. Fountoulakis, N. J. Cairns, M. Dierssen, K. Herkner, and G. Lubec. 2001. "Decreased Protein Levels of Stathmin in Adult Brains with Down Syndrome and Alzheimer's Disease." *Journal of Neural Transmission, Supplement* (61):281–88.

Chien, David T., Shadfar Bahri, A. Katrin Szardenings, Joseph C. Walsh, Fanrong Mu, Min Ying Su, William R. Shankle, Arkadij Elizarov, and Hartmuth C. Kolb. 2013. "Early Clinical PET Imaging Results with the Novel PHF-Tau Radioligand [F-18]-T807." *Journal of Alzheimer's Disease* 34(2):457–68.

Chien, David T., A. Katrin Szardenings, Shadfar Bahri, Joseph C. Walsh, Fanrong Mu, Chunfang Xia, William R. Shankle, Alan J. Lerner, Min Ying Su, Arkadij Elizarov, and Hartmuth C. Kolb. 2014. "Early Clinical PET Imaging Results with the Novel PHF-Tau Radioligand [F18]-T808." *Journal of Alzheimer's Disease* 38(1):171–84.

Citron, Martin, Tilman Oltersdorf, Christian Haass, Lisa Mcconlogue, Albert Y. Hung, Peter Seubert, Carmen Vigo-pelfrey, Ivan Lieberburg, and Dennis J. Selkoe. 1992. "Mutation of the B-Amyloid Precursor Protein in Familial Alzheimer's Disease

Increases b-Protein Production." 360(December):1991–93.

Citron, Martin, David Westaway, Weiming Xia, George Carlson, Thekla Diehl, Georges Levesque, Kelly Johnson-Wood, Michael Lee, Peter Seubert, Angela Davis, Dora Kholodenko, Ruth Motter, Robin Sherrington, Billie Perry, Hong Yao, Robert Strome, Ivan Lieberburg, Johanna Rommens, Soyeon Kim, Dale Schenk, Paul Fraser, Peter St. George Hyslop, and Dennis J. Selkoe. 1997. "Mutant Presenilins of Alzheimer's Disease Increase Production of 42-Residue Amyloid β-Protein in Both Transfected Cells and Transgenic Mice." *Nature Medicine* 3(1):67–72.

Clem, Rollie. 2007. "Baculoviruses and Apoptosis: A Diversity of Genes and Responses." *Current Drug Targets* 8(10):1069–74.

Colasanti, Tania, Cristiana Barbati, Giuseppe Rosano, Walter Malorni, and Elena Ortona. 2010. "Autoantibodies in Patients with Alzheimer's Disease: Pathogenetic Role and Potential Use as Biomarkers of Disease Progression." *Autoimmunity Reviews* 9(12):807–11.

Contreras-Gómez, A., A. Sánchez-Mirón, F. García-Camacho, E. Molina-Grima, and Y. Chisti. 2014. "Protein Production Using the Baculovirus-Insect Cell Expression System." *Biotechnology Progress* 30(1):1–18.

Corder, E. H., A. M. Saunders, W. J. Strittmatter, D. E. Schmechel, P. C. Gaskell, G. W. Small, A. D. Roses, J. L. Haines, and M. A. Pericak-Vance. 1993. "Gene Dose of Apolipoprotein E Type 4 Allele and the Risk of Alzheimer's Disease in Late Onset Families." *Science* 261(5123):921–23.

Correale, Jorge and Andrés Villa. 2007. "The Blood-Brain-Barrier in Multiple Sclerosis: Functional Roles and Therapeutic Targeting." *Autoimmunity* 40(2):148–60.

Coulibaly, Fasséli, Elaine Chiu, Sascha Gutmann, Chitra Rajendran, Peter W. Haebel, Keiko Ikeda, Hajime Mori, Vernon K. Ward, Clemens Schulze-Briese, and Peter Metcalf. 2009. "The Atomic Structure of Baculovirus Polyhedra Reveals the Independent Emergence of Infectious Crystals in DNA and RNA Viruses." *Proceedings of the National Academy of Sciences of the United States of America* 106(52):22205–10.

Coulibaly, Fasséli, Elaine Chiu, Keiko Ikeda, Sascha Gutmann, Peter W. Haebel, Clemens Schulze-Briese, Hajime Mori, and Peter Metcalf. 2007. "The Molecular Organization of Cypovirus Polyhedra." *Nature* 446(7131):97–101.

Counts, Scott E., Milos D. Ikonomovic, Natosha Mercado, Irving E. Vega, and Elliott J. Mufson. 2017. "Biomarkers for the Early Detection and Progression of Alzheimer's Disease." *Neurotherapeutics* 14(1):35–53.

Craig-Schapiro, Rebecca, Richard J. Perrin, Catherine M. Roe, Chengjie Xiong, Deborah Carter, Nigel J. Cairns, Mark A. Mintun, Elaine R. Peskind, Ge Li, Douglas R. Galasko, Christopher M. Clark, Joseph F. Quinn, Gina D'Angelo, James P. Malone, R. Reid Townsend, John C. Morris, Anne M. Fagan, and David M. Holtzman. 2010. "YKL-40: A Novel Prognostic Fluid Biomarker for Preclinical Alzheimer's Disease." *Biological Psychiatry* 68(10):903–12.

D'Andrea, Michael R. 2003. "Evidence Linking Neuronal Cell Death to Autoimmunity in Alzheimer's Disease." *Brain Research* 982(1):19–30.

D'Andrea, Michael R. 2005. "Add Alzheimer's Disease to the List of Autoimmune Diseases." *Medical Hypotheses* 64(3):458–63.

Dahlström, A., A. McRae, R. Polinsky, L. Nee, B. Sadasivan, and E. A. Ling. 1994. "Alzheimer's Disease Cerebrospinal Fluid Antibodies Display Selectivity for Microglia - Investigations with Cell Cultures and Human Cortical Biopsies." *Molecular Neurobiology* 9(1–3):41–54.

Davis, Judianne and William E. Van Nostrand. 1996. "Enhanced Pathologic Properties of Dutch-Type Mutant Amyloid β-Protein." *Proceedings of the National Academy of Sciences of the United States of America* 93(7):2996–3000.

Davis, Kenneth L., Leon J. Thal, Elkan R. Gamzu, Charles S. Davis, Robert F. Woolson, Stephen I. Gracon, David A. Drachman, Lon S. Schneider, Peter J. Whitehouse, Toni M. Hoover, John C. Morris, Claudia H. Kawas, David S. Knopman, Nancy L. Earl, Vinod Kumar, and Rachelle S. Doody. 1992. "A Double-Blind, Placebo-Controlled Multicenter Study of Tacrine for Alzheimer's Disease." *New England Journal of Medicine* 327(18):1253–59.

Deane, Rashid, Shi Du Yan, Ram Kumar Submamaryan, Barbara LaRue, Suzana Jovanovic, Elizabeth Hogg, Deborah Welch, Lawrence Manness, Chang Lin, Jin Yu, Hong Zhu, Jorge Ghiso, Blas Frangione, Alan Stern, Ann Marie Schmidt, Don L. Armstrong, Bernd Arnold, Birgit Liliensiek, Peter Nawroth, Florence Hofman, Mark Kindy, David Stern, and Berislav Zlokovic. 2003. "RAGE Mediates Amyloid-β Peptide Transport across the Blood-Brain Barrier and Accumulation in Brain." *Nature Medicine* 9(7):907–13.

DeKosky, Steven T. and Stephen W. Scheff. 1990. "Synapse Loss in Frontal Cortex Biopsies in Alzheimer's Disease: Correlation with Cognitive Severity." *Annals of Neurology* 27(5):457–64.

Delunardo, Federica, Paola Margutti, Simona Pontecorvo, Tania Colasanti, Fabrizio Conti, Rachele Riganò, Elisabetta Profumo, Alessandra Siracusano, Antonella Capozzi, Massimiliano Prencipe, Maurizio Sorice, Ada Francia, and Elena Ortona. 2007. "Screening of a Microvascular Endothelial CDNA Library Identifies Rabaptin 5 as a Novel Autoantigen in Alzheimer's Disease." *Journal of Neuroimmunology* 192(1–2):105–12.

DeMarshall, Cassandra A., Eric P. Nagele, Abhirup Sarkar, Nimish K. Acharya, George Godsey, Eric L. Goldwaser, Mary Kosciuk, Umashanger Thayasivam, Min Han, Benjamin Belinka, and Robert G. Nagele. 2016. "Detection of Alzheimer's Disease at Mild Cognitive Impairment and Disease Progression Using Autoantibodies as Blood-Based Biomarkers." *Alzheimer's and Dementia: Diagnosis, Assessment and Disease Monitoring* 3:51–62.

Derman, Alan I., William A. Prinz, Dominique Belin, and Jon Beckwith. 1993. "Mutations That Allow Disulfide Bond Formation in the Cytoplasm of Escherichia Coli." *Science* 262(5140):1744–47.

Disease, A. candidate plasma protein classifier to identify Alzheimer's. 2015. "A Candidate Plasma Protein Classifier to Identify Alzheimer's Disease." *Journal of Alzheimer's Disease* 43(2):549–63.

Doecke, James D., Simon M. Laws, Noel G. Faux, William Wilson, Samantha C. Burnham, Chiou Peng Lam, Alinda Mondal, Justin Bedo, Ashley I. Bush, Belinda Brown, Karl De Ruyck, Kathryn A. Ellis, Christopher Fowler, Veer B. Gupta, Richard Head, S. Lance Macaulay, Kelly Pertile, Christopher C. Rowe, Alan Rembach, Mark Rodrigues, Rebecca Rumble, Cassandra Szoeke, Kevin Taddei, Tania Taddei, Brett Trounson, David Ames, Colin L. Masters, and Ralph N. Martins. 2012. "Blood-Based Protein Biomarkers for Diagnosis of Alzheimer Disease." *Archives of Neurology* 69(10):1318–25.

Doglio, LE, R. Kanwar, GR Jackson, M. Perez, and J. Avila. 2006. "RETRACTED: γ-Cleavage-Independent Functions of Presenilin, Nicastrin, and Aph-1 Regulate Cell-Junction Organization and Prevent Tau Toxicity In Vivo." 50:359–75.

Doye, Jonathan P. K. and Wilson C. K. Poon. 2006. "Protein Crystallization in Vivo." *Current Opinion in Colloid and Interface Science* 11(1):40–46.

Drolle, Elizabeth, Francis Hane, Brenda Lee, and Zoya Leonenko. 2014. "Atomic Force Microscopy to Study Molecular Mechanisms of Amyloid Fibril Formation and Toxicity in Alzheimer's Disease." *Drug Metabolism Reviews* 46(2):207–23.

Du, Yansheng, Xing Wei, Richard Dodel, Norbert Sommer, Harald Hampel, Feng Gao, Zhizhong Ma, Liming Zhao, Wolfgang H. Oertel, and Martin Farlow. 2003. "Human Anti-β-Amyloid Antibodies Block β-Amyloid Fibril Formation and Prevent β-Amyloid-Induced Neurotoxicity." *Brain* 126(9):1935–39.

Duda, Sabrina, Torsten Witte, Martin Stangel, Jan Adams, Reinhold E. Schmidt, and Niklas T. Baerlecken. 2017. "Autoantibodies Binding to Stathmin-4: New Marker for Polyneuropathy in Primary Sjögren's Syndrome." *Immunologic Research* 65(6):1099–1102.

Duncan, Jason E., Nikki K. Lytle, Alfredo Zuniga, and Lawrence S. B. Goldstein. 2013. "The Microtubule Regulatory Protein Stathmin Is Required to Maintain the Integrity of Axonal Microtubules in Drosophila" edited by M. B. Feany. *PLoS ONE* 8(6):e68324.

Duszenko, Michael, Lars Redecke, Celestin Nzanzu Mudogo, Benjamin Philip Sommer, Stefan Mogk, Dominik Oberthuer, and Christian Betzel. 2015. "*In Vivo* Protein Crystallization in Combination with Highly Brilliant Radiation Sources Offers Novel Opportunities for the Structural Analysis of Post-Translationally Modified Eukaryotic Proteins." *Acta Crystallographica Section F Structural Biology Communications* 71(8):929–37.

E. Counts, Scott, Bin He, John G. Prout, Bernadeta Michalski, Lucia Farotti, Margaret Fahnestock, and Elliott J. Mufson. 2016. "Cerebrospinal Fluid ProNGF: A Putative Biomarker for Early Alzheimer's Disease." *Current Alzheimer Research* 13(7):800–808.

Edbauer, Dieter, Edith Winkler, Joerg T. Regula, Brigitte Pesold, Harald Steiner, and Christian Haass. 2003. "Reconstitution of γ-Secretase Activity." *Nature Cell Biology* 5(5):486–88.

Elkon, Keith B. and Gregg J. Silverman. 2012. "Naturally Occurring Autoantibodies to Apoptotic Cells." *Advances in Experimental Medicine and Biology* 750:14–26.

Fagan, Anne M., Mark A. Mintun, Robert H. Mach, Sang-Yoon Lee, Carmen S. Dence, Aarti R. Shah, Gina N. LaRossa, Michael L. Spinner, William E. Klunk, Chester A. Mathis, Steven T. DeKosky, John C. Morris, and David M. Holtzman. 2006. "Inverse Relation between in Vivo Amyloid Imaging Load and Cerebrospinal Fluid $A\beta_{42}$ in Humans." *Annals of Neurology* 59(3):512–19.

Fan, G. Y., Fausto Maldonado, Y. Zhang, Randall Kincaid, Mark H. Ellisman, and Louis N. Gastinel. 1996. "In Vivo Calcineurin Crystals Formed Using the Baculovirus Expression System." *Microscopy Research and Technique* 34(1):77–86.

Fernández, Francisco J. and M. Cristina Vega. 2013. "Technologies to Keep an Eye on: Alternative Hosts for Protein Production in Structural Biology." *Current Opinion in Structural Biology* 23(3):365–73.

Ferrer-Miralles, Neus, Joan Domingo-Espín, José Corchero, Esther Vázquez, and Antonio Villaverde. 2009. "Microbial Factories for Recombinant Pharmaceuticals." *Microbial Cell Factories* 8:1–8.

Festa, Fernanda, Jason Steel, Xiaofang Bian, and Joshua Labaer. 2013. "High-Throughput Cloning and Expression Library Creation for Functional Proteomics." *Proteomics* 13(9):1381–99.

Fialová, Lenka, Ales Bartos, Jana Švarcová, and Ivan Malbohan. 2011. "Increased Intrathecal High-Avidity Anti-Tau Antibodies in Patients with Multiple Sclerosis." *PLoS ONE* 6(11):1–7.

Forsberg, Anton, Henry Engler, Ove Almkvist, Gunnar Blomquist, Göran Hagman, Anders Wall, Anna Ringheim, Bengt Långström, and Agneta Nordberg. 2008. "PET Imaging of Amyloid Deposition in Patients with Mild Cognitive Impairment." *Neurobiology of Aging* 29(10):1456–65.

Fragoso-Loyo, Hilda, Javier Cabiedes, Alejandro Orozco-Narváez, Luis Dávila-Maldonado, Yemil Atisha-Fregoso, Betty Diamond, Luis Llorente, and Jorge Sánchez-Guerrero. 2008. "Serum and Cerebrospinal Fluid Autoantibodies in Patients with Neuropsychiatric Lupus Erythematosus. Implications for Diagnosis and Pathogenesis." *PLoS ONE* 3(10).

Friesen, Paul D. 1997. "Regulation of Baculovirus Early Gene Expression." Pp. 141–70 in *The Baculoviruses*. Springer US.

Froger, Alexandrine and James E. Hall. 2007. "Transformation of Plasmid DNA into E. Coli Using the Heat Shock Method." *Journal of Visualized Experiments* (6):2007.

Funk, C. Joel, Sharon C. Braunagel, and George F. Rohrmann. 1997. "Baculovirus

Structure." Pp. 7–32 in *The Baculoviruses*. Springer US.

Furst, Ansgar J., Gil D. Rabinovici, Ara H. Rostomian, Tyler Steed, Adi Alkalay, Caroline Racine, Bruce L. Miller, and William J. Jagust. 2012. "Cognition, Glucose Metabolism and Amyloid Burden in Alzheimer's Disease." *Neurobiology of Aging* 33(2):215–25.

Gallat, François Xavier, Naohiro Matsugaki, Nathan P. Coussens, Koichiro J. Yagi, Marion Boudes, Tetsuya Higashi, Daisuke Tsuji, Yutaka Tatano, Mamoru Suzuki, Eiichi Mizohata, Kensuke Tono, Yasumasa Joti, Takashi Kameshima, Jaehyun Park, Changyong Song, Takaki Hatsui, Makina Yabashi, Eriko Nango, Kohji Itoh, Fasséli Coulibaly, Stephen Tobe, S. Ramaswamy, Barbara Stay, So Iwata, and Leonard M. G. Chavas. 2014. "In Vivo Crystallography at X-Ray Freeelectron Lasers: The next Generation of Structural Biology?" *Philosophical Transactions of the Royal Society B: Biological Sciences* 369(1647):20130497.

Gao, Runping, Christopher J. McCormick, Michael J. P. Arthur, Richard Ruddell, Fiona Oakley, David E. Smart, Frank R. Murphy, Mark P. G. Harris, and Derek A. Mann. 2002. "High Efficiency Gene Transfer into Cultured Primary Rat and Human Hepatic Stellate Cells Using Baculovirus Vectors." *Liver* 22(1):15–22.

Gati, Cornelius, Gleb Bourenkov, Marco Klinge, Dirk Rehders, Francesco Stellato, Dominik Oberthür, Oleksandr Yefanov, Benjamin P. Sommer, Stefan Mogk, Michael Duszenko, Christian Betzel, Thomas R. Schneider, Henry N. Chapman, and Lars Redecke. 2014. "Serial Crystallography on in Vivo Grown Microcrystals Using Synchrotron Radiation." *IUCrJ* 1:87–94.

Gati, Cornelius, Dominik Oberthuer, Oleksandr Yefanov, Richard D. Bunker, Francesco Stellato, Elaine Chiu, Shin Mei Yeh, Andrew Aquila, Shibom Basu, Richard Bean, Kenneth R. Beyerlein, Sabine Botha, Sébastien Boutet, Daniel P. DePonte, R. Bruce Doak, Raimund Fromme, Lorenzo Galli, Ingo Grotjohann, Daniel R. James, Christopher Kupitz, Lukas Lomb, Marc Messerschmidt, Karol Nass, Kimberly Rendek, Robert L. Shoeman, Dingjie Wang, Uwe Weierstall, Thomas A. White, Garth J. Williams, Nadia A. Zatsepin, Petra Fromme, John C. H. Spence, Kenneth N. Goldie, Johannes A. Jehle, Peter Metcalf, Anton Barty, and Henry N. Chapman. 2017. "Atomic Structure of Granulin Determined from Native Nanocrystalline Granulovirus Using an X-Ray Free-Electron Laser." *Proceedings of the National Academy of Sciences of the United States of America* 114(9):2247–52.

Gaudet, Pascale, Pierre André Michel, Monique Zahn-Zabal, Aurore Britan, Isabelle Cusin, Marcin Domagalski, Paula D. Duek, Alain Gateau, Anne Gleizes, Valérie Hinard, Valentine Rech De Laval, Jin Jin Lin, Frederic Nikitin, Mathieu Schaeffer, Daniel Teixeira, Lydie Lane, and Amos Bairoch. 2017. "The NeXtProt Knowledgebase on Human Proteins: 2017 Update." *Nucleic Acids Research* 45(D1):D177–82.

Gavet, Olivier, Sa&#65533;d El Messari, Sylvie Ozon, and Andr&#65533; Sobel. 2002. "Regulation and Subcellular Localization of the Microtubule-Destabilizing Stathmin Family Phosphoproteins in Cortical Neurons." *Journal of Neuroscience Research* 68(5):535–50.

Ghosh, Sudip, Md Khalid Parvez, Kakoli Banerjee, Shiv K. Sarin, and Seyed E.

Hasnain. 2002. "Baculovirus as Mammalian Cell Expression Vector for Gene Therapy: An Emerging Strategy." *Molecular Therapy* 6(1):5–11.

Giil, Lasse M., Einar K. Kristoffersen, Christian A. Vedeler, Dag Aarsland, Jan Erik Nordrehaug, Bengt Winblad, Angel Cedazo-Minguez, Anders Lund, and Tove Ragna Reksten. 2015. "Autoantibodies toward the Angiotensin 2 Type 1 Receptor: A Novel Autoantibody in Alzheimer's Disease." *Journal of Alzheimer's Disease* 47(2):523–29.

Ginn, Helen M., Marc Messerschmidt, Xiaoyun Ji, Hanwen Zhang, Danny Axford, Richard J. Gildea, Graeme Winter, Aaron S. Brewster, Johan Hattne, Armin Wagner, Jonathan M. Grimes, Gwyndaf Evans, Nicholas K. Sauter, Geoff Sutton, and David I. Stuart. 2015. "Structure of CPV17 Polyhedrin Determined by the Improved Analysis of Serial Femtosecond Crystallographic Data." *Nature Communications* 6(1):1–8.

Giraldo, P. and L. Montoliu. 2001. "Size Matters: Use of YACs, BACs and PACs in Transgenic Animals." *Transgenic Research* 10(2):83–103.

Gisslén, Magnus, Richard W. Price, Ulf Andreasson, Niklas Norgren, Staffan Nilsson, Lars Hagberg, Dietmar Fuchs, Serena Spudich, Kaj Blennow, and Henrik Zetterberg. 2016. "Plasma Concentration of the Neurofilament Light Protein (NFL) Is a Biomarker of CNS Injury in HIV Infection: A Cross-Sectional Study." *EBioMedicine* 3:135–40.

Goedert, M., C. M. Wischik, R. A. Crowther, J. E. Walker, and A. Klug. 1988. "Cloning and Sequencing of the CDNA Encoding a Core Protein of the Paired Helical Filament of Alzheimer Disease: Identification as the Microtubule-Associated Protein Tau." *Proceedings of the National Academy of Sciences of the United States of America* 85(11):4051–55.

Goedert, Michel and Maria Grazia Spillantini. 2006. "REVIEWS A Century of Alzheimer ' s Disease." *Science* 314:777–81.

Golde, Todd E., Steven Estus, Linda H. Younkin, Dennis J. Selkoe, and Steven G. Younkin. 1992. "Processing of the Amyloid Protein Precursor to Potentially Amyloidogenic Derivatives." *Science* 255(5045):728–30.

Gómez-Isla, Teresa, Joseph L. Price, Daniel W. McKeel, John C. Morris, John H. Growdon, and Bradley T. Hyman. 1996. "Profound Loss of Layer II Entorhinal Cortex Neurons Occurs in Very Mild Alzheimer's Disease." *Journal of Neuroscience* 16(14):4491–4500.

Gottesman, Susan. 1996. " PROTEASES AND THEIR TARGETS IN ESCHERICHIA COLI ." *Annual Review of Genetics* 30(1):465–506.

Götz, J., F. Chen, J. Van Dorpe, and R. M. Nitsch. 2001. "Formation of Neurofibrillary Tangles in P301L Tau Transgenic Mice Induced by Aβ42 Fibrils." *Science* 293(5534):1491–95.

Grabowski, Thomas J., Hyun Soon Cho, Jean Paul G. Vonsattel, G. William Rebeck, and Steven M. Greenberg. 2001. "Novel Amyloid Precursor Protein Mutation in an Iowa Family with Dementia and Severe Cerebral Amyloid Angiopathy." *Annals of Neurology* 49(6):697–705.

Graham, F. L., J. Smiley, W. C. Russell, and R. Nairn. 1977. "Characteristics of a Human Cell Line Transformed by DNA from Human Adenovirus Type 5." *Journal of General Virology* 36(1):59–72.

Graves, W. S., J. P. J. Chen, P. Fromme, M. R. Holl, R. Kirian, L. E. Malin, K. E. Schmidt, J. C. H. Spence, M. Underhill, U. Weierstall, N. A. Zatsepin, and C. Zhang. 2018. "ASU COMPACT XFEL*." *38th Int. Free Electron Laser Conf.* TUB03:225–28.

Greenberg, Steven M., G. William Rebeck, Jean Paul G. Vonsattel, Teresa Gomez-Isla, and Bradley T. Hyman. 1995. "Apolipoprotein E E4 and Cerebral Hemorrhage Associated with Amyloid Angiopathy." *Annals of Neurology* 38(2):254–59.

Grodberg, J. and J. J. Dunn. 1988. "OmpT Encodes the Escherichia Coli Outer Membrane Protease That Cleaves T7 RNA Polymerase during Purification." *Journal of Bacteriology* 170(3):1245–53.

Grover, J., D. Tilman, C. N. Vargas, J. Adams, R. R. Sharp, D. S. Treves, J. Adams, V. Souza, R. E. Lenski, S. Manning, J. Adams, R. E. Lenski, M. Travisano, U. Dieckmann, G. Saxer, M. Travisano, M. Doebeli, C. Adami, C. O. Wilke, C. Ofria, R. T. Pennock, C. Adami, C. Ofria, R. Standish, H. A. Abbass, L. Pauling, V. Bryson, and H. J. Vogel. 2004. "Self-Assembling Protein Microarrays." *Science* 305(July):86–91.

Gruden, Marina A., Tatyana B. Davidova, Mantas Mališauskas, Robert D. E. Sewell, Nina I. Voskresenskaya, Kristina Wilhelm, Elena I. Elistratova, Vladimir V. Sherstnev, and Ludmilla A. Morozova-Roche. 2007. "Differential Neuroimmune Markers to the Onset of Alzheimer's Disease Neurodegeneration and Dementia: Autoantibodies to Aβ(25-35) Oligomers, S100b and Neurotransmitters." *Journal of Neuroimmunology* 186(1–2):181–92.

Grundke-Iqbal, I., K. Iqbal, Y. C. Tung, M. Quinlan, H. M. Wisniewski, and L. I. Binder. 1986. "Abnormal Phosphorylation of the Microtubule-Associated Protein Tau (Tau) in Alzheimer Cytoskeletal Pathology." *Proceedings of the National Academy of Sciences of the United States of America* 83(13):4913–17.

Gustaw, Katarzyna A., Matthew R. Garrett, Hyoung Gon Lee, Rudy J. Castellani, Michael G. Zagorski, Annamalai Prakasam, Sandra L. Siedlak, Xiongwei Zhu, George Perry, Robert B. Petersen, Robert P. Friedland, and Mark A. Smith. 2008. "Antigen-Antibody Dissociation in Alzheimer Disease: A Novel Approach to Diagnosis." *Journal of Neurochemistry* 106(3):1350–56.

Guzman, L. M., D. Belin, M. J. Carson, and J. Beckwith. 1995. "Tight Regulation, Modulation, and High-Level Expression by Vectors Containing the Arabinose P(BAD) Promoter." *Journal of Bacteriology* 177(14):4121–30.

Haass, Christian, Michael G. Schlossmacher, Albert Y. Hung, Carmen Vigo-Pelfrey, Angela Mellon, Beth L. Ostaszewski, Ivan Lieberburg, Edward H. Koo, Dale Schenk, David B. Teplow, and Dennis J. Selkoe. 1992. "Amyloid β-Peptide Is Produced by Cultured Cells during Normal Metabolism." *Nature* 359(6393):322–25.

Hanes, Jozef and Andreas Plückthun. 1997. "In Vitro Selection and Evolution of Functional Proteins by Using Ribosome Display." *Proceedings of the National*

Academy of Sciences of the United States of America 94(10):4937–42.

Hansson, Oskar, Henrik Zetterberg, Eugeen Vanmechelen, Hugo Vanderstichele, Ulf Andreasson, Elisabet Londos, Anders Wallin, Lennart Minthon, and Kaj Blennow. 2010. "Evaluation of Plasma Aβ 40 and Aβ 42 as Predictors of Conversion to Alzheimer's Disease in Patients with Mild Cognitive Impairment." *Neurobiology of Aging* 31(3):357–67.

Harada, Ryuichi, Nobuyuki Okamura, Shozo Furumoto, Tetsuro Tago, Masahiro Maruyama, Makoto Higuchi, Takeo Yoshikawa, Hiroyuki Arai, Ren Iwata, Yukitsuka Kudo, and Kazuhiko Yanai. 2013. "Comparison of the Binding Characteristics of [18F]THK-523 and Other Amyloid Imaging Tracers to Alzheimer's Disease Pathology." *European Journal of Nuclear Medicine and Molecular Imaging* 40(1):125–32.

Harrison, Robert L., Elisabeth A. Herniou, Johannes A. Jehle, David A. Theilmann, John P. Burand, James J. Becnel, Peter J. Krell, Monique M. van Oers, Joseph D. Mowery, and Gary R. Bauchan. 2018. "ICTV Virus Taxonomy Profile: Baculoviridae." *Journal of General Virology* 99(9):1185–86.

Harrison, Robert L. and Donald L. Jarvis. 2016. "Transforming Lepidopteran Insect Cells for Continuous Recombinant Protein Expression." *Methods in Molecular Biology* 1350:329–48.

Hartig, T. 1855. "About the Gluten Flour." *Botanische Zeitung* 13:881–82.

Hartley, J. L., G. F. Temple, and M. A. Brasch. 2000. "DNA Cloning Using in Vitro Site-Specific Recombination." *Genome Research* 10(11):1788–95.

Hasegawa, Haruki, John Wendling, Feng He, Egor Trilisky, Riki Stevenson, Heather Franey, Francis Kinderman, Gary Li, Deirdre Murphy Piedmonte, Timothy Osslund, Min Shen, and Randal R. Ketchem. 2011. "In Vivo Crystallization of Human IgG in the Endoplasmic Reticulum of Engineered Chinese Hamster Ovary (CHO) Cells." *Journal of Biological Chemistry* 286(22):19917–31.

Hashimoto, Hiroki, Kazunori Kawamura, Nobuyuki Igarashi, Makoto Takei, Tomoya Fujishiro, Yoshiharu Aihara, Satoshi Shiomi, Masatoshi Muto, Takehito Ito, Kenji Furutsuka, Tomoteru Yamasaki, Joji Yui, Lin Xie, Maiko Ono, Akiko Hatori, Kazuyoshi Nemoto, Tetsuya Suhara, Makoto Higuchi, and Ming Rong Zhang. 2014. "Radiosynthesis, Photoisomerization, Biodistribution, and Metabolite Analysis of 11C-PBB3 as a Clinically Useful PET Probe for Imaging of Tau Pathology." *Journal of Nuclear Medicine* 55(9):1532–38.

Hatterer, Eric, Monique Touret, Marie-Françoise Belin, Jérôme Honnorat, and Serge Nataf. 2008. "Cerebrospinal Fluid Dendritic Cells Infiltrate the Brain Parenchyma and Target the Cervical Lymph Nodes under Neuroinflammatory Conditions" edited by J. Kanellopoulos. *PLoS ONE* 3(10):e3321.

Hebert, Liesi E., Paul A. Scherr, Julia L. Bienias, David A. Bennett, and Denis A. Evans. 2003. "Alzheimer Disease in the US Population: Prevalence Estimates Using the 2000 Census." *Archives of Neurology* 60(8):1119–22.

Hebert, Liesi E., Jennifer Weuve, Paul A. Scherr, and Denis A. Evans. 2013. "Alzheimer Disease in the United States (2010–2050) Estimated Using the 2010 Census." *Neurology* 80(19):1778–83.

Hellwig, Konstantin, Hlin Kvartsberg, Erik Portelius, Ulf Andreasson, Timo Jan Oberstein, Piotr Lewczuk, Kaj Blennow, Johannes Kornhuber, Juan Manuel Maler, Henrik Zetterberg, and Philipp Spitzer. 2015. "Neurogranin and YKL-40: Independent Markers of Synaptic Degeneration and Neuroinflammation in Alzheimer's Disease." *Alzheimer's Research and Therapy* 7(1).

Herniou, Elisabeth and Johannes Jehle. 2007. "Baculovirus Phylogeny and Evolution." *Current Drug Targets* 8(10):1043–50.

Heron, MP. 2018. "Deaths: Leading Causes for 2016."

Hippius, Hanns and Gabriele Neundörfer. 2003. "The Discovery of Alzheimer's Disease." *Dialogues in Clinical Neuroscience* 5(1):101–8.

Hirokawa, Nobutaka, Takeshi Funakoshi, Reiko Sato-Harada, and Yoshimitsu Kanai. 1996. "Selective Stabilization of Tau in Axons and Microtubule-Associated Protein 2C in Cell Bodies and Dendrites Contributes to Polarized Localization of Cytoskeletal Proteins in Mature Neurons." *Journal of Cell Biology* 132(4):667–79.

Hitchman, Richard B., Robert D. Possee, Andrew T. Crombie, Adam Chambers, Kim Ho, Evangelia Siaterli, Olga Lissina, Heather Sternard, Robert Novy, Kathryn Loomis, Louise E. Bird, Raymond J. Owens, and Linda A. King. 2010. "Genetic Modification of a Baculovirus Vector for Increased Expression in Insect Cells." *Cell Biology and Toxicology* 26(1):57–68.

Hitchman, Richard B., Robert D. Possee, and Linda A. King. 2009. "Baculovirus Expression Systems for Recombinant Protein Production in Insect Cells." *Recent Patents on Biotechnology* 46–54.

Hitchman, Richard B., Robert D. Possee, and Linda A. King. 2012. "High-Throughput Baculovirus Expression in Insect Cells." *Methods in Molecular Biology* 824:609–27.

Hitzeman, R. A., C. N. Chang, C. Y. Chen, A. Singh, T. Etcheverry, V. Chisholm, W. Kohr, G. Vehar, M. Renz, and D. Dowbenko. 1988. "Hansenula Polymorpha as a Novel Yeast System for the Expression of Heterologous Genes." *Biochemical Society Transactions* 16(6):1081.

Hitzeman, Ronald A., Frank E. Hagie, Howard L. Levine, David V. Goeddel, Gustav Ammerer, and Benjamin D. Hall. 1981. "Expression of a Human Gene for Interferon in Yeast." *Nature* 293(October):1–6.

Hoffmann, Frank and Ursula Rinas. 2004. "Roles of Heat-Shock Chaperones in the Production of Recombinant Proteins in Escherichia Coli." *Advances in Biochemical Engineering/Biotechnology* 89:143–61.

Hofte, H. and H. R. Whiteley. 1989. "Insecticidal Crystal Proteins of Bacillus Thuringiensis." *Microbiological Reviews* 53(2):242–55.

Holtzman, David M., Kelly R. Bales, Tanya Tenkova, Anne M. Fagan, Maia Parsadanian, Leah J. Sartorius, Brian Mackey, John Olney, Daniel McKeel, David Wozniak, and Steven M. Paul. 2000. "Apolipoprotein E Isoform-Dependent Amyloid Deposition and Neuritic Degeneration in a Mouse Model of Alzheimer's Disease." *Proceedings of the National Academy of Sciences of the United States of America* 97(6):2892–97.

Holtzman, David M., Joachim Herz, and Guojun Bu. 2012. "Apolipoprotein E and Apolipoprotein E Receptors: Normal Biology and Roles in Alzheimer Disease." *Cold Spring Harbor Perspectives in Medicine* 2(3):1–24.

Holtzman, David M., John C. Morris, and Alison M. Goate. 2011. "Alzheimer's Disease: The Challenge of the Second Century." *Science Translational Medicine* 3(77).

Hoover, Brian R., Miranda N. Reed, Jianjun Su, Rachel D. Penrod, Linda A. Kotilinek, Marianne K. Grant, Rose Pitstick, George A. Carlson, Lorene M. Lanier, Li Lian Yuan, Karen H. Ashe, and Dezhi Liao. 2010. "Tau Mislocalization to Dendritic Spines Mediates Synaptic Dysfunction Independently of Neurodegeneration." *Neuron* 68(6):1067–81.

Hu, Chaojun, Wei Huang, Hua Chen, Guang Song, Ping Li, Qiang Shan, Xuan Zhang, Fengchun Zhang, Heng Zhu, Lin Wu, and Yongzhe Li. 2015. "Autoantibody Profiling on Human Proteome Microarray for Biomarker Discovery in Cerebrospinal Fluid and Sera of Neuropsychiatric Lupus." *PLoS ONE* 10(5).

Hu, Yuan Yuan, Shan Shu He, Xiaochuan Wang, Qiu Hong Duan, Inge Grundke-Iqbal, Khalid Iqbal, and Jianzhi Wang. 2002. "Levels of Nonphosphorylated and Phosphorylated Tau in Cerebrospinal Fluid of Alzheimer's Disease Patients: An Ultrasensitive Bienzyme-Substrate-Recycle Enzyme-Linked Immunosorbent Assay." *American Journal of Pathology* 160(4):1269–78.

Huang, Yadong and Lennart Mucke. 2012. "Alzheimer Mechanisms and Therapeutic Strategies." *Cell* 148(6):1204–22.

Hunter, Molly, Ping Yuan, Divya Vavilala, and Mark Fox. 2019. "Optimization of Protein Expression in Mammalian Cells." *Current Protocols in Protein Science* 95(1):1–28.

Ijkel, Wilfred F. J., Marcel Westenberg, Rob W. Goldbach, Gary W. Blissard, Just M. Vlak, and Douwe Zuidema. 2000. "A Novel Baculovirus Envelope Fusion Protein with a Proprotein Convertase Cleavage Site." *Virology* 275(1):30–41.

Iwatsubo, Takeshi, Asano Odaka, Nobuhiro Suzuki, Hidehiro Mizusawa, Nobuyuki Nukina, and Yasuo Ihara. 1994. "Visualization of Aβ42(43) and Aβ40 in Senile Plaques with End-Specific Aβ Monoclonals: Evidence That an Initially Deposited Species Is Aβ42(43)." *Neuron* 13(1):45–53.

J. Baranello, Robert, Krishna L. Bharani, Vasudevaraju Padmaraju, Nipun Chopra, Debomoy K. Lahiri, Nigel H. Greig, Miguel A. Pappolla, and Kumar Sambamurti. 2015. "Amyloid-Beta Protein Clearance and Degradation (ABCD) Pathways and Their

Role in Alzheimer’s Disease." *Current Alzheimer Research* 12:32–46.

Jack, Clifford R., Marilyn S. Albert, David S. Knopman, Guy M. McKhann, Reisa A. Sperling, Maria C. Carrillo, Bill Thies, and Creighton H. Phelps. 2011. "Introduction to the Recommendations from the National Institute on Aging-Alzheimer's Association Workgroups on Diagnostic Guidelines for Alzheimer's Disease." *Alzheimer's and Dementia* 7(3):257–62.

Jack, Clifford R., David S. Knopman, William J. Jagust, Ronald C. Petersen, Michael W. Weiner, Paul S. Aisen, Leslie M. Shaw, Prashanthi Vemuri, Heather J. Wiste, Stephen D. Weigand, Timothy G. Lesnick, Vernon S. Pankratz, Michael C. Donohue, and John Q. Trojanowski. 2013. "Tracking Pathophysiological Processes in Alzheimer's Disease: An Updated Hypothetical Model of Dynamic Biomarkers." *The Lancet Neurology* 12(2):207–16.

Jack, Clifford R., David S. Knopman, William J. Jagust, Leslie M. Shaw, Paul S. Aisen, Michael W. Weiner, Ronald C. Petersen, and John Q. Trojanowski. 2010. "Hypothetical Model of Dynamic Biomarkers of the Alzheimer's Pathological Cascade." *The Lancet Neurology* 9(1):119–28.

Jäger, Stefanie, Peter Cimermancic, Natali Gulbahce, Jeffrey R. Johnson, Kathryn E. McGovern, Starlynn C. Clarke, Michael Shales, Gaelle Mercenne, Lars Pache, Kathy Li, Hilda Hernandez, Gwendolyn M. Jang, Shoshannah L. Roth, Eyal Akiva, John Marlett, Melanie Stephens, Iván D'Orso, Jason Fernandes, Marie Fahey, Cathal Mahon, Anthony J. Oĝdonoghue, Aleksandar Todorovic, John H. Morris, David A. Maltby, Tom Alber, Gerard Cagney, Frederic D. Bushman, John A. Young, Sumit K. Chanda, Wesley I. Sundquist, Tanja Kortemme, Ryan D. Hernandez, Charles S. Craik, Alma Burlingame, Andrej Sali, Alan D. Frankel, and Nevan J. Krogan. 2012. "Global Landscape of HIV-Human Protein Complexes." *Nature* 481(7381):365–70.

Janelidze, Shorena, Erik Stomrud, Sebastian Palmqvist, Henrik Zetterberg, Danielle Van Westen, Andreas Jeromin, Linan Song, David Hanlon, Cristina A. Tan Hehir, David Baker, Kaj Blennow, and Oskar Hansson. 2016. "Plasma β-Amyloid in Alzheimer's Disease and Vascular Disease." *Scientific Reports* 6:26801.

Jarvis, Donald L. 2009. "Chapter 14 Baculovirus-Insect Cell Expression Systems." Pp. 191–222 in *Methods in Enzymology*. Vol. 463. Academic Press Inc.

Jarvis, Donald L., Carla Weinkauf, and Linda A. Guarino. 1996. "Immediate-Early Baculovirus Vectors for Foreign Gene Expression in Transformed or Infected Insect Cells." *Protein Expression and Purification* 8(2):191–203.

Jehle, J. A., G. W. Blissard, B. C. Bonning, J. S. Cory, E. A. Herniou, G. F. Rohrmann, D. A. Theilmann, S. M. Thiem, and J. M. Vlak. 2006. "On the Classification and Nomenclature of Baculoviruses: A Proposal for Revision." *Archives of Virology* 151(7):1257–66.

Jha, Prakash K., Rahul Pal, Bita Nakhai, Padma Sridhar, and Seyed E. Hasnain. 1992. "Simultaneous Synthesis of Enzymatically Active Luciferase and Biologically Active β Subunit of Human Chorionic Gonadotropin in Caterpillars Infected with a Recombinant Baculovirus." *FEBS Letters* 310(2):148–52.

Ji, Xiaoyun, Danny Axford, Robin Owen, Gwyndaf Evans, Helen M. Ginn, Geoff Sutton, and David I. Stuart. 2015. "Polyhedra Structures and the Evolution of the Insect Viruses." *Journal of Structural Biology* 192(1):88–99.

Jiang, X., O. Gurel, E. A. Mendiaz, G. W. Stearns, C. L. Clogston, H. S. Lu, T. D. Osslund, R. S. Syed, K. E. Langley, and W. A. Hendrickson. 2000. "Structure of the Active Core of Human Stem Cell Factor and Analysis of Binding to Its Receptor Kit." *The EMBO Journal* 19(13):3192–3203.

Jin, LW, E. Masliah, D. Iimoto, R. Deteresa, M. Mallory, M. Sundsmon, N. Mori, A. Sobel, and T. Saitoh. 1996. "Neurofibrillary Tangle-Associated Alteration of S Tathmin in Alzheimer ' s Disease." 17(3):331–41.

Jones, Richard B., Andrew Gordus, Jordan A. Krall, and Gavin MacBeath. 2006. "A Quantitative Protein Interaction Network for the ErbB Receptors Using Protein Microarrays." *Nature* 439(7073):168–74.

Jorio, Hasnaa, Rosa Tran, and Amine Kamen. 2006. "Stability of Serum-Free and Purified Baculovirus Stocks under Various Storage Conditions." *Biotechnology Progress* 22(1):319–25.

Kadavath, Harindranath, Romina V. Hofele, Jacek Biernat, Satish Kumar, Katharina Tepper, Henning Urlaub, Eckhard Mandelkow, and Markus Zweckstetter. 2015. "Tau Stabilizes Microtubules by Binding at the Interface between Tubulin Heterodimers." *Proceedings of the National Academy of Sciences of the United States of America* 112(24):7501–6.

Kane, James F. and Donna L. Hartley. 1988. "Formation of Recombinant Protein Inclusion Bodies in Escherichia Coli." *Trends in Biotechnology* 6(5):95–101.

Kang, Ju Hee, Magdalena Korecka, Jon B. Toledo, John Q. Trojanowski, and Leslie M. Shaw. 2013. "Clinical Utility and Analytical Challenges in Measurement of Cerebrospinal Fluid Amyloid-B1-42 and τ Proteins as Alzheimer Disease Biomarkers." *Clinical Chemistry* 59(6):903–16.

Karimi, Kamran, Joshua D. Fortriede, Vaneet S. Lotay, Kevin A. Burns, Dong Zhou Wang, Malcom E. Fisher, Troy J. Pells, Christina James-Zorn, Ying Wang, V. G. Ponferrada, Stanley Chu, Praneet Chaturvedi, Aaron M. Zorn, and Peter D. Vize. 2017. "Xenbase: A Genomic, Epigenomic and Transcriptomic Model Organism Database." *Nucleic Acids Research* 46:861–68.

Karthikeyan, Kailash, Kristi Barker, Yanyang Tang, Peter Kahn, Peter Wiktor, Al Brunner, Vinicius Knabben, Bharath Takulapalli, Jane Buckner, Gerald Nepom, Joshua La Baer, and Ji Qiu. 2016. "A Contra Capture Protein Array Platform for Studying Post-Translationally Modified (PTM) Auto-Antigenomes." *Molecular & Cellular Proteomics* 15(7):2324–37.

Kärtner, F. X., F. Ahr, A. L. Calendron, H. Çankaya, S. Carbajo, G. Chang, G. Cirmi, K. Dörner, U. Dorda, A. Fallahi, A. Hartin, M. Hemmer, R. Hobbs, Y. Hua, W. R. Huang, R. Letrun, N. Matlis, V. Mazalova, O. D. Mücke, E. Nanni, W. Putnam, K. Ravi, F. Reichert, I. Sarrou, X. Wu, A. Yahaghi, H. Ye, L. Zapata, D. Zhang, C. Zhou, R. J.

D. Miller, K. K. Berggren, H. Graafsma, A. Meents, R. W. Assmann, H. N. Chapman, and P. Fromme. 2016. "AXSIS: Exploring the Frontiers in Attosecond X-Ray Science, Imaging and Spectroscopy." *Nuclear Instruments and Methods in Physics Research, Section A: Accelerators, Spectrometers, Detectors and Associated Equipment* 829:24–29.

Katzen, Federico. 2007. "Gateway® Recombinational Cloning: A Biological Operating System." *Expert Opinion on Drug Discovery* 2(4):571–89.

Katzen, Federico, Geoffrey Chang, and Wieslaw Kudlicki. 2005. "The Past, Present and Future of Cell-Free Protein Synthesis." *Trends in Biotechnology* 23(3):150–56.

Katzen, Federico, Todd C. Peterson, and Wieslaw Kudlicki. 2009. "Membrane Protein Expression: No Cells Required." *Trends in Biotechnology* 27(8):455–60.

Kaushansky, Alexis, Andrew Gordus, Bogdan A. Budnik, William S. Lane, John Rush, and Gavin MacBeath. 2008. "System-Wide Investigation of ErbB4 Reveals 19 Sites of Tyr Phosphorylation That Are Unusually Selective in Their Recruitment Properties." *Chemistry and Biology* 15(8):808–17.

Kellner, Alexander, Jakob Matschke, Christian Bernreuther, Holger Moch, Isidro Ferrer, and Markus Glatzel. 2009. "Autoantibodies against β-Amyloid Are Common in Alzheimer's Disease and Help Control Plaque Burden." *Annals of Neurology* 65(1):24–31.

Khalil, Michael, Charlotte E. Teunissen, Markus Otto, Fredrik Piehl, Maria Pia Sormani, Thomas Gattringer, Christian Barro, Ludwig Kappos, Manuel Comabella, Franz Fazekas, Axel Petzold, Kaj Blennow, Henrik Zetterberg, and Jens Kuhle. 2018. "Neurofilaments as Biomarkers in Neurological Disorders." *Nature Reviews Neurology* 14(10):577–89.

Kidd, M. 1963. "Paired Helical Filaments in Electron Microscopy of Alzheimer's Disease." 197:192–93.

Kim, Jungsu, Jacob M. Basak, and David M. Holtzman. 2009. "The Role of Apolipoprotein E in Alzheimer's Disease." *Neuron* 63(3):287–303.

Kim, Min Sik, Sneha M. Pinto, Derese Getnet, Raja Sekhar Nirujogi, Srikanth S. Manda, Raghothama Chaerkady, Anil K. Madugundu, Dhanashree S. Kelkar, Ruth Isserlin, Shobhit Jain, Joji K. Thomas, Babylakshmi Muthusamy, Pamela Leal-Rojas, Praveen Kumar, Nandini A. Sahasrabuddhe, Lavanya Balakrishnan, Jayshree Advani, Bijesh George, Santosh Renuse, Lakshmi Dhevi N. Selvan, Arun H. Patil, Vishalakshi Nanjappa, Aneesha Radhakrishnan, Samarjeet Prasad, Tejaswini Subbannayya, Rajesh Raju, Manish Kumar, Sreelakshmi K. Sreenivasamurthy, Arivusudar Marimuthu, Gajanan J. Sathe, Sandip Chavan, Keshava K. Datta, Yashwanth Subbannayya, Apeksha Sahu, Soujanya D. Yelamanchi, Savita Jayaram, Pavithra Rajagopalan, Jyoti Sharma, Krishna R. Murthy, Nazia Syed, Renu Goel, Aafaque A. Khan, Sartaj Ahmad, Gourav Dey, Keshav Mudgal, Aditi Chatterjee, Tai Chung Huang, Jun Zhong, Xinyan Wu, Patrick G. Shaw, Donald Freed, Muhammad S. Zahari, Kanchan K. Mukherjee, Subramanian Shankar, Anita Mahadevan, Henry Lam, Christopher J. Mitchell, Susarla Krishna Shankar, Parthasarathy Satishchandra, John

T. Schroeder, Ravi Sirdeshmukh, Anirban Maitra, Steven D. Leach, Charles G. Drake, Marc K. Halushka, T. S. Keshav. Prasad, Ralph H. Hruban, Candace L. Kerr, Gary D. Bader, Christine A. Iacobuzio-Donahue, Harsha Gowda, and Akhilesh Pandey. 2014. "A Draft Map of the Human Proteome." *Nature* 509(7502):575–81.

King, L. A. (Linda A. .. and R. D. (Robert D. .. Possee. 1992. *The Baculovirus Expression System : A Laboratory Guide*. Chapman & Hall.

Kitts, P. A. and R. D. Possee. 1993. "A Method for Producing Recombinant Baculovirus Expression Vectors at High Frequency." *BioTechniques* 14(5):810-812+814+816.

Kitts, Paul A., Martin D. Ayres, and Robert D. Possee. 1990. "Linearization of Baculovirus DNA Enhances the Recovery of Recombinant Virus Expression Vectors." *Nucleic Acids Research* 18(19):5667–72.

Klammt, Christian, Daniel Schwarz, Nora Eifler, Andreas Engel, Jacob Piehler, Winfried Haase, Steffen Hahn, Volker Dötsch, and Frank Bernhard. 2007. "Cell-Free Production of G Protein-Coupled Receptors for Functional and Structural Studies." *Journal of Structural Biology* 158(3):482–93.

Klaver, Andrea C., Mary P. Coffey, Lynnae M. Smith, David A. Bennett, John M. Finke, Loan Dang, and David A. Loeffler. 2011. "ELISA Measurement of Specific Non-Antigen-Bound Antibodies to Aβ1-42 Monomer and Soluble Oligomers in Sera from Alzheimer's Disease, Mild Cognitively Impaired, and Noncognitively Impaired Subjects." *Journal of Neuroinflammation* 8:1–11.

Klunk, William E., Henry Engler, Agneta Nordberg, Yanming Wang, Gunnar Blomqvist, Daniel P. Holt, Mats Bergström, Irina Savitcheva, Guo Feng Huang, Sergio Estrada, Birgitta Ausén, Manik L. Debnath, Julien Barletta, Julie C. Price, Johan Sandell, Brian J. Lopresti, Anders Wall, Pernilla Koivisto, Gunnar Antoni, Chester A. Mathis, and Bengt Långström. 2004. "Imaging Brain Amyloid in Alzheimer's Disease with Pittsburgh Compound-B." *Annals of Neurology* 55(3):306–19.

Ko, Li Wen, Eric C. Ko, Parimala Nacharaju, Wan Kyng Liu, Emmanuel Chang, Agnes Kenessey, and Shu Hui C. Yen. 1999. "An Immunochemical Study on Tau Glycation in Paired Helical Filaments." *Brain Research* 830(2):301–13.

Kohlbrenner, Erik, George Aslanidi, Kevin Nash, Stanislav Shklyaev, Martha Campbell-Thompson, Barry J. Byrne, Richard O. Snyder, Nicholas Muzyczka, Kenneth H. Warrington, and Sergei Zolotukhin. 2005. "Successful Production of Pseudotyped RAAV Vectors Using a Modified Baculovirus Expression System." *Molecular Therapy* 12(6):1217–25.

Kohnken, Russell, Katharina Buerger, Raymond Zinkowski, Caudill Miller, Daniel Kerkman, John Debernardis, Jifang Shen, Hans Jürgen Möller, Peter Davies, and Harald Hampel. 2000. "Detection of Tau Phosphorylated at Threonine 231 in Cerebrospinal Fluid of Alzheimer's Disease Patients." *Neuroscience Letters* 287(3):187–90.

Koivunen, J., N. Scheinin, JR Virta, and S. Aalto. 2011. "Amyloid PET Imaging in

Patients with Mild Cognitive Impairment: A 2-Year Follow-up Study." *Neurology* 76:1085–90.

Kolarova, Michala, Francisco García-Sierra, Ales Bartos, Jan Ricny, and Daniela Ripova. 2012. "Structure and Pathology of Tau Protein in Alzheimer Disease." *International Journal of Alzheimer's Disease* 2012.

Kool, M., C. H. Ahrens, J. M. Vlak, and G. F. Rohrmann. 1995. "Replication of Baculovirus DNA." *Journal of General Virology* 76(9):2103–18.

Koopmann, Rudolf, Karolina Cupelli, Lars Redecke, Karol Nass, Daniel P. Deponte, Thomas A. White, Francesco Stellato, Dirk Rehders, Mengning Liang, Jakob Andreasson, Andrew Aquila, Sasa Bajt, Miriam Barthelmess, Anton Barty, Michael J. Bogan, Christoph Bostedt, Sébastien Boutet, John D. Bozek, Carl Caleman, Nicola Coppola, Jan Davidsson, R. Bruce Doak, Tomas Ekeberg, Sascha W. Epp, Benjamin Erk, Holger Fleckenstein, Lutz Foucar, Heinz Graafsma, Lars Gumprecht, Janos Hajdu, Christina Y. Hampton, Andreas Hartmann, Robert Hartmann, Gülnter Hauser, Helmut Hirsemann, Peter Holl, Mark S. Hunter, Stephan Kassemeyer, Richard A. Kirian, Lukas Lomb, Filipe R. N. C. Maia, Nils Kimmel, Andrew V. Martin, Marc Messerschmidt, Christian Reich, Daniel Rolles, Benedikt Rudek, Artem Rudenko, Ilme Schlichting, Joachim Schulz, M. Marvin Seibert, Robert L. Shoeman, Raymond G. Sierra, Heike Soltau, Stephan Stern, Lothar Strülder, Nicusor Timneanu, Joachim Ullrich, Xiaoyu Wang, Georg Weidenspointner, Uwe Weierstall, Garth J. Williams, Cornelia B. Wunderer, Petra Fromme, John C. H. Spence, Thilo Stehle, Henry N. Chapman, Christian Betzel, and Michael Duszenko. 2012. "In Vivo Protein Crystallization Opens New Routes in Structural Biology." *Nature Methods* 9(3):259–62.

Kost, Thomas A., J. Patrick Condreay, and Donald L. Jarvis. 2005. "Baculovirus as Versatile Vectors for Protein Expression in Insect and Mammalian Cells." *Nature Biotechnology* 23(5):567–75.

Kost, Thomas A. and Christopher W. Kemp. 2016a. *Fundamentals of Baculovirus Expression and Applications.* Vol. 896.

Kost, Thomas A. and Christopher W. Kemp. 2016b. *Fundamentals of Expression in Mammalian Cells*. Vol. 896.

Kraepelin, E. 1910. *Psychiatrie: Klinische Psychiatrie; T. 1*.

Krammer, Florian and Reingard Grabherr. 2010. "Alternative Influenza Vaccines Made by Insect Cells." *Trends in Molecular Medicine* 16(7):313–20.

Krammer, Florian, Sabine Nakowitsch, Paul Messner, Dieter Palmberger, Boris Ferko, and Reingard Grabherr. 2010. "Swine-Origin Pandemic H1N1 Influenza Virus-like Particles Produced in Insect Cells Induce Hemagglutination Inhibiting Antibodies in BALB/c Mice." *Biotechnology Journal* 5(1):17–23.

Krogan, Nevan J., Gerard Cagney, Haiyuan Yu, Gouqing Zhong, Xinghua Guo, Alexandr Ignatchenko, Joyce Li, Shuye Pu, Nira Datta, Aaron P. Tikuisis, Thanuja Punna, José M. Peregrín-Alvarez, Michael Shales, Xin Zhang, Michael Davey, Mark D.

Robinson, Alberto Paccanaro, James E. Bray, Anthony Sheung, Bryan Beattie, Dawn P. Richards, Veronica Canadien, Atanas Lalev, Frank Mena, Peter Wong, Andrei Starostine, Myra M. Canete, James Vlasblom, Samuel Wu, Chris Orsi, Sean R. Collins, Shamanta Chandran, Robin Haw, Jennifer J. Rilstone, Kiran Gandi, Natalie J. Thompson, Gabe Musso, Peter St Onge, Shaun Ghanny, Mandy H. Y. Lam, Gareth Butland, Amin M. Altaf-Ul, Shigehiko Kanaya, Ali Shilatifard, Erin O'Shea, Jonathan S. Weissman, C. James Ingles, Timothy R. Hughes, John Parkinson, Mark Gerstein, Shoshana J. Wodak, Andrew Emili, and Jack F. Greenblatt. 2006. "Global Landscape of Protein Complexes in the Yeast Saccharomyces Cerevisiae." *Nature* 440(7084):637–43.

Kuhlmann, Julia, Ulf Andreasson, Josef Pannee, Maria Bjerke, Erik Portelius, Andreas Leinenbach, Tobias Bittner, Magdalena Korecka, Rand G. Jenkins, Hugo Vanderstichele, Erik Stoops, Piotr Lewczuk, Leslie M. Shaw, Ingrid Zegers, Heinz Schimmel, Henrik Zetterberg, and Kaj Blennow. 2017. "CSF Aβ1–42 – an Excellent but Complicated Alzheimer's Biomarker – a Route to Standardisation." *Clinica Chimica Acta* 467:27–33.

Kuleshov, Maxim V., Matthew R. Jones, Andrew D. Rouillard, Nicolas F. Fernandez, Qiaonan Duan, Zichen Wang, Simon Koplev, Sherry L. Jenkins, Kathleen M. Jagodnik, Alexander Lachmann, Michael G. McDermott, Caroline D. Monteiro, Gregory W. Gundersen, and Avi Ma'ayan. 2016. "Enrichr: A Comprehensive Gene Set Enrichment Analysis Web Server 2016 Update." *Nucleic Acids Research* 44:W90–97.

Kvartsberg, Hlin, Flora H. Duits, Martin Ingelsson, Niels Andreasen, Annika Öhrfelt, Kerstin Andersson, Gunnar Brinkmalm, Lars Lannfelt, Lennart Minthon, Oskar Hansson, Ulf Andreasson, Charlotte E. Teunissen, Philip Scheltens, Wiesje M. Van Der Flier, Henrik Zetterberg, Erik Portelius, and Kaj Blennow. 2015. "Cerebrospinal Fluid Levels of the Synaptic Protein Neurogranin Correlates with Cognitive Decline in Prodromal Alzheimer's Disease." *Alzheimer's and Dementia* 11(10):1180–90.

Kvartsberg, Hlin, Erik Portelius, Ulf Andreasson, Gunnar Brinkmalm, Konstantin Hellwig, Natalia Lelental, Johannes Kornhuber, Oskar Hansson, Lennart Minthon, Philipp Spitzer, Juan M. Maler, Henrik Zetterberg, Kaj Blennow, and Piotr Lewczuk. 2015. "Characterization of the Postsynaptic Protein Neurogranin in Paired Cerebrospinal Fluid and Plasma Samples from Alzheimer's Disease Patients and Healthy Controls." *Alzheimer's Research and Therapy* 7(1):1–9.

Lamesch, Philippe, Ning Li, Stuart Milstein, Changyu Fan, Tong Hao, Gabor Szabo, Zhenjun Hu, Kavitha Venkatesan, Graeme Bethel, Paul Martin, Jane Rogers, Stephanie Lawlor, Stuart McLaren, Amélie Dricot, Heather Borick, Michael E. Cusick, Jean Vandenhaute, Ian Dunham, David E. Hill, and Marc Vidal. 2007. "HORFeome v3.1: A Resource of Human Open Reading Frames Representing over 10,000 Human Genes." *Genomics* 89(3):307–15.

Landau, S. M., B. A. Thomas, L. Thurfjell, M. Schmidt, R. Margolin, M. Mintun, M. Pontecorvo, S. L. Baker, and W. J. Jagust. 2014. "Amyloid PET Imaging in Alzheimer's Disease: A Comparison of Three Radiotracers." *European Journal of Nuclear Medicine and Molecular Imaging* 41(7):1398–1407.

Landy, Arthur. 1989. "Dynamic, Structural, and Regulatory Aspects of λ Site-Specific

Recombination." *Annual Review Biochemistry* 58:913–49.

Lange, R. H., Z. Grodziński, and W. Kilarski. 1982. "Yolk-Platelet Crystals in Three Ancient Bony Fishes: Polypterus Bichir (Polypteri), Amia Calva L., and Lepisosteus Osseus (L.) (Holostei)." *Cell and Tissue Research* 222(1):159–65.

Laske, Christoph, Hamid R. Sohrabi, Shaun M. Frost, Karmele López-De-Ipiña, Peter Garrard, Massimo Buscema, Justin Dauwels, Surjo R. Soekadar, Stephan Mueller, Christoph Linnemann, Stephanie A. Bridenbaugh, Yogesan Kanagasingam, Ralph N. Martins, and Sid E. O'bryant. 2015. "Innovative Diagnostic Tools for Early Detection of Alzheimer's Disease." *Alzheimer's and Dementia* 11(5):561–78.

Lee, H. H. and L. K. Miller. 1978. "Isolation of Genotypic Variants of Autographa Californica Nuclear Polyhedrosis Virus." *Journal of Virology* 27(3):754–67.

Lee, Virginia M. Y., Brian J. Balin, Laszlo Otvos, and John Q. Trojanowski. 1991. "A68: A Major Subunit of Paired Helical Filaments and Derivatized Forms of Normal Tau." *Science* 251(4994):675–78.

Lehrer, Steven and Peter H. Rheinstein. 2015. "Is Alzheimer's Disease Autoimmune Inflammation of the Brain That Can Be Treated with Nasal Nonsteroidal Anti-Inflammatory Drugs?" *American Journal of Alzheimer's Disease and Other Dementias* 30(3):225–27.

Levine, Harry. 1995. "Soluble Multimeric Alzheimer β(1-40) Pre-Amyloid Complexes in Dilute Solution." *Neurobiology of Aging* 16(5):755–64.

Lewczuk, Piotr, Natalia Ermann, Ulf Andreasson, Christian Schultheis, Jana Podhorna, Philipp Spitzer, Juan Manuel Maler, Johannes Kornhuber, Kaj Blennow, and Henrik Zetterberg. 2018. "Plasma Neurofilament Light as a Potential Biomarker of Neurodegeneration in Alzheimer's Disease." *Alzheimer's Research and Therapy* 10(1).

Lewis, J., D. W. Dickson, W. L. Lin, L. Chisholm, A. Corral, G. Jones, S. H. Yen, N. Sahara, L. Skipper, D. Yager, C. Eckman, J. Hardy, M. Hutton, and E. McGowan. 2001. "Enhanced Neurofibrillary Degeneration in Transgenic Mice Expressing Mutant Tau and APP." *Science* 293(5534):1487–91.

Li, Chuanzhou and Jürgen Götz. 2017. "Somatodendritic Accumulation of Tau in Alzheimer's Disease Is Promoted by Fyn-mediated Local Protein Translation." *The EMBO Journal* 36(21):3120–38.

Liang, Winnie S., Eric M. Reiman, Jon Valla, Travis Dunckley, Thomas G. Beach, Andrew Grover, Tracey L. Niedzielko, Lonnie E. Schneider, Diego Mastroeni, Richard Caselli, Walter Kukull, John C. Morris, Christine M. Hulette, Donald Schmechel, Joseph Rogers, and Dietrich A. Stephan. 2008. "Alzheimer's Disease Is Associated with Reduced Expression of Energy Metabolism Genes in Posterior Cingulate Neurons." *Proceedings of the National Academy of Sciences of the United States of America* 105(11):4441–46.

Liedtke, Wolfgang, Elizabeth E. Leman, Robert E. W. Fyffe, Cedric S. Raine, and

Ulrich K. Schubart. 2002. "Stathmin-Deficient Mice Develop an Age-Dependent Axonopathy of the Central and Peripheral Nervous Systems." *The American Journal of Pathology* 160(2):469–80.

Lin, Meng-Ju and Shyh-Jye Lee. 2016. "Stathmin-like 4 Is Critical for the Maintenance of Neural Progenitor Cells in Dorsal Midbrain of Zebrafish Larvae." *Scientific Reports* 6:36188.

Lindsay, Joan, Danielle Laurin, René Verreault, Réjean Hébert, Barbara Helliwell, Gerry B. Hill, and Ian McDowell. 2002. "Risk Factors for Alzheimer's Disease: A Prospective Analysis from the Canadian Study of Health and Aging." *American Journal of Epidemiology* 156(5):445–53.

Lister, James P. and Carol A. Barnes. 2009. "Neurobiological Changes in the Hippocampus during Normative Aging." *Archives of Neurology* 66(7):829–33.

Liu, Chaoting, Brian Dalby, Weixing Chen, Jennifer M. Kilzer, and Henry C. Chiou. 2008. "Transient Transfection Factors for High-Level Recombinant Protein Production in Suspension Cultured Mammalian Cells." Pp. 141–53 in *Molecular Biotechnology*. Vol. 39. Springer.

Lopresti, Patrizia, Sara Szuchet, Sozos Ch Papasozomenos, Raymond P. Zinkowski, and Lester I. Binder. 1995. "Functional Implications for the Microtubule-Associated Protein Tau: Localization in Oligodendrocytes." *Proceedings of the National Academy of Sciences of the United States of America* 92(22):10369–73.

Loy, Clement T., Peter R. Schofield, Anne M. Turner, and John B. J. Kwok. 2014. "Genetics of Dementia." *The Lancet* 383(9919):828–40.

Lübbert, Hermann, Inge Kruczek, Sian Tjia, and Walter Doerfler. 1981. "The Cloned EcoRI Fragments of Autographa Californica Nuclear Polyhedrosis Virus DNA." *Gene* 16(1–3):343–45.

Luckow, V. A., S. C. Lee, G. F. Barry, and P. O. Olins. 1993. "Efficient Generation of Infectious Recombinant Baculoviruses by Site-Specific Transposon-Mediated Insertion of Foreign Genes into a Baculovirus Genome Propagated in Escherichia Coli." *Journal of Virology* 67(8):4566–79.

Lynn, Dwight E. and Robert L. Harrison. 2016. "Available Lepidopteran Insect Cell Lines." Pp. 119–42 in *Methods in Molecular Biology*. Vol. 1350. Humana Press Inc.

Macauley-Patrick, Sue, Mariana L. Fazenda, Brian McNeil, and Linda M. Harvey. 2005. "Heterologous Protein Production Using the Pichia Pastoris Expression System." *Yeast* 22(4):249–70.

Maftei, Madalina, Franka Thurm, Cathrin Schnack, Hayrettin Tumani, Markus Otto, Thomas Elbert, Iris Tatjana Kolassa, Michael Przybylski, Marilena Manea, and Christine A. F. von Arnim. 2013. "Increased Levels of Antigen-Bound β-Amyloid Autoantibodies in Serum and Cerebrospinal Fluid of Alzheimer's Disease Patients." *PLoS ONE* 8(7).

Mahley, Robert W. 1988. "Apolipoprotein E: Cholesterol Transport Protein with Expanding Role in Cell Biology." *Science* 240(4852):622–30.

Makrides, Savvas C. 1996. "Strategies for Achieving High-Level Expression of Genes in Escherichia Coli." *Microbiological Reviews* 60(3):512–38.

Mapstone, Mark, Amrita K. Cheema, Massimo S. Fiandaca, Xiaogang Zhong, Timothy R. Mhyre, Linda H. Macarthur, William J. Hall, Susan G. Fisher, Derick R. Peterson, James M. Haley, Michael D. Nazar, Steven A. Rich, Dan J. Berlau, Carrie B. Peltz, Ming T. Tan, Claudia H. Kawas, and Howard J. Federoff. 2014. "Plasma Phospholipids Identify Antecedent Memory Impairment in Older Adults." *Nature Medicine* 20(4):415–18.

Marchese, Monica, David Cowan, Elizabeth Head, Donglai Ma, Khalil Karimi, Vanessa Ashthorpe, Minesh Kapadia, Hui Zhao, Paulina Davis, and Boris Sakic. 2014. "Autoimmune Manifestations in the 3xTg-AD Model of Alzheimer's Disease." *Journal of Alzheimer's Disease* 39(1):191–210.

Marquié, Marta, Marc D. Normandin, Charles R. Vanderburg, Isabel M. Costantino, Elizabeth A. Bien, Lisa G. Rycyna, William E. Klunk, Chester A. Mathis, Milos D. Ikonomovic, Manik L. Debnath, Neil Vasdev, Bradford C. Dickerson, Stephen N. Gomperts, John H. Growdon, Keith A. Johnson, Matthew P. Frosch, Bradley T. Hyman, and Teresa Gómez-Isla. 2015. "Validating Novel Tau Positron Emission Tomography Tracer [F-18]-AV-1451 (T807) on Postmortem Brain Tissue." *Annals of Neurology* 78(5):787–800.

Masliah, Eliezer, Leslie Crews, and Lawrence Hansen. 2006. "Synaptic Remodeling during Aging and in Alzheimer's Disease." *Journal of Alzheimer's Disease* 9(SUPPL. 3):91–99.

Massover, William H. 1971. "Intramitochondrial Yolk-Crystals of Frog Oocytes: I. Formation of Yolk-Crystal Inclusions by Mitochondria during Bullfrog Oogenesis." *Journal of Cell Biology* 48(2):266–79.

Mastroeni, Diego, Jennifer Nolz, Omar M. Khdour, Shobana Sekar, Elaine Delvaux, Lori Cuyugan, Winnie S. Liang, Sidney M. Hecht, and Paul D. Coleman. 2018. "Oligomeric Amyloid β Preferentially Targets Neuronal and Not Glial Mitochondrial-Encoded MRNAs." *Alzheimer's and Dementia* 14(6):775–86.

Mathis, Chester A., Yanming Wang, Daniel P. Holt, Guo Feng Huang, Manik L. Debnath, and William E. Klunk. 2003. "Synthesis and Evaluation of 11C-Labeled 6-Substituted 2-Arylbenzothiazoles as Amyloid Imaging Agents." *Journal of Medicinal Chemistry* 46(13):2740–54.

Matsubayashi, Hideaki, Yutetsu Kuruma, and Takuya Ueda. 2014. "In Vitro Synthesis of the E. Coli Sec Translocon from DNA." *Angewandte Chemie - International Edition* 53(29):7535–38.

Mattsson, Niklas, Ulf Andreasson, Staffan Persson, Hiroyuki Arai, Sat Dev Batish, Sergio Bernardini, Luisella Bocchio-Chiavetto, Marinus A. Blankenstein, Maria C. Carrillo, Sonia Chalbot, Els Coart, Davide Chiasserini, Neal Cutler, Gunilla Dahlfors,

Stefan Duller, Anne M. Fagan, Orestes Forlenza, Giovanni B. Frisoni, Douglas Galasko, Daniela Galimberti, Harald Hampel, Aase Handberg, Michael T. Heneka, Adrianna Z. Herskovits, Sanna Kaisa Herukka, David M. Holtzman, Christian Humpel, Bradley T. Hyman, Khalid Iqbal, Mathias Jucker, Stephan A. Kaeser, Elmar Kaiser, Elisabeth Kapaki, Daniel Kidd, Peter Klivenyi, Cindy S. Knudsen, Markus P. Kummer, James Lui, Albert Lladó, Piotr Lewczuk, Qiao Xin Li, Ralph Martins, Colin Masters, John McAuliffe, Marc Mercken, Abhay Moghekar, José Luis Molinuevo, Thomas J. Montine, William Nowatzke, Richard O'Brien, Markus Otto, George P. Paraskevas, Lucilla Parnetti, Ronald C. Petersen, David Prvulovic, Herman P. M. De Reus, Robert A. Rissman, Elio Scarpini, Alessandro Stefani, Hilkka Soininen, Johannes Schröder, Leslie M. Shaw, Anders Skinningsrud, Brith Skrogstad, Annette Spreer, Leda Talib, Charlotte Teunissen, John Q. Trojanowski, Hayrettin Tumani, Robert M. Umek, Bianca Van Broeck, Hugo Vanderstichele, Laszlo Vecsei, Marcel M. Verbeek, Manfred Windisch, Jing Zhang, Henrik Zetterberg, and Kaj Blennow. 2011. "The Alzheimer's Association External Quality Control Program for Cerebrospinal Fluid Biomarkers." *Alzheimer's and Dementia* 7(4):386–95.

Mattsson, Niklas, Ulf Andreasson, Henrik Zetterberg, Kaj Blennow, Michael W. Weiner, Paul Aisen, Arthur W. Toga, Ronald Petersen, Clifford R. Jack, William Jagust, John Q. Trojanowki, Leslie M. Shaw, Laurel Beckett, Robert C. Green, Andrew J. Saykin, John C. Morris, Zaven Khachaturian, Greg Sorensen, Maria Carrillo, Lew Kuller, Marc Raichle, David Holtzman, Steven Paul, Peter Davies, Howard Fillit, Franz Hefti, M. Marcel Mesulam, William Potter, Peter Snyder, Eli Lilly, Adam Schwartz, Tom Montine, Ronald G. Thomas, Michael Donohue, Sarah Walter, Devon Gessert, Tamie Sather, Gus Jiminez, Archana B. Balasubramanian, Jennifer Mason, Iris Sim, Danielle Harvey, Matthew Bernstein, Bret Borowski, Jeff Gunter, Matt Senjem, Prashanthi Vemuri, David Jones, Kejal Kantarci, Chad Ward, Nick Fox, Paul Thompson, Norbert Schuff, Charles DeCarli, Susan Landau, Robert A. Koeppe, Norm Foster, Eric M. Reiman, Kewei Chen, Chet Mathis, Nigel J. Cairns, Erin Franklin, Lisa Taylor-Reinwald, Virginia Lee, Magdalena Korecka, Michal Figurski, Karen Crawford, Scott Neu, Tatiana M. Foroud, Li Shen, Kelley Faber, Sungeun Kim, Kwangsik Nho, Steven Potkin, Lean Thal, Marilyn Albert, Richard Frank, John Hsiao, Jeffrey Kaye, Joseph Quinn, Lisa Silbert, Betty Lind, Raina Carter, Sara Dolen, Lon S. Schneider, Sonia Pawluczyk, Mauricio Becerra, Liberty Teodoro, Bryan M. Spann, James Brewer, Helen Vanderswag, Adam Fleisher, Judith L. Heidebrink, Joanne L. Lord, Sara S. Mason, Colleen S. Albers, David Knopman, Kris Johnson, Rachelle S. Doody, Javier Villanueva-Meyer, Valory Pavlik, Victoria Shibley, Munir Chowdhury, Susan Rountree, Mimi Dang, Yaakov Stern, Lawrence S. Honig, Karen L. Bell, Beau Ances, Maria Carroll, Mary L. Creech, Mark A. Mintun, Stacy Schneider, Angela Oliver, Daniel Marson, David Geldmacher, Marissa Natelson Love, Randall Griffith, David Clark, John Brockington, Erik Roberson, Hillel Grossman, Effie Mitsis, Raj C. Shah, Leyla De Toledo-Morrell, Ranjan Duara, Maria T. Greig-Custo, Warren Barker, Chiadi Onyike, Daniel D'Agostino, Stephanie Kielb, Martin Sadowski, Mohammed O. Sheikh, Anaztasia Ulysse, Mrunalini Gaikwad, P. Murali Doraiswamy, Jeffrey R. Petrella, Salvador Borges-Neto, Terence Z. Wong, Edward Coleman, Steven E. Arnold, Jason H. Karlawish, David A. Wolk, Christopher M. Clark, Charles D. Smith, Greg Jicha, Peter Hardy, Partha Sinha, Elizabeth Oates, Gary Conrad, Oscar L. Lopez, Mary Ann Oakley, Donna M. Simpson, Anton P. Porsteinsson, Bonnie S. Goldstein, Kim Martin, Kelly M. Makino, M. Saleem Ismail, Connie Brand, Adrian Preda, Dana Nguyen, Kyle Womack, Dana Mathews, Mary Quiceno, Allan I. Levey, James J. Lah, Janet S. Cellar, Jeffrey M. Burns, Russell H. Swerdlow, William M. Brooks, Liana Apostolova, Kathleen

Tingus, Ellen Woo, Daniel H. S. Silverman, Po H. Lu, George Bartzokis, Neill R. Graff-Radford, Francine Parfitt, Kim Poki-Walker, Martin R. Farlow, Ann Marie Hake, Brandy R. Matthews, Jared R. Brosch, Scott Herring, Christopher H. Van Dyck, Richard E. Carson, Martha G. MacAvoy, Pradeep Varma, Howard Chertkow, Howard Bergman, Chris Hosein, Sandra Black, Bojana Stefanovic, Curtis Caldwell, Ging Yuek Robin Hsiung, Benita Mudge, Vesna Sossi, Howard Feldman, Michele Assaly, Elizabeth Finger, Stephen Pasternack, Irina Rachisky, Dick Trost, Andrew Kertesz, Charles Bernick, Donna Munic, Emily Rogalski, Kristine Lipowski, Sandra Weintraub, Borna Bonakdarpour, Diana Kerwin, Chuang Kuo Wu, Nancy Johnson, Carl Sadowsky, Teresa Villena, Raymond Scott Turner, Kathleen Johnson, Brigid Reynolds, Reisa A. Sperling, Gad Marshall, Jerome Yesavage, Joy L. Taylor, Barton Lane, Allyson Rosen, Jared Tinklenberg, Marwan N. Sabbagh, Christine M. Belden, Sandra A. Jacobson, Sherye A. Sirrel, Neil Kowall, Ronald Killiany, Andrew E. Budson, Alexander Norbash, Patricia Lynn Johnson, Thomas O. Obisesan, Saba Wolday, Joanne Allard, Alan Lerner, Paula Ogrocki, Curtis Tatsuoka, Parianne Fatica, Evan Fletcher, Pauline Maillard, John Olichney, Owen Carmichael, Smita Kittur, Michael Borrie, T. Y. Lee, Rob Bartha, Sterling Johnson, Sanjay Asthana, Cynthia M. Carlsson, Pierre Tariot, Anna Burke, Ann Marie Milliken, Nadira Trncic, Stephanie Reeder, Vernice Bates, Horacio Capote, Michelle Rainka, Douglas W. Scharre, Maria Kataki, Brendan Kelley, Earl A. Zimmerman, Dzintra Celmins, Alice D. Brown, Godfrey D. Pearlson, Karen Blank, Karen Anderson, Laura A. Flashman, Marc Seltzer, Mary L. Hynes, Robert B. Santulli, Kaycee M. Sink, Leslie Gordineer, Jeff D. Williamson, Pradeep Garg, Franklin Watkins, Brian R. Ott, Geoffrey Tremont, Lori A. Daiello, Stephen Salloway, Paul Malloy, Stephen Correia, Howard J. Rosen, Bruce L. Miller, David Perry, Jacobo Mintzer, Kenneth Spicer, David Bachman, Stephen Pasternak, Irina Rachinsky, John Rogers, Dick Drost, Nunzio Pomara, Raymundo Hernando, Antero Sarrael, Susan K. Schultz, Karen Ekstam Smith, Hristina Koleva, Ki Won Nam, Hyungsub Shim, Norman Relkin, Gloria Chiang, Michael Lin, Lisa Ravdin, Amanda Smith, Balebail Ashok Raj, and Kristin Fargher. 2017. "Association of Plasma Neurofilament Light with Neurodegeneration in Patients with Alzheimer Disease." *JAMA Neurology* 74(5):557–66.

Mattsson, Niklas, Henrik Zetterberg, Shorena Janelidze, Philip S. Insel, Ulf Andreasson, Erik Stomrud, Sebastian Palmqvist, David Baker, Cristina A. Tan Hehir, Andreas Jeromin, David Hanlon, Linan Song, Leslie M. Shaw, John Q. Trojanowski, Michael W. Weine, and Blennow Kaj. 2016. "Plasma Tau in Alzheimer Disease." *Neurology* 87:1827–37.

Maurer, Konrad, Stephan Volk, and Hector Gerbaldo. 1997. "Auguste D and Alzheimer's Disease." *Lancet* 349(9064):1546–49.

Max, D. Summers and E. Smit Gale. 1987. "A Manual of Methods for Baculovirus Vectors and Insect Cell Culture Procedures."

Mayeux, Richard, Ann M. Saunders, Steven Shea, Suzanne Mirra, Denis Evans, Allen D. Roses, Bradley T. Hyman, Barbara Crain, Ming-Xin Tang, and Creighton H. Phelps. 1998. "Utility of the Apolipoprotein E Genotype in the Diagnosis of Alzheimer's Disease." *New England Journal of Medicine* 338(8):506–11.

Mcdaniel, Leslie D., Timothy Lukovits, and Keith D. Mcdaniel. 1993. "Alzheimer's Disease: The Problem of Incorrect Clinical Diagnosis." *Journal of Geriatric Psychiatry*

and Neurology 6(4):230–34.

McKenzie, Edward A. and W. Mark Abbott. 2018. "Expression of Recombinant Proteins in Insect and Mammalian Cells." *Methods* 147(May):40–49.

Mecocci, P., L. Parnetti, G. Romano, A. Scarelli, F. Chionne, R. Cecchetti, M. C. Polidori, B. Palumbo, A. Cherubini, and U. Senin. 1995. "Serum Anti-GFAP and Anti-S100 Autoantibodies in Brain Aging, Alzheimer's Disease and Vascular Dementia." *Journal of Neuroimmunology* 57(1–2):165–70.

Mehta, Dev, Robert Jackson, Gaurav Paul, Jiong Shi, and Marwan Sabbagh. 2017. "Why Do Trials for Alzheimer's Disease Drugs Keep Failing? A Discontinued Drug Perspective for 2010-2015." *Expert Opinion on Investigational Drugs* 26(6):735–39.

Mehta, Pankaj D., Tuula Pirttilä, Sangita P. Mehta, Eugene A. Sersen, Paul S. Aisen, and Henryk M. Wisniewski. 2000. "Plasma and Cerebrospinal Fluid Levels of Amyloid β Proteins 1-40 and 1- 42 in Alzheimer Disease." *Archives of Neurology* 57(1):100–105.

Mena, Jimmy A. and Amine A. Kamen. 2011. "Insect Cell Technology Is a Versatile and Robust Vaccine Manufacturing Platform." *Expert Review of Vaccines* 10(7):1063–81.

Metz, Stefan W. and Gorben P. Pijlman. 2011. "Arbovirus Vaccines; Opportunities for the Baculovirus-Insect Cell Expression System." *Journal of Invertebrate Pathology* 107(SUPPL.):S16–30.

Michaelson, Daniel M. 2014. "APOE E4: The Most Prevalent yet Understudied Risk Factor for Alzheimer's Disease." *Alzheimer's and Dementia* 10(6):861–68.

Mielke, Michelle M., Clinton E. Hagen, Jing Xu, Xiyun Chai, Prashanthi Vemuri, Val J. Lowe, David C. Airey, David S. Knopman, Rosebud O. Roberts, Mary M. Machulda, Clifford R. Jack, Ronald C. Petersen, and Jeffrey L. Dage. 2018. "Plasma Phospho-Tau181 Increases with Alzheimer's Disease Clinical Severity and Is Associated with Tau- and Amyloid-Positron Emission Tomography." *Alzheimer's and Dementia* 14(8):989–97.

Miersch, Shane, Xiaofang Bian, Garrick Wallstrom, Sahar Sibani, Tanya Logvinenko, Clive H. Wasserfall, Desmond Schatz, Mark Atkinson, Ji Qiu, and Joshua LaBaer. 2013. "Serological Autoantibody Profiling of Type 1 Diabetes by Protein Arrays." *Journal of Proteomics* 94:486–96.

Miersch, Shane and Joshua LaBaer. 2011. "Nucleic Acid Programmable Protein Arrays: Versatile Tools for Array-Based Functional Protein Studies." *Current Protocols in Protein Science* 27.2.1-27.2.26.

Minton, Nigel P. 1984. "Improved Plasmid Vectors for the Isolation of Translational Lac Gene Fusions." *Gene* 31(1–3):269–73.

Mintun, M. A., G. N. Larossa, Y. I. Sheline, C. S. Dence, S. Y. Lee, R. H. MacH, W. E. Klunk, C. A. Mathis, S. T. Dekosky, and J. C. Morris. 2006. "[11C]PIB in a

Nondemented Population: Potential Antecedent Marker of Alzheimer Disease." *Neurology* 67(3):446–52.

Mishra, Seema. 1998. "Baculoviruses as Biopesticides." *Current Science* 75:1015–22.

Mitchell, MB, JJ Buccafusco, RF Schade, SJ Webster, S. Mruthinti, DU Harrell, NK Gulati, and LS. Miller. 2010. "RAGE and Aβ Immunoglobulins: Relation to Alzheimer's Disease-Related Cognitive Function." *The Journnal of the International Neuropsychological Society* 16(4):672–78.

Mokdad-Gargouri, Raja, Salma Abdelmoula-Soussi, Nadia Hadiji-Abbès Amor, and Ines Yacoubi-Hadj. 2004. *Recombinant Gene Expression*.

Monsma, S. A., A. G. Oomens, and G. W. Blissard. 1996. "The GP64 Envelope Fusion Protein Is an Essential Baculovirus Protein Required for Cell-to-Cell Transmission of Infection." *Journal of Virology* 70(7):4607–16.

Montor, Wagner R, Jin Huang, Yanhui Hu, Eugenie Hainsworth, Susan Lynch, Jeannine-Weiner Kronish, Claudia L. Ordonez, Tanya Logvinenko, Stephen Lory, and Joshua Labaer. 2009. "Genome-Wide Study of Pseudomonas Aeruginosa Outer Membrane Protein Immunogenicity Using Self-Assembling Protein Microarrays †." *INFECTION AND IMMUNITY* 77(11):4877–86.

Montor, Wagner R., Jin Huang, Yanhui Hu, Eugenie Hainsworth, Susan Lynch, Jeannine Weiner Kronish, Claudia L. Ordonez, Tanya Logvinenko, Stephen Lory, and Joshua LaBaer. 2009. "Genome-Wide Study of Pseudomonas Aeruginosa Outer Membrane Protein Immunogenicity Using Self-Assembling Protein Microarrays." *Infection and Immunity* 77(11):4877–86.

Mor, Felix, Marina Izak, and Irun R. Cohen. 2005. "Identification of Aldolase as a Target Antigen in Alzheimer's Disease." *The Journal of Immunology* 175(5):3439–45.

Mori, Hiroshi, Jun Kondo, and Yasuo Ihara. 1987. "Ubiquitin Is a Component of Paired Helical Filaments in Alzheimer's Disease." *Science* 235(4796):1641–44.

Mori, Hirosi, Kenji Hosoda, Etsuro Matsubara, Tadakatsu Nakamoto, Yoshiko Furiya, Riuko Endoh, Mihoko Usami, Mikio Shoji, Shoichi Maruyama, and Shunsaku Hirai. 1995. "Tau in Cerebrospinal Fluids: Establishment of the Sandwich ELISA with Antibody Specific to the Repeat Sequence in Tau." *Neuroscience Letters* 186(2–3):181–83.

Mormino, Elizabeth C., Michael G. Brandel, Cindee M. Madison, Gil D. Rabinovici, Shawn Marks, Suzanne L. Baker, and William J. Jagust. 2012. "Not Quite PIB-Positive, Not Quite PIB-Negative: Slight PIB Elevations in Elderly Normal Control Subjects Are Biologically Relevant." *Neuroimage* 59(2):1152–60.

Moscardi, Flavio, Marlinda Lobo De Souza, Maria Elita Batista De Castro, Mauricio Lara Moscardi, and Boguslaw Szewczyk. 2011. "Baculovirus Pesticides: Present State and Future Perspectives." Pp. 415–45 in *Microbes and Microbial Technology: Agricultural and Environmental Applications*. Springer New York.

Mruthinti, Shyamala, Jerry J. Buccafusco, William D. Hill, Jennifer L. Waller, Thomas W. Jackson, Edward Y. Zamrini, and Rosann F. Schade. 2004. "Autoimmunity in Alzheimer's Disease: Increased Levels of Circulating IgGs Binding Aβ and RAGE Peptides." *Neurobiology of Aging* 25(8):1023–32.

Mullan, Mike, Fiona Crawford, Karin Axelman, Henry Houlden, Lena Lilius, Bengt Winblad, and Lars Lannfelt. 1992. "A Pathogenic Mutation for Probable Alzheimer's Disease in the APP Gene at the N–Terminus of β–Amyloid." *Nature Genetics* 1(5):345–47.

Nagaratnam, Nirupa, Yanyang Tang, Ji Qiu, Justin Saul, Sabine Botha, Chufeng Li, Hao Hu, Sahba Zaare, Sebastien Boutet, Mark Hunter, David Lowry, Uwe Weierstall, Nadia Zatsepin, John C. H. Spence, Joshua LaBaer, Petra Fromme, and Jose M. Martin-Garcia. n.d. "Enhanced X-Ray Diffraction of in Vivo Grown MNS Crystals by Viscous Jets at XFELs." Manuscript Submitted to *Acta Crystallographica Section F*.

Nagele, Eric, Min Han, Cassandra DeMarshall, Benjamin Belinka, and Robert Nagele. 2011. "Diagnosis of Alzheimer's Disease Based on Disease-Specific Autoantibody Profiles in Human Sera." *PLoS ONE* 6(8).

Nagele, Eric P., Min Han, Nimish K. Acharya, Cassandra DeMarshall, Mary C. Kosciuk, and Robert G. Nagele. 2013. "Natural IgG Autoantibodies Are Abundant and Ubiquitous in Human Sera, and Their Number Is Influenced By Age, Gender, and Disease." *PLoS ONE* 8(4).

Nakamura, Akinori, Naoki Kaneko, Victor L. Villemagne, Takashi Kato, James Doecke, Vincent Doré, Chris Fowler, Qiao Xin Li, Ralph Martins, Christopher Rowe, Taisuke Tomita, Katsumi Matsuzaki, Kenji Ishii, Kazunari Ishii, Yutaka Arahata, Shinichi Iwamoto, Kengo Ito, Koichi Tanaka, Colin L. Masters, and Katsuhiko Yanagisawa. 2018. "High Performance Plasma Amyloid-β Biomarkers for Alzheimer's Disease." *Nature* 554(7691):249–54.

Ni, Ye and Rachel Chen. 2009. "Extracellular Recombinant Protein Production from Escherichia Coli." *Biotechnology Letters* 31(11):1661–70.

Nicoll, James A. R., Masahito Yamada, Janusz Frackowiak, Bozena Mazur-Kolecka, and Roy O. Weller. 2004. "Cerebral Amyloid Angiopathy Plays a Direct Role in the Pathogenesis of Alzheimer's Disease: Pro-CAA Position Statement." Pp. 589–97 in *Neurobiology of Aging*. Vol. 25.

Van Nostrand, William E., Jerry P. Melchor, Hyun Soon Cho, Steven M. Greenberg, and G. William Rebeck. 2001. "Pathogenic Effects of D23N Iowa Mutant Amyloid β-Protein." *Journal of Biological Chemistry* 276(35):32860–66.

Nussbaum, Robert L. and Christopher E. Ellis. 2003. "Alzheimer's Disease and Parkinson's Disease" edited by A. E. Guttmacher and F. S. Collins. *New England Journal of Medicine* 348(14):1356–64.

O'Bryant, Sid E., Guanghua Xiao, Robert Barber, Ryan Huebinger, Kirk Wilhelmsen, Melissa Edwards, Neill Graff-Radford, Rachelle Doody, and Ramon Diaz-Arrastia. 2011. "A Blood-Based Screening Tool for Alzheimer's Disease That Spans Serum and

Plasma: Findings from TARC and ADNI." *PLoS ONE* 6(12).

O'Reilly, D. R., L. K. Miller, and V. A. Luckow. 1992. "Baculovirus Expression Vectors: A Laboratory Manual." *Baculovirus Expression Vectors: A Laboratory Manual.*

O'Reilly, J. J., P. M. Lane, R. Heidemann, and R. Hofstetter. 1992. "Optical Generation of Very Narrow Linewidth Millimetre Wave Signals." 28(25):3–5.

Oberthuer, Dominik, Juraj Knoška, Max O. Wiedorn, Kenneth R. Beyerlein, David A. Bushnell, Elena G. Kovaleva, Michael Heymann, Lars Gumprecht, Richard A. Kirian, Anton Barty, Valerio Mariani, Aleksandra Tolstikova, Luigi Adriano, Salah Awel, Miriam Barthelmess, Katerina Dörner, P. Lourdu Xavier, Oleksandr Yefanov, Daniel R. James, Garrett Nelson, Dingjie Wang, George Calvey, Yujie Chen, Andrea Schmidt, Michael Szczepek, Stefan Frielingsdorf, Oliver Lenz, Edward Snell, Philip J. Robinson, Böidar Šarler, Grega Belšak, Marjan Maček, Fabian Wilde, Andrew Aquila, Sébastien Boutet, Mengning Liang, Mark S. Hunter, Patrick Scheerer, John D. Lipscomb, Uwe Weierstall, Roger D. Kornberg, John C. H. Spence, Lois Pollack, Henry N. Chapman, and Saša Bajt. 2017. "Double-Flow Focused Liquid Injector for Efficient Serial Femtosecond Crystallography." *Scientific Reports* 7(1):1–12.

Oddo, Salvatore, Antonella Caccamo, Jason D. Shepherd, M. Paul Murphy, Todd E. Golde, Rakez Kayed, Raju Metherate, Mark P. Mattson, Yama Akbari, and Frank M. LaFerla. 2003. "Triple-Transgenic Model of Alzheimer's Disease with Plaques and Tangles: Intracellular Aβ and Synaptic Dysfunction." *Neuron* 39(3):409–21.

van Oers, Monique M. 2011. "Opportunities and Challenges for the Baculovirus Expression System." *Journal of Invertebrate Pathology* 107(SUPPL.):S3–15.

Van Oers, Monique M., Gorben P. Pijlman, and Just M. Vlak. 2015. "Thirty Years of Baculovirus-Insect Cell Protein Expression: From Dark Horse to Mainstream Technology." *Journal of General Virology* 96(1):6–23.

Van Oers, Monique M. and Just M. Vlak. 1997. "The Baculovirus 10-KDa Protein." *Journal of Invertebrate Pathology* 70(1):1–17.

Ohkawa, Taro, Loy E. Volkman, and Matthew D. Welch. 2010. "Actin-Based Motility Drives Baculovirus Transit to the Nucleus and Cell Surface." *Journal of Cell Biology* 190(2):187–95.

Olsson, Bob, Ronald Lautner, Ulf Andreasson, Annika Öhrfelt, Erik Portelius, Maria Bjerke, Mikko Hölttä, Christoffer Rosén, Caroline Olsson, Gabrielle Strobel, Elizabeth Wu, Kelly Dakin, Max Petzold, Kaj Blennow, and Henrik Zetterberg. 2016. "CSF and Blood Biomarkers for the Diagnosis of Alzheimer's Disease: A Systematic Review and Meta-Analysis." *The Lancet Neurology* 15(7):673–84.

Ovod, Vitaliy, Kara N. Ramsey, Kwasi G. Mawuenyega, Jim G. Bollinger, Terry Hicks, Theresa Schneider, Melissa Sullivan, Katrina Paumier, David M. Holtzman, John C. Morris, Tammie Benzinger, Anne M. Fagan, Bruce W. Patterson, and Randall J. Bateman. 2017. "Amyloid β Concentrations and Stable Isotope Labeling Kinetics of Human Plasma Specific to Central Nervous System Amyloidosis." *Alzheimer's & Dementia* 13(8):841–49.

Ozon, Sylvie, Salah El Mestikawy, and André Sobel. 1999. "Differential, Regional, and Cellular Expression of the Stathmin Family Transcripts in the Adult Rat Brain." *Journal of Neuroscience Research* 56(5):553–64.

Palmqvist, Sebastian, Henrik Zetterberg, Kaj Blennow, Susanna Vestberg, Ulf Andreasson, David J. Brooks, Rikard Owenius, Douglas Hägerström, Per Wollmer, Lennart Minthon, and Oskar Hansson. 2014. "Accuracy of Brain Amyloid Detection in Clinical Practice Using Cerebrospinal Fluid β-Amyloid 42: A Cross-Validation Study against Amyloid Positron Emission Tomography." *JAMA Neurology* 71(10):1282–89.

Palmqvist, Sebastian, Henrik Zetterberg, Niklas Mattsson, Per Johansson, Lennart Minthon, Kaj Blennow, Mattias Olsson, and Oskar Hansson. 2015. "Detailed Comparison of Amyloid PET and CSF Biomarkers for Identifying Early Alzheimer Disease." *Neurology* 85(14):1240–49.

Palop, Jorge J. and Lennart Mucke. 2010. "Amyloid-B-Induced Neuronal Dysfunction in Alzheimer's Disease: From Synapses toward Neural Networks." *Nature Neuroscience* 13(7):812–18.

Panda, A. K. 1985. *Bioprocessing of Therapeutic Proteins from the Inclusion Bodies of Escherichia Coli*. Vol. 13.

Park, Jaehong, Andrea L. Throop, and Joshua LaBaer. 2015. "Site-Specific Recombinational Cloning Using Gateway and In-Fusion Cloning Schemes." *Current Protocols in Molecular Biology* 110(1):3.20.1-3.20.23.

Passarelli, A. and Linda Guarino. 2007. "Baculovirus Late and Very Late Gene Regulation." *Current Drug Targets* 8(10):1103–15.

Passarelli, A. Lorena. 2007. "Baculovirus RNA Polymerase: Activities, Composition, and Evolution." *Virologica Sinica* 22(2):94–107.

Payne, Christopher C. and Peter P. C. Mertens. 1983. "Cytoplasmic Polyhedrosis Viruses." Pp. 425–504 in *The Reoviridae*. Springer US.

Pennock, G. D., C. Shoemaker, and L. K. Miller. 1984. "Strong and Regulated Expression of Escherichia Coli Beta-Galactosidase in Insect Cells with a Baculovirus Vector." *Molecular and Cellular Biology* 4(3):399–406.

Perusini, G. 1909. "Über Klinisch Und Histologisch Eigenartige Psychische Erkrankungen Des Späteren Lebensalters." *Histologische Und Histopathologische Arbeiten Über Die Gehirnrinde* 297–351.

Petersen, Ronald C., Glenn E. Smith, Stephen C. Waring, Robert J. Ivnik, Eric G. Tangalos, and Emre Kokmen. 1999. "Mild Cognitive Impairment: Clinical Characterization and Outcome." *Archives of Neurology* 56(3):303–8.

Pidre, L. Matias, Leticia M. Ferrelli, Santiago Haase, and Victor Romanowski. 2013. "Baculovirus Display: A Novel Tool for Vaccination." in *Current Issues in Molecular Virology - Viral Genetics and Biotechnological Applications*. InTech.

Pijlman, Gorben P., Jessica E. van Schinjndel, and Just M. Vlak. 2003. "Spontaneous Excision of BAC Vector Sequences from Bacmid-Derived Baculovirus Expression Vectors upon Passage in Insect Cells." *Journal of General Virology* 84(10):2669–78.

Plegaria, Jefferson S. and Cheryl A. Kerfeld. 2018. "Engineering Nanoreactors Using Bacterial Microcompartment Architectures." *Current Opinion in Biotechnology* 51:1–7.

Plump, A. S. 1995. "Apolipoprotein E and the Apolipoprotein E-Deficient Mouse." *Annual Review of Nutrition* 15(1):495–518.

Pope, Brian and Helen M. Kent. 1996. "High Efficiency 5 Min Transformation of Escherichia Coli." *Nucleic Acids Research* 24(3):536–37.

Porro, Danilo, Marina Venturini, Luca Brambilla, Lilia Alberghina, and Marco Vanoni. 2000. "Relating Growth Dynamics and Glucoamylase Excretion of Individual Saccharomyces Cerevisiae Cells." *Journal of Microbiological Methods* 42(1):49–55.

Portelius, Erik, Henrik Zetterberg, Tobias Skillbäck, Ulrika Törnqvist, Ulf Andreasson, John Q. Trojanowski, Michael W. Weiner, Leslie M. Shaw, Niklas Mattsson, and Kaj Blennow. 2015. "Cerebrospinal Fluid Neurogranin: Relation to Cognition and Neurodegeneration in Alzheimer's Disease." *Brain* 138(11):3373–85.

Possee, Robert D. 1993. "Baculovirus Expression Vectors — A Laboratory Manual." *Trends in Biotechnology* 11(6):267–68.

Possee, Robert D., Caroline M. Griffiths, Richard B. Hitchman, Adam Chambers, Fernanda Murguia-Meca, John Danquah, Ananya Jeshtadi, Linda A. King, Sassan Asgari, and Karyn N. Johnson. 2011. "Baculoviruses: Biology, Replication and Exploitation - NERC Open Research Archive." in *Baculoviruses: biology, replication and exploitation*.

Possee, Robert D., Richard B. Hitchman, Kevin S. Richards, Susan G. Mann, Evangelia Siaterli, Clare P. Nixon, Helen Irving, Rene Assenberg, David Alderton, Raymond J. Owens, and Linda A. King. 2008. "Generation of Baculovirus Vectors for the High-Throughput Production of Proteins in Insect Cells." *Biotechnology and Bioengineering* 101(6):1115–22.

Possee, Robert D. and Linda A. King. 2016. "Baculovirus Transfer Vectors." Pp. 51–71 in *Methods in Molecular Biology*. Vol. 1350. Humana Press Inc.

Poulain, FE and A. Sobel. 2007. "The 'SCG10-LIke Protein' SCLIP Is a Novel Regulator of Axonal Branching in Hippocampal Neurons, Unlike SCG10." *Molecular and Cellular Neuroscience* 34(2):137–46.

Preische, Oliver, Stephanie A. Schultz, Anja Apel, Jens Kuhle, Stephan A. Kaeser, Christian Barro, Susanne Gräber, Elke Kuder-Buletta, Christian LaFougere, Christoph Laske, Jonathan Vöglein, Johannes Levin, Colin Masters, Ralph Martins, Peter Schofield, Martin N. Rossor, Neill Graff-Radford, Stephen Salloway, Bernardino Ghetti, John Ringman, James Noble, Jasmeer Chhatwal, Alison Goate, Tammie Benzinger, John Morris, Randall Bateman, Guoqiao Wang, Anne Fagan, Eric McDade,

Brian Gordon, Mathias Jucker, Ricardo Allegri, Fatima Amtashar, Sarah Berman, Courtney Bodge, Susan Brandon, William Brooks, Jill Buck, Virginia Buckles, Sochenda Chea, Patricio Chrem, Helena Chui, Jake Cinco, Jack Clifford, Carlos Cruchaga, Mirelle D'Mello, Tamara Donahue, Jane Douglas, Noelia Edigo, Nilufer Erekin-Taner, Marty Farlow, Angela Farrar, Howard Feldman, Gigi Flynn, Nick Fox, Erin Franklin, Hisako Fujii, Cortaiga Gant, Samantha Gardener, Jill Goldman, Julia Gray, Jenny Gurney, Jason Hassenstab, Mie Hirohara, David Holtzman, Russ Hornbeck, Siri Houeland DiBari, Takeshi Ikeuchi, Snezana Ikonomovic, Gina Jerome, Celeste Karch, Kensaku Kasuga, Takeshi Kawarabayashi, William Klunk, Robert Koeppe, Jae Hong Lee, Daniel Marcus, Neal Scott Mason, Denise Maue-Dreyfus, Lucy Montoya, Hiroshi Mori, Akem Nagamatsu, Katie Neimeyer, Joanne Norton, Richard Perrin, Marc Raichle, Jee Hoon Roh, Hiroyuki Shimada, Tomoyo Shiroto, Mikio Shoji, Wendy Sigurdson, Hamid Sohrabi, Paige Sparks, Kazushi Suzuki, Laura Swisher, Kevin Taddei, Jen Wang, Peter Wang, Mike Weiner, Mary Wolfsberger, Chengjie Xiong, and Xiong Xu. 2019. "Serum Neurofilament Dynamics Predicts Neurodegeneration and Clinical Progression in Presymptomatic Alzheimer's Disease." *Nature Medicine* 25(2):277–83.

Proteome, Tissue-Based Map of the Human. 2015. "Tissue-Based Map of the Human Proteome." *Science* 347(6220):1260419.

Puck, Theodore T., Steven J. Cieciura, and Arthur Robinson. 1958. "GENETICS OF SOMATIC MAMMALIAN CELLS III. LONG-TERM CULTIVATION OF EUPLOID CELLS FROM HUMAN AND ANIMAL SUBJECTS." *Journal of Experimental Medicine* 108(6):945–56.

Pullen, S. S. and P. D. Friesen. 1995. "Early Transcription of the Ie-1 Transregulator Gene of Autographa Californica Nuclear Polyhedrosis Virus Is Regulated by DNA Sequences within Its 5' Noncoding Leader Region." *Journal of Virology* 69(1):156–65.

Putnam, Karen T., David L. Friedman, Lida H. Kimmel, Judy Bergeson, Guy J. Manetti, John J. Bartko, and Robert M. Cohen. 2015. "Decreased [illegible] -Amyloid 1-42 and Increased Tau Levels in Cerebrospinal Fluid of Patients With Alzheimer Disease." *Jamanetwork.Com* 289(16).

Qiu, Ji and Joshua Labaer. 2011. "Nucleic Acid Programmable Protein Array: A Just-in-Time Multiplexed Protein Expression and Purification Platform." Pp. 151–63 in *Methods in Enzymology*. Vol. 500. Academic Press Inc.

Qu, Bao Xi, Yunhua Gong, Carol Moore, Min Fu, Dwight C. German, Ling Yu Chang, Roger Rosenberg, and Ramon Diaz-Arrastia. 2014. "Beta-Amyloid Auto-Antibodies Are Reduced in Alzheimer's Disease." *Journal of Neuroimmunology* 274(1–2):168–73.

Querfurth, Henry W. and Frank M. Laferla. 2010. "Alzheimer's Disease." *N Engl J Med* 329–44.

Querfurth, HW and FM LaFerla. 2010. "Mechanisms of Disease Alzheimer's Disease." *The New England Journal of Medicine* 362:329–44.

Radad, Khaled, Rudolf Moldzio, Mubarak Al-Shraim, Barbara Kranner, Christopher Krewenka, and Wolf-Dieter Rausch. 2017. "Recent Advances on the Role of Neurogenesis in the Adult Brain: Therapeutic Potential in Parkinson's and Alzheimer's Diseases." *CNS & Neurological Disorders - Drug Targets* 16(7).

Radner, Stephan, Patrick H. N. Celie, Karoline Fuchs, Werner Sieghart, Titia K. Sixma, and Mariano Stornaiuolo. 2012. "Transient Transfection Coupled to Baculovirus Infection for Rapid Protein Expression Screening in Insect Cells." *Journal of Structural Biology* 179(1):46–55.

Rajan, Kumar B., Lisa L. Barnes, Robert S. Wilson, Elizabeth A. McAninch, Jennifer Weuve, Dominique Sighoko, and Denis A. Evans. 2017. "Racial Differences in the Association Between Apolipoprotein E Risk Alleles and Overall and Total Cardiovascular Mortality Over 18 Years." *Journal of the American Geriatrics Society* 65(11):2425–30.

Ramachandran, Niroshan, Eugenie Hainsworth, Bhupinder Bhullar, Samuel Eisenstein, Benjamin Rosen, Albert Y. Lau, Johannes C. Walter, and Joshua LaBaer. 2004. "Self-Assembling Protein Microarrays." *Science* 305(5680):86–90.

Ramachandran, Niroshan, Jacob V. Raphael, Eugenie Hainsworth, Gokhan Demirkan, Manuel G. Fuentes, Andreas Rolfs, Yanhui Hu, and Joshua LaBaer. 2008. "Next-Generation High-Density Self-Assembling Functional Protein Arrays." *Nature Methods* 5(6):535–38.

Ramani, Sree R., Irene Tom, Nicholas Lewin-Koh, Bernd Wranik, Laura Depalatis, Jianjun Zhang, Dan Eaton, and Lino C. Gonzalez. 2012. "A Secreted Protein Microarray Platform for Extracellular Protein Interaction Discovery." *Analytical Biochemistry* 420(2):127–38.

Randall, Jeffrey, Erik Mörtberg, Gail K. Provuncher, David R. Fournier, David C. Duffy, Sten Rubertsson, Kaj Blennow, Henrik Zetterberg, and David H. Wilson. 2013. "Tau Proteins in Serum Predict Neurological Outcome after Hypoxic Brain Injury from Cardiac Arrest: Results of a Pilot Study." *Resuscitation* 84(3):351–56.

Rauf, Femina, Fernanda Festa, Jin G. Park, Mitchell Magee, Seron Eaton, Capria Rinaldi, Carlos Morales Betanzos, Laura Gonzalez-Malerva, and Joshua Labaer. 2018. "Ibrutinib Inhibition of ERBB4 Reduces Cell Growth in a WNT5A-Dependent Manner." *Oncogene* 37(17):2237–50.

Ray, Sandip, Markus Britschgi, Charles Herbert, Yoshiko Takeda-Uchimura, Adam Boxer, Kaj Blennow, Leah F. Friedman, Douglas R. Galasko, Marek Jutel, Anna Karydas, Jeffrey A. Kaye, Jerzy Leszek, Bruce L. Miller, Lennart Minthon, Joseph F. Quinn, Gil D. Rabinovici, William H. Robinson, Marwan N. Sabbagh, Yuen T. So, D. Larry Sparks, Massimo Tabaton, Jared Tinklenberg, Jerome A. Yesavage, Tibshirani Robert, and Wyss-Coray Tony. 2007. "Classification and Prediction of Clinical Alzheimer's Diagnosis Based on Plasma Signaling Proteins." *Natural Medicine* 13:1359–62.

Reddy, M. Muralidhar, Rosemary Wilson, Johnnie Wilson, Steven Connell, Anne Gocke, Linda Hynan, Dwight German, and Thomas Kodadek. 2011. "Identification of

Candidate IgG Biomarkers for Alzheimer's Disease via Combinatorial Library Screening." *Cell* 144(1):132–42.

Redecke, Lars, Karol Nass, Daniel P. DePonte, Thomas A. White, Dirk Rehders, Anton Barty, Francesco Stellato, Mengning Liang, Thomas R. M. Barends, Sébastien Boutet, Garth J. Williams, Marc Messerschmidt, M. Marvin Seibert, Andrew Aquila, David Arnlund, Sasa Bajt, Torsten B. Barth, Michael J. Bogan, Carl Caleman, Tzu Chiao Chao, R. Bruce Doak, Holger Fleckenstein, Matthias Frank, Raimund Fromme, Lorenzo Galli, Ingo Grotjohann, Mark S. Hunter, Linda C. Johansson, Stephan Kassemeyer, Gergely Katona, Richard A. Kirian, Rudolf Koopmann, Chris Kupitz, Lukas Lomb, Andrew V. Martin, Stefan Mogk, Richard Neutze, Robert L. Shoeman, Jan Steinbrener, Nicusor Timneanu, Dingjie Wang, Uwe Weierstall, Nadia A. Zatsepin, John C. H. Spence, Petra Fromme, Ilme Schlichting, Michael Duszenko, Christian Betzel, and Henry N. Chapman. 2013. "Natively Inhibited Trypanosoma Brucei Cathepsin B Structure Determined by Using an X-Ray Laser." *Science* 339(6116):227–30.

Reece-Hoyes, John S. and Albertha J. M. Walhout. 2018. "Gateway Recombinational Cloning." *Cold Spring Harbor Protocols* 2018(1):1–6.

Reiman, Eric M., Kewei Chen, Xiaofen Liu, Daniel Bandy, Meixiang Yu, Wendy Lee, Napatkamon Ayutyanont, Jennifer Keppler, Stephanie A. Reeder, Jessica B. S. Langbaum, Gene E. Alexander, William E. Klunk, Chester A. Mathis, Julie C. Price, Howard J. Aizensteini, Steven T. DeKosky, and Richard J. Caselli. 2009. "Fibrillar Amyloid-β Burden in Cognitively Normal People at 3 Levels of Genetic Risk for Alzheimer's Disease." *Proceedings of the National Academy of Sciences of the United States of America* 106(16):6820–25.

Reiser, J., V. Glumoff, M. Kälin, and U. Ochsner. 1990. "Transfer and Expression of Heterologous Genes in Yeasts Other than Saccharomyces Cerevisiae." *Advances in Biochemical Engineering/Biotechnology* 43:75–102.

Restrepo, Lucas, Phillip Stafford, and Stephen Albert Johnston. 2013. "Feasibility of an Early Alzheimer's Disease Immunosignature Diagnostic Test." *Journal of Neuroimmunology* 254(1–2):154–60.

Restrepo, Lucas, Phillip Stafford, D. Mitch Magee, and Stephen Albert Johnston. 2011. "Application of Immunosignatures to the Assessment of Alzheimer's Disease." *Annals of Neurology* 70(2):286–95.

Riederer, Beat M. and Lester I. Binder. 1994. "Differential Distribution of Tau Proteins in Developing Cat Cerebellum." *Brain Research Bulletin* 33(2):155–61.

Ring, Sabine, Sascha W. Weyer, Susanne B. Kilian, Elaine Waldron, Claus U. Pietrzik, Mikhail A. Filippov, Jochen Herms, Christian Buchholz, Christopher B. Eckman, Martin Korte, David P. Wolfer, and Ulrike C. Müller. 2007. "The Secreted β-Amyloid Precursor Protein Ectodomain APPsα Is Sufficient to Rescue the Anatomical, Behavioral, and Electrophysiological Abnormalities of APP-Deficient Mice." *Journal of Neuroscience* 27(29):7817–26.

Rio, Donald C., Scott G. Clark, and Robert Tjian. 1985. "A Mammalian Host-Vector

System That Regulates Expression and Amplification of Transfected Genes by Temperature Induction." *Science* 227(4682):23–28.

Roedig, Philip, Helen M. Ginn, Tim Pakendorf, Geoff Sutton, Karl Harlos, Thomas S. Walter, Jan Meyer, Pontus Fischer, Ramona Duman, Ismo Vartiainen, Bernd Reime, Martin Warmer, Aaron S. Brewster, Iris D. Young, Tara Michels-Clark, Nicholas K. Sauter, Abhay Kotecha, James Kelly, David J. Rowlands, Marcin Sikorsky, Silke Nelson, Daniel S. Damiani, Roberto Alonso-Mori, Jingshan Ren, Elizabeth E. Fry, Christian David, David I. Stuart, Armin Wagner, and Alke Meents. 2017. "High-Speed Fixed-Target Serial Virus Crystallography." *Nature Methods* 14(8):805–10.

Rohrmann, G. F. 1986. "Polyhedrin Structure." *The Journal of General Virology* 67:1499–1513.

Romanos, Michael A., Carol A. Scorer, and Jeffrey J. Clare. 1992. "Foreign Gene Expression in Yeast: A Review." *Yeast* 8(6):423–88.

Rooney, Isabelle, Kristine Butrovich, and Carl F. Ware. 2000. *Expression of Lymphotoxins and Their Receptor-Fc Fusion Proteins by Baculovirus*. Vol. 322. ACADEMIC PRESS.

Rosenmann, Hanna, Zeev Meiner, Valeria Geylis, Oded Abramsky, and Michael Steinitz. 2006. "Detection of Circulating Antibodies against Tau Protein in Its Unphosphorylated and in Its Neurofibrillary Tangles-Related Phosphorylated State in Alzheimer's Disease and Healthy Subjects." *Neuroscience Letters* 410(2):90–93.

Rovelet-Lecrux, Anne, Didier Hannequin, Gregory Raux, Nathalie Le Meur, Annie Laquerrière, Anne Vital, Cécile Dumanchin, Sébastien Feuillette, Alexis Brice, Martine Vercelletto, Frédéric Dubas, Thierry Frebourg, and Dominique Campion. 2006. "APP Locus Duplication Causes Autosomal Dominant Early-Onset Alzheimer Disease with Cerebral Amyloid Angiopathy." *Nature Genetics* 38(1):24–26.

Rowe, Christopher C., Kathryn A. Ellis, Miroslava Rimajova, Pierrick Bourgeat, Kerryn E. Pike, Gareth Jones, Jurgen Fripp, Henri Tochon-Danguy, Laurence Morandeau, Graeme O'Keefe, Roger Price, Parnesh Raniga, Peter Robins, Oscar Acosta, Nat Lenzo, Cassandra Szoeke, Olivier Salvado, Richard Head, Ralph Martins, Colin L. Masters, David Ames, and Victor L. Villemagne. 2010. "Amyloid Imaging Results from the Australian Imaging, Biomarkers and Lifestyle (AIBL) Study of Aging." *Neurobiology of Aging* 31(8):1275–83.

Rozenblatt-Rosen, Orit, Rahul C. Deo, Megha Padi, Guillaume Adelmant, Michael A. Calderwood, Thomas Rolland, Miranda Grace, Amélie Dricot, Manor Askenazi, Maria Tavares, Samuel J. Pevzner, Fieda Abderazzaq, Danielle Byrdsong, Anne Ruxandra Carvunis, Alyce A. Chen, Jingwei Cheng, Mick Correll, Melissa Duarte, Changyu Fan, Mariet C. Feltkamp, Scott B. Ficarro, Rachel Franchi, Brijesh K. Garg, Natali Gulbahce, Tong Hao, Amy M. Holthaus, Robert James, Anna Korkhin, Larisa Litovchick, Jessica C. Mar, Theodore R. Pak, Sabrina Rabello, Renee Rubio, Yun Shen, Saurav Singh, Jennifer M. Spangle, Murat Tasan, Shelly Wanamaker, James T. Webber, Jennifer Roecklein-Canfield, Eric Johannsen, Albert László Barabási, Rameen Beroukhim, Elliott Kieff, Michael E. Cusick, David E. Hill, Karl Münger, Jarrod A. Marto, John Quackenbush, Frederick P. Roth, James A. Decaprio, and Marc Vidal.

2012. "Interpreting Cancer Genomes Using Systematic Host Network Perturbations by Tumour Virus Proteins." *Nature* 487(7408):491–95.

Rychlowska, Malgorzata, Beata Gromadzka, Krystyna Bienkowska-Szewczyk, and Boguslaw Szewczyk. 2011. "Baculovirus-Insect Cell Expression System for Human Therapy." *Current Pharmaceutical Biotechnology* 12(11):1840–49.

Saarenpää, Tuulia, Veli Pekka Jaakola, and Adrian Goldman. 2015. "Baculovirus-Mediated Expression of GPCRs in Insect Cells." *Methods in Enzymology* 556:185–218.

Saitoh, Tsunao, Karen Horsburgh, and Eliezer Masliah. 1993. "Hyperactivation of Signal Transduction Systems in Alzheimer's Disease." *Annals of the New York Academy of Sciences* 695(1):34–41.

Sardi, F., L. Fassina, L. Venturini, M. Inguscio, F. Guerriero, E. Rolfo, and G. Ricevuti. 2011. "Alzheimer's Disease, Autoimmunity and Inflammation. The Good, the Bad and the Ugly." *Autoimmunity Reviews* 11(2):149–53.

Sato, Chihiro, Nicolas R. Barthélemy, Kwasi G. Mawuenyega, Bruce W. Patterson, Brian A. Gordon, Jennifer Jockel-Balsarotti, Melissa Sullivan, Matthew J. Crisp, Tom Kasten, Kristopher M. Kirmess, Nicholas M. Kanaan, Kevin E. Yarasheski, Alaina Baker-Nigh, Tammie L. S. Benzinger, Timothy M. Miller, Celeste M. Karch, and Randall J. Bateman. 2018. "Tau Kinetics in Neurons and the Human Central Nervous System." *Neuron* 97(6):1284-1298.e7.

Satoh, K., A. Kawakami, S. Shirabe, M. Tamai, A. Sato, M. Tsujihata, K. Nagasato, and K. Eguchi. 2010. "Anti-Cyclic Citrullinated Peptide Antibody (Anti-CCP Antibody) Is Present in the Sera of Patients with Dementia of Alzheimer's Type in Asian." *Acta Neurologica Scandinavica* 121(5):338–41.

Saul, Justin, Brianne Petritis, Sujay Sau, Femina Rauf, Michael Gaskin, Benjamin Ober-Reynolds, Irina Mineyev, Mitch Magee, John Chaput, Ji Qiu, and Joshua LaBaer. 2014. "Development of a Full-Length Human Protein Production Pipeline." *Protein Science* 23(8):1123–35.

Schiller, John T., Xavier Castellsagué, Luisa L. Villa, and Allan Hildesheim. 2008. "An Update of Prophylactic Human Papillomavirus L1 Virus-like Particle Vaccine Clinical Trial Results." *Vaccine* 26(SUPPL. 10):53–61.

Schmechel, D. E., A. M. Saunders, W. J. Strittmatter, B. J. Crain, C. M. Hulette, S. H. Joo, M. A. Pericak-Vance, D. Goldgaber, and A. D. Roses. 1993. "Increased Amyloid β-Peptide Deposition in Cerebral Cortex as a Consequence of Apolipoprotein E Genotype in Late-Onset Alzheimer Disease." *Proceedings of the National Academy of Sciences of the United States of America* 90(20):9649–53.

Schönherr, R., M. Klinge, J. M. Rudolph, K. Fita, D. Rehders, F. Lübber, S. Schneegans, I. V. Majoul, M. Duszenko, C. Betzel, A. Brandariz-Nuñez, J. Martinez-Costas, R. Duden, and L. Redecke. 2015. "Real-Time Investigation of Dynamic Protein Crystallization in Living Cells." *Structural Dynamics* 2(4):041712.

Schönherr, Robert, Janine Mia Rudolph, and Lars Redecke. 2018. "Protein Crystallization in Living Cells." *Biological Chemistry* 399(7):751–72.

Schott, Klaus, Henning Wormstall, Maren Dietrich, Reinhild Klein, and Anil Batra. 1996. "Autoantibody Reactivity in Serum of Patients with Alzheimer's Disease and Other Age-Related Dementias." *Psychiatry Research* 59(3):251–54.

Seiler, Catherine Y., Jin G. Park, Amit Sharma, Preston Hunter, Padmini Surapaneni, Casey Sedillo, James Field, Rhys Algar, Andrea Price, Jason Steel, Andrea Throop, Michael Fiacco, and Joshua Labaer. 2014. "DNASU Plasmid and PSI:Biology-Materials Repositories: Resources to Accelerate Biological Research." *Nucleic Acids Research* 42(D1):1253–60.

Service, Robert F. 2002. "Tapping DNA for Structures Produces a Trickle." *Science* 298(5595):948–50.

Seubert, Peter, Carmen Vigo-Pelfrey, Fred Esch, Michael Lee, Harry Dovey, Dave Davis, Sukanto Sinha, Michael Schiossmacher, Justine Whaley, Cathy Swindlehurst, Robert McCormack, Robert Wolfert, Dennis Selkoe, Ivan Lieberburg, and Dale Schenk. 1992. "Isolation and Quantification of Soluble Alzheimer's β-Peptide from Biological Fluids." *Nature* 359(6393):235–37.

Sezonov, Guennadi, Danièle Joseleau-Petit, and Richard D'Ari. 2007. "Escherichia Coli Physiology in Luria-Bertani Broth." *Journal of Bacteriology* 189(23):8746–49.

Shah, Dipti, Frederick Rohlfing, and Evan Johnson. 2016. "Discovery and Subsequent Confirmation of Novel Serum Biomarkers Diagnosing Alzheimer's Disease Swati Anand Agilent Technologies 6 PUBLICATIONS 58 CITATIONS SEE PROFILE."

Shapira, Sagi D., Irit Gat-Viks, Bennett O. V. Shum, Amelie Dricot, Marciela M. de Grace, Liguo Wu, Piyush B. Gupta, Tong Hao, Serena J. Silver, David E. Root, David E. Hill, Aviv Regev, and Nir Hacohen. 2009. "A Physical and Regulatory Map of Host-Influenza Interactions Reveals Pathways in H1N1 Infection." *Cell* 139(7):1255–67.

Shiloach, Joseph and Rephael Fass. 2005. "Growing E. Coli to High Cell Density - A Historical Perspective on Method Development." *Biotechnology Advances* 23(5):345–57.

Sibani, Sahar and Joshua LaBaer. 2011. "Immunoprofiling Using NAPPA Protein Microarrays." *Methods in Molecular Biology (Clifton, N.J.)* 723:149–61.

Slack, Jeffery and Basil M. Arif. 2006. "The Baculoviruses Occlusion-Derived Virus: Virion Structure and Function." *Advances in Virus Research* 69:99–165.

Smith, G. E., M. D. Summers, and M. J. Fraser. 1992. "Production of Human Beta Interferon in Insect Cells Infected with a Baculovirus Expression Vector. 1983." *Biotechnology (Reading, Mass.)* 24:434–43.

Smith, Gale E., M. J. Fraser, and Max D. Summers. 1983. "Molecular Engineering of the Autographa Californica Nuclear Polyhedrosis Virus Genome: Deletion Mutations Within the Polyhedrin Gene." *Journal of Virology* 46(2):584–93.

Smith, Gale E., Just M. Vlak, and Max D. Summers. 1983. "Physical Analysis of Autographa Californica Nuclear Polyhedrosis Virus Transcripts for Polyhedrin and 10,000-Molecular-Weight Protein." *Journal of Virology* 45(1):215–25.

Smith, K. M. 1976. "Virus-Insect Relationships." *Virus-Insect Relationships.*

Snigirevskaya, Ekaterina S., Alan R. Hays, and Alexander S. Raikhel. 1997. "Secretory and Internalization Pathways of Mosquito Yolk Protein Precursors." *Cell and Tissue Research* 290(1):129–42.

Spence, J. C. H. 2017. "XFELs for Structure and Dynamics in Biology." *IUCrJ* 4(Pt 4):322–39.

Sridhar, P., A. K. Awasthi, A. A. Azim, S. Burma, S. Habib, A. Jain, B. Mukherjee, A. Ranjan, and Seyed E. Hasnain. 1994. "Baculovirus Vector-Mediated Expression of Heterologous Genes in Insect Cells." *J Biosci* 19(5):603–14.

Steiner, Johann and Matthias L. Schroeter. 2011. "S100B Protein in Neurodegenerative Disorders."

Stewart, Walter F., Claudia Kawas, Maria Corrada, and E. Jeffrey Metter. 1997. "Risk of Alzheimer's Disease and Duration of NSAID Use." *Neurology* 48(3):626–32.

Strausberg, Robert L. and Susan L. Strausberg. 1995. "Overview of Protein Expression in Saccharomyces Cerevisiae." *Current Protocols in Protein Science* 5.6.1-5.6.7.

Strittmatter, Warren J., Ann M. Saunders, Donald Schmechel, Margaret Pericak-Vance, Jan Enghild, Guy S. Salvesen, and Allen D. Roses. 1993. "Apolipoprotein E: High-Avidity Binding to β-Amyloid and Increased Frequency of Type 4 Allele in Late-Onset Familial Alzheimer Disease." *Proceedings of the National Academy of Sciences of the United States of America* 90(5):1977–81.

Strooper, Bart De. 2007. "Loss-of-Function Presenilin Mutations in Alzheimer Disease. Talking Point on the Role of Presenilin Mutations in Alzheimer Disease." *EMBO Reports* 8(2):141–46.

Strooper, De Bart, P. Saftig, K. Craessaerts, H. Vanderstichele, G. Guhde, W. Annaert, K. Von Figura, and F. Van Leuven. 1998. "Deficiency of Presenilin-1 Inhibits the Normal Cleavage of Amyloid Precursor Protein." *Nature* 391(January):387–90.

Studier, F. William and Barbara A. Moffatt. 1986. "Use of Bacteriophage T7 RNA Polymerase to Direct Selective High-Level Expression of Cloned Genes." *Journal of Molecular Biology* 189(1):113–30.

Swamy-Mruthinti, S., Shyamala Mruthinti, Jerry J. Buccafusco, William D. Hill, Jennifer L. Waller, Thomas W. Jackson, Edward Y. Zamrini, and Rosann F. Schade. 2004. "Autoimmunity in Alzheimers Disease as Evidenced by Plasma Immunoreactivity Against RAGE and Aβ42: Complication of Diabetes Autoimmunity in Alzheimer's Disease: Increased Levels of Circulating IgGs Binding A and RAGE Peptides." *Neurobiology of Aging* 25:1023–32.

Swartz, James R. 2009. "Universal Cell-Free Protein Synthesis." *Nature Biotechnology* 27(8):731–32.

Szabo, Paul, Norman Relkin, and Marc E. Weksler. 2008. "Natural Human Antibodies to Amyloid Beta Peptide." *Autoimmunity Reviews* 7(6):415–20.

Szewczyk, Boguslaw, Liliana Hoyos-Carvajal, Maria Paluszek, Iwona Skrzecz, and Marlinda Lobo De Souza. 2006. "Baculoviruses - Re-Emerging Biopesticides." *Biotechnology Advances* 24(2):143–60.

Tafforeau, Lionel, Chantal Rabourdin-Combe, and Vincent Lotteau. 2012. "Virus-Human Cell Interactomes." *Methods in Molecular Biology* 812:103–20.

Takasugi, Nobumasa, Taisuke Tomita, Ikuo Hayashi, Makiko Tsuruoka, Manabu Niimura, Yasuko Takahashi, Gopal Thinakaran, and Takeshi Iwatsubo. 2003. "The Role of Presenilin Cofactors in the γ-Secretase Complex." *Nature.Com* 422:438–41.

Tanaka, J., K. Nakamura, M. Takeda, K. Tada, H. Suzuki, H. Morita, T. Okado, S. Hariguchi, and T. Nishimura. 1989. "Enzyme-linked Immunosorbent Assay for Human Autoantibody to Glial Fibrillary Acidic Protein: Higher Titer of the Antibody Is Detected in Serum of Patients with Alzheimer's Disease." *Acta Neurologica Scandinavica* 80(6):554–60.

Tang, Yanyang, Ji Qiu, Matthias Machner, and Joshua LaBaer. 2017. "Discovering Protein-Protein Interactions Using Nucleic Acid Programmable Protein Arrays." *Current Protocols in Cell Biology* 2017:15.21.1-15.21.14.

Tarawneh, Rawan, Gina D'Angelo, Elizabeth MacY, Chengjie Xiong, Deborah Carter, Nigel J. Cairns, Anne M. Fagan, Denise Head, Mark A. Mintun, Jack H. Ladenson, Jin Moo Lee, John C. Morris, and David M. Holtzman. 2011. "Visinin-like Protein-1: Diagnostic and Prognostic Biomarker in Alzheimer Disease." *Annals of Neurology* 70(2):274–85.

Terry, Robert D., Eliezer Masliah, David P. Salmon, Nelson Butters, Richard DeTeresa, Robert Hill, Lawrence A. Hansen, and Robert Katzman. 1991. "Physical Basis of Cognitive Alterations in Alzheimer's Disease: Synapse Loss Is the Major Correlate of Cognitive Impairment." *Annals of Neurology* 30(4):572–80.

Terryberry, J. W., G. Thor, and J. B. Peter. 1998. "Autoantibodies in Neurodegenerative Diseases: Antigen-Specific Frequencies and Intrathecal Analysis." *Neurobiology of Aging* 19(3):205–16.

Thorsell, Annika, Maria Bjerke, Johan Gobom, Eva Brunhage, Eugeen Vanmechelen, Niels Andreasen, Oskar Hansson, Lennart Minthon, Henrik Zetterberg, and Kaj Blennow. 2010. "Neurogranin in Cerebrospinal Fluid as a Marker of Synaptic Degeneration in Alzheimer's Disease." *Brain Research* 1362:13–22.

Todd, Jason W., A. Lorena Passarelli, and Lois K. Miller. 1995. *Eighteen Baculovirus Genes, Including Lef-11, P35, 39K, and P47, Support Late Gene Expression*. Vol. 69.

Tsutsui, Hidekazu, Yuka Jinno, Keiko Shoda, Akiko Tomita, Makoto Matsuda, Eiki

Yamashita, Hiroyuki Katayama, Atsushi Nakagawa, and Atsushi Miyawaki. 2015. "A Diffraction-Quality Protein Crystal Processed as an Autophagic Cargo." *Molecular Cell* 58(1):186–93.

Tyagi, Manoj, Kosuke Hashimoto, Benjamin A. Shoemaker, Stefan Wuchty, and Anna R. Panchenko. 2012. "Large-Scale Mapping of Human Protein Interactome Using Structural Complexes." *EMBO Reports* 13(3):266–71.

Tzen, Kai-Yuan, Shieh-Yueh Yang, Ta-Fu Chen, Ting-Wen Cheng, Herng-Er Horng, Hsiang-Ping Wen, Ya-Yao Huang, Chyng-Yann Shiue, and Ming-Jang Chiu. 2014. "Plasma Aβ but Not Tau Is Related to Brain PiB Retention in Early Alzheimer's Disease." *ACS Chemical Neuroscience* 5(9):830–36.

Uetz, Peter, Loic Glot, Gerard Cagney, Traci A. Mansfield, Richard S. Judson, James R. Knight, Daniel Lockshon, Vaibhav Narayan, Malthreyan Srinivasan, Pascale Pochart, Alla Qureshi-Emlli, Ying Li, Brian Godwin, Diana Conover, Theodore Kalbfleisch, Govindan Vijayadamodar, Meijia Yang, Mark Johnston, Stanley Fields, and Jonathan M. Rothberg. 2000. "A Comprehensive Analysis of Protein-Protein Interactions in Saccharomyces Cerevisiae." *Nature* 403(6770):623–27.

Vacirca, D., F. Delunardo, P. Matarrese, T. Colasanti, P. Margutti, A. Siracusano, S. Pontecorvo, A. Capozzi, M. Sorice, A. Francia, W. Malorni, and E. Ortona. 2012. "Autoantibodies to the Adenosine Triphosphate Synthase Play a Pathogenetic Role in Alzheimer's Disease." *Neurobiology of Aging* 33(4):753–66.

Vail, P. V., G. Sutter, D. L. Jay, and D. Gough. 1971. "Reciprocal Infectivity of Nuclear Polyhedrosis Viruses of the Cabbage Looper and Alfalfa Looper." *Journal of Invertebrate Pathology* 17(3):383–88.

Vandenberghe, Rik, Koen Van Laere, Adrian Ivanoiu, Eric Salmon, Christine Bastin, Eric Triau, Steen Hasselbalch, Ian Law, Allan Andersen, Alex Korner, Lennart Minthon, Gaëtan Garraux, Natalie Nelissen, Guy Bormans, Chris Buckley, Rikard Owenius, Lennart Thurfjell, Gill Farrar, and David J. Brooks. 2010. "18F-Flutemetamol Amyloid Imaging in Alzheimer Disease and Mild Cognitive Impairment a Phase 2 Trial." *Annals of Neurology* 68(3):319–29.

Vanmechelen, E., H. Vanderstichele, P. Davidsson, E. Van Kerschaver, B. Van Der Perre, M. Sjögren, N. Andreasen, and K. Blennow. 2000. "Quantification of Tau Phosphorylated at Threonine 181 in Human Cerebrospinal Fluid: A Sandwich ELISA with a Synthetic Phosphopeptide for Standardization." *Neuroscience Letters* 285(1):49–52.

Vaughn, J. L. and P. Faulkner. 1963. "Susceptibility of an Insect Tissue Culture to Infection by Virus Preparations of the Nuclear Polyhedrosis of the Silkworm (Bombyx Mori L.)." *Virology* 20(3):484–89.

Vaughn, J. L., R. H. Goodwin, G. J. Tompkins, and P. McCawley. 1977. "The Establishment of Two Cell Lines from the Insect Spodoptera Frugiperda." *In Vitro* 13(4):213–17.

Venkatesan, Krishnan, Joel Green, Steven R. Shapiro, and George F. Steinhardt.

2009. "Correlation of Hydronephrosis Index to Society of Fetal Urology Hydronephrosis Scale." *Advances in Urology*.

Vicente, Tiago, António Roldão, Cristina Peixoto, Manuel J. T. Carrondo, and Paula M. Alves. 2011. "Large-Scale Production and Purification of VLP-Based Vaccines." *Journal of Invertebrate Pathology* 107(SUPPL.):S42–48.

Vigo-Pelfrey, C., P. Seubert, R. Barbour, C. Blomquist, M. Lee, D. Lee, F. Coria, L. Chang, B. Miller, I. Lieberburg, and D. Schenk. 1995. "Elevation of Microtubule-Associated Protein Tau in the Cerebrospinal Fluid of Patients with Alzheimer's Disease." *Neurology* 45(4):788–93.

Villemagne, Victor L. 2016. "Amyloid Imaging: Past, Present and Future Perspectives." *Ageing Research Reviews* 30:95–106.

Vinarov, Dmitriy A., Betsy L. Lytle, Francis C. Peterson, Ejan M. Tyler, Brian F. Volkman, and John L. Markley. 2004. "Cell-Free Protein Production and Labeling Protocol for NMR-Based Structural Proteomics." *Nature Methods* 1(2):149–53.

Vlak, Just M., Alexander Schouten, Magda Usmany, Graham J. Belsham, Els C. Klinge-Roode, Andrew J. Maule, Jan W. M. Van Lent, and Douwe Zuidema. 1990. "Expression of Cauliflower Mosaic Virus Gene I Using a Baculovirus Vector Based upon the P10 Gene and a Novel Selection Method." *Virology* 179(1):312–20.

Volkman, Loy E. and Phyllis A. Goldsmith. 1985. "Mechanism of Neutralization of Budded Autographs Californica Nuclear Polyhedrosis Virus by a Monoclonal Antibody: Inhibition of Entry by Adsorptive Endocytosis." *Virology* 143(1):185–95.

Volkman, Loy E. and Max D. Summers. 1977. "Autographa Californica Nuclear Polyhedrosis Virus: Comparative Infectivity of the Occluded, Alkali-Liberated, and Nonoccluded Forms." *Journal of Invertebrate Pathology* 30(1):102–3.

Volkman, Loy E., Max D. Summers, and Ching-Hsiu Hsieh. 1976. "Occluded and Nonoccluded Nuclear Polyhedrosis Virus Grown in Trichoplusia Ni: Comparative Neutralization, Comparative Infectivity, and In Vitro Growth Studies." *Journal of Virology* 19(3):820–32.

Walhout, A. J. M., G. F. Temple, M. A. Brasch, J. L. Hartley, M. A. Lorson, S. Van den Heuvel, and M. Vidal. 2000. "GATEWAY Recombinational Cloning: Application to the Cloning of Large Numbers of Open Reading Frames or ORFeomes." *Methods in Enzymology* 328:575–92.

Wampler, Ronald D., David J. Kissick, Christopher J. Dehen, Ellen J. Gualtieri, Jessica L. Grey, Hai-Feng Wang, David H. Thompson, Ji-Xin Cheng, and Garth J. Simpson. 2008. "Selective Detection of Protein Crystals by Second Harmonic Microscopy." *Journal of the American Chemical Society* 130(43):14076–77.

Wang, Haoyu, Gokhan Demirkan, Xiaofang Bian, Garrick Wallstrom, Kristi Barker, Kailash Karthikeyan, Yanyang Tang, Shabana F. Pasha, Jonathan A. Leighton, Ji Qiu, and Joshua LaBaer. 2017. "Identification of Antibody against SNRPB, Small Nuclear Ribonucleoprotein-Associated Proteins B and B', as an Autoantibody Marker in

Crohn's Disease Using an Immunoproteomics Approach." *Journal of Crohn's and Colitis* 11(7):848–56.

Wang, Jie, Shilpa Shivakumar, Kristi Barker, Yanyang Tang, Garrick Wallstrom, Jin G. Park, Jun Chieh J. Tsay, Harvey I. Pass, William N. Rom, Joshua LaBaer, and Ji Qiu. 2016. "Comparative Study of Autoantibody Responses between Lung Adenocarcinoma and Benign Pulmonary Nodules." *Journal of Thoracic Oncology* 11(3):334–45.

Wang, Yipeng and Eckhard Mandelkow. 2016. "Tau in Physiology and Pathology." *Nature Reviews Neuroscience* 17(1):5–21.

Ward, Alex, Sheila Crean, Catherine J. Mercaldi, Jenna M. Collins, Dylan Boyd, Michael N. Cook, and H. Michael Arrighi. 2012. "Fax +41 61 306 12 34 E-Mail Karger@karger.Ch Systematic Review Prevalence of Apolipoprotein E4 Genotype and Homozygotes (APOE E4/4) among Patients Diagnosed with Alzheimer's Disease: A Systematic Review and Meta-Analysis."

Weingarten, M. D., A. H. Lockwood, S. Y. Hwo, and M. W. Kirschner. 1975. "A Protein Factor Essential for Microtubule Assembly." *Proceedings of the National Academy of Sciences of the United States of America* 72(5):1858–62.

Wellington, Henrietta, Ross W. Paterson, Erik Portelius, Ulrika Törnqvist, Nadia Magdalinou, Nick C. Fox, Kaj Blennow, Jonathan M. Schott, and Henrik Zetterberg. 2016. "Increased CSF Neurogranin Concentration Is Specific to Alzheimer Disease." *Neurology* 86(9):829–35.

Weyer, U. and R. D. Possee. 1991. "A Baculovirus Dual Expression Vector Derived from the Autographa Californica Nuclear Polyhedrosis Virus Polyhedrin and P10 Promoters: Co-Expression of Two Influenza Virus Genes in Insect Cells." *Journal of General Virology* 72(12):2967–74.

Wickham, T. J. and G. R. Nemerow. 1993. "Optimization of Growth Methods and Recombinant Protein Production in BTI-Tn-5B1-4 Insect Cells Using the Baculovirus Expression System." *Biotechnology Progress* 9(1):25–30.

Wiemann, Stefan, Christa Pennacchio, Yanhui Hu, Preston Hunter, Matthias Harbers, Alexandra Amiet, Graeme Bethel, Melanie Busse, Piero Carninci, Mark Diekhans, Ian Dunham, Tong Hao, J. Wade Harper, Yoshihide Hayashizaki, Oliver Heil, Steffen Hennig, Agnes Hotz-Wagenblatt, Wonhee Jang, Anika Jöcker, Jun Kawai, Christoph Koenig, Bernhard Korn, Cristen Lambert, Anita LeBeau, Sun Lu, Johannes Maurer, Troy Moore, Osamu Ohara, Jin Park, Andreas Rolfs, Kourosh Salehi-Ashtiani, Catherine Seiler, Blake Simmons, Anja Van Brabant Smith, Jason Steel, Lukas Wagner, Tom Weaver, Ruth Wellenreuther, Shuwei Yang, Marc Vidal, Daniela S Gerhard, Joshua La Baer, Gary Temple, and David E. Hill. 2016. "The ORFeome Collaboration: A Genome-Scale Human ORF-Clone Resource." *Nature Methods* 13(3):191–92.

Wolfe, Michael S., Weiming Xia, Beth L. Ostaszewski, Thekla S. Diehl, W. Taylor Kimberly, and Dennis J. Selkoe. 1999. "Two Transmembrane Aspartates in Presenilin-1 Required for Presenilin Endoproteolysis and γ-Secretase Activity." *Nature*

398(6727):513–17.

Wu, Jianming and Ling Li. 2016. "Autoantibodies in Alzheimer's Disease: Potential Biomarkers, Pathogenic Roles, and Therapeutic Implications." *Journal of Biomedical Research* 30(5):361–72.

Wurm, Florian M. 2004. "Production of Recombinant Protein Therapeutics in Cultivated Mammalian Cells." *Nature Biotechnology* 22(11):1393–98.

Wyss-Coray, Tony and Joseph Rogers. 2012. "Inflammation in Alzheimer Disease-A Brief Review of the Basic Science and Clinical Literature." *Cold Spring Harbor Perspectives in Medicine* 2(1):1–23.

Xu, Zhinan, Haiqin Chen, Xiufei Yin, Naizheng Xu, and Peilin Cen. 2005. "High-Level Expression of Soluble Human β-Defensin-2 Fused with Green Fluorescent Protein in Escherichia Coli Cell-Free System." *Applied Biochemistry and Biotechnology* 127(1):53–62.

Yang, Ning Sun, Joe Burkholder, Beth Roberts, Brian Martinell, and Dennis Mccabe. 1990. "In Vivo and in Vitro Gene Transfer to Mammalian Somatic Cells by Particle Bombardment." *Proceedings of the National Academy of Sciences of the United States of America* 87(24):9568–72.

Yates, John L., Noreen Warren, and Bill Sugden. 1985. "Stable Replication of Plasmids Derived from Epstein-Barr Virus in Various Mammalian Cells." *Nature* 313(6005):812–15.

Yokoyama, Jennifer S., Yunpeng Wang, Andrew J. Schork, Wesley K. Thompson, Celeste M. Karch, Carlos Cruchaga, Linda K. McEvoy, Aree Witoelar, Chi Hua Chen, Dominic Holland, James B. Brewer, Andre Franke, William P. Dillon, David M. Wilson, Pratik Mukherjee, Christopher P. Hess, Zachary Miller, Luke W. Bonham, Jeffrey Shen, Gil D. Rabinovici, Howard J. Rosen, Bruce L. Miller, Bradley T. Hyman, Gerard D. Schellenberg, Tom H. Karlsen, Ole A. Andreassen, Anders M. Dale, and Rahul S. Desikan. 2016. "Association between Genetic Traits for Immune-Mediated Diseases and Alzheimer Disease." *JAMA Neurology* 73(6):691–97.

Yokoyama, Shigeyuki. 2003. "Protein Expression Systems for Structural Genomics and Proteomics." *Current Opinion in Chemical Biology* 7(1):39–43.

Yoshie, Mikihiro, Kazuhiro Tamura, Takahiko Hara, and Hiroshi Kogo. 2006. "Expression of Stathmin Family Genes in the Murine Uterus during Early Pregnancy." *Molecular Reproduction and Development* 73(2):164–72.

Yoshimura, Toru, Kenju Fujita, Satoshi Kawakami, Katsumichi Takeda, Sabrina Chan, Gangamani Beligere, and Barry Dowell. 2008. "Stability of Pro-Gastrin-Releasing Peptide in Serum versus Plasma." *Tumor Biology* 29(4):224–30.

Young-Pearse, Tracy L., Seiyam Suth, Eric S. Luth, Akira Sawa, and Dennis J. Selkoe. 2010. "Biochemical and Functional Interaction of Disrupted-in-Schizophrenia 1 and Amyloid Precursor Protein Regulates Neuronal Migration during Mammalian Cortical Development." *Journal of Neuroscience* 30(31):10431–40.

Yu, Xiaobo, Kimberly B. Decker, Kristi Barker, M. Ramona Neunuebel, Justin Saul, Morgan Graves, Nathan Westcott, Howard Hang, Joshua Labaer, Ji Qiu, and Matthias P. Machner. 2015. "Host-Pathogen Interaction Profiling Using Self-Assembling Human Protein Arrays." *Journal of Proteome Research* 14(4):1920–36.

Yu, Xiaobo and Joshua Labaer. 2015. "High-Throughput Identification of Proteins with AMPylation Using Self-Assembled Human Protein (NAPPA) Microarrays." *Nature Protocols* 10(5):756–67.

Yu, Xiaobo, Andrew R. Woolery, Phi Luong, Yi Heng Hao, Markus Grammel, Nathan Westcott, Jin Park, Jie Wang, Xiaofang Bian, Gokhan Demirkan, Howard C. Hang, Kim Orth, and Joshua LaBaer. 2014. "Click Chemistry-Based Detection of Global Pathogen-Host AMPylation on Self-Assembled Human Protein Microarrays." *Molecular & Cellular Proteomics* 13(11):3164–76.

Yuan, Ping, Gregory Jedd, Desigan Kumaran, Subramanyam Swaminathan, Helen Shio, David Hewitt, Nam Hai Chua, and Kunchithapadam Swaminathan. 2003. "A HEX-1 Crystal Lattice Required for Woronin Body Function in Neurospora Crassa." *Nature Structural Biology* 10(4):264–70.

Zemella, Anne, Lena Thoring, Christian Hoffmeister, and Stefan Kubick. 2015. "Cell-Free Protein Synthesis: Pros and Cons of Prokaryotic and Eukaryotic Systems." *ChemBioChem* 16(17):2420–31.

Zetterberg, Henrik. 2016. "Neurofilament Light: A Dynamic Cross-Disease Fluid Biomarker for Neurodegeneration." *Neuron* 91(1):1–3.

Zetterberg, Henrik. 2019. "Blood-Based Biomarkers for Alzheimer's Disease—An Update." *Journal of Neuroscience Methods* 319:2–6.

Zetterberg, Henrik, Erik Mörtberg, Linan Song, Lei Chang, Gail K. Provuncher, Purvish P. Patel, Evan Ferrell, David R. Fournier, Cheuk W. Kan, Todd G. Campbell, Ray Meyer, Andrew J. Rivnak, Brian A. Pink, Kaitlin A. Minnehan, Tomasz Piech, David M. Rissin, David C. Duffy, Sten Rubertsson, David H. Wilson, and Kaj Blennow. 2011. "Hypoxia Due to Cardiac Arrest Induces a Time-Dependent Increase in Serum Amyloid β Levels in Humans." *PLoS ONE* 6(12).

Zetterberg, Henrik, David Wilson, Ulf Andreasson, Lennart Minthon, Kaj Blennow, Jeffrey Randall, and Oskar Hansson. 2013. "Plasma Tau Levels in Alzheimer's Disease." *Alzheimer's Research & Therapy* 5(2):9.